EUROPEAN
JOURNAL OF
BIOLOGY

OFFICIAL JOURNAL OF ISTANBUL UNIVERSITY'S SCIENCE FACULTY

https://iupress.istanbul.edu.tr/en/journal/ejb/home

ISTANBUL
UNIVERSITY
P R E S S
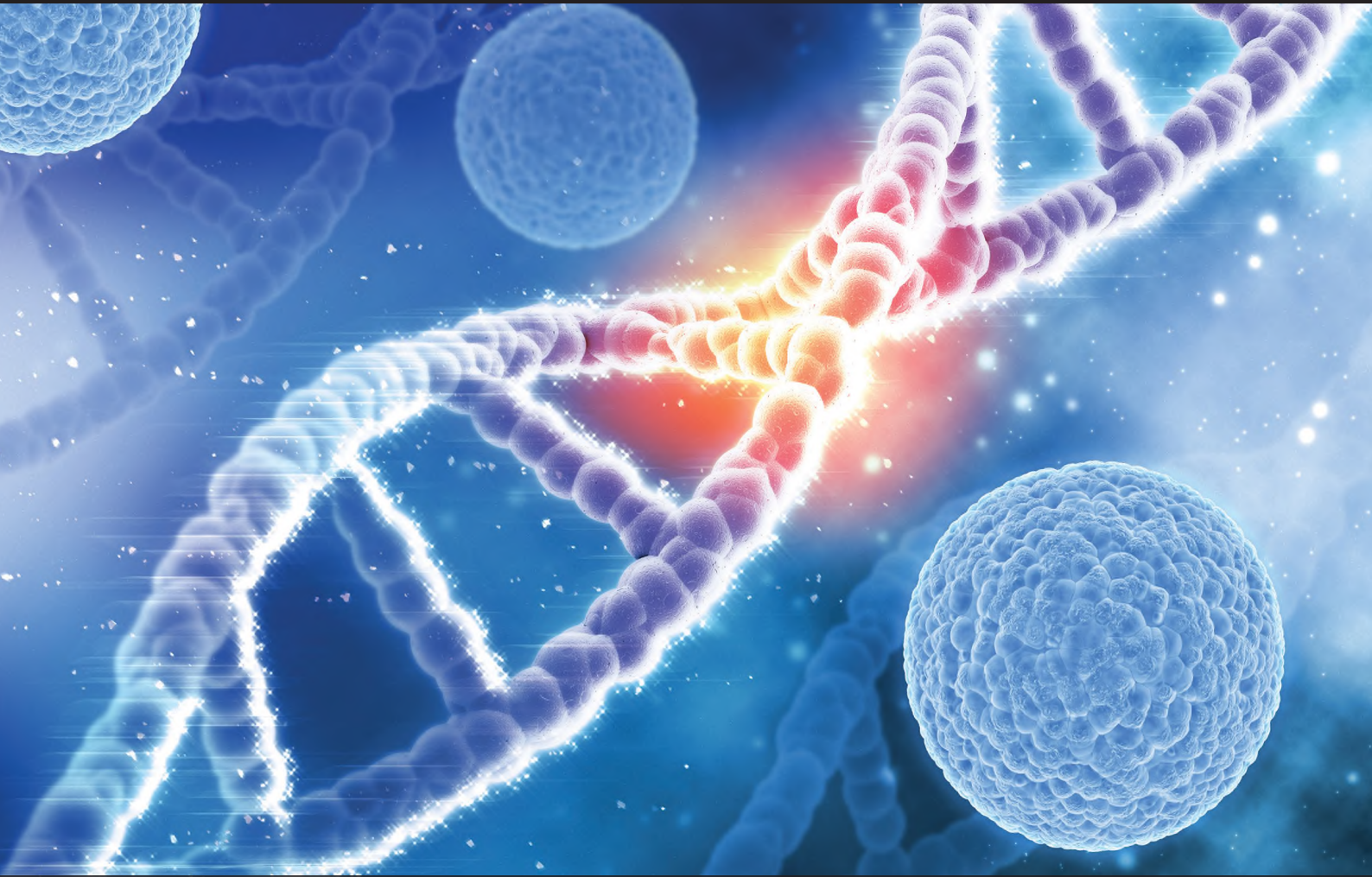
Indexing and Abstracting

SCOPUS
TUBITAK ULAKBIM TR Index
Zoological Record - Clarivate Analytics
CAB Abstracts
DOAJ
CABI
- AgBiotechNet Database
- Animal Science Database
- VetMed Resource
- Environmental Impact Database
- Horticultural Science Database
- Nutrition and Food Sciences Database
Chemical Abstracts Service (CAS)
EBSCO Central & Eastern European Academic Source
SOBIAD
Cabells Journalytics

II

EDITORIAL MANAGEMENT BOARD

İSTANBUL
UNIVERSITY
PRESS

EDITORIAL MANAGEMENT BOARD

AIMS AND SCOPE

European Journal of Biology (Eur J Biol) is an international, scientific, open access periodical published in accordance with independent, unbiased, and double-blinded peer-review principles. The journal is the official publication of Istanbul University Faculty of Science and it is published biannually on June and December. The publication language of the journal is English. European Journal of Biology has been previously published as IUFS Journal of Biology. It has been published in continuous publication since 1940.

European Journal of Biology aims to contribute to the literature by publishing manuscripts at the highest scientific level on all fields of biology. The journal publishes original research and review articles, and short communications that are prepared in accordance with the ethical guidelines in all fields of biology and life sciences.

The scope of the journal includes but not limited to; animal biology and systematics, plant biology and systematics, hydrobiology, ecology and environmental biology, microbiology, cell and molecular biology, biochemistry, biotechnology and genetics, physiology, toxicology, cancer biology, developmental and stem cell biology.

The target audience of the journal includes specialists and professionals working and interested in all disciplines of biology.

The editorial and publication processes of the journal are shaped in accordance with the guidelines of the International Committee of Medical Journal Editors (ICMJE), World Association of Medical Editors (WAME), Council of Science Editors (CSE), Committee on Publication Ethics (COPE), European Association of Science Editors (EASE), and National Information Standards Organization (NISO). The journal is in conformity with the Principles of Transparency and Best Practice in Scholarly Publishing (doaj.org/bestpractice).

European Journal of Biology is currently indexed SCOPUS, TUBITAK ULAKBIM TR Index, Zoological Record - Clarivate Analytics, CAB Abstracts, DOAJ, CABI, Chemical Abstracts Service (CAS), EBSCO Central & Eastern European Academic Source, SOBIAD, Cabells Journalytics.

Processing and publication are free of charge with the journal. No fees are requested from the authors at any point throughout the evaluation and publication process. All manuscripts must be submitted via the online submission system, which is available at dergipark. gov.tr/iufsjb. The journal guidelines, technical information, and the required forms are available on the journal's web page.

All expenses of the journal are covered by the Istanbul University.

Statements or opinions expressed in the manuscripts published in the journal reflect the views of the author(s) and not the opinions of the Istanbul University Faculty of Science, editors, editorial board, and/or publisher; the editors, editorial board, and publisher disclaim any responsibility or liability for such materials.

All published content is available online, free of charge at https://dergipark.org.tr/tr/pub/iufsjb. Printed copies of the journal are distributed free of charge.

Editor in Chief: Prof. Dr. Fusun OZTAY
Address: Istanbul University, Faculty of Science, Department of Biology, 34134 Vezneciler, Fatih, Istanbul, Türkiye
Phone: +90 212 4555700 (Ext. 20319)
Fax: +90 212 5280527
E-mail: fusoztay@istanbul.edu.tr; ejb@istanbul.edu.tr

INSTRUCTIONS TO AUTHORS

European Journal of Biology (Eur J Biol) is an international, scientific, open access periodical published in accordance with independent, unbiased, and double-blinded peer-review principles. The journal is the official publication of Istanbul University Faculty of Science and it is published biannually on June and December. The publication language of the journal is English. European Journal of Biology has been previously published as IUFS Journal of Biology. It has been published in continuous publication since 1940.

European Journal of Biology aims to contribute to the literature by publishing manuscripts at the highest scientific level on all fields of biology. The journal publishes original research and review articles, and short communications that are prepared in accordance with the ethical guidelines in all fields of biology and life sciences.

The scope of the journal includes but not limited to; animal biology and systematics, plant biology and systematics, hydrobiology, ecology and environmental biology, microbiology, cell and molecular biology, biochemistry, biotechnology and genetics, physiology, toxicology, cancer biology, developmental and stem cell biology.

The editorial and publication processes of the journal are shaped in accordance with the guidelines of the International Council of Medical Journal Editors (ICMJE), the World Association of Medical Editors (WAME), the Council of Science Editors (CSE), the Committee on Publication Ethics (COPE), the European Association of Science Editors (EASE), and National Information Standards Organization (NISO). The journal conforms to the Principles of Transparency and Best Practice in Scholarly Publishing (doaj.org/bestpractice).

Originality, high scientific quality, and citation potential are the most important criteria for a manuscript to be accepted for publication. Manuscripts submitted for evaluation should not have been previously presented or already published in an electronic or printed medium. Manuscripts that have been presented in a meeting should be submitted with detailed information on the organization, including the name, date, and location of the organization.

Manuscripts submitted to European Journal of Biology will go through a double-blind peer-review process. Each submission will be reviewed by at least three external, independent peer reviewers who are experts in their fields in order to ensure an unbiased evaluation process. The editorial board will invite an external and independent editor to manage the evaluation processes of manuscripts submitted by editors or by the editorial board members of the journal. The Editor in Chief is the final authority in the decision-making process for all submissions.

An approval of research protocols by the Ethics Committee in accordance with international agreements (World Medical Association Declaration of Helsinki "Ethical Principles for Medical Research Involving Human Subjects," amended in October 2013, www.wma.net) is required for experimental, clinical, and drug studies. If required, ethics committee reports or an equivalent official document will be requested from the authors.

The Journal takes as principle to comply with the ethical standards of Basel Declaration and WMA Statement on Animal Use in Biomedical Research and World Medical Association (WMA) Declaration of Helsinki – Ethical Principles for Medical Research Involving Human Subjects.

The journal requires experimental research studies on vertebrates or any regulated invertebrates to comply with relevant institutional, national and/or international guidelines, and authors are advised to clearly state their compliance with relevant guidelines. For studies involving animals, it is required to obtain approval of research protocols from an ethics committee. The committee reviews protocols to ensure compliance with applicable regulations and guidelines, including the Guide for the Care and Use of Laboratory Animals (8th Edition, 2011), International Council for Laboratory Animal Science (ICLAS), and the International Guiding Principles for Biomedical Research Involving Animals (2012). These guidelines offer comprehensive instructions on how to carry out animal research ethically and humanely and are widely acknowledged as the benchmark for such research. Authors should provide detailed explanation of the ethical treatment of animals in their manuscripts, including measures taken to avoid pain and distress. This is crucial to ensure the humane conduct of the study and enable verification that it conforms to the relevant ethical criteria. The ARRIVE checklist is a useful tool authors can use to present this information clearly and thoroughly.

European Journal of Biology advises authors to comply with IUCN Policy Statement on research Involving Species at Risk of Extinction and the Convention on the Trade in Endangered Species of Wild IUCN Policy Statement on Research Involving Species at Risk of Extinction and the Convention on the Trade in Endangered Species of Wild Fauna and Flora.

An approval of research protocols by the Ethics Committee in accordance with international standards mentioned above is required for experimental, clinical, and

drug studies and for some case reports. If required, ethics committee reports or an equivalent official document will be requested from the authors. For manuscripts concerning experimental research on humans, a statement should be included that shows that written informed consent of patients and volunteers was obtained following a detailed explanation of the procedures that they may undergo. Information on patient consent, the name of the ethics committee, and the ethics committee approval number should also be stated in the Materials and Methods section of the manuscript. It is the authors' responsibility to carefully protect the patients' anonymity. For photographs that may reveal the identity of the patients, signed releases of the patient or of their legal representative should be enclosed.

All submissions are screened by a similarity detection software (iThenticate by CrossCheck).

In the event of alleged or suspected research misconduct, e.g., plagiarism, citation manipulation, and data falsification/fabrication, the Editorial Board will follow and act in accordance with COPE guidelines.

Each individual listed as an author should fulfil the authorship criteria recommended by the International Committee of Medical Journal Editors (ICMJE - www.icmje.org). The ICMJE recommends that authorship be based on the following 4 criteria:

1. Substantial contributions to the conception or design of the work; or the acquisition, analysis, or interpretation of data for the work; AND
2. Drafting the work or revising it critically for important intellectual content; AN
3. Final approval of the version to be published; AND
4. Agreement to be accountable for all aspects of the work in ensuring that questions related to the accuracy or integrity of any part of the work are appropriately investigated and resolved.

In addition to being accountable for the parts of the work he/she has done, an author should be able to identify which co-authors are responsible for specific other parts of the work. In addition, authors should have confidence in the integrity of the contributions of their co-authors.

All those designated as authors should meet all four criteria for authorship, and all who meet the four criteria should be identified as authors. Those who do not meet all four criteria should be acknowledged in the title page of the manuscript.

European Journal of Biology requires corresponding authors to submit a signed and scanned version of the authorship contribution form (available for download through the journal's web page) during the initial submission process in order to act appropriately on authorship rights and to prevent ghost or honorary authorship. If the editorial board suspects a case of "gift authorship," the submission will be rejected without further review. As part of the submission of the manuscript, the corresponding author should also send a short statement declaring that he/she accepts to undertake all the responsibility for authorship during the submission and review stages of the manuscript.

European Journal of Biology requires and encourages the authors and the individuals involved in the evaluation process of submitted manuscripts to disclose any existing or potential conflicts of interests, including financial, consultant, and institutional, that might lead to potential bias or a conflict of interest. Any financial grants or other supports received for a submitted study from individuals or institutions should be disclosed to the Editorial Board. To disclose a potential conflict of interest, the ICMJE Potential Conflict of Interest Disclosure Form should be filled and submitted by all contributing authors. Cases of a potential conflict of interest of the editors, authors, or reviewers are resolved by the journal's Editorial Board within the scope of COPE and ICMJE guidelines.

The Editorial Board of the journal handles all appeal and complaint cases within the scope of COPE guidelines. In such cases, authors should get in direct contact with the editorial office regarding their appeals and complaints. When needed, an ombudsperson may be assigned to resolve cases that cannot be resolved internally. The Editor in Chief is the final authority in the decision-making process for all appeals and complaints.

When submitting a manuscript to European Journal of Biology, authors accept to assign the copyright of their manuscript to Istanbul University Faculty of Science. If rejected for publication, the copyright of the manuscript will be assigned back to the authors. European Journal of Biology requires each submission to be accompanied by a Copyright Transfer Form (available for download at the journal's web page). When using previously published content, including figures, tables, or any other material in both print and electronic formats, authors must obtain permission from the copyright holder. Legal, financial and criminal liabilities in this regard belong to the author(s).

Statements or opinions expressed in the manuscripts published in European Journal of Biology reflect the views of the author(s) and not the opinions of the editors, the editorial board, or the publisher; the editors, the editorial board, and the publisher disclaim any responsibility

or liability for such materials. The final responsibility in regard to the published content rests with the authors.

MANUSCRIPT SUBMISSION

European Journal of Biology endorses ICMJE-Recommendations for the Conduct, Reporting, Editing, and Publication of Scholarly Work in Medical Journals (updated in December 2015 - http:/ / www.icmje.org/ icmje-recommendations.pdf). Authors are required to prepare manuscripts in accordance with the CONSORT guidelines for randomized research studies, STROBE guidelines for observational original research studies, STARD guidelines for studies on diagnostic accuracy, PRISMA guidelines for systematic reviews and meta-analysis, ARRIVE guidelines for experimental animal studies, TREND guidelines for non-randomized public behaviour, and COREQ guidelines for qualitative research.

Manuscripts can only be submitted through the journal's online manuscript submission and evaluation system, available at the journal's web page. Manuscripts submitted via any other medium will not be evaluated.

Manuscripts submitted to the journal will first go through a technical evaluation process where the editorial office staff will ensure that the manuscript has been prepared and submitted in accordance with the journal's guidelines. Submissions that do not conform to the journal's guidelines will be returned to the submitting author with technical correction requests.

During the initial submission, authors are required to submit the following:

- Copyright Agreement Form,
- Author Contributions Form, and

ICMJE Potential Conflict of Interest Disclosure Form (should be filled in by all contributing authors). These forms are available for download at the journal's web page.

Preparation of the Manuscript

Title page: A separate title page should be submitted with all submissions and this page should include:

- The full title of the manuscript as well as a short title (running head) of no more than 50 characters,
- Name(s), affiliations, and highest academic degree(s) of the author(s),
- Grant information and detailed information on the other sources of support,

- Name, address, telephone (including the mobile phone number) and fax numbers, and email address of the corresponding author,
- Acknowledgment of the individuals who contributed to the preparation of the manuscript but who do not fulfil the authorship criteria.

Abstract: Abstract with subheadings should be written as structured abstract in submitted papers except for Review Articles and Letters to the Editor. Please check Table 1 below for word count specifications (250 words).

Keywords: Each submission must be accompanied by a minimum of three to a maximum of six keywords for subject indexing at the end of the abstract. The keywords should be listed in full without abbreviations.

Manuscript Types

Original Articles: This is the most important type of article since it provides new information based on original research. A structured abstract is required with original articles and it should include the following subheadings: Objective, Materials and Methods, Results and Conclusion. The main text of original articles should be structured with Introduction, Materials and Methods, Results, Discussion, and Conclusion subheadings. Please check Table 1 for the limitations of Original Articles. Statistical analysis to support conclusions is usually necessary. Statistical analyses must be conducted in accordance with international statistical reporting standards. Information on statistical analyses should be provided with a separate subheading under the Materials and Methods section and the statistical software that was used during the process must be specified. Units should be prepared in accordance with the International System of Units (SI).

Short Communications: Short communication is for a concise, but independent report representing a significant contribution to Biology. Short communication is not intended to publish preliminary results. But if these results are of exceptional interest and are particularly topical and relevant will be considered for publication. Short Communications should include an abstract and should be structed with the following subheadings: "Introduction", "Materials and Methods", "Results and Discussion".

Editorial Comments: Editorial comments aim to provide a brief critical commentary by reviewers with expertise or with high reputation in the topic of the research article published in the journal. Authors are selected and invited by the journal to provide such comments. Abstract, Keywords, and Tables, Figures, Images, and other media are not included.

Review Articles: Reviews prepared by authors who have extensive knowledge on a particular field and whose scientific background has been translated into a high volume of publications with a high citation potential are welcomed. These authors may even be invited by the journal. Reviews should describe, discuss, and evaluate the current level of knowledge of a topic in clinical practice and should guide future studies. The main text should contain Introduction, Experimental and Clinical Research Consequences, and Conclusion sections. Please check Table 1 for the limitations for Review Articles.

Letters to the Editor: This type of manuscript discusses important parts, overlooked aspects, or lacking parts of a previously published article. Articles on subjects within the scope of the journal that might attract the readers' attention, particularly educative cases, may also be submitted in the form of a "Letter to the Editor." Readers can also present their comments on the published manuscripts in the form of a "Letter to the Editor." Abstract, Keywords, and Tables, Figures, Images, and other media should not be included. The text should be unstructured. The manuscript that is being commented on must be properly cited within this manuscript.

Tables

Tables should be included in the main document, presented after the reference list, and they should be numbered consecutively in the order they are referred to within the main text. A descriptive title must be placed above the tables. Abbreviations used in the tables should be defined below the tables by footnotes (even if they are defined within the main text). Tables should be created using the "insert table" command of the word processing software and they should be arranged clearly to provide easy reading. Data presented in the tables should not be a repetition of the data presented within the main text but should be supporting the main text.

Figures and Figure Legends

Figures, graphics, and photographs should be submitted as separate files (in TIFF or JPEG format with 1200 dpi for graphic and 600 dpi for colour images) through the submission system. The files should not be embedded in a Word document or the main document. When there are figure subunits, the subunits should be labeled merged to form a single image. Each subunit should be submitted separately through the submission system. Images should be labeled (a, b, c, etc.) to indicate figure subunits.

Thick and thin arrows, arrowheads, stars, asterisks, and similar marks can be used on the images to support fig-

ure legends. Like the rest of the submission, the figures too should be blind. Any information within the images that may indicate an individual or institution should be blinded. The minimum resolution of each submitted figure should be 300 DPI. To prevent delays in the evaluation process, all submitted figures should be clear in resolution and large in size (minimum dimensions: 100 × 100 mm). Figure legends should be listed at the end of the main document.

All acronyms and abbreviations used in the manuscript should be defined at first use, both in the abstract and in the main text. The abbreviation should be provided in parentheses following the definition.

When a drug, chemical, product, hardware, or software program is mentioned within the main text, product information, including the name of the product, the producer of the product, and city and the country of the company (including the state if in USA), should be provided in parentheses in the following format: "Discovery St PET/CT scanner (General Electric, Milwaukee, WI, USA)"

All references, tables, and figures should be referred to within the main text, and they should be numbered consecutively in the order they are referred to within the main text.

Limitations, drawbacks, and the shortcomings of original articles should be mentioned in the Discussion section before the conclusion paragraph.

References

European Journal of Biology uses the **AMA citation style.** In the paper, you are writing, materials are cited using superscript numerals. The first reference used in a written document is listed as 1 in the reference list, and a 1 is inserted into the document immediately next to the fact, concept, or quotation being cited. If the same reference is used multiple times in one document, use the same number to refer to it throughout the document.

Example:

Finding treatments for breast cancer is a major goal for scientists.[1,2] Some classes of drugs show more promise than others. Gradishar evaluated taxanes as a class.[3] Other scientists have investigated individual drugs within this class, including Andre and Zielinski[2] and Joensuu and Gligorov.[4] Mita et al's investigation of cabazitaxel 5 seems to indicate a new role for this class of drugs.

While citing publications, preference should be given to the latest, most up to date publications. If an ahead of print publication is cited, the DOI number should be pro-

Table 1. Limitations for each manuscript type					
Type of manuscript	**Word limit**	**Abstract word limit**	**Reference limit**	**Table limit**	**Figure limit**
Original Article	4500	250 (Structured)	No limit	6	Maximum 8
Short Communication	2500	200	30	3	4
Review Article	5500	250	No limit	5	6
Letter to the Editor	500	No abstract	5	No tables	No media

vided. Authors are responsible for the accuracy of references. Journal titles should be abbreviated in accordance with the journal abbreviations in Index Medicus/ MEDLINE/PubMed. When there are six or fewer authors, all authors should be listed. If there are seven or more authors, the first six authors should be listed followed by "et al."

At the end of the document, include a reference list with full citations to each item. The reference styles for different types of publications are presented in the following examples.

Print journal article with six or fewer authors:

Kayalar O, Oztay F, Ongen HG. Gastrin-releasing peptide induces fibrotic response in MRC5s and proliferation in A549s. *Cell Commun Signal.* 2020;18(1):96-107.

Kazerouni NN, Currier RJ, Hodgkinson C, Goldman S, Lorey F, Roberson M. Ancillary benefits of prenatal maternal serum screening achieved in the California program. *Prenat Diagn.* 2010;30 (10):981-987.

Print journal article with more than six authors:

Baba Y, Yoshida N, Kinoshita K, et al. Clinical and prognostic features of patients with esophageal cancer and multiple primary cancers: A retrospective single-institution study. *Ann Surg.* 2018;267(3):478-483.

Online journal article:

Florez H, Martinez R, Chakra W, Strickman-Stein M, Levis S. Outdoor exercise reduces the risk of hypovitaminosis D in the obese. *J Steroid Biochem Mol Bio.* 2007;103(3-5):679-681. doi:10.1016/j.jsbmb.2006.12.032.

Journal article with no named author or group name:

Centers for Disease Control and Prevention (CDC). Licensure of a meningococcal conjugate vaccine (Menveo) and guidance for use-Advisory Committee on Immunization Practices (ACIP), 2010. *MMWR Morb Mortal Wkly Rep.* 2010;59(9):273

Book:

Brownson RC. *Evidence-based Public Health.* 2nd ed. New York, N.Y.: Oxford University Press; 2011.

Book Chapter:

Guyton JL, Crockarell JR. Fractures of acetabulum and pelvis. In: Canale ST, ed. *Campbell's Operative Orthopaedics.* 10th ed. Philadelphia, PA: Mosby, Inc; 2003:2939-2984.

Webpage:

Fast facts. National Osteoporosis Foundation website. http://www.nof.org/osteoporosis/diseasefacts.htm. Accessed August 27, 2007.

Official organization report published on a webpage:

Office of Women's Health, California Department of Public Health. California Adolescent Health 2009. http://www.cdph.ca.gov/pubsforms/Pubs/OWH-AdolHealthReport09.pdf. Accessed January 5, 2011.

Conference Proceedings:

Fritz TC, Soni MG. Use of dietary supplements in sports drinks: Consumption and safety determinations for regulatory compliance. Poster presented at: *Annual International Society of Sports Nutrition Conference and Expo*; June 16-18, 2005; New Orleans, LA.

Thesis

Yildirim M. The determination of effective long non-coding RNA on human pulmonary fibrosis in an in vitro model. Istanbul University, Science Institute, Master Thesis, 2018.

REVISIONS

When submitting a revised version of a paper, the author must submit a detailed "Response to the reviewers" that states point by point how each issue raised by the reviewers has been covered and where it can be found

(each reviewer's comment, followed by the author's reply and line numbers where the changes have been made) as well as an annotated copy of the main document. Revised manuscripts must be submitted within 30 days from the date of the decision letter. If the revised version of the manuscript is not submitted within the allocated time, the revision option may be cancelled. If the submitting author(s) believe that additional time is required, they should request this extension before the initial 30-day period is over. Accepted manuscripts are copy-edited for grammar, punctuation, and format. Once the publication process of a manuscript is completed, it is published online on the journal's webpage as an ahead-of-print publication before it is included in its scheduled issue. A PDF proof of the accepted manuscript is sent to the corresponding author and their publication approval is requested within 2 days of their receipt of the proof.

Editor in Chief: Prof. Dr. Fusun OZTAY
Address: Istanbul University, Faculty of Science, Department of Biology,
34134 Vezneciler, Fatih, Istanbul, Türkiye
Phone: +90 212 4555700 (Ext. 20319)
Fax: +90 212 5280527
E-mail: fusoztay@istanbul.edu.tr

CONTENTS

İSTANBUL UNIVERSITY PRESS

CONTENTS

İSTANBUL UNIVERSITY PRESS

RESEARCH ARTICLE

Astragaloside-IV Inhibits Metastasis by Suppressing the SDF-1/CXCR4 Axis and Activating Apoptosis in Cisplatin-Resistant Ovarian Cancer Cells

Burcin Irem Abas[1], Omer Erdogan[1], Ozge Cevik[1]

[1]Aydin Adnan Menderes University, Faculty of Medicine, Medical Biochemistry Department, Aydin, Türkiye

ABSTRACT

Objective: Ovarian cancer has the highest mortality rate in women and it has a poor response rate to treatment due to its late diagnosis and is frequently resistant to currently used cisplatin-based treatment methods. Astragaloside IV (As-IV), a bioactive compound and natural tripeptide glycoside known as an antioxidant, has drawn attention in Chinese medicine for its healing properties. Many studies have shown that it has anti-inflammatory, antidiabetic, antitumoral, and anti-angiogenic properties.

Materials and Methods: In our study, we first rendered ovarian cancer cells (OVCAR-3) resistant to cisplatin and then applied determined doses of As-IV (40 µg/mL) and (70 µg/mL) to OVCAR-3 cells and cisplatin-resistant ovarian cancer cells (OVCAR-3-CisR). The cell viability capacity, variation of *BAX/BCL-2* gene expression, and regulation of the *SDF-1/CXCR4* chemokine axis protein and their gene expressions were investigated.

Results: According to the findings, As-IV administration suppressed metastasis by lowering the colony formation potential of cisplatin-resistant ovarian cancer and down-regulating the *SDF-1/CXCR4* axis, and increasing the ratio of *BAX/BCL-2* mRNA and protein levels due to *BAX* up-regulation and *BCL-2* down-regulation.

Conclusion: As a result, we showed that As-IV, used as an antioxidant, can be used as an effective anticancer agent to improve response to the currently used cisplatin-based treatment in cases of drug resistance in ovarian cancer.

Keywords: Ovarian cancer, Cisplatin, Astragaloside IV, Chemokine, Apoptosis, Antioxidant

INTRODUCTION

One of the most common cancers of the woman's reproductive system is ovarian cancer, with 313,959 new cases and 207,252 fatalities anticipated in 2020.[1] Ovarian cancer was the leading cause of death among all gynecologic cancer patients, outpacing only endometrial and cervical cancers in incidence rate.[2] The high death rate of ovarian cancer is attributed to delayed diagnosis and a lack of suitable treatments for resistant disease.[3] Despite advances in diagnostic strategies, surgical techniques, and novel therapeutic drugs, long-term survival in patients with ovarian cancer remains discouraging. Maximum tumor debulking followed by postoperative platinum-based chemotherapy is the current standard of care for ovarian cancer.[4] Cisplatin, a platinum-based antitumoral agent, is one of the most widely used chemotherapy drugs in the treatment of cancer patients suffering from lung, bladder, esophageal, testicular, ovarian, cervical, or breast cancer.[5] The cornerstone of current ovarian cancer chemotherapy, cisplatin-based chemotherapy showed favorable survival and response rates, and toxicity.[6] But as a result of drug resistance, cisplatin's effectiveness in ovarian cancer cells diminished or vanished.[7]

One of the main active components of Astragalus membranaceus is Astragaloside IV (As-IV), which is also referred to as astragalus saponin IV. Astragalus membranaceus is among the 50 most essential herbs used in traditional Chinese medicine, known as "Huang qi" in the Chinese Pharmacopoeia.[8] The chemical formula of AS-IV is 3-O-beta-D-xylopyranosyl-6-O-beta-D-glucopyranosyl-cycloastragenol and the molecular formula of As-IV is $C14H68O14$.[9] As-IV has a broad range of pharmacological effects, including cardioprotective, antioxidant, anti-diabetes, anti-bacterial, anti-inflammatory, anti-fibrosis, anti-viral, and immunoregulation effects. It also has protective effects against respiratory, cardiovascular, kidney, and immune system disease.[10] Furthermore, administration of the antioxidant As-IV was shown to increase the expression of the tight junction proteins occludin and zona occludens-1 and to protect the blood-brain barrier by contributing to the regulation of

endothelial cells of mice subjected to ischemia/reperfusion.[11] In a study of rats with myocardial ischemia, As-IV was shown to increase myocardial antioxidant enzyme superoxide dismutase activity and to contribute to protection against ischemia through regulation of the nitric oxide inducing system.[12]

Numerous studies have shown that As-IV has anti-cancer effects against several tumor types by enhancing immune function, tumor growth inhibition, and tumor migration and invasion inhibition.We investigated the effect of treating cisplatin-resistant ovarian cancer cells with As-IV on chemokine receptors and apoptotic markers, as well as whether As-IV can be used as a potential treatment agent in ovarian cancer types that develop drug resistance.

MATERIALS AND METHODS

Ovarian Cancer Cells and Resistant to Cisplatin

Human ovarian cancer cells (OVCAR-3, ATCC-HTB-161) were used for MTT at 1-1000 µM cisplatin for 24, 48 and 72 h. The IC_{50} dose was 26.37 µM (Figure 1a). First, the living OVCAR-3 cells were passaged and incubated for 48 h with 10 µM cisplatin in the medium.[13] Second, the living OVCAR-3 cells were passaged and 5 µM cisplatin was added to the medium and incubated for 48 h. Finally, the OVCAR-3 living cells were passaged and incubated for 20 days with 2.5 µM cisplatin in the medium. In this way, there was a gradual reduction in the amount of cisplatin in the medium and the growth of OVCAR-3 cells with resistance. At this point the OVCAR-3 cisplatin resistance cells (OVCAR-3-CisR) were cultured in RPMI-1640 Medium (Gibco), including 2 mM glutamine, 10% FBS, 100 Units penicillin/streptomycin at 37°C in a humidified atmosphere containing 5% CO_2.

Cytotoxicity Assay

The MTT (3-(4,5-dimethylthiazol-2-yl)-2,5-diphenyl-2H-tetrazolium bromide) test was performed for the determination of cell viability. The OVCAR-3 and OVCAR-3-CisR cells were cultured in 96-well plates which designed to be 10,000 cells per well in order to obtain the desired results. Following overnight incubation at 37°C, OVCAR-3 and OVCAR-3-CisR cells were exposed to increasing (1-100 µg/mL) doses of As-IV (Sigma 74777) for 24 h.[14] As-IV substance was dissolved with dimethyl sulfoxide (DMSO) and an equal amount of DMSO was applied to the medium as a control batch in the cells. A 10 µL volume of MTT (final concentration: 5 µg/mL) was added to each well and incubated for 4 h at 37°C. After this, 100 µL of DMSO was added and the absorbance was measured at 570 nm.[15] The cell viability of the cells was calculated with the percentage of the treatment batch collate with the control.

Colony Formation Assay

Colony assay studies in OVCAR-3 and OVCAR-3-CisR cells were performed at concentrations closest to the IC_{50} of As-IV. For the colony formation experiment, 500 cells/well were cultured in a 24-well plate for 24 h. After 24 h of incubation, the OVCAR-3 cells were incubated 40 µg/mL As-IV and the OVCAR-3-CisR cells were incubated 70 µg/mL As-IV, both cells of which were incubated for 7 days. After removing the culture medium, the cells were fixed with a 1:1 solution of methanol and acetic acid, and then incubated for 20 min with crystal violet dye (0.5% in methanol).[15] The dye was then washed out with distilled water. The colonies formed were photographed in microscope (Axiovert, Zeiss), dissolved in ethanol and measured for absorbance at 595 nm. The percentage of formed colonies was calculated to collate with the control.

Measurement of CXCR4 and SDF-1 Protein Levels

OVCAR-3 and OVCAR-3-CisR cells ($1x10^6$ cells/well) were cultured in 6-well plates. As-IV (40 µg/mL or 70 µg/mL) was applied to the cells and incubated for 24 h. For the measurement of SDF-1 release, the cell medium was collected after incubation. For the measurement of CXCR4, the cell pellet was used. The plate was rinsed twice with PBS after collecting the cell medium. The cells were then harvested with trypsin-EDTA and centrifuged at 1000 x g for 10 min. The centrifuged OVCAR-3 and OVCAR-3-CisR cells were blasted with a cell lysis buffer containing 2% Triton X-100 and centrifugation was repeated at 4°C. After centrifugation, CXCR4 was measured using the supernatant. The measurements were carried out according to the protocol of the commercial ELISA kit used (CXCR4 ELISA kit CSB-E12825h-Cusabio Technology; SDF-1 ELISA kit CSB-E04722h-Cusabio Technology). After measuring the absorbance in an ELISA reader (Biotek, Epoch) at 450 nm, changes in protein levels were calculated according to the standard curve.

Measurement of *CXCR4, SDF1, BAX* and *BCL2* Gene Expression Levels

Apoptotic changes were analyzed by *BAX* and *BCL2* gene expression, and chemokine changes were analyzed by *CXCR4* and *SDF-1* gene expression using the qPCR technique. OVCAR-3 and OVCAR-3-CisR cells ($1x10^6$ cells/well) were cultured in 6-well plates and cells were incubated As-IV (40 µg/mL or 70 µg/mL) for 24 h. After incubation, cells were collected and lysed with cell lysis buffer in the total RNA isolation kit. The manufacturer's instructions for the RNA extraction kit (PureLink, Life Technologies) were followed to isolate total RNA. Using the High Capacity cDNA Reverse Transcription Kit (Applied Biosystem) in accordance with the manufacturer's instructions, 1 µg of total RNA was reverse transcribed.
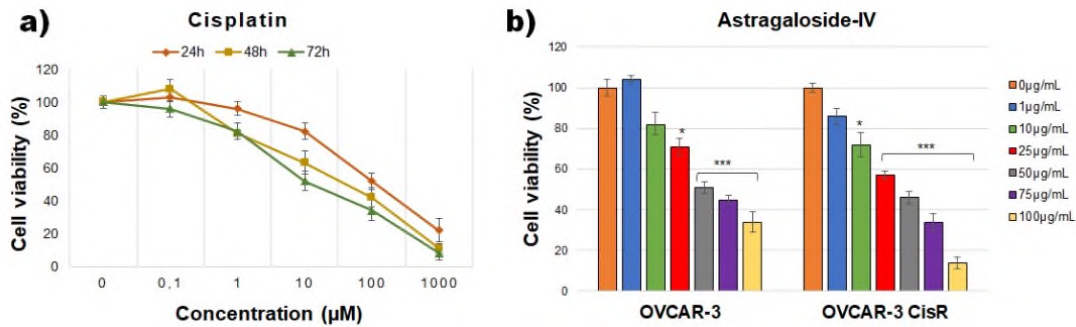
Figure 1. MTT cytotoxicity test results are depicted graphically. a) A percentage representation of the change in cell viability caused by the application of cisplatin doses ranging from 1-100 µM to OVCAR-3 cells for 24, 48, and 72 h. b) Percentage change in the viability of OVCAR-3 and OVCAR-3-CisR cells after 24 h incubation with As-IV doses ranging from 1-100 µg/mL

Statistical Analysis

Statistical analysis was accomplished with GraphPad Prism version 7.0 software. Data's significancy described as respectively *, $p<0.05$; ***, $p<0.01$; +++, $p<0.001$)

RESULTS

Effects of As-IV on Cell Viability in OVCAR-3 and OVCAR-3-CisR Cells

To determine the cytotoxic effect, As-IV was used in the concentration range of 1-100 µg/mL and incubated for 24 h, resulting in an IC$_{50}$ dose of 43.11±4.36 µg/mL for OVCAR-3 cells, 71.02 ± 3.21 µg/mL for OVCAR-3-CisR cells found (Figure 1). In the experimental models, the dose of As-IV to be used in 24 h incubations was 40 µg/mL for OVCAR-3 cells and 70 µg/mL for OVCAR-3-CisR cells. As-IV appears to have a toxic effect on OVCAR-3 cells starting from 25 µg/mL ($p<0.05$) at concentrations above 50 µg/mL, and momentously reduce cell proliferation ($p<0.001$). It can be seen that As-IV momentously reduces cell proliferation in OVCAR-3-CisR cells starting from 10 µg/mL ($p<0.05$) at concentrations above 25 µg/mL ($p<0.001$).

Effect of As-IV on *BAX/BCL-2* Rate in OVCAR-3 and OVCAR-3-CisR Cells

Gene expression levels of *BAX* and *BCL2* markers were examined in order to understand whether the administration of As-IV treatment suppresses the apoptotic cascade in cells. According to the data obtained, it was observed that As-IV administration suppressed apoptosis in cells (Figure 2). *BAX* is an apoptotic gene and its protein forms localized to the mitochondria. *BAX* mRNA levels increased momentously with As-IV administration in OVCAR-3 cells versus the DMSO (Figure 2a, $p<0.001$). When the OVCAR-3-CisR cells were versus the OVCAR-3 cells control, there was no momentous change in

BAX mRNA levels. In the OVCAR-3-CisR cells, As-IV administration momentously increased *BAX* mRNA levels versus the DMSO ($p<0.001$). At the same time, a momentous increase was found when this condition was against the OVCAR-3 cells control ($p<0.001$). *BCL2* is an apoptotic gene and its protein form is found in mitochondria and protects the cell from apoptosis. *BCL2* mRNA levels decreased momentously with As-IV administration in OVCAR-3 cells versus with the DMSO (Figure 2b, $p<0.001$). When the OVCAR-3 CisR cells were versus with the OVCAR-3 cells control, there was increased momentous change in *BCL2* mRNA levels ($p<0.05$). In the OVCAR-3-CisR cells, As-IV administration momentously decreased *BCL2* mRNA levels versus the DMSO ($p<0.001$). At the same time, a momentous decrease *BCL2* levels were found versus the OVCAR-3 control ($p<0.001$). The *BAX/BCL2* scale is more effective in assessing the severity of apoptosis. As-IV treatment momentously increased the *BAX/BCL2* scale in both OVCAR-3 and OVCAR-3-CisR cells (Figure 2c, $p<0.001$).

Effect of As-IV on Colony Formation in OVCAR-3 and OVCAR-3-CisR Cells

To assess the metastatic effect in colony formation, cells are assessed for their ability to proliferate alone in their region and for their behavior. Colonies formed as a result of incubation of OVCAR-3 and OVCAR-3 CisR cells with As-IV for 7 days were visualized by crystal violet staining (Figure 3a). It was shown that As-IV treatment momentously reduced colony formation (Figure 3b) in OVCAR-3 cells versus the DMSO ($p<0.01$). Colony formation in the OVCAR-3-CisR cells were found to be faster than in the OVCAR-3 cells and to increase momentously with cisplatin resistance ($p<0.001$). Colony formation was momentously reduced in OVCAR-3-CisR cells when the As-IV treatment was versus the DMSO ($p<0.001$). Compare with the OVCAR-3 cells DMSO, the OVCAR-3 CisR cells As-IV treatment had momentously reduced colony formation ($p<0.05$).
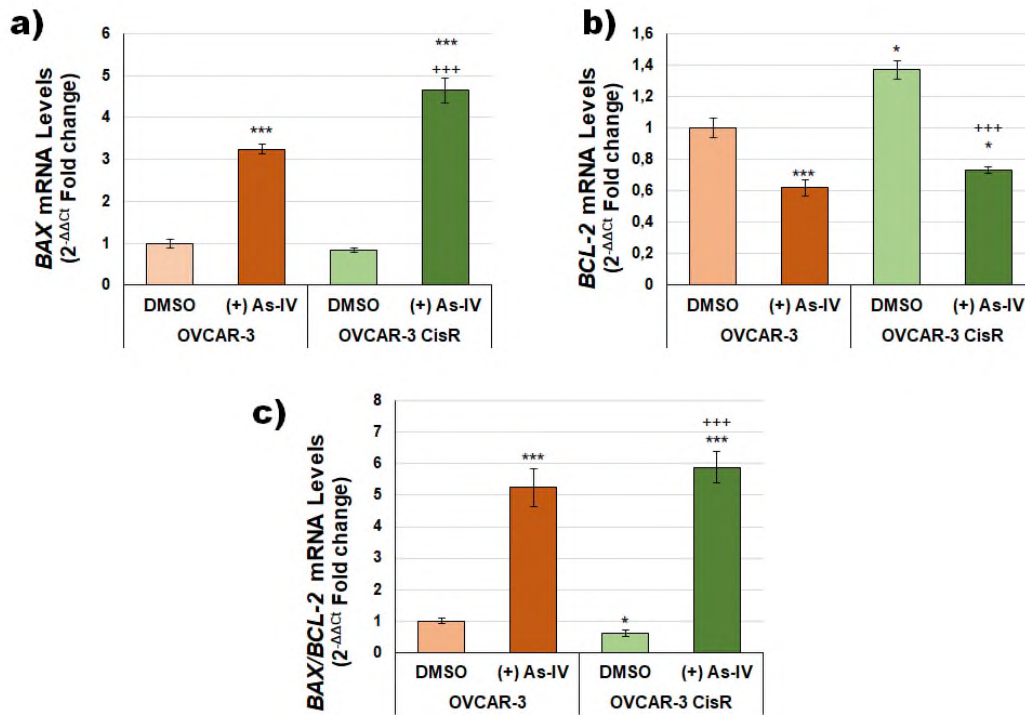
Figure 2. Apoptosis related gene expression levels of -/+As-IV on OVCAR-3 and OVCAR-3 CisR cells. (a) The change in *BAX* mRNA levels, (b) The change in *BCL2* mRNA levels, (c) The change mRNA levels ratio of *BAX/BCL2* (* p<0.05, ***p<0.001 compare to DMSO in OVCAR-3 cells, +++p<0.001 compare to DMSO in OVCAR-3-CisR cells).

Effect of As-IV on SDF-1 and CXCR4 in OVCAR-3 and OVCAR-3-CisR Cells

CXCR4 and SDF-1 are important chemokines for the evaluation of tumor microenvironment and drug resistance mechanisms. CXCR4 protein levels decreased momentously with As-IV administration in OVCAR-3 cells versus the DMSO (Figure 4a, p<0.001). When the OVCAR-3-CisR cells were versus the OVCAR-3 control batch, there was increased momentous change in CXCR4 protein levels (p<0.001). In the OVCAR-3-CisR cells, As-IV administration momentously decreased CXCR4 protein levels versus the DMSO (p<0.001). A momentous decrease in CXCR4 protein levels was found when As-IV administration was versus the OVCAR-3 cells control (p<0.01). SDF-1 protein levels decreased momentously with As-IV administration in OVCAR-3 cells versus the DMSO (Figure 4b, p<0.01). When the OVCAR-3-CisR cells were versus the OVCAR-3 control batch, there was increased momentous change in SDF-1 protein levels (p<0.001). In the OVCAR-3-CisR cells, As-IV administration momentously decreased SDF-1 protein levels versus the DMSO (p<0.001). There were no momentous changes in SDF-1 protein levels in As-IV treated OVCAR-3-CisR cells versus to OVCAR-3 control.

According to the data, *CXCR4* mRNA levels decreased momentously with As-IV administration in OVCAR-3 cells versus the DMSO (Figure 4c, p<0.001). When the OVCAR-3-CisR cells were versus the OVCAR-3 control, there was a momentous increase in *CXCR4* mRNA levels (p<0.001). In the OVCAR-3-CisR cells, As-IV administration momentously decreased *CXCR4* mRNA levels versus the DMSO (p<0.001). A momentous decrease *CXCR4* mRNA levels was found in As-IV administration OVCAR-3-CisR versus the OVCAR-3 control (p<0.001). *SDF-1* mRNA levels decreased momentously with As-IV administration in OVCAR-3 cells versus the DMSO (Figure 4d, p<0.001). When the OVCAR-3-CisR cells were versus the OVCAR-3 cells control, there was increased momentous change in *SDF-1* mRNA levels (p<0.001). In the OVCAR-3-CisR cells, As-IV administration momentously decreased *SDF-1* mRNA levels versus the DMSO (p<0.01). There were no momentous changes in *SDF-1* mRNA levels in As-IV treated OVCAR-3-CisR cells versus the OVCAR-3 cells control.

DISCUSSION

Ovarian cancer is the fifth deadliest cancer in the world and the most commonly diagnosed gynecological malignancy. Epidemiologic data show that over 22,000 new cases of ovarian cancer were diagnosed in 2018, with approximately 14,000 deaths occurring as a result of increased life expectancy worldwide, particularly among older women aged >65 years. Because of the inconspicuous location of the ovaries in the female reproductive tract, ovarian cancer is often referred to as a "silent
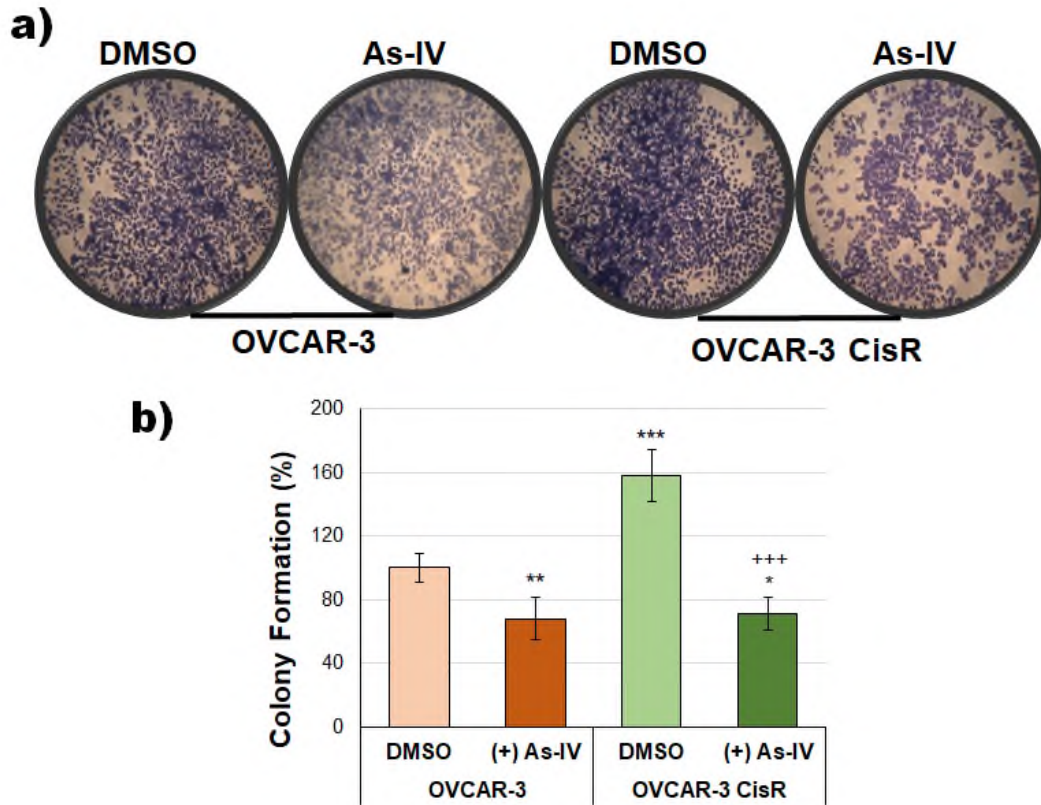
Figure 3. Colony formation of -/+As-IV on OVCAR-3 and OVCAR-3-CisR cells (a) Microscope images (4X) and (b) Colony formation graphics of percentage of cells (* p<0.05, ** p<0.01, ***p<0.001 compare to DMSO in OVCAR-3 cells, +++p<0.001 compare to DMSO in OVCAR-3-CisR cells).

killer," and nearly 70% of cases are prognosed with the progressive disease. Despite advances in detection and treatment, women with progressive ovarian cancer regularly have a five-year survival rate of only 30%.[16] Due to the increasing popularity of Chinese medicine, it has been widely used as an effective adjunct to standard cancer treatment. In Chinese medicine, the use of herbs included in the Chinese pharmacopoeia is important for their safety and includes herbs containing As-IV. As-IV is an important biomarker used for saponin screening in plants, and its importance in Chinese medicine is increasing day by day due to its antioxidant properties.[17] It can help reduce the side effects of chemotherapy and radiotherapy.[18,19] The main effects of the drug As-IV are its ability to induce cell cycle arrest and apoptosis[20,21] There are studies showing that As-IV has antioxidant effects.[22,23] As-IV acts as an antioxidant by increasing glutathione, superoxide dismutase, and catalase to reduce malondialdehyde release and increasing Nrf2 to increase NQO1 and HO-1 expression.[24] It has been proven that it reduces oxidative stress due to free oxygen radicals and has neuroprotective [25] and cardioprotective effects.[26] There are datas that the flavonoid components in its content can be used as an effective anticancer agent, by activating apoptotic mechanisms in the treatment of many cancers by showing anti-tumoral effect

and leading to programmed death of cells.[10] As-IV also helps prevent cancer cells from growing and spreading.[27,28] In addition, the drug can improve the sensitivity of cancer cells to various chemotherapy drugs. It can also prevent tumor growth in models of cancer. [29] These effects were restricted to tumor cells and did not result in cytotoxicity in normal cells. Some of the other common cancers that can be affected by this drug include liver, lung, colorectal, ovarian, and breast cancer.[16,30−33] It also affects glioma[34], gastric cancer,[35] cervical cancer,[27] prostate cancer,[36] abdominal aortic aneurysm,[37] osteosarcoma,[38] and vulvar cancer.[39] As a result, As-IV is a promising anticancer agent with beneficial pharmacological effects. The diversity of pharmacological effects of As-IV is due to its structure. As-IV has high polarity due to its saponin derivative structure. Since As-IV is a tetracyclic triterpenoid saponin in the form of a lanolin alcohol, it has a high binding capacity to plasma proteins, but it has a low bioavailability due to its low lipophilicity.[40,41] The potential of an antioxidant molecule such as As-IV, which can bind to plasma proteins, to act on cancer cells is very important for studies. Antioxidants that are able to bind to plasma proteins will interact with cancer cells and cause them to undergo apoptosis while leaving healthy cells unharmed.

Apoptosis, also known as programmed cell death, is advan-
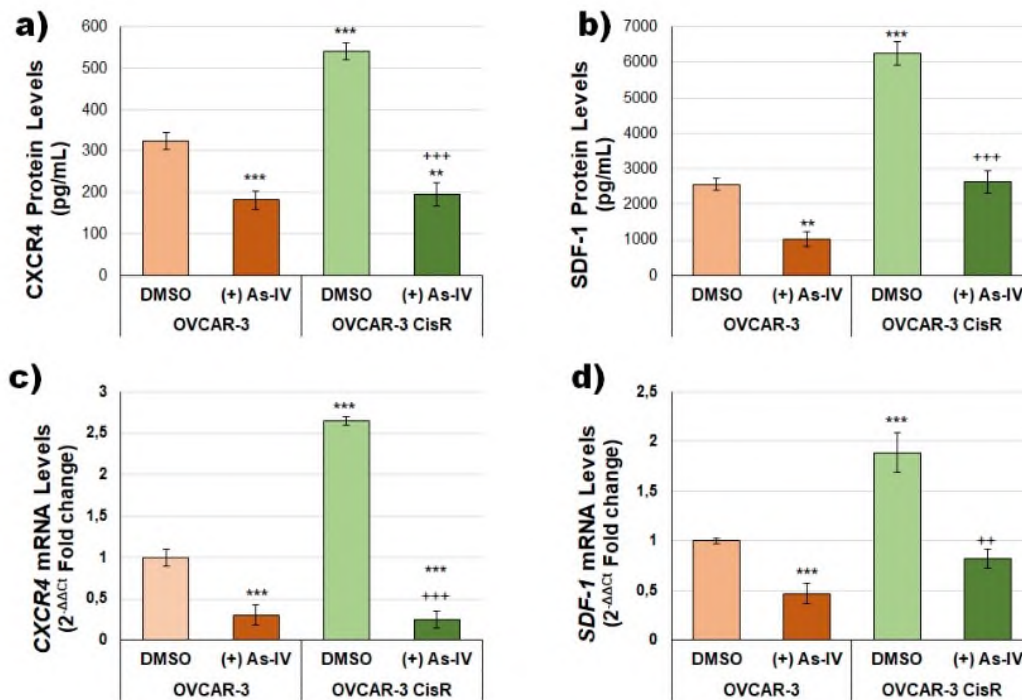
Figure 4. Demonstration of the effect of As-IV administration to OVCAR-3 and OVCAR-3 CisR cells on protein and gene expressions of CXCR4 and SDF-1 chemokines. (a) CXCR4 protein levels, (b) SDF-1 protein levels, (c) *CXCR4* mRNA levels, (d) *SDF1* mRNA levels. (** p<0.01, ***p<0.001 compare to DMSO in OVCAR-3 cells, ++p<0.001, +++p<0.001 compare to DMSO in OVCAR-3-CisR cells).

tageous for healthy cell division, organ development, and tissue homeostasis.[42] Apoptosis is a healthy physiological process that is crucial to the growth and homeostasis of living things. Most cancers have apoptosis defects.[43] The BCL-2 family has been found to play a vital role in stimulating or restraining the intrinsic apoptotic pathway caused by mitochondrial dysfunction. [44,45] As a result, the equity of pro- and anti-apoptotic members of this family can effect cellular fate. The main members of the BCL-2 family are BAX and BCL-2, whose potential roles in tumor advancement and diagnosis of various human malignancies have piqued the interest of several studies over the last decade. BAX causes the mitochondrial outer membrane to become permeable in reply to various cellular stresses, which encourages cell death. BCL-2, however, prevents apoptosis by inhibiting BAX activity.[46,47] Numerous studies have demonstrated that As-IV can affect the levels of *BCL2*, *BAX* expression, and the scale of *BAX/BCL2* in various cancer types, including lung, nonsmall-cell lung, liver, colorectal, breast, and vulvar cancers. It is shown in a study that by suppressing *BCL2* and *BCL-XL* levels and upregulating *BAX* and cleaved caspase 3 expression, As-IV treatment increased the mortality of vulvar squamous cancer cells.[39] In our study, we have showed that giving AS-IV to cisplatin-resistant ovarian cancer cells increases the *BAX/BCL2* scale by upregulating *BAX* expression while downregulating *BCL2* expression.

CXCR4 is usually overexpressed in cancerous cells of the breast, brain, lung, pancreas, colorectal, prostate, and ovarian, as well as melanoma and leukemia.[48−51] CXCR4 promotes epithelial cell migration by activating matrix metalloproteinases,[52] and elevates cancer cell motility by activating the NF-B and ERK-dependent pathways.[53] SDF-1 (also called CXCL-12), a chemokine, has been found in typical regions of tumor metastasis such as lungs and lymph nodes.[54] Tumor cells form metastatic tumors as a result of their interaction with SDF-1 and CXCR4.[55] Furthermore, SDF1 hypermethylation has been reported in a variety of cancers, including gastric, breast, colon, lung, and prostate cancer,[56] suggesting that SDF-1 may play a key role in carcinogenesis.[57] The SDF-1/CXCR4 axis promotes cancer progression and metastasis,[58,59] regulates angiogenesis,[60,61] induces epithelial-mesenchymal transition.[62,63] As-IV treatment may inhibit cancer cell migration, metastasis, and induce apoptosis by blocking the SDF-1/CXCR4 axis. The cisplatin resistance in ovarian cancer cells treated with As-IV showed a statistically momentous decrease trend in SDF-1 and CXCR4 protein and gene expression levels, and as a result, the chemoresistance developed against drug resistance was suppressed.

CONCLUSION

Ovarian cancer is one of the leading cancer types in the world in terms of mortality in women, and because it can progress

insidiously, its treatment is delayed. Chemotherapy based on cisplatin administration is one of the most effective treatment methods currently available. However, in most cases, resistance to cisplatin is observed, and the survival rate decreases due to poor response to treatment. As-IV is a natural triterpene glycoside that is very important in Chinese medicine due to its anti-tumoral and antioxidant effects. In our study, we looked at its anti-metastatic and apoptotic effects in ovarian cancer cells that had developed resistance to cisplatin. As a result, it has been demonstrated that As-IV administration can prevent metastasis to distant tissues caused by an epithelial-mesenchymal transition in drug-resistant ovarian cancer cells by inhibiting the SDF-1/CXCR4 axis, and can also induce apoptosis due to an increase in the *BAX/BCL2* scale. We believe As-IV has the potential to be used as an anticancer therapeutic agent in the treatment of patients with resistant ovarian cancer.

Ethics Committee Approval: Ethics committee approval is not required for the study.

Peer Review: Externally peer-reviewed.

Author Contributions: Concept: B.I.A, O.C; Design: B.I.A, O.C; Supervision: B.I.A, O.C; Materials: O.C; Data Collection and/or Processing: B.I.A, O.E, O.C; Analysis and/or Interpretation: B.I.A, O.E Literature Search: B.I.A, O.C; Writing: B.I.A, O.C; Critical Reviews: B.I.A, O.E, O.C.

Conflict of Interest: The authors declare that they have no conflicts of interest to disclose.

Financial Disclosure: There are no funders to report for this submission.

ORCID IDs of the authors

Burcin Irem Abas   0000-0002-1018-5577
Omer Erdogan   0000-0002-8327-7077
Ozge Cevik   0000-0002-9325-3757

REFERENCES

1. Sung H, Ferlay J, Siegel RL, et al. Global cancer statistics 2020: GLOBOCAN estimates of incidence and mortality worldwide for 36 cancers in 185 countries. *CA Cancer J Clin*. 2021;71(3):209-249.

2. Siegel RL, Miller KD, Jemal A. Cancer statistics, 2019. *CA Cancer J Clin*. 2019;69(1):7-34.

3. Gorshkov K, Sima N, Sun W, et al. Quantitative chemotherapeutic profiling of gynecologic cancer cell lines using approved drugs and bioactive compounds. *Transl Oncol*. 2019;12(3):441-452.

4. Song M, Cui M, Liu K. Therapeutic strategies to overcome cisplatin resistance in ovarian cancer. *Eur J Med Chem*. 2022;232:114205. doi:https://doi.org/10.1016/j.ejmech.2022.114205

5. Chen SH, Chang JY. New ınsights into mechanisms of cisplatin resistance: From tumor cell to microenvironment. *Int J Mol Sci*. 2019;20(17):4136. doi:10.3390/ijms20174136

6. McQuade RM, Stojanovska V, Bornstein JC, Nurgali K. PARP inhibition in platinum-based chemotherapy: Chemopotentiation and neuroprotection. *Pharmacol Res*. 2018;137:104-113.

7. Amable L. Cisplatin resistance and opportunities for precision medicine. *Pharmacol Res*. 2016;106:27-36.

8. Liu P, Zhao H, Luo Y. Anti-aging implications of *Astragalus membranaceus* (Huangqi): A well-known Chinese tonic. *Aging Dis*. 2017;8(6):868-886.

9. Song H, Qiu J, Yu C, et al. Traditional Chinese Medicine prescription Huang-Qi-Jian-Zhong-Tang ameliorates indomethacin-induced duodenal ulcers in rats by affecting NF-κ B and STAT signaling pathways. *Biomed Pharmacother*. 2022;156:113866. doi:https://doi.org/10.1016/j.biopha.2022.113866

10. Zhang J, Wu C, Gao L, Du G, Qin X. Astragaloside IV derived from *Astragalus membranaceus:* A research review on the pharmacological effects. *Adv Pharmacol*. 2020;87:89-112.

11. Qu YZ, Li M, Zhao YL, et al. Astragaloside IV attenuates cerebral ischemia–reperfusion-induced increase in permeability of the blood-brain barrier in rats. *Eur J Pharmacol*. 2009;606(1):137-141.

12. Zhang WD, Chen H, Zhang C, Liu RH, Li HL, Chen HZ. Astragaloside IV from *Astragalus membranaceus* shows cardioprotection during myocardial ischemia *in vivo* and *in vitro*. *Planta Med*. 2006;72(1):4-8.

13. Lai ST, Wang Y, Peng F. Astragaloside IV sensitizes non-small cell lung cancer cells to cisplatin by suppressing endoplasmic reticulum stress and autophagy. *J Thorac Dis*. 2020;12(7):3715-3724.

14. Min L, Wang H, Qi H. Astragaloside IV inhibits the progression of liver cancer by modulating macrophage polarization through the TLR4/NF-κB/STAT3 signaling pathway. *Am J Transl Res*. 2022;14(3):1551–1566.

15. Abas BI, Demirbolat GM, Cevik O. Wharton jelly-derived mesenchymal stem cell exosomes induce apoptosis and suppress EMT signaling in cervical cancer cells as an effective drug carrier system of paclitaxel. *PLoS One*. 2022;17(9):e0274607. https://doi.org/10.1371/journal.pone.0274607.

16. Wang X, Gao S, Song L, Liu M, Sun Z, Liu J. Astragaloside IV antagonizes M2 phenotype macrophage polarization-evoked ovarian cancer cell malignant progression by suppressing the HMGB1–TLR4 axis. *Mol Immunol*. 2021;130:113-121.

17. Qi L-W, Yu Q-T, Yi L, et al. Simultaneous determination of 15 marker constituents in various Radix Astragali preparations by solid-phase extraction and high-performance liquid chromatography. *J Sep Sci*. 2008;31(1):97-106.

18. Qi F, Zhao L, Zhou A, et al. The advantages of using traditional Chinese medicine as an adjunctive therapy in the whole course of cancer treatment instead of only terminal stage of cancer. *Biosci Trends*. 2015;9(1):16-34.

19. Tao F, Zhang Y, Zhang Z. The role of herbal bioactive components in mitochondria function and cancer therapy. *Evid Based Complement Altern Med*. 2019;2019:3868354. doi:10.1155/2019/3868354

20. Jiang Z, Mao Z. Astragaloside IV (AS-IV) alleviates the malignant biological behavior of hepatocellular carcinoma via Wnt/β-catenin signaling pathway. *RSC Adv*. 2019;9(61):35473-35482.

21. Liu F, Ran F, He H, Chen L. Astragaloside IV exerts anti-tumor effect on murine colorectal cancer by re-educating tumor-associated macrophage. *Arch Immunol Ther Exp (Warsz)*. 2020;68(6):33. doi:10.1007/s00005-020-00598-y

22. Gui D, Guo Y, Wang F, et al. Astragaloside IV, a novel antioxidant, prevents glucose-ınduced podocyte apoptosis *in vitro* and *in vivo*. *PLoS One*. 2012;7(6):e39824. https://doi.org/10.1371/journal.pone.0039824.

23. Ji C, Luo Y, Zou C, Huang L, Tian R, Lu Z. Effect of astragaloside IV on indoxyl sulfate-induced kidney injury in mice via attenuation of oxidative stress. *BMC Pharmacol Toxicol*. 2018;19(1):53. doi:10.1186/s40360-018-0241-2

24. Wang H, Zhuang Z, Huang YY, et al. Protective effect and possible mechanisms of astragaloside IV in animal models of diabetic nephropathy: A preclinical systematic review and meta-analysis. *Front Pharmacol*. 2020;11:988. doi:10.3389/fphar.2020.00988

25. Yao M, Zhang L, Wang L. Astragaloside IV: A promising natural neuroprotective agent for neurological disorders. *Biomed Pharmacother*. 2023;159:114229. doi:https://doi.org/10.1016/j.biopha.2023.114229

26. Tan YQ, Chen HW, Li J. Astragaloside IV: An effective drug for the treatment of cardiovascular diseases. *Drug Des Devel Ther*. 2020;14:3731-3746.

27. Xia C, He Z, Cai Y. Quantitative proteomics analysis of differentially expressed proteins induced by astragaloside IV in cervical cancer cell invasion. *Cell Mol Biol Lett*. 2020;25(1):25. doi:10.1186/s11658-020-00218-9

28. Zhang L, Zhou J, Qin X, Huang H, Nie C. Astragaloside IV inhibits the invasion and metastasis of SiHa cervical cancer cells via the TGF-β1-mediated PI3K and MAPK pathways. *Oncol Rep*. 2019;41(5):2975-2986.

29. He C-S, Liu Y-C, Xu Z-P, Dai P-C, Chen X-W, Jin D-H. Astragaloside IV enhances cisplatin chemosensitivity in non-small cell lung cancer cells through inhibition of B7-H3. *Cell Physiol Biochem*. 2016;40(5):1221-1229.

30. Li L, Li G, Chen M, Cai R. Astragaloside IV enhances the sensibility of lung adenocarcinoma cells to bevacizumab by inhibiting autophagy. *Drug Dev Res*. 2022;83(2):461-469.

31. Qu X, Gao H, Zhai J, et al. Astragaloside IV enhances cisplatin chemosensitivity in hepatocellular carcinoma by suppressing MRP2. *Eur J Pharm Sci*. 2020;148:105325. doi:https://doi.org/10.1016/j.ejps.2020.105325

32. Wang S, Mou J, Cui L, Wang X, Zhang Z. Astragaloside IV inhibits cell proliferation of colorectal cancer cell lines through down-regulation of B7-H3. *Biomed Pharmacother*. 2018;102:1037-1044.

33. Hu S, Zheng W, Jin L. Astragaloside IV inhibits cell proliferation and metastasis of breast cancer via promoting the long noncoding RNA TRHDE-AS1. *J Nat Med*. 2021;75(1):156-166.

34. Han J, Shen X, Zhang Y, Wang S, Zhou L. Astragaloside IV suppresses transforming growth factor-β1-induced epithelial–mesenchymal transition through inhibition of Wnt/β-catenin pathway in glioma U251 cells. *Biosci Biotechnol Biochem*. 2020;84(7):1345-1352.

35. Liu W, Chen H, Wang D. Protective role of astragaloside IV in gastric cancer through regulation of microRNA-195-5p-mediated PD-L1. *Immunopharmacol Immunotoxicol*. 2021;43(4):443-451.

36. He Y, Zhang Q, Chen H, et al. Astragaloside IV enhanced carboplatin sensitivity in prostate cancer by suppressing AKT/NF-κB signaling pathway. *Biochem Cell Biol*. 2020;99(2):214-222.

37. Wang J, Zhou Y, Wu S, et al. Astragaloside IV attenuated 3,4-benzopyrene-ınduced abdominal aortic aneurysm by ameliorating macrophage-mediated inflammation. *Front Pharmacol*. 2018;9:496. doi:10.3389/fphar.2018.00496

38. Hu T, Fei Z, Wei N. Chemosensitive effects of Astragaloside IV in osteosarcoma cells via induction of apoptosis and regulation of caspase-dependent Fas/FasL signaling. *Pharmacol Reports*. 2017;69(6):1159-1164.

39. Zhao Y, Wang L, Wang Y, et al. Astragaloside IV inhibits cell proliferation in vulvar squamous cell carcinoma through the TGF-β/Smad signaling pathway. *Dermatol Ther*. 2019;32(4):e12802. doi:https://doi.org/10.1111/dth.12802

40. Zhang Q, Zhu L-L, Chen G-G, Du Y. Pharmacokinetics of astragaloside IV in beagle dogs. *Eur J Drug Metab Pharmacokinet*. 2007;32(2):75-79.

41. Huang CR, Wang GJ, Wu XL, et al. Absorption enhancement study of astragaloside IV based on its transport mechanism in Caco-2 cells. *Eur J Drug Metab Pharmacokinet*. 2006;31(1):5-10.

42. Rogers C, Alnemri E. Gasdermins in apoptosis: New players in an old game. *Yale J Biol Med*. 2019;92:603-617.

43. Tang C, Zhao C-C, Yi H, et al. Traditional Tibetan Medicine in cancer therapy by targeting apoptosis pathways. *Front Pharmacol*. 2020;11:976. doi:10.3389/fphar.2020.00976

44. Yip KW, Reed JC. Bcl-2 family proteins and cancer. *Oncogene*. 2008;27(50):6398-6406.

45. Mohan S, Abdelwahab SI, Kamalidehghan B, et al. Involvement of NF-κ B and Bcl2/Bax signaling pathways in the apoptosis of MCF7 cells induced by a xanthone compound pyranocycloartobiloxanthone A. *Phytomedicine*. 2012;19(11):1007-1015.

46. Khodapasand E, Jafarzadeh N, Farrokhi F, Kamalidehghan B, Houshmand M. Is Bax/Bcl-2 ratio considered as a prognostic marker with age and tumor location in colorectal cancer? *Iran Biomed J*. 2015;19:69-75.

47. Hector S, Prehn JHM. Apoptosis signaling proteins as prognostic biomarkers in colorectal cancer: A review. *Biochim Biophys Acta (BBA)-Reviews Cancer*. 2009;1795(2):117-129.

48. Gangadhar T, Nandi S, Salgia R. The role of chemokine receptor CXCR4 in lung cancer. *Cancer Biol Ther*. 2010;9(6):409-416.

49. Xu C, Zhao H, Chen H, Yao Q. CXCR4 in breast cancer: Oncogenic role and therapeutic targeting. *Drug Des Devel Ther*. 2015;9:4953-4964.

50. Zhao H, Guo L, Zhao H, Zhao J, Weng H, Zhao B. CXCR4 overexpression and survival in cancer: A system review and meta-analysis. *Oncotarget*. 2015;6(7):5022-5040.

51. Balkwill F. The significance of cancer cell expression of the chemokine receptor CXCR4. *Semin Cancer Biol*. 2004;14(3):171-179.

52. Ghosh MC, Makena PS, Gorantla V, Sinclair SE, Waters CM. CXCR4 regulates migration of lung alveolar epithelial cells through activation of Rac1 and matrix metalloproteinase-2. *Am J Physiol Cell Mol Physiol*. 2012;302(9):L846-L856.

53. Huang Y-C, Hsiao Y-C, Chen Y-J, Wei Y-Y, Lai T-H, Tang C-H. Stromal cell-derived factor-1 enhances motility and integrin up-regulation through CXCR4, ERK and NF-κB-dependent pathway in human lung cancer cells. *Biochem Pharmacol*. 2007;74(12):1702-1712.

54. Phillips RJ, Burdick MD, Lutz M, Belperio JA, Keane MP, Strieter RM. The stromal derived factor–1/CXCL12–CXC chemokine receptor 4 biological axis in non–small cell lung cancer metastases. *Am J Respir Crit Care Med*. 2003;167(12):1676-1686.

55. Müller A, Homey B, Soto H, et al. Involvement of chemokine receptors in breast cancer metastasis. *Nature*. 2001;410(6824):50-56.

56. Abas BI, Büyükkarıncali N, Cevik O. IRF5 inhibits

prostate cancer metastasis and drug resistance by decreasing CXCR4/CXCL12 complex. *Cukurova Med J.* 2021;46(4):1632-1639.

57. Zhou W, Guo S, Liu M, Burow M, Wang G. Targeting CXCL12/CXCR4 Axis in tumor immunotherapy. *Curr Med Chem.* 2017;24. doi:10.2174/0929867324666170830111531

58. Su L, Zhang J, Xu H, et al. Differential expression of CXCR4 is associated with the metastatic potential of human non–small cell lung cancer cells. *Clin cancer Res.* 2005;11(23):8273-8280.

59. Wagner PL, Hyjek E, Vazquez MF, et al. CXCL12 and CXCR4 in adenocarcinoma of the lung: association with metastasis and survival. *J Thorac Cardiovasc Surg.* 2009;137(3):615-621.

60. Wang M, Chen GY, Song HT, Hong X, Yang ZY, Sui GJ. Significance of CXCR4, phosphorylated STAT3 and VEGF-A expression in resected non-small cell lung cancer. *Exp Ther Med.* 2011;2(3):517-522.

61. Cai X, Chen Z, Pan X, et al. Inhibition of angiogenesis, fibrosis and thrombosis by tetramethylpyrazine: mechanisms contributing to the SDF-1/CXCR4 axis. *PLoS One*. 2014;9(2):e88176. doi:10.1371/journal.pone.0088176

62. Onoue T, Uchida D, Begum NM, Tomizuka Y, Yoshida H, Sato M. Epithelial-mesenchymal transition induced by the stromal cell-derived factor-1/CXCR4 system in oral squamous cell carcinoma cells. *Int J Oncol*. 2006;29(5):1133-1138.

63. Bertolini G, D'Amico L, Moro M, et al. Microenvironment-modulated metastatic CD133+/CXCR4+/EpCAM lung cancer–initiating cells sustain tumor dissemination and correlate with poor prognosis. *Cancer Res.* 2015;75(17):3636-3649.

How cite this article

Susceptibility of *Staphylococcus aureus* Isolated from Different Raw Meat Products to Disinfectants

Fatma Ozdemir[1] , Seza Arslan[1]

[1]Bolu Abant Izzet Baysal University, Faculty of Arts and Sciences, Department of Biology, Bolu, Türkiye

ABSTRACT

Objective: *Staphylococcus aureus*, a severe public health hazard, causes foodborne diseases from the consumption of contaminated food. Various antimicrobials and disinfectants are used throughout the food chain to reduce microbial contamination or eliminate microorganisms on food contact surfaces. However, little is known about the susceptibility of disinfectants to food pathogens, including *S. aureus*, which can develop resistance to antimicrobials and cause severe diseases.

Materials and Methods: The antimicrobial activity of triclosan, cetyltrimethylammonium bromide (CTAB), acetic acid, citric acid, and lactic acid against 50 *S. aureus* isolates, including multidrug-resistant (MDR) isolates originating from ground beef, chicken, and fish, was investigated using the broth microdilution method.

Results: The minimal inhibitory concentrations (MICs) of triclosan, CTAB, acetic acid, citric acid, and lactic acid against the isolates were 0.125-16 µg/mL, 0.25-32 µg/mL, 102.5-26250 µg/mL, 187.5-12000 µg/mL, and 703-22500 µg/mL, respectively. Almost all MDR isolates showed resistance to triclosan. There was a statistically significant difference in MICs between triclosan and organic acids, as well as between CTAB and organic acids ($p < 0.05$). However, a statistically significant difference was not observed in triclosan and CTAB, as well as in acetic acid and lactic acid ($p > 0.05$). Pearson correlation coefficient revealed a strong relationship between triclosan and multidrug resistance. Based on the multiple linear regression analysis, triclosan had a positive effect on multidrug resistance ($p < 0.05$).

Conclusion: This research gives helpful information on the susceptibility of disinfectants to *S. aureus*, particularly to resistant *S. aureus* isolates from meats, which may help to recommend proper disinfectant use in food production.

Keywords: *Staphylococcus aureus*, Triclosan, Cetyltrimethylammonium bromide, Organic acids, Minimum inhibitory concentration.

INTRODUCTION

Staphylococcus aureus is a significant pathogen that causes a wide range of illnesses including skin and soft tissue infections, foodborne poisoning, pneumonia, bacteremia, endocarditis, osteomyelitis, meningitis, enterocolitis, urinary tract infections, toxic shock syndrome.[1,2] Consumption of contaminated food, such as meat and meat products, with this pathogen is the major source of *S. aureus* foodborne illnesses and poses a serious threat to human health. The presence of foodborne pathogens including *S. aureus* in processed foods or on food processing equipment because of contact by humans or cross-contamination could indicate poor handling or sanitation.[2,3] It is important to avoid cross-contamination of food and possible foodborne disease. It is recommended to clean surfaces; either the organisms must be removed, or they must be inactivated in

situ using a disinfection method. Disinfectants and sanitizers are considered more efficient since they make more effective contact with surface-attached microorganisms.[4]

Disinfectants, sanitizing agents, and cleaning chemical agents are widely utilized in the food industry to inhibit the growth or kill microorganisms involved in food spoilage and foodborne diseases on food contact surfaces and reduce them to safe levels in food manufacturing facilities.[3,5] Sanitizers and disinfectants such as triclosan, quaternary ammonium compounds, chlorohexidine, benzalkonium chloride, chlorine and chlorine-based derivatives, hydrogen peroxide, acid anionic agents, peracetic acid, and weak organic acids play essential roles in the food and health care industries.[3,5-7] These sanitizing agents are extensively used in the food industry for disinfecting and cleaning floors, walls, drains, and fields associated

with livestock and crop production, including farm buildings, equipment, and vehicles, as well as on animals, such as in footbaths or udder cleansing.[5,6] The antimicrobial effectiveness of these chemicals and the amount of residue left on surfaces after application can vary. Several factors that influence antimicrobial efficiency include exposure time, temperature, chemical formulation, concentration, pH, microbiological load and type, microbial adhesion to the surface, and application.[3,5]

Triclosan, 2,4,4'-trichloro-2'-hydroxydiphenyl ether, is a synthetic bisphenol antibacterial agent present in various hygiene products, including soaps and mouthwashes. It has activity against both Gram-positive and Gram-negative bacteria.[8] Triclosan is commonly used in community environments for personal hygiene purposes and to avoid cross-contamination with bacteria in domestic environments and during food processing, as well as in industrial environments.[9,10] It is used as a material preservative in kitchen equipment, including cutting boards, plastic utensils, storage containers, and counters which contact with foodstuffs.[11] The triclosan residue detection in various foodstuffs has previously been reported in China and Spain.[12,13] Furthermore, triclosan has been successfully used in hospital environments to control methicillin-resistant *Staphylococcus aureus* (MRSA) infections and reduce nosocomial outbreaks of antimicrobial-resistant bacteria.[8-10,14] As in clinical settings, disinfectants and preservatives could give selective pressure for the development and isolation of antimicrobial-resistant bacteria.[5,15] Several studies have been published showing the emergence of triclosan resistance in *S.aureus*.[8,15,16] In addition, triclosan resistance has been studied in *Escherichia coli*[17], *Pseudomonas aeruginosa*[18], vancomycin-resistant *Enterococcus faecium*[19], and *Salmonella* strains.[20]

Quaternary ammonium compounds (QACs) are a broad class of chemicals that include central nitrogen, which is bound to four (quaternary) organic groups. The interaction of positively charged quaternary nitrogen with the polar head groups of phospholipids mediates QAC antibacterial activity. This activity restricts the uptake of nutrients into the microbial cell and waste discharge.[9,21] QACs are widely used as disinfectants for the control of bacterial growth in clinical and food production environments because they have antimicrobial effects on a wide variety of microorganisms but have no effect on the spore phase.[3,21] Gram-positive bacteria are more sensitive to QACs at lower concentrations than Gram-negative bacteria.[3,21,22] Cetyltrimethylammonium bromide (CTAB) is a quaternary ammonium compound and cationic detergent that acts as an antibacterial agent by inducing superoxide stress in bacteria.[23,24]

Organic acids are natural compounds present in a variety of fruits and fermented products that have antimicrobial activity against microorganisms.[3,6,25] They can inhibit microorganism growth by decreasing the pH, altering the proton gradient across

the membrane, acidifying the cytoplasm, and impeding chemical transport across the cell membrane.[3,7] Organic acids are considered "generally recognized as safe" additives in many foods for people by the U.S. Food and Drug Administration.[3] The major organic acids are acetic, citric, and lactic acids, which can be used in the sanitization process due to their efficacy and cost.[6,7,25-27] Previous studies have demonstrated differences in the antibacterial activity of organic acids such as acetic, lactic, and citric acids against foodborne pathogens.[25-29]

Several chemical sanitizers and disinfectants, including triclosan[8,15,30], CTAB[18,20], and organic acids like acetic, citric, and lactic acid[7,25-27], have been investigated for their efficacy against pathogens in previous studies. These compounds have commonly been used as disinfectants, sanitizers, antiseptics, and surface decontaminants in food and meat processing industries, animal farms, poultry, household cleaning products, hospitals, and other health care settings, and as preservatives in food industries, cosmetics, pharmaceuticals, textiles, and laundry detergents.[10,21,25] Many studies have demonstrated the effects of sanitizers and disinfectants on the growth inhibition of pathogens in food.[7,28,31,32] However, few studies have been conducted to evaluate the effectiveness of disinfectants on multidrug-resistant pathogens from food, which constitute a potential threat to human health.[25,27] Therefore, this study aimed to investigate the susceptibility of *S. aureus* isolates, including multidrug-resistant isolates from meat products to some of the most widely used disinfectants, such as triclosan, CTAB, acetic acid, lactic acid, and citric acid.

MATERIALS AND METHODS

Bacterial Isolates

Fifty *S. aureus* isolates from meat were used in this study. They comprised 20 fish samples: 11 from seawater fish *(Sparus aurata)*, 8 from freshwater fish *(Oncorhynchus mykiss)*, 1 from seawater fish *(Dicentrarchus labrax)*, 17 from ground beef (cow's meat), 13 from chicken meat (breast and leg parts) isolates. All meat samples, including fish samples from local fish markets and supermarkets, ground beef samples from butcher shops, and chicken meat samples from supermarkets and butchers, were collected. The isolates had already been identified using biochemical tests and a PCR for the species-specific fragment (Sa442) and thermonuclease gene *(nucA)*.[1,33,34]

Disinfectants

The disinfectants tested were triclosan, CTAB, acetic acid, citric acid, and lactic acid. Triclosan, CTAB, and citric acid were purchased from Sigma-Aldrich (MO, USA). Acetic acid and lactic acid were obtained from Merck (Darmstadt, Ger-

many). Stock solutions of triclosan and CTAB were prepared in dimethyl sulfoxide (DMSO) (Applichem, Darmstadt, Germany). As in the previous studies [24,30], the level of DMSO in the final working solutions was below 5%. Organic acids were prepared in Mueller-Hinton broth (Merck, Germany). Disinfectants were tested at the following concentrations: triclosan (0.125-64 µg/mL), CTAB (0.25-128 µg/mL), acetic acid (51.45-26250 µg/mL), citric acid (93.75-48000 µg/mL), and lactic acid (43.9-22500 µg/mL). All stock solutions were sterilized before use by syringe filtration through 0.22 µm membrane filters (Sartorius AG, Goettingen, Germany).

Determination of Minimum Inhibitory Concentration (MIC) of Disinfectants

The susceptibility of disinfectants was tested using the broth microdilution method, as defined by the Clinical and Laboratory Standards Institute (CLSI).[35,36] Before the experiment, all *S. aureus* isolates used in this study were activated in Tryptic Soy Broth (TSB) (Merck, Darmstadt, Germany), incubated at 37 ºC for 24 h, streaked on Tryptic Soy Agar (TSA) (Merck, Germany) plates, and incubated overnight at 37 ºC. Several colonies from the TSA plates were taken and suspended in Mueller Hinton broth (Merck) to adjust the bacterial turbidity to 0.5 McFarland standard (approximately 10^8 Colony-Forming Units (CFU)/mL). The isolates were diluted to the final concentration of 1×10^6 CFU/mL and added to each well of a 96-microtiter plate (Lp Italiana, U-bottom). The MIC value of *Staphylococcus aureus* ATCC 29213 as a quality control strain according to the CLSI against gentamicin was used in all experiments. The microtiter plates were incubated at 37 ºC for 16-20 h. The optical density was measured at 600 nm using a microplate reader (Thermo Electron Corporation, Vantaa, Finland). MIC experiments were carried out in triplicates. The MIC for each isolate was determined as the lowest concentration that inhibited growth.[35] The MIC was recorded as the lowest concentration of disinfectant at which no visible bacterial growth was considered.[37] The MIC_{50} and MIC_{90} results showed that the MIC values inhibited 50% and 90% of the isolates, respectively. The previously published susceptible/resistant criterion was used to determine triclosan resistance.[38] *S. aureus* was classified as susceptible at MICs of < 0.5 µg/mL, intermediate at MICs of 0.5 to 2 µg/mL, and resistant at MICs of > 2 µg/mL.

Statistical Analysis

The MIC values of the disinfectants against the *S. aureus* isolates were evaluated using one-way analysis of variance (ANOVA) with Tukey's multiple comparison test. Pearson's correlation test was used to evaluate the correlations between disinfectant susceptibility and multidrug resistance. Multiple linear regression was performed using multidrug resistance as the dependent variable and triclosan, CTAB, acetic acid, citric acid, and lactic acid as the independent variables. All analyses were conducted using SigmaPlot 12.3 (Systat Software Inc., USA). The results with a *p*-value of less than 0.05 were regarded as statistically significant.

RESULTS

MICs, MIC_{50}, and MIC_{90} values of disinfectants tested against the *S. aureus* isolates from raw meat products are shown in Table 1. Triclosan MICs ranged between 0.125 and 16 µg/mL. Twenty-eight percent (28%) of the isolates tested positive for triclosan resistance (MIC > 2 µg/mL), while 18% were positive for triclosan intermediate resistance (MIC in the range of 0.5-2 µg/mL). The *S. aureus* isolates (54%) had susceptible triclosan MICs that ranged from 0.125-0.25 µg/mL. The MIC_{50} and MIC_{90} values for triclosan were 0.25 and 4 µg/mL, respectively. Among the tested *S. aureus* isolates, all 13 multidrug-resistant (MDR) isolates exhibited resistance (11 isolates) or intermediate resistance (2 isolates) to triclosan (Figure 1). The Pearson correlation test revealed a significant relationship between triclosan resistance and multidrug resistance in the *S. aureus* isolates (r = 0.752, *p* < 0.05). There was no significant relationship between the other disinfectants tested and multidrug resistance (*p* > 0.05). According to the multiple linear regression analysis, only triclosan had a positive effect on multidrug resistance in a 95% confidence level (R = 0.766).

The MIC levels for the disinfectant CTAB were between 0.25 and 32 µg/mL. MIC values of CTAB for the 18 isolates (36%) were 1 µg/mL, while 12 isolates (24%) were at 2 µg/mL. The MIC_{50} and MIC_{90} of CTAB were 1 and 8 µg/mL, respectively. The MIC values of CTAB against MDR isolates ranged from 0.5 to 32 µg/mL (Figure 1). Moreover, CTAB MIC values for 75% of the MDR isolates from chicken meat ranged from 4 to 8 µg/mL (Figure 1).

Table 2 shows the triclosan and CTAB susceptibilities among the *S. aureus* isolates from different raw meat products. Resistance to triclosan was detected most frequently in chicken meat at a rate of 46.1% and in ground beef at a rate of 35.3%. On the other hand, the highest sensitivity to triclosan was detected in the isolates from freshwater fish, seawater fish, ground beef, and chicken meat, with 87.5%, 66.7%, 47.1%, and 30.8%, respectively. Considering the effect of CTAB on the susceptibilities of the isolates from meat products, one isolate from ground beef and one from seawater fish showed the highest MIC values at 32 µg/mL and 16 µg/mL, respectively. Among all meat isolates, 41.2% of the ground beef isolates demonstrated activity against CTAB with a MIC of 1 µg/mL.

The MICs of organic acids, including acetic acid, citric acid, and lactic acid against *S. aureus* isolates were determined, and the results are presented in Table 1 and Figure 2. Organic acids tested were efficient against the *S. aureus* meat isolates, with

Table 1. Distributions of disinfectant MIC values for *Staphylococcus aureus* isolates from raw meat products.

Disinfectants	Number of the isolates at each MIC (µg/mL) of disinfectant																							MIC_{50}	MIC_{90}
	0.125	0.25	0.5	1	2	4	8	16	32	102.5	187.5	703	750	820	1406	1500	1641	2812.5	3000	3281	5625	6000	>6000		
Triclosan	15	12		4	5	**8**	**5**	**1**																0.25	4
CTAB		2	6	18	12	5	5	1	1															1	8
Acetic acid										1				13			23			8			5	1641	3281
Citric acid											1		9			21			13			4	2	1500	6000
Lactic acid												2			29		13				5		1	1406	5625

The concentrations of disinfectants were tested: triclosan (0.125–64 µg/mL), CTAB, cetyltrimethylammonium bromide (0.25–128 µg/mL), acetic acid 51.45–26250 µg/mL), citric acid (93.75–48000 µg/mL), and lactic acid (43.9–22500 µg/mL). Bold numbers indicate triclosan-resistant isolates. *S. aureus* isolates were classified as susceptible to triclosan at MICs of < 0.5 µg/mL, intermediate at MICs of 0.5 to 2 µg/mL, and resistant at MICs of > 2 µg/mL.[38]
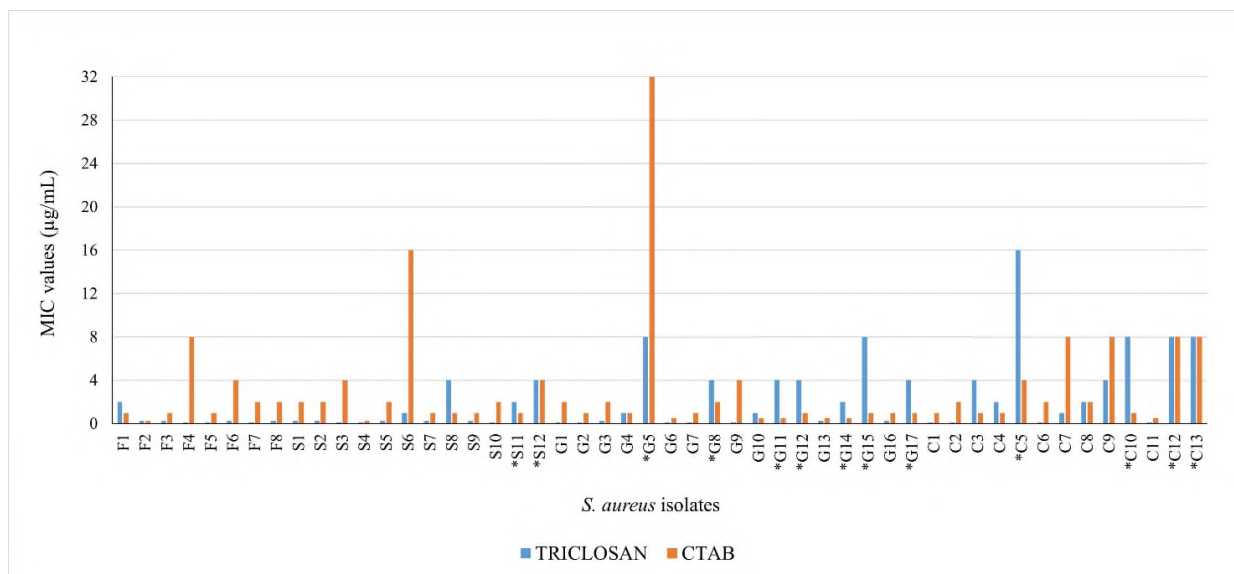
Figure 1. MIC values of triclosan and CTAB (cetyltrimethylammonium bromide) against *Staphylococcus aureus* isolates from meat. Isolate F, freshwater fish; S, seawater fish; G, ground beef; C, chicken meat. The stars (*) indicate the multidrug-resistant isolates.

MICs ranging between 102.5-26250 µg/mL for acetic acid, with MICs ranging between 187.5-12000 µg/mL for citric acid, and with MICs ranging between 703-22500 µg/mL for lactic acid. Acetic acid, citric acid, and lactic acid MICs were 1641 µg/mL for 23 isolates (46%), 1500 µg/mL for 21 isolates (42%), and 1406 µg/mL for 29 isolates (58%), respectively (Table 1). *S. aureus* meat isolates had MIC_{50} values of 1641 µg/mL for acetic acid, 1500 µg/mL for citric acid, and 1406 µg/mL for lactic acid (Table 1). The *S. aureus* meat isolates had MIC_{90} values of 3281 µg/mL for acetic acid, 5625 µg/mL for lactic acid, and 6000 µg/mL for citric acid (Table 1). The MIC > 6000 µg/mL comprised one isolate from ground beef with 22500 µg/mL for lactic acid, one isolate from freshwater fish and one isolate from chicken meat with 12000 µg/mL for citric acid, and one isolate from chicken meat with 6562.5 µg/mL, two isolates from ground beef with 13125 µg/mL, and one isolate from ground beef and one isolate from chicken meat with 26250 µg/mL for acetic acid.

Furthermore, organic acid MICs of *S. aureus* isolated from different meat products are represented in Table 3. In particular, the MIC value of acetic acid for all (100%) freshwater fish isolates was 1641 µg/mL. The acetic acid MIC value of 820 µg/mL was found in more than half of the ground beef isolates (52.9%). In addition, 58.3% of seawater fish isolates had MICs of 1641 µg/mL for acetic acid and 1500 µg/mL for citric acid. More than half of the isolates obtained from ground beef (64.7%), freshwater fish (62.5%), chicken meat (53.8%), and seawater fish (50%) had an MIC of 1406 µg/mL for lactic acid.

The *S. aureus* isolates had lower MICs for the triclosan and CTAB than for the organic acids among the disinfectants tested. Based on the MIC data, there was a statistically significant difference between triclosan, and the organic acids tested ($p < 0.05$). Similarly, the difference between CTAB and the organic acids tested was statistically significant ($p < 0.05$). However, the

Table 2. Triclosan and CTAB susceptibilities of the isolates based on raw meat products.

Origin	MIC (µg/mL)	No. (%) of the isolates	
		Triclosan	CTAB
Freshwater fish (n=8)	0.125	3 (37.5)	-ᵃ
	0.25	4 (50)	1 (12.5)
	1	-	3 (37.5)
	2	1 (12.5)	2 (25)
	4	-	1 (12.5)
	8	-	1 (12.5)
Seawater fish (n=12)	0.125	3 (25)	-
	0.25	5 (41.7)	1 (8.3)
	1	1 (8.3)	4 (33.3)
	2	1 (8.3)	4 (33.3)
	4	2 (16.7)	2 (16.7)
	8	-	-
	16	-	1 (8.3)
Ground beef (n=17)	0.125	5 (29.4)	-
	0.25	3 (17.6)	-
	0.5	-	5 (29.4)
	1	2 (11.8)	7 (41.2)
	2	1 (5.9)	3 (17.6)
	4	4 (23.5)	1 (5.9)
	8	2 (11.8)	-
	32	-	1 (5.9)
Chicken meat (n=13)	0.125	4 (30.8)	-
	0.5	-	1 (7.7)
	1	1 (7.7)	4 (30.8)
	2	2 (15.4)	3 (23.1)
	4	2 (15.4)	1 (7.7)
	8	3 (23.1)	4 (30.8)
	16	1 (7.7)	-

ᵃ Not detected.

MIC, minimum inhibitory concentration; CTAB, cetyltrimethylammonium bromide.
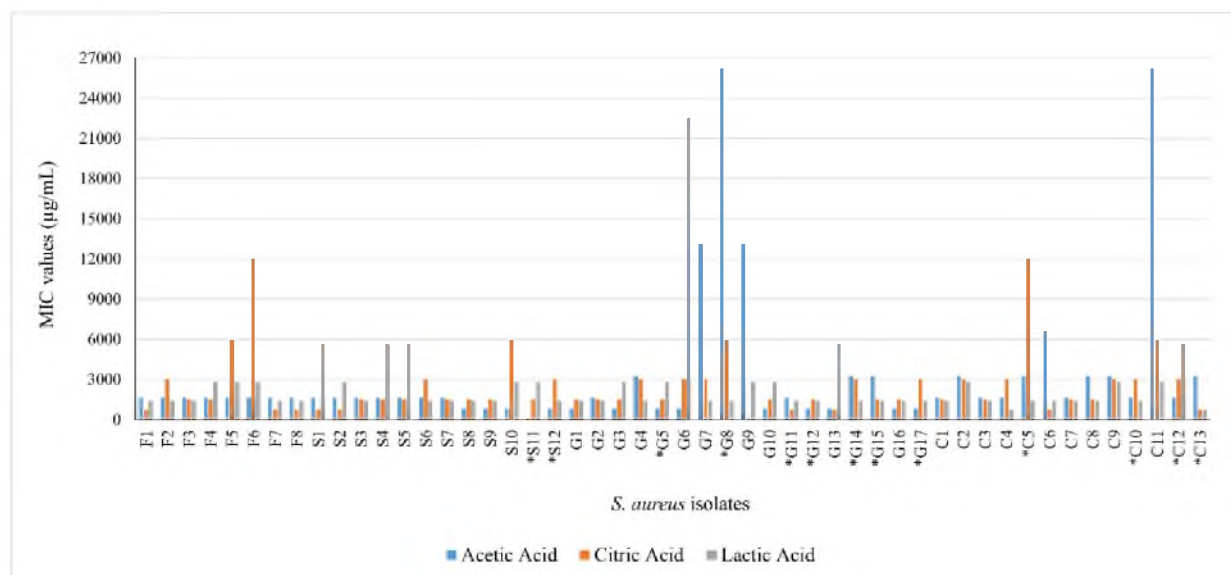
Figure 2. MIC values of three different organic acids against *Staphylococcus aureus* isolates from meat. Isolate F, freshwater fish; S, seawater fish; G, ground beef; C, chicken meat. The stars (*) indicate the multidrug-resistant isolates.

Table 3. Organic acid MICs of *Staphylococcus aureus* isolated from different meat products.

Origin	MIC (µg/mL)	No. (%) of the isolates		
		Acetic acid	Citric acid	Lactic acid
Freshwater fish (n=8)	750	-[a]	3 (37.5)	-
	1406	-	-	5 (62.5)
	1500	-	2 (25)	-
	1641	8 (100)	1 (12.5)	-
	2812.5	-	-	3 (37.5)
	3000	-	-	-
	6000	-	1 (12.5)	-
	> 6000	-	1 (12.5)	-
Seawater fish (n=12)	102.5	1 (8.3)	-	-
	750	-	2 (16.7)	-
	820	4 (33.3)	-	-
	1406	-	-	6 (50)
	1500	-	7 (58.3)	-
	1641	7 (58.3)	-	-
	2812.5	-	-	3 (25)
	3000	-	2 (16.7)	-
	5625	-	-	3 (25)
	6000	-	1 (8.3)	-
Ground Beef (n=17)	187.5	-	1 (5.9)	-
	703	-	-	1 (5.9)
	750	-	2 (11.7)	-
	820	9 (52.9)	-	-
	1406	-	-	11 (64.7)
	1500	-	8 (47.1)	-
	1641	2 (11.8)	-	-
	2812.5	-	-	4 (23.5)
	3000	-	5 (29.4)	-
	3281	3 (17.6)	-	-
	5625	-	-	1 (5.9)
	6000	-	1 (5.9)	-
	> 6000	3 (17.6)	-	-
Chicken meat (n=13)	703	-	-	2 (15.4)
	750	-	2 (15.4)	-
	1406	-	-	7 (53.8)
	1500	-	4 (30.7)	-
	1641	6 (46.1)	-	-
	2812.5	-	-	3 (23.1)
	3000	-	5 (38.5)	-
	3281	5 (38.5)	-	-
	5625	-	-	1 (7.7)
	6000	-	1 (7.7)	-
	> 6000	2 (15.4)	1 (7.7)	-

a Not detected.
MIC, minimum inhibitory concentration.

DISCUSSION

Sanitizers and disinfectants are necessary for ensuring food safety. They are critical for controlling pathogen spread and are beneficial to public health.[5] Several parameters influence disinfectant effectiveness, including concentration, bacterial state, and the presence of interfering components such as organic waste.[3,6,9] The concentration of disinfectant utilized is the most essential component in pathogen control, together with other

difference in MIC values between triclosan and CTAB, as well as acetic acid and lactic acid, was not considered significant (*p* > 0.05).

physical and chemical parameters such as temperature, pH, humidity, and organic load.[3,25]

Triclosan, as a disinfectant and antiseptic, is widely used in personal hygiene and disinfection and has good antimicrobial activity against a broad range of microorganisms, including antimicrobial-resistant bacteria, since it has a specific bacterial cellular target.[8,15] Many investigations have reported resistance to triclosan in *S. aureus* and other bacteria.[16-18,24] In the present study,[23] (46%) *S. aureus* isolates demonstrated intermediate resistance or resistance to triclosan (MIC ≥ 1 µg/mL) (Table 1). All (13) MDR isolates had MICs to triclosan ranging from 2 to 16 µg/mL among the 50 *S. aureus* isolates from raw meat products (Figure 1). All MDR isolates obtained from chicken meat were resistant to triclosan, with MICs of 8 to 16 µg/mL.

Pearson's test showed a strong correlation (r = 0.752) between triclosan and multidrug resistance. In contrast to our study, all *S. aureus* strains from swine mandibular lymph node tissue and commercial pork sausage meat were susceptible to triclosan.[24] All *Pseudomonas aeruginosa* veterinary isolates were resistant to triclosan.[18] Similarly, 99% of *Campylobacter jejuni* strains recovered from broiler chicken house environments were triclosan resistant.[30]

CTAB, a quaternary ammonium compound, is a widely used antimicrobial cationic surfactant.[3,18,24,30] The MICs for CTAB ranged between 0.25 and 32 µg/mL among the *S. aureus* meat isolates. The MIC_{50} and MIC_{90} values for the CTAB were 1 µg/mL and 8 µg/mL, respectively (Table 1). The disinfectant CTAB MICs in this study were higher than the MICs (range from 0.25 to 2 µg/mL) for the *S. aureus* strains isolated from swine feces reported by Beier et al.[24] In contrast to the current study, the researchers observed higher MIC_{50} values for CTAB (4 µg/mL) in *C. jejuni* strains from the litter of broiler chicken houses.[30] However, in this study, the isolates from chicken meat with a rate of 38.5% demonstrated high CTAB MIC values ($\geq$ 4 µg/mL) (Table 2).

Organic acids have strong bactericidal effects and can be applied in the sanitization process of food and food environments.[7,25,27] The susceptibility of three organic acids, including acetic acid, citric acid, and lactic acid, against *S. aureus*, isolates from various types of meat are shown in Table 1 and Figure 2. The MIC_{50} results of acetic, lactic, and citric acids against *S. aureus* isolates were 1641, 1406, and 1500 µg/mL, respectively (Table 1). The MICs for acetic, lactic, and citric acids against *S. aureus* isolates that inhibited 90% of isolates (MIC_{90}) were 3281, 5625, and 6000 µg/mL, respectively (Table 1).

In overall, the antimicrobial effectiveness of acids follows the order acetic > lactic > citric under similar conditions[3], consistent with the results of this study. In a study, acetic, lactic, and citric acids all had high MICs (1024 to 4096 µg/mL) against *E. coli* O157:H7 strains from cattle carcasses, feces, hides, and ground beef.[17] Acetic acids, also known as vinegar (5 to 10%), have antibacterial activity at low concentrations and have been used commonly in food and medicine.[3,29] In the present study, freshwater fish (100%), seawater fish (58.3%), ground beef (52.9%), and chicken meat (46.1%) had the highest percentages of acetic acid with MICs of 1641 µg/mL and 820 µg/mL (Table 3). In et al.[28] reported that acetic acid exhibited relatively high antimicrobial activity (the lowest MIC among organic acids) against all *Shigella* species, which was in parallel to our findings. Furthermore, the results showed that acetic acid had greater germicidal activity against most pathogens than lactic acid.[29] Humayoun et al.[25] found that the MIC_{50} of the tested multidrug-resistant *Salmonella* was 1640 µg/mL, which was like our acetic acid results. However, they found higher MIC_{50} values for lactic acid (5664 µg/mL) and

citric acid (3156 µg/mL). In a study documented by Hussain et al.[31], citric acid was a more efficient agent than lactic acid at the tested concentrations in reducing *E. coli* and *Salmonella* growth. Acetic and citric acids were effective in inhibiting *Salmonella typhimurium*, *E. coli* O157:H7, and *S. aureus* in tabbouleh salad.[32] The organic acid disinfectants, including lactic acid and citric acid, exhibited good bactericidal activity against drug-resistant foodborne pathogens, including *Salmonella* and *Campylobacter*.[27] This study did not indicate a relationship between multi-drug resistance and susceptibility to organic acids in the *S. aureus* isolates from raw meat products. In medicine, Burns et al.[26] reported that all organic acids tested had antibacterial properties against the uropathogens, *Proteus mirabilis, S. aureus, E. coli*, and *P. aeruginosa*.

CONCLUSION

Sanitizers and disinfectants are widely used to prevent contamination by foodborne pathogens. Different disinfectants have varying degrees of antibacterial activity against numerous bacteria. In this study, susceptibility values of *S. aureus* originating from raw meat products to various disinfectants were determined. Triclosan and CTAB were more effective than organic acids, including acetic, lactic, and citric acids against the *S. aureus* isolates from meats. Resistance to triclosan was detected in 46% of the isolates, but almost all multidrug-resistant *S. aureus* isolates were triclosan-resistant. Among the organic acids tested, acetic acid had the most inhibitory effect on the *S. aureus* isolates from raw meats. The difference in MIC values between triclosan and organic acids, as well as between CTAB and organic acids, was statistically significant. *S. aureus* isolates from meat with high MIC values against disinfectants may pose a risk of growing antimicrobial resistance. The results of this study might be useful for evaluating the efficacy of disinfectants against *S. aureus* as a food pathogen and determining the development of resistance to them.

ORCID IDs of the authors

Fatma Ozdemir   0000-0002-4804-936X

Seza Arslan   0000-0002-2478-6875

REFERENCES

1. Götz F, Bannerman T, Schleifer KH. The genera *Staphylococcus* and *Macrococcus*. In: Dworkin M, Falkow S,E, Rosenberg E, Schleifer KH, Stackebrandt E, eds. *The Prokaryotes*. 3rd ed. New York, N.Y.: Springer; 2006:5-75.

2. Bhunia AK. *Foodborne microbial pathogens: Mechanisms and pathogenesis*. New York, N.Y.: Springer; 2008.

3. Ray B. *Fundamental Food Microbiology*. 3rd ed. Boca Raton, Florida: CRC press; 2004.

4. Bloomfield SF, Exner M, Fara GM, Nath KJ, Scott EA. Hygiene procedures in the home and their effectiveness: A review of the scientific evidence base. International Scientific Forum on Home Hygiene. 2013. https://ifh-homehygiene.org/review-best-practice/hygiene-procedures-home-and-their-effectiveness-review-scientific-evidence-base/.

5. Donaghy JA, Jagadeesan B, Goodburn K, et al. Relationship of sanitizers, disinfectants, and cleaning agents with antimicrobial resistance. *J Food Prot.* 2019;82(5):889-902.

6. Beuchat LR. Surface decontamination of fruits and vegetables eaten raw: A review. World Health Organization. 1998.

7. Lepaus BM, Rdcha JS, Sadjse JFB. Organic acids and hydrogen peroxide can replace chlorinated compounds as sanitizers on strawberries, cucumbers and rocket leaves. *Food Sci Technol.* 2020;40:242-249.

8. Suller MTE, Russell AD. Triclosan and antibiotic resistance in *Staphylococcus aureus. J Antimicrob Chemother.* 2000;46:11-18.

9. Sheldon AT. Antiseptic "Resistance": Real or perceived threat? *Clin Infect Dis.* 2005;40:1650-1656.

10. Jones RD, Jampani HB, Newman JL, Lee AS. Triclosan: A review of effectiveness and safety in health care settings. *Am J Infect Control.* 2000;28:184-196.

11. Glaser A. The ubiquitous triclosan: A common antibacterial agent exposed. *Pesticides and You NCODM.* 2004;24(3):12-17.

12. Yao K, Wen K, Shan W, Jiang H, Shao B. An immunoaffinity purification method for the simultaneous analysis triclocarban and triclosan in foodstuffs by liquid chromatography tandem mass spectrometry. *J Agric Food Chem.* 2019;67:9088-9095.

13. Azzouz A, Colon LP, Hejji L, Ballesteros E. Determination of alkylphenols, phenylphenols, bisphenol A, parabens, organophosphorus pesticides and triclosan in different cereal-based foodstuffs by gas chromatography–mass spectrometry. *Anal Bioanal Chem.* 2020;412:2621-2631.

14. Coia JE, Duckworth GJ, Edwards DI, et al. Guidelines for the control and prevention of meticillin-resistant *Staphylococcus aureus* (MRSA) in healthcare facilities. *J Hosp Infect.* 2006;63S:S1-S44.

15. Ciusa ML, Furi L, Knight D, et al. A novel resistance mechanism to triclosan that suggests horizontal gene transfer and demonstrates a potential selective pressure for reduced biocide susceptibility in clinical strains of *Staphylococcus aureus. Int J Antimicrob Agents.* 2012;40:210-220.

16. Fan F, Yan K, Wallis NG, et al. Defining and combating the mechanisms of triclosan resistance in clinical isolates of *Staphylococcus aureus. Antimicrob Agents Chemother.* 2002;46(11):3343-3347.

17. Beier RC, Poole TL, Brichta-Harhay DM, et al. Disinfectant and antibiotic susceptibility profiles of *Escherichia coli* O157:H7 strains from cattle carcasses, feces, and hides and ground beef from the United States. *J Food Prot.* 2013;76:6-17.

18. Beier RC, Foley SL, Davidson MK, et al. Characterization of antibiotic and disinfectant susceptibility profiles among *Pseudomonas aeruginosa* veterinary isolates recovered during 1994-2003. *J Appl Microbiol.* 2014;118:326-342.

19. Beier RC, Duke SE, Ziprin RL, et al. Antibiotic and disinfectant susceptibility profiles of vancomycin-resistant *Enterococcus faecium* (VRE) isolated from community wastewater in Texas. *Bull Environ Contam Toxicol.* 2008;80:188-194.

20. Beier RC, Callaway TR, Andrews K, et al. Disinfectant and antimicrobial susceptibility profiles of *Salmonella* strains from feedlot water-sprinkled cattle: Hides and feces. *J Food Chem Nanotechnol.* 2017;3:50-59.

21. McBain AJ, Ledder RG, Moore LE, Catrenich CE, Gilbert P. Effects of quaternary-ammonium–based formulations on bacterial community dynamics and antimicrobial susceptibility. *Appl Environ Microbiol.* 2004;70(6):3449-3456.

22. To MS, Favrin S, Romanova N, Griffiths MW. Postadaptational resistance to benzalkonium chloride and subsequent physicochemical modifications of *Listeria monocytogenes. Appl Environ Microbiol.* 2002;68(11):5258-5264.

23. Nakata K, Tsuchido T, Matsumura Y. Antimicrobial cationic surfactant, cetyltrimethylammonium bromide, induces superoxide stress in *Escherichia coli* cells. *J Appl Microbiol.* 2011;110:568-579.

24. Beier RC, Andrews K, Hume ME, et al. Disinfectant and antimicrobial susceptibility studies of *Staphylococcus aureus* strains and ST398-MRSA and ST5-MRSA strains from swine mandibular lymph node tissue, commercial pork sausage meat and swine feces. *Microorganisms.* 2021;9:2401. doi.org/10.3390/microorganisms9112401.

25. Humayoun SB, Hiott LM, Gupta SK, et al. An assay for determining the susceptibility of *Salmonella* isolates to commercial and household biocides. *PloS one.* 2018;13(12):e0209072. doi.org/10.1371/journal.pone.0209072.

26. Burns J, McCoy CP, Irwin NC. Synergistic activity of weak organic acids against uropathogens. *J Hosp Infect.* 2021;111:78-88.

27. Bai Y, Ding X, Zhao Q, et al. Development of an organic acid compound disinfectant to control food-borne pathogens and its application in chicken slaughterhouses. *Poult Sci.* 2022;101:101842. doi.org/10.1016/j.psj.2022.101842.

28. In YW, Kim JJ, Kim HJ, Oh SW. Antimicrobial activities of acetic acid, citric acid and lactic acid against *Shigella species. J Food Saf.* 2013; 33:79-85.

29. Pangprasit N, Srithanasuwan A, Suriyasathaporn W, et al. Antibacterial activities of acetic acid against major and minor pathogens isolated from mastitis in dairy cows. *Pathogens.* 2020; 9:961. doi:10.3390/pathogens9110961.

30. Beier RC, Byrd JA, Andrews K, et al. Disinfectant and antimicrobial susceptibility studies of the foodborne pathogen *Campylobacter jejuni* isolated from the litter of broiler chicken houses. *Poult Sci.* 2021;100:1024-1033.

31. Hussain G, Rahman A, Hussain T, Uddin S, Ali T. Citric and lactic acid effects on the growth inhibition of *E. coli* and *S. typhymurium* on beef during storage. *Sarhad J Agric.* 2015;31(3):183-190.

32. Al-Rousan WM, Olaimat AN, Osaili TM, Al-Nabulsi AA, Ajo RY, Holley RA. Use of acetic and citric acids to inhibit *Escherichia coli* O157:H7, *Salmonella Typhimurium* and *Staphylococcus aureus* in tabbouleh salad. *Food Microbiol.* 2018;73:61-66.

33. Brakstad OG, Aasbakk K, Maeland JA. Detection of *Staphylococcus aureus* by polymerase chain reaction amplification of the nuc gene. *J Clin Microbiol*. 1992;30(7):1654-1660.

34. Bannerman TL, Peacock SJ. *Staphylococcus, Micrococcus*, and other catalase-positive cocci. In: Versalovic J, Carroll KC, Funke G, Jorgensen JH, Landry ML, Warnock DW, eds. Manual of clinical microbiology, Washington, D.C: ASM Press; 2011:308-330.

35. Clinical and Laboratory Standards Institute (CLSI), Methods for dilution antimicrobial susceptibility tests for bacteria that grow aerobically; Ninth edition, M7-A9, in, Wayne, PA, USA, 2012.

36. Clinical and Laboratory Standards Institute (CLSI), Performance standards for antimicrobial susceptibility testing; 32nd edition, in, Malvern, PA, USA, 2022.

37. Andrews JM. Determination of minimum inhibitory concentrations. *J Antimicrob Chemother*. 2001;48:5-16.

38. Heath RJ, Rock CO. A triclosan-resistant bacterial enzyme. *Nature*. 2000;406:145-146.

How to cite this article

Retrospective Analysis of Transcriptomic Differences between Triple-Negative Breast Cancer (TNBC) and non-TNBC

Caglar Berkel[1] 🆔

[1]Tokat Gaziosmanpasa University, Faculty of Science and Arts, Department of Molecular Biology and Genetics, Tokat, Türkiye

ABSTRACT

Objective: Triple-negative breast cancer (TNBC), which has no expression of estrogen receptor, progesterone receptor and HER2, is an aggressive subgroup. Molecular differences between TNBC and non-TNBC should be better understood to develop tailored treatment strategies.

Materials and Methods: The expression of the most frequently mutated genes, and of genes for which copy number variation events are observed in the highest percentage of breast cancer patients, was compared between TNBC and non-TNBC samples, in R programming environment, using TCGA-BRCA transcriptomics dataset.

Results: 70% of the most frequently mutated genes in breast cancer (*CDH1, GATA3, MLL3 (KMT2C), MAP3K1, PTEN, NCOR1, FAT3, MAP2K4, NF1, ARID1A, LRP1B, RUNX1, MLL2 (KMT2D)* and *TBX3*) was found to have decreased expression in TNBC compared to non-TNBC. The expression of 40% of the genes with the highest frequency of copy number gain events in breast cancer (*SLC45A3, PTPRC, ELF3, FCGR2B, AKT3, FH, TPM3* and *SETDB1*) was increased in TNBC compared with non-TNBC. The half of the genes with the highest percentage of copy number loss events in breast cancer (*CBFA2T3, CDH1, ZFHX3, CDH11, MAP2K4, GAS7, PER1, RABEP1, NCOR1* and *PCM1*) was observed to have decreased expression in TNBC compared to non-TNBC. Lastly, the expression of BRCA2, but not of BRCA1, was found to be higher in TNBC than in non-TNBC.

Conclusion: This study provides further evidence in support of previous research, which show the presence of a large number of molecular differences between TNBC and non-TNBC, pointing to the need for more tailored treatment strategies for patients with TNBC.

Keywords: Breast cancer; Estrogen receptor; Progesterone receptor; HER2; Copy number variation; Transcriptomics; Triple-negative breast cancer.

INTRODUCTION

Breast cancer is the most common cause of cancer-associated deaths in female patients, with an estimate of more than 2,000,000 new cases and approximately 700,000 deaths each year worldwide.[1,2] This malignancy has been classified into different subgroups, mainly based on the presence/absence of the expression of three receptors: estrogen receptor (ER), progesterone receptor (PR), and human epidermal growth factor receptor (HER2/ERBB2). Despite the presence of high levels of heterogeneity at the molecular and cellular levels in breast tumors, the majority of the patients with breast cancer are treated with untailored therapies with certain chemotherapeutics or hormone therapies, including tamoxifen, a selective ER modulator, neglecting the molecular diversity and heterogeneity between the subgroups of the disease. Therefore, there is an im-

mediate need to develop novel targeted therapy modalities that are matched to the particular molecular and cellular changes in a breast tumor, with the ultimate purpose of achieving improved treatment benefits and avoiding excessive therapy.[3]

Triple-negative breast cancer (TNBC), which does not have hormone receptor (ER and PR) and HER2 expression, is an aggressive subtype of breast cancer for which novel therapy strategies need to be developed.[4,5] TNBC represents around 10–15% of all tumors of the breast, with an unfavorable prognosis at the clinic compared with non-TNBC.[6-9] Using current standard treatment options, the median overall survival for patients with TNBC is around 10.2 months. The 5-year survival rate is approximately 65% for patients whose tumors have spread to nearby lymph nodes, local tissues, or organs, and 11% for patients whose disease has metastasized from

breast tissue to distant organs in the body.[10,11] In addition to the aggressive characteristics of this subtype, the limited targeted therapy options and insensitivity to endocrine agents contribute significantly to poor disease-free and overall survival in this patient group.[6,9] Although therapeutic strategies such as immune checkpoint inhibitors and PARP (Poly (ADP-ribose) polymerase) inhibitors (also known as PARPi) including olaparib are changing the treatment landscape[12], TNBC currently has the worst prognosis among all breast cancer subtypes. This indicates an urgent need for a more complete understanding of TNBC which might help researchers develop therapeutic strategies with higher efficacy for patients with this subtype of breast cancer.

In the present study, molecular differences at the transcript level between TNBC and non-TNBC were studied. Between TNBC and non-TNBC samples, the expression of the most frequently mutated genes and of genes for which copy number variation (CNV) events (gain and loss) are observed in the highest percentage of breast cancer patients, were compared to identify essential genes that possibly contribute to clinical differences between TNBC and non-TNBC. Seventy percent of the most frequently mutated genes (*CDH1, GATA3, MLL3 (KMT2C), MAP3K1, PTEN, NCOR1, FAT3, MAP2K4, NF1, ARID1A, LRP1B, RUNX1, MLL2 (KMT2D)* and *TBX3*) in breast cancer was found to have decreased expression in TNBC compared to non-TNBC. Forty percent of the genes with the highest frequency of copy number gain events in breast cancer (*SLC45A3, PTPRC, ELF3, FCGR2B, AKT3, FH, TPM3* and *SETDB1*) was shown to have increased expression in TNBC compared with non-TNBC. The half of the genes with the highest frequency of copy number loss events in breast cancer (*CBFA2T3, CDH1, ZFHX3, CDH11, MAP2K4, GAS7, PER1, RABEP1, NCOR1* and *PCM1*) was observed to have decreased expression in TNBC compared to non-TNBC. Lastly, the expression of *BRCA2*, but not of *BRCA1*, was found to be higher in TNBC than in non-TNBC. This study points to the presence of many molecular differences between TNBC and non-TNBC at the expression level of genes of clinical importance, pointing to the need for more tailored treatment strategies for breast cancer patients with triple-negative status.

MATERIALS AND METHODS

Datasets

In the present study, mutation percentage and copy number variation (CNV) data were obtained from the Genomic Data Commons (GDC) Data Portal of The National Cancer Institute, which can be accessed at https://portal.gdc.cancer.gov/, which includes data from TCGA (The Cancer Genome Atlas)-BRCA project in addition to other projects.[13-17] The most frequently mutated genes were defined as genes with the highest percentage of cases affected by mutations in these genes (for instance,

442 out of 1387 patients with breast cancer have a mutation in the *TP53* gene, the most frequently mutated gene in breast cancer). Only the top 20 most commonly mutated genes were included in this analysis.

For transcriptomic analysis, processed and compiled RNA sequencing and clinical data for breast cancer patient samples from the TCGA project (GSE62944) were used.[18-20] In more detail, in the construction of datasets, authors aligned the fastq files.[18] First, they aligned the reads with the align function to the UCSC hg19 reference genome. Second, they used the featureCounts function to summarize the gene expression values as integers. Lastly, these summarized gene values were normalized to FPKM and TPM values.[18] The total sample size (n) for the number of patients after the filtering steps is 703. Sample sizes (i.e., number of patients) for subgroups are as follows: non-TNBC (non-triple negative breast cancer): 591; TNBC (triple-negative breast cancer):112. TNBC is defined as ER- (estrogen receptor-negative), PR- (progesterone receptor-negative), and HER2- (human epidermal growth factor receptor 2-negative). This dataset can also be accessed in SummarizedExperiment format through Bioconductor (in Experiment Packages » GSE62944).[21-23] This dataset also includes clinical variables for patients other than those used in the present study. Raw data for this dataset can be found at GEO using the given accession ID. In this dataset, ER, PR, and HER2 status from patient breast tumor samples were determined using immunohistochemistry.[19]

Data Analysis and Visualization

Analysis and visualization of the obtained data in the present study were conducted in R statistical programming environment (R version 4.2.1 (2022-06-23)) using R Studio IDE from posit.[24] These R/Bioconductor packages (https://bioconductor.org/) were used throughout the analysis[22,23]: tidyverse (a collection of R packages written for data science applications including ggplot2 and tidyr)[25-27], readxl[28], ExperimentHub[29], SummarizedExperiment[30], ggpubr[31] (for statistical tests), rmarkdown[32] and knitr.[33] After processing, TCGA gene expression data (GSE62944) was accessed using the ExperimentHub package for all cancer types with the query function from the AnnotationHub package; as the "CancerType" variable, "BRCA" was selected (CancerType== "BRCA"), which is short for breast cancer. R script used in the analysis is available as a supplementary document for reproducibility purposes.

The Wilcoxon test was performed when the expression data was not normally distributed.[31] Otherwise (when we can assume normality, i.e., p-value> 0.05 for Shapiro-Wilk test of normality), the *t-test* was used in the comparison of group means. Functions (ggqqplot for quantile-quantile plot and shapiro.test for Shapiro-Wilk normality test) from stats and ggpubr packages were used in the analysis of the distribution (normal dis-
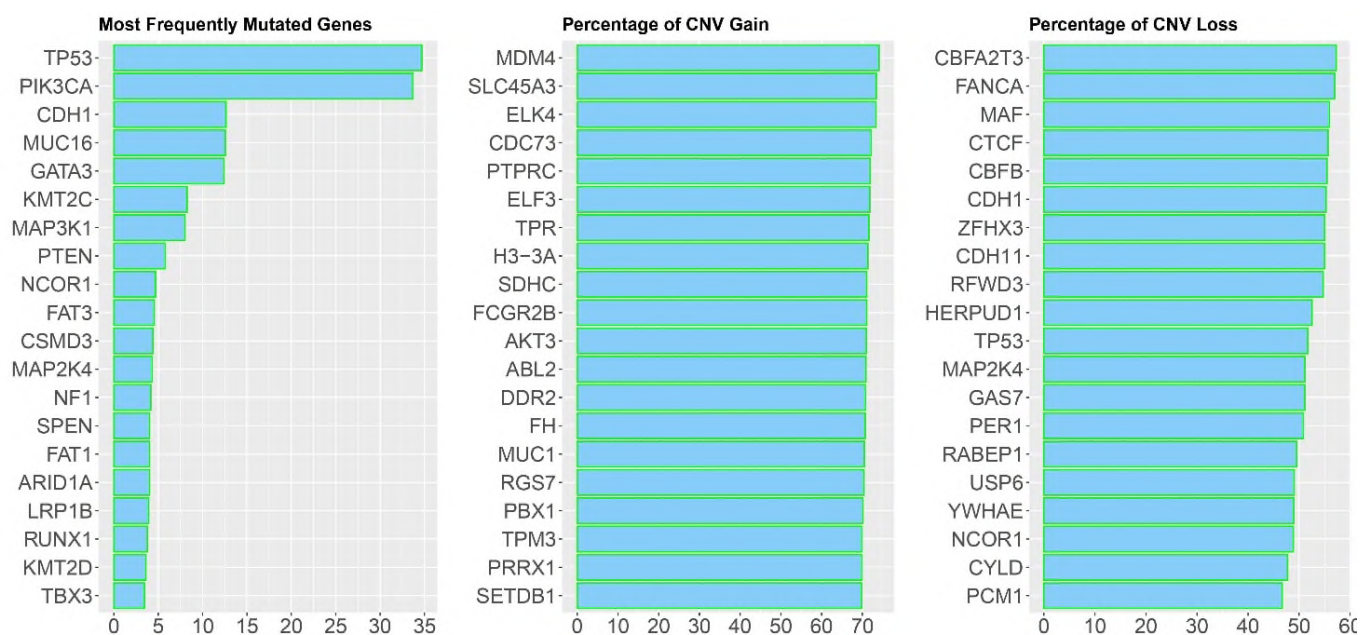
Figure 1. The list of the top 20 genes with the highest percentage of mutations (first panel), the highest percentage of copy number gain events (middle panel), or copy number loss events (last panel) in breast cancer. The x-axis in the first panel shows the number of cases in which a gene is mutated divided by the number of cases investigated for the presence of simple somatic mutations. CNV: copy number variation.

tribution or not).[24] Relative expression values shown in plots are log10 transformations of read counts from the dataset. Data analysis and visualization were performed as reported in our previous studies.[34,35]

RESULTS

Seventy Percent of the Most Frequently Mutated Genes in Patients with Breast Cancer Shows Decreased Expression in TNBC compared to Non-TNBC.

Firstly, the transcript levels of the top 20 most frequently mutated genes in breast cancer (namely, *TP53, PIK3CA, CDH1, MUC16, GATA3, MLL3, MAP3K1, PTEN, NCOR1, FAT3, CSMD3, MAP2K4, NF1, FAT1, SPEN, ARID1A, LRP1B, RUNX1, MLL2* and *TBX3*) (Figure 1) were compared between tumors from breast cancer patients with triple negative status (ER-, PR-, HER2-) and non-TNBC. Fourteen genes out of these 20 genes (70%) were found to have decreased expression in TNBC compared to non-TNBC (Figure 2). These 14 genes are: *CDH1, GATA3, MLL3 (KMT2C), MAP3K1, PTEN, NCOR1, FAT3, MAP2K4, NF1, ARID1A, LRP1B, RUNX1, MLL2 (KMT2D)* and *TBX3* (Figure 2). In contrast, PIK3CA, MUC16 and FAT1 showed increased expression in TNBC compared to non-TNBC (Figure 2). TP53, CSMD3, and SPEN expression did not change between patients with TNBC and non-TNBC at the transcript level (Figure 2).

Forty Percent of the Genes with the Highest Percentage of CNV Gain Events in Breast Cancer Shows Increased Expression in TNBC compared to Non-TNBC.

Next, mRNA levels of the top 20 genes for which the highest percentage of CNV gain events are observed in patients with breast cancer (namely, *MDM4, SLC45A3, ELK4, CDC73, PT-PRC, ELF3, TPR, H3-3A (H3F3A), FCGR2B, SDHC, AKT3, ABL2, DDR2, FH, MUC1, RGS7, PBX1, PRRX1, TPM3* and *SETDB1*) (Figure 1), were compared between tumors from patients with TNBC and non-TNBC (Figure 3). The expression of 5 genes (*MDM4, MUC1, RGS7, PBX1,* and *PRRX1*) (25%) was found to be decreased in TNBC compared to non-TNBC (Figure 3). In contrast, the expression of *SLC45A3, PTPRC, ELF3, FCGR2B, AKT3, FH, TPM3,* and *SETDB1* (8 genes out of 20; 40%) was shown to be higher in breast tumors with triple-negative status than in those with non-triple negative status (Figure 3). The other seven genes did not show significantly different expression between patients with TNBC and non-TNBC (Figure 3).

Half of the Genes with the Highest Percentage of CNV Loss Events in Breast Cancer Shows Lower Expression in TNBC than in Non-TNBC.

Then, the expression levels of the top 20 genes for which the highest percentage of CNV loss events are observed in breast cancer patients (that are *CBFA2T3, FANCA, MAF, CTCF, CBFB, CDH1, ZFHX3, CDH11, RFWD3, HERPUD1, TP53, MAP2K4, GAS7, PER1, RABEP1, USP6, YWHAE, NCOR1,*
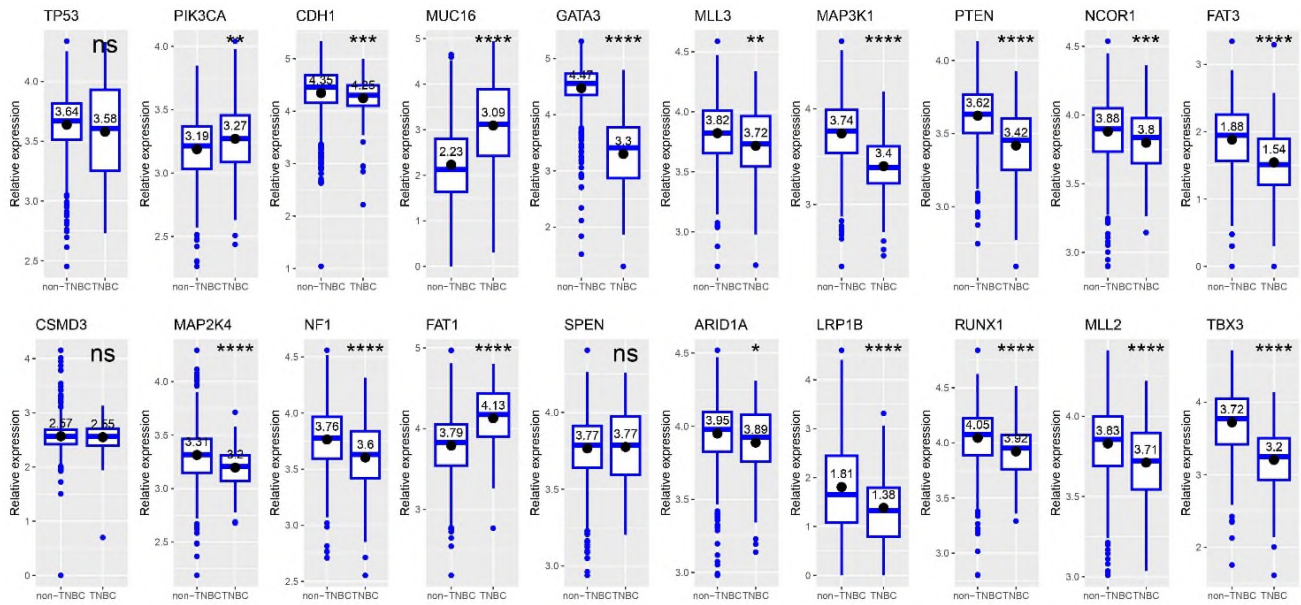
Figure 2. Comparative expression of the most frequently mutated genes in breast cancer between triple-negative breast cancer (TNBC) and with non-TNBC. The following convention of star symbols for statistical significance was used in the comparison of group means: ns (non-significant): p > 0.05; *: p ≤ 0.05; **: p ≤ 0.01; ***: p ≤ 0.001; ****: p ≤ 0.0001.
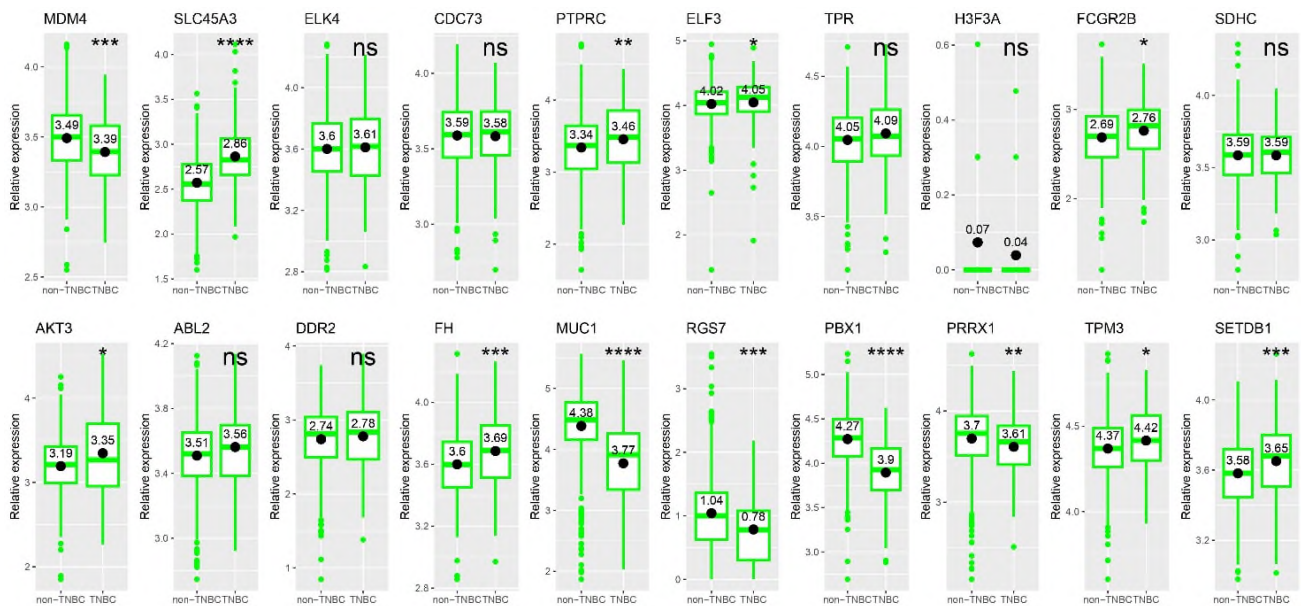
Figure 3. Comparative expression of the genes with the highest percentage of copy number gain events in breast cancer between triple-negative breast cancer (TNBC) and non-TNBC. The following convention of star symbols for statistical significance was used in the comparison of group means: ns (non-significant): p > 0.05; *: p ≤ 0.05; **: p ≤ 0.01; ***: p ≤ 0.001; ****: p ≤ 0.0001.

CYLD and *PCM1*) (Figure 1), were comparatively analyzed between tumors from patients with TNBC and non-TNBC (Figure 4). The half of these genes (*CBFA2T3, CDH1, ZFHX3, CDH11, MAP2K4, GAS7, PER1, RABEP1, NCOR1* and *PCM1*) was observed to have decreased expression in TNBC compared to non-TNBC (Figure 4). *FANCA, CBFB, RFWD3*, and *YWHAE*

expression were higher in breast tumors with triple-negative status than in those with non-TNBC (Figure 4). The other six genes (30%) (*MAF, CTCF, HERPUD1, TP53, USP6*, and *CYLD*) did not exhibit differential expression in breast cancer based on triple negativity status (TNBC vs non-TNBC) (Figure 4).
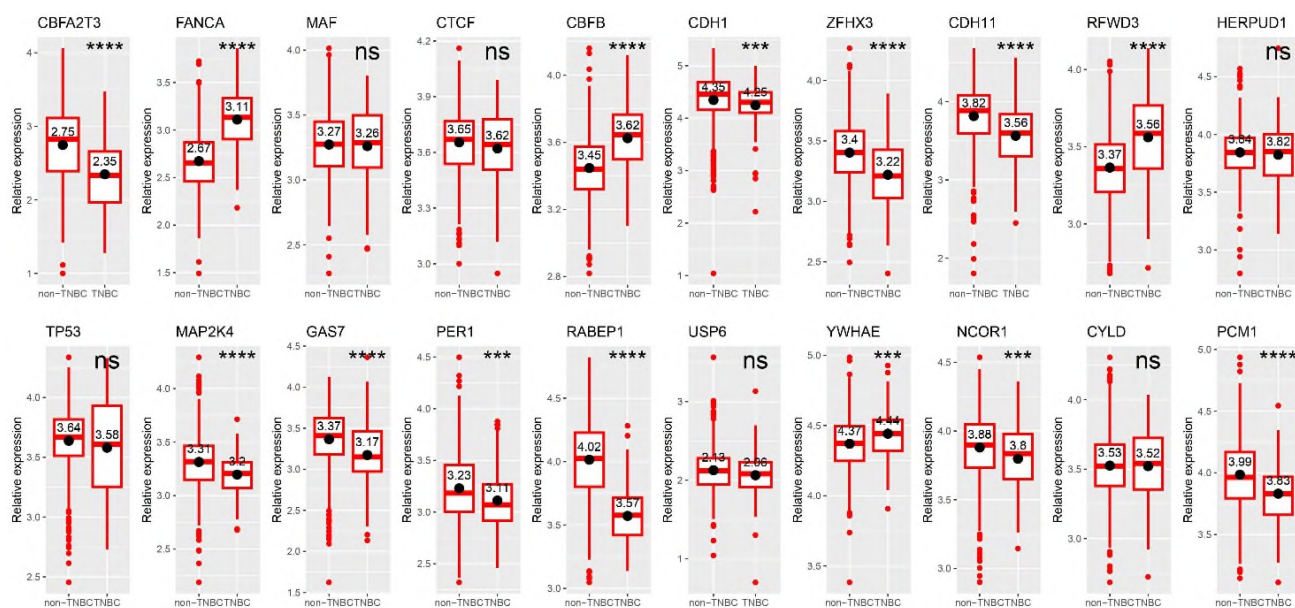
Figure 4. Comparative expression of the genes with the highest percentage of copy number loss events in breast cancer between triple-negative breast cancer (TNBC) and non-TNBC. The following convention of star symbols for statistical significance was used in the comparison of group means: ns (non-significant): p > 0.05; *: p ≤ 0.05; **: p ≤ 0.01; ***: p ≤ 0.001; ****: p ≤ 0.0001.

The Expression of BRCA2, but not of BRCA1, Is Higher in TNBC than in Non-TNBC.

Finally, the expression of the two most essential genes in the context of breast cancer (*BRCA1* and *BRCA2*) was compared between TNBC and non-TNBC samples (Figure 5). The expression of *BRCA2* was higher in TNBC than in non-TNBC (p = 2e-05) (Figure 5). However, the expression of *BRCA1* did not change between breast tumors depending on triple negativity status (TNBC vs. non-TNBC) (p = 0.16) (Figure 5).

DISCUSSION

The treatment of TNBC, the subtype with the least favorable outcome with an early tendency to metastasize to other tissues and an increased recurrence rate, remains challenging.[36,37] A better understanding of the molecular differences between TNBC and non-TNBC might contribute to the development of more targeted and molecularly guided treatment modalities with improved efficacies.

The most frequently mutated genes in patients with breast cancer are already known based on previous research; however, differential expression of these genes based on triple-negativity status has not been studied previously in a comprehensive manner. Here, 70% of the most frequently mutated genes in patients with breast cancer was first found to have decreased expression in TNBC than in non-TNBC. One of the genes whose expression was decreased in TNBC is *GATA3*. The *GATA3* functions to limit epithelial-mesenchymal transition (EMT) and metastasis in breast cancer, supporting previous observations
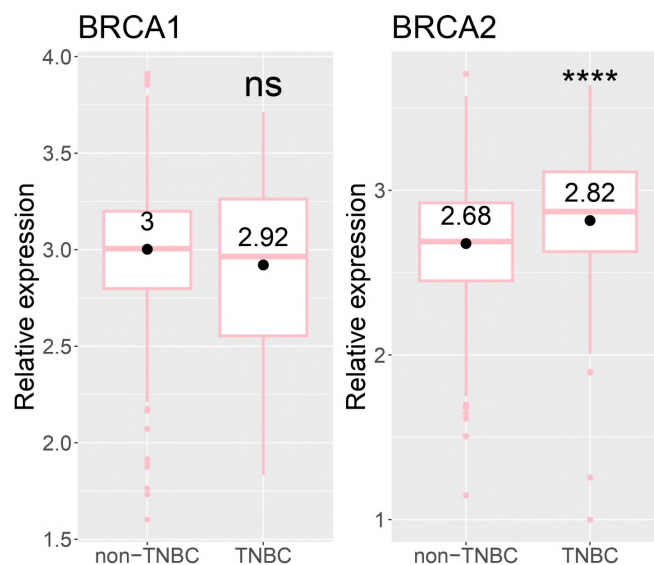
Figure 5. The expression of BRCA2, but not of BRCA1, is higher in triple-negative breast cancer (TNBC) than in non-TNBC. The following convention of star symbols for statistical significance was used in the comparison of group means: ns (non-significant): p > 0.05; *: p ≤ 0.05; **: p ≤ 0.01; ***: p ≤ 0.001; ****: p ≤ 0.0001.

that *GATA3* loss is associated with aggressive breast cancer development.[38,39] In more detail, it was found that the GATA3-UTX-Dicer axis can inhibit EMT, invasion, and metastasis of breast cancer cells *in vitro* and the dissemination of breast cancer *in vivo*.[38,39] Therefore, its decreased expression (or loss) in TNBC might contribute to, at least to a certain level, poor

prognosis observed in patients with TNBC by limiting the inhibition of EMT, invasion, and metastasis of breast cancer cells. One of the other genes whose expression was lower in TNBC than in non-TNBC is *PTEN*. Li et al. reported that PTEN loss might be associated with more aggressive characteristics and worse outcomes in breast cancer patients[40], again showing that decreased PTEN expression in TNBC might influence prognosis in this patient group. They found that PTEN loss is associated with larger tumor size, lymph node metastasis, high TNM stage (stage III-IV), and poor differentiation. Most importantly, their analysis showed that PTEN loss is associated with a triple-negative phenotype, supporting our findings.[40] RUNX1 transcript levels were lower in TNBC than in non-TNBC. Since RUNX1 limits aggressiveness in most subtypes of breast cancer, and RUNX1 was identified to have a role in the repression of epithelial-to-mesenchymal transition in breast cancer[41], its decreased expression in TNBC might potentially lead to increased metastatic events in this subtype of breast cancer, leading to poor prognosis. More recent studies showed that RUNX1 can repress cancer stem cells and tumorsphere formation in breast cancer.[41] Decreased RUNX1 expression in TNBC might lead to higher numbers of cancer stem cells and increased tumorsphere formation, negatively influencing prognosis in TNBC. *MUC16* expression was also observed to be higher in patients with TNBC compared with those with non-TNBC. In a very recent study, *MUC16* was shown to promote triple-negative breast cancer metastasis to the lung; thus, increased levels of MUC16 might contribute to worse outcomes in patients with TNBC.[42] Besides, although p53 is a known genetic marker for TNBCs (as the most frequently mutated gene), there was no difference in its expression between TNBC and non-TNBC at the transcript level, possibly pointing to other levels of regulation, such as protein activity or functionality or this non-significance observed can be caused due to the short half-life of p53 mRNA. Here, it also should be stated that although the difference in mean expression values for some genes between TNBC and non-TNBC is higher compared to some others, no statistically significant difference was observed as opposed to others due to the high range of distribution of expression values in each group (in TNBC and non-TNBC) for the former case.

Next, 40% of the genes with the highest percentage of copy number gain events in breast cancer showed increased expression in TNBC compared to non-TNBC. One of these genes, whose expression was increased in TNBC, is SETDB1. SETDB1, a histone methyltransferase, is known to regulate and support breast cancer metastasis.[43,44] SETDB1 is a target of miR-381-3p, whose overexpression suppresses cell proliferation, cell cycle progression, and migration in breast cancer.[44] Increased expression of SETDB1 in TNBC might contribute to disease progression into advanced tumor stages and even to endocrine therapy resistance in breast cancer.[45] Besides, the expression of MDM4 was found to be lower in TNBC compared

with non-TNBC. Swetzig et al. showed that estrogen receptor alpha (ERα; ESR1) promotes the upregulation of *MDM4* in breast cancer cells, and the expression of *MDM4* is associated with ERα-positive disease[46]; therefore, decreased expression of *MDM4* in TNBC might be in part due to the absence of ERs in this subtype. Furthermore, ELF3 expression was observed to be slightly increased in TNBC. Zhang et al. showed that ELF3 is associated with a worse prognosis in patients with breast cancer.[47] Therefore, its higher levels in TNBC might influence survival negatively in patients with TNBC. Mechanistically, miR-320 (functioning as a tumor suppressor) might downregulate *ELF3* by directly binding to its 3' untranslated regions in non-TNBC cells, in addition to its function in the inhibition of the EMT and the PI3K/AKT signaling pathway in breast cancer.[47]

The half the genes with the highest percentage of copy number loss events in breast cancer was found to have decreased expression in TNBC compared to non-TNBC. The expression of *CBFA2T3* was found to be lower in TNBC. *CBFA2T3* was previously proposed as a gene with breast tumor suppressor activity.[48] ZFHX3 transcript levels were also lower in TNBC than in non-TNBC. Dong et al. reported that ZFHX3 promotes the proliferation of breast cancer cells with ER-positive status (i.e., non-TNBC), leading to tumor growth[49], possibly explaining its increased expression observed in non-TNBC. In more detail, authors showed that ZFHX3 promotes the proliferation and tumor growth of ER-positive breast cancer cells, likely by enhancing stem-like features and *MYC* and *TBX3* transcription, since they found that ZFHX3 transcriptionally activates these two genes via promoter binding.[49] mRNA levels of GAS7 were similarly shown to be decreased in TNBC. Since GAS7 was shown to reduce the number of metastatic events in particular breast cancer cells (mechanistically, GAS7 blocks CYFIP1 and Rac1 protein interaction, actin polymerization, and β1-integrin/FAK/Src signaling, leading to the suppression of breast cancer metastasis)[50], its lower levels in TNBC might conversely increase the number of metastatic events in patients with TNBC, due to the absence (or decreased activity) of this suppression axis. *CBFB* expression was found to be higher in TNBC. Hsu et al. found recently that circulating exosomes isolated from patients whose breast cancer has metastasized to the bone were rich in CBFB, and that this protein promotes more aggressive behavior in breast cancer.[51] The authors found that silencing *CBFB* in metastatic cells suppresses migration and invasion and downregulates vimentin, CXCR4, Snail1, Runx2, CD44, and OPN. Conversely, CBFB overexpression increases Runx2, vimentin, Snail1, CD44, and OPN in nonmetastatic cells.[51] Thus, it can be suggested that increased levels of *CBCF* in TNBC might influence prognosis negatively by at least promoting metastasis to the bone via the upregulation of specific genes involved in cell migration.[51] Besides, this analysis showed that *NCOR1* expression is lower in TNBC compared to non-TNBC. Since the level of *NCOR1* gene expression is an

independent prognostic factor for patients with breast cancer, and patients with high mRNA levels of *NCOR1* have a more favorable prognosis compared to those with low expression[52], its lower expression in TNBC might contribute, at least in part, to the unfavorable prognosis observed in patients with TNBC. In support, Zhang et al.[52] reported that NCOR1 mRNA is expressed at significantly higher levels in patients without axillary lymph node involvement, with a tumor size less than 2 cm, with a low or intermediate histological grade, and with ER-alpha/PR-positive and with HER2 negative tumors (i.e., non-TNBC).

Here, it should be noted that although only some of the genes studied in the present work were discussed, future work is required to better understand the functional and mechanistic details of the most of the genes covered in the context of breast cancer. Currently, studies on the most of these genes in breast cancer are highly limited. Lastly, the expression of *BRCA2*, but not of *BRCA1*, was shown to be higher in TNBC than in non-TNBC. In breast cancer patients, the tumor phenotype differs depending on the status of *BRCA1* or *BRCA2* germline mutations. Patients who carry *BRCA1* mutations mainly develop TNBC, whereas patients who carry BRCA2 mutations are more likely to have ER- and/or PR-positive breast tumors.[53-58] Therefore, it can be speculated that non-functional BRCA2 (for instance, mutant BRCA2) might be associated with ER- and/or PR-positivity in breast cancer, in parallel to the observation made in the present study that BRCA2 transcript levels are lower in breast cancer cells with ER- and/or PR-positive status. However, these inferences should be experimentally tested to make stronger assumptions.

CONCLUSION

This study provides a better understanding of the molecular differences between TNBC and non-TNBC, highlighting the need for further research to characterize the functional and clinical outcomes of these changes at the expression level between these two groups of breast cancer patients to be able to develop more personalized treatment strategies based on ER, PR and HER2 status. However, as a limitation, it should be noted that TNBC tumors also display high heterogeneity within themselves, and they can be further sub-classified based on specific driver signaling pathways, which should be taken into account when assigning TNBC patients to appropriate targeted therapies.[59,60] In other words, in addition to identifying molecular differences between TNBC and non-TNBC, determining the molecular differences within TNBC might also be of high clinical importance, considering the presence of high heterogeneity within this subtype of breast cancer.

ORCID IDs of the author

Caglar Berkel   0000-0003-4787-5157

REFERENCES

1. Harding C, Pompei F, Burmistrov D, Welch HG, Abebe R, Wilson R. Breast cancer screening, incidence, and mortality across US counties. *JAMA Intern Med*. 2015;175(9):1483-1489.

2. Sung H, Ferlay J, Siegel RL et al. Global cancer statistics 2020: GLOBOCAN estimates of incidence and mortality worldwide for 36 cancers in 185 countries. *CA Cancer J Clin*. 2021;71(3):209-249.

3. Kim M, Park J, Bouhaddou M, et al. A protein interaction landscape of breast cancer. *Science*. 2021;374(6563):eabf3066. doi: 10.1126/science.abf3066

4. Bianchini G, Balko JM, Mayer IA, Sanders ME, Gianni L. Triple-negative breast cancer: Challenges and opportunities of a heterogeneous disease. *Nat Rev Clin Oncol*. 2016;13(11):674-690.

5. Bianchini G, De Angelis C, Licata L, Gianni L. Treatment landscape of triple-negative breast cancer-expanded options, evolving needs. *Nat Rev Clin Oncol*. 2022;19(2):91-113.

6. Fallahpour S, Navaneelan T, De P, Borgo A. Breast cancer survival by molecular subtype: A population-based analysis of cancer registry data. *CMAJ Open*. 2017;5:E734–E739.

7. Dent R, Trudeau M, Pritchard KI, et al. Triple-negative breast cancer: Clinical features and patterns of recurrence. *Clin Cancer Res*. 2007;13:4429-4434.

8. Tan AR, Swain SM. Therapeutic strategies for triple-negative breast cancer. *Cancer J*. 2008;14:343–351.

9. Kaplan HG, Malmgren JA, Atwood M. T1N0 triple negative breast cancer: Risk of recurrence and adjuvant chemotherapy. *Breast J*. 2009;15:454–460.

10. Won KA, Spruck C. Triple negative breast cancer therapy: Current and future perspectives (Review). *Int J Oncol*. 2020;57:1245–1261.

11. Almansour NM. Triple-negative breast cancer: A brief review about epidemiology, risk factors, signaling pathways, treatment and role of artificial intelligence. *Front Mol Biosci*. 2022;9:836417. doi:10.3389/fmolb.2022.836417.

12. Berkel C, Kucuk B, Usta M, Yılmaz E, Cacan E. The effect of olaparib and bortezomib combination treatment on ovarian cancer cell lines. *Eur J Biol*. 2020;79(2):115-123.

13. Ciriello G, Gatza ML, Beck AH, et al. Comprehensive molecular portraits of ınvasive lobular breast cancer. *Cell*. 2015;163(2):506-519.

14. Jensen MA, Ferretti V, Grossman RL, Staudt LM. The NCI Genomic Data Commons as an engine for precision medicine. *Blood*. 2017;130(4):453-459.

15. Zhang Z, Hernandez K, Savage J, et al. Uniform genomic data analysis in the NCI Genomic Data Commons. *Nat Commun*. 2021;12(1):1226. doi: 10.1038/s41467-021-21254-9.

16. Berger AC, Korkut A, Kanchi RS, et al. A Comprehensive pan-cancer molecular study of gynecologic and breast cancers. *Cancer Cell*. 20189;33(4):690-705.e9. doi: 10.1016/j.ccell.2018.03.014.

17. Cancer Genome Atlas Network. Comprehensive molecular portraits of human breast tumours. *Nature*. 2012;490(7418):61-70.

18. Rahman M, Jackson LK, Johnson WE, Li DY, Bild AH, Piccolo SR. Alternative preprocessing of RNA-Sequencing data in The Cancer Genome Atlas leads to improved analysis results. *Bioinformatics*. 2015;31(22):3666-3672.

19. Weinstein JN, Collisson EA, Mills GB, et al. Cancer Genome Atlas Research Network; The Cancer Genome Atlas Pan-Cancer analysis project. *Nat Genet*. 2013;45(10):1113-1120.

20. Wilks C, Cline MS, Weiler E, et al. The Cancer Genomics Hub (CGHub): Overcoming cancer through the power of torrential data. *Database*. 2014:1–10.

21. Arora S. GSE62944: GEO accession data GSE62944 as a SummarizedExperiment. R package version 1.28.1;2023. http://bioconductor.org/packages/release/bioc/html/GSE62944.html

22. Huber W, Carey VJ, Gentleman R, et al. Orchestrating high-throughput genomic analysis with bioconductor. *Nat Methods*. 2015;12(2):115-121.

23. Gentleman RC, Carey VJ, Bates DM, et al. Bioconductor: Open software development for computational biology and bioinformatics. *Genome Biol*. 2004;5(10):R80. doi:10.1186/gb-2004-5-10-r80

24. R Core Team. R: A language and environment for statistical computing. R Foundation for Statistical Computing; 2022. Vienna, Austria. URL https://www.R-project.org/

25. Wickham H, Averick M, Bryan J, et al. Welcome to the tidyverse. *J Open Source Softw.* 2019;4(43):1686. doi:10.21105/joss.01686

26. Wickham H. stringr: Simple, consistent wrappers for common string operations. R package version 1.5.0;2022. https://CRAN.R-project.org/package=stringr

27. Wickham H. ggplot2: Elegant Graphics for Data Analysis. Springer-Verlag New York, 2016.

28. Wickham H, Bryan J. readxl: Read Excel Files. R package version 1.4.2;2023. https://CRAN.R-project.org/package=readxl

29. Morgan M, Shepherd L. ExperimentHub: Client to access ExperimentHub resources. R package version 2.4.0;2022.

30. Morgan M, Obenchain V, Hester J, Pagès H. SummarizedExperiment: SummarizedExperiment container. R package version 1.26.1;2022. https://bioconductor.org/packages/SummarizedExperiment

31. Kassambara A. ggpubr: 'ggplot2' Based Publication Ready Plots. R package version 0.6.0;2023. https://CRAN.R-project.org/package=ggpubr

32. Allaire J, Xie Y, Dervieux C, et al. rmarkdown: Dynamic Documents for R. R package version 2.21;2023. https://github.com/rstudio/rmarkdown

33. Xie Y. knitr: A General-Purpose Package for Dynamic Report Generation in R. R package version 1.42;2023.

34. Berkel C, Cacan E. *In silico* analysis of DYNLL1 expression in ovarian cancer chemoresistance. *Cell Biol Int*. 2020;44(8):1598-1605.

35. Berkel C, Cacan E. Transcriptomic analysis reveals tumor stage- or grade-dependent expression of miRNAs in serous ovarian cancer. *Hum Cell*. 2021;34(3):862-877.

36. Li X, Yang J, Peng L, et al. Triple-negative breast cancer has worse overall survival and cause-specific survival than non-triple-negative breast cancer. *Breast Cancer Res Treat.* 2017;161(2):279-287.

37. Bai X, Ni J, Beretov J, Graham P, Li Y. Triple-negative breast cancer therapeutic resistance: Where is the Achilles' heel? *Cancer Lett*. 2021;497:100-111.

38. Bai F, Zhang LH, Liu X, et al. GATA3 functions downstream of BRCA1 to suppress EMT in breast cancer. *Theranostics*. 2021;11(17):8218-8233.

39. Yu W, Huang W, Yang Y, et al. GATA3 recruits UTX for gene transcriptional activation to suppress metastasis of breast cancer. *Cell Death Dis*. 2019;10(11):832. doi:10.1038/s41419-019-2062-7

40. Li S, Shen Y, Wang M, et al. Loss of PTEN expression in breast cancer: Association with clinicopathological characteristics and prognosis. *Oncotarget*. 2017;8(19):32043-32054.

41. Hong D, Fritz AJ, Gordon JA, et al. RUNX1-dependent mechanisms in biological control and dysregulation in cancer. *J Cell Physiol*. 2019;234(6):8597-8609.

42. Chaudhary S, Appadurai MI, Maurya SK, et al. MUC16 promotes triple-negative breast cancer lung metastasis by modulating RNA-binding protein ELAVL1/HUR. *Breast Cancer Res*. 2023;25(1):25. doi:10.1186/s13058-023-01630-7

43. Ryu TY, Kim K, Kim SK, et al. SETDB1 regulates SMAD7 expression for breast cancer metastasis. *BMB Rep*. 2019;52(2):139-144.

44. Wu M, Fan B, Guo Q, et al. Knockdown of SETDB1 inhibits breast cancer progression by miR-381-3p-related regulation. *Biol Res*. 2018;51(1):39. doi: 10.1186/s40659-018-0189-0

45. Liu Z, Liu J, Ebrahimi B, et al. SETDB1 interactions with PELP1 contributes to breast cancer endocrine therapy resistance. *Breast Cancer Res.* 2022;24(1):26. doi: 10.1186/s13058-022-01520-4

46. Swetzig WM, Wang J, Das GM. Estrogen receptor alpha (ERα/ESR1) mediates the p53-independent overexpression of MDM4/MDMX and MDM2 in human breast cancer. *Oncotarget*. 2016;7(13):16049-16069.

47. Zhang Z, Zhang J, Li J, et al. miR-320/ELF3 axis inhibits the progression of breast cancer via the PI3K/AKT pathway. *Oncol Lett*. 2020;19(4):3239-3248.

48. Kochetkova M, McKenzie OL, Bais AJ, et al. CBFA2T3 (MTG16) is a putative breast tumor suppressor gene from the breast cancer loss of heterozygosity region at 16q24.3. *Cancer Res*. 2002;62(16):4599-4604.

49. Dong G, Ma G, Wu R, et al. ZFHX3 promotes the proliferation and tumor growth of ER-positive breast cancer cells likely by enhancing stem-like features and MYC and TBX3 transcription. *Cancers (Basel)*. 2020;12(11):3415. doi: 10.3390/cancers12113415

50. Chang JW, Kuo WH, Lin CM, et al. Wild-type p53 upregulates an early onset breast cancer-associated gene GAS7 to suppress metastasis via GAS7-CYFIP1-mediated signaling pathway. *Oncogene*. 2018;37(30):4137-4150.

51. Hsu CH, Ma HP, Ong JR, et al. Cancer-associated exosomal CBFB facilitates the aggressive phenotype, evasion of oxidative stress, and preferential predisposition to bone prometastatic factor of breast cancer progression. *Dis Markers*. 2022;2022:8446629. doi: 10.1155/2022/8446629

52. Zhang Z, Yamashita H, Toyama T, et al. NCOR1 mRNA is an independent prognostic factor for breast cancer. *Cancer Lett*. 2006;237(1):123-129.

53. Mavaddat N, Barrowdale D, Andrulis IL, et al. Consortium

of Investigators of Modifiers of BRCA1/2. Pathology of breast and ovarian cancers among BRCA1 and BRCA2 mutation carriers: results from the Consortium of Investigators of Modifiers of BRCA1/2 (CIMBA). *Cancer Epidemiol Biomarkers Prev*. 2012;21(1):134-147.

54. De Talhouet S, Peron J, Vuilleumier A, et al. Clinical outcome of breast cancer in carriers of BRCA1 and BRCA2 mutations according to molecular subtypes. *Sci Rep*. 202027;10(1):7073. doi:10.1038/s41598-020-63759-1 Erratum in: *Sci Rep*. 2020;10(1):19248.

55. Lakhani SR, Reis-Filho JS, Fulford L, et al. Prediction of BRCA1 status in patients with breast cancer using estrogen receptor and basal phenotype. *Clin Cancer Res*. 2005;11:5175–5180.

56. Armes JE, Trute L, White D, et al. Distinct molecular pathogeneses of early-onset breast cancers in BRCA1 and BRCA2 mutation carriers: a population-based study. *Cancer Res*. 1999;59:2011–2017.

57. Palacios J, Honrado E, Osorio A, et al. Phenotypic characterization of BRCA1 and BRCA2 tumors based in a tissue microarray study with 37 immunohistochemical markers. *Breast Cancer Res Treat*. 2005;90:5–14.

58. Lakhani SR, Van De Vijver MJ, Jacquemier J, et al. The pathology of familial breast cancer: predictive value of immunohistochemical markers estrogen receptor, progesterone receptor, HER-2, and p53 in patients with mutations in BRCA1 and BRCA2. *J Clin Oncol*. 2002;20:2310–2318.

59. Lehmann BD, Bauer JA, Chen X, et al. Identification of human triple-negative breast cancer subtypes and preclinical models for selection of targeted therapies. *J Clin Invest*. 2011;121(7):2750-2767.

60. Sporikova Z, Koudelakova V, Trojanec R, Hajduch M. Genetic markers in triple-negative breast cancer. *Clin Breast Cancer*. 2018;18(5):e841-e850. doi: 10.1016/j.clbc.2018.07.023

How to cite this article

Investigation of the Relationship between the Multidrug Resistance 1 Gene Polymorphisms and Bronchodilator Response in COPD

Ersan Atahan[1] 📍, Buket Caliskaner Ozturk[1] 📍, Suat Saribas[2] 📍, Bulent Tutluoglu[3] 📍

[1]Istanbul University-Cerrahpaşa, Cerrahpaşa Faculty of Medicine, Department of Pulmonary Diseases, Istanbul, Türkiye
[2]Istanbul University-Cerrahpasa, Cerrahpasa Faculty of Medicine, Department of Microbiology, Istanbul, Türkiye
[3]Acıbadem University, Acıbadem Faculty of Medicine, Department of Pulmonary Diseases, Istanbul, Türkiye

ABSTRACT

Objective: Chronic obstructive pulmonary disease (COPD) is described as partially reversible airflow limitation. P-glycoprotein (P-gp/MDR1), encoded by the Multidrug Resistance 1 (*MDR1*) gene, is regarded as a protective component for the respiratory tract and is present in tracheobronchial epithelium and lung parenchyma, and removes particles from cells and protects against various xenobiotics. Polymorphisms of *MDR1* gene and the alteration in the expression of P-gp are considered to have a negative effect on the severity of COPD pathogenesis and treatment efficacy. We aimed to investigate the relationship of the *MDR1* gene polymorphisms with reversibility in COPD patients.

Materials and Methods: The *MDR1* polymorphisms, specifically the 3435C>T and 2677A/G variations, were analyzed in 90 COPD patients.

Results: 15 of the 90 COPD patients had positive reversibility tests. 2677TT (p=0.044) and 3435TT (p=0.003) alleles related to positive reversibility tests. There were no significant differences in the distribution of the *MDR1* C3435 alleles and the G2677 alleles (p> 0.05).

Conclusion: COPD patients with the TT allele have a higher rate of early reversibility positivity; this suggests that those carrying the allele may respond better to bronchodilator therapy. These markers could help to distinguish COPD patients who respond better to β2-agonists or who may not benefit much and, therefore, need different drugs.

Keywords: COPD, MDR1, polymorphism

INTRODUCTION

Chronic obstructive pulmonary disease (COPD), which may cause considerable mortality and morbidity, is a significant health issue worldwide.[1] As an external factor, smoking may contribute to the progression of COPD by affecting the detoxification system and causing an imbalance in the protease-anti-protease system.[2] The airway epithelium protects from irritants breathed in and reduces the absorption of foreign substances.

The pulmonary epithelium of the airway is the first barrier for drug delivery following inhalation. The amount of target molecule that reaches the final site of action through the epithelium can be reduced by blood flow, absorption, surface binding, mucociliary clearance, and metabolism.[3] Transporters in the pulmonary epithelium, the first barrier for inhaled drugs, may play a vital role in delivering drugs administered by inhaler. The plasma membrane glycoprotein (P-gp) may limit the absorption of substances breathed in through the bronchial ep-

ithelium. P-gp expression occurs in ciliated collecting ducts and epithelial cells or bronchial glands in the human lung.[4] The presence and functions of many ABC transporters are essential for the application of drugs to the site of action, and multidrug resistance-associated protein 1 (MRP1) is amongst ATP binding cassette (ABC) transporters. However, changes in the Multidrug Resistance 1 (*MDR1*) gene's genetic structure or the alteration of P-gp expression may change its functions.[5]

The *MDR1* gene is located in human chromosome 7 and encodes P-gp (170-kDa). This P-gp belongs to the ABC transporters family, also named ABCB1. There are 28 exons (49 to 209 base pairs) in the *MDR1* gene, and it encodes an mRNA (4.5 kb). More than 50 SNPs and insertion/deletion polymorphisms were identified in the *MDR1* gene.[6] Most SNPs are silent (synonymous), and no change can be seen in the amino acid sequence. In the different ethnic populations, 1236C>T and 2677G>T/A/C polymorphisms were detected in the MDR1

gene. The most commonly seen polymorphism was 3435C>T.[7] Specifically, the C3435T single nucleotide polymorphism identified in exon 26 is considered to be associated with P-gp levels and substrate uptake.[8] Although some studies indicate the role of altered expression of P-gp and the *MDR1* gene polymorphisms for the development of respiratory diseases, their exact role and clinical relevance are not fully understood.

COPD is described as airflow limitation, and a full recovery is impossible. Treatments include bronchodilator drugs for these patients. Variabilities for bronchodilator response (BDR) in COPD patients may be associated with several factors such as age, baseline lung function, and eosinophil biomarkers.[9-11] Depending on these findings, the differences in COPD patients may be related to interindividual variability in the pharmacological response to bronchodilator drugs β2-agonist bronchodilators used for symptomatic treatment in COPD. Genetic variants that determine the bronchodilator response in COPD are being investigated. These markers could help to find COPD patients who respond better to β2-agonists or who may not benefit much and, therefore, need different drugs.

In this study, we aimed to investigate the relationship of the *MDR1* gene polymorphisms with reversibility in COPD patients.

MATERIALS AND METHODS

Study Design

A cross-sectional, real-life prospective study is compatible with the ethical guidelines of the Declaration of Helsinki and was approved by our Institutional Ethics Committee Board (No: 3773 Date: 06.02.2007). Each patient or their relatives gave signed informed consent forms.

Settings

Eligible patients were recruited between January 2010 and July 2010 in our department's COPD outpatient clinics.

Participants

Patients with COPD over 40 years of age who had stopped smoking at least five years ago were included in the study. The patients were in a stable period. Patients who had cancer, cardiac disease, and a COPD attack in the last three months were excluded from the study. Patients with a family history of atopy and allergic complaints with an eosinophil of more than 3% in plasma and patients with positive skin tests for allergies were excluded from the study.

Blood Analysis

Five ml of blood was collected from each patient. Blood samples taken in vacuum sterile K3-EDTA tubes were stored at -20°C, and their DNAs were isolated within the first week. DNA isolation was performed using the Roche DNA kit. The polymorphisms of *MDR1* C3435T and G2677T/As were detected by the PCR-RFLP method.

Pulmonary Function Tests

All subjects performed standardized spirometry according to European Respiratory Society guidelines. It was ensured that the patients did not use bronchodilator drugs for 24 h before the pulmonary function test. A pulmonary function test was performed 15-20 min after Salbutamol 400 mcg, and the response to the bronchodilator was measured by reversibility test. The reversibility test was considered positive if forced expiratory volume (FEV1) increased by 200 mL and the expected FEV1 percentage increased by 12%.

The COPD patients were divided into mild, moderate, and severe according to their FEV1 values. Those with FEV1>80% were assessed as mild, 80%>FEV1>50% as moderate, and those with FEV1<50% as severe. Patient groups were determined according to the GOLD 2005 update.

Study Size

Three groups of 30 patients, each with mild, moderate, and severe obstruction, were included in the study.

Statistical Analysis

All analyses were performed using Epi Info Software version 3.2.2 (CDC, Atlanta, GA). The MDR1 gene polymorphism distribution was compared using χ^2 or Fisher test. Significance was concluded with a p-value $\leq$ 0.05. When the p-value was < 0.05, the odds ratio with a 95% confidence interval was calculated.

RESULTS

Participants

150 consecutive COPD patients were studied. Sixty patients were excluded because they did not meet the criteria. Ninety patients with a smoking history of more than 20 packs/year participated in this study. Patients with mild, moderate and severe obstruction were adjusted to 30 people each, and patient recruitment was carried out.

Descriptive and Outcome Data

Subjects (n=90, M/F: 83/7) mean age was 62.3 ± 12.4 years. The smoking duration of the patients was 38.1 ± 19.4 packs/year. The patients' mean FEV1 and FEV1/FVC (Forced vital capacity) values were 1804 ± 444 ml and 55.6 ± 5.5%, respectively (Table 1).

The Polymorphisms of *MDR1* C3435T and G2677T/As

The allele frequencies for the C3435 single nucleotide polymorphism of the *MDR1* gene for COPD patients were detected and recorded (Table 2, Figure 1). C alleles distribution of the*MDR1* gene was found to be 47.7%, and T alleles were found to be 53.3%. CC alleles distribution of the MDR-1 was found (n:22) 33.3%, and CT and TT alleles were detected as (n:42) 51.1% and (n:26) 31.9%, respectively, in COPD patients. The allele frequencies for G2677 single nucleotide polymorphism of the MDR1 genes were determined (Table 3, Figure 2). The *MDR1* gene G allele distribution was 49.4%, the T allele was 87.3%, and the A allele was 0.2% in the COPD group. The MDR genotype distribution was found to be 24.4% for GG, 46.7% for GT, 24.4% for TT, 0.3% for GA, and 0.1% for TA in the COPD group.

Early reversibility test was positive in six patients with mild obstruction, five with moderate obstruction, and four with severe obstruction (a total of 15). No statistical difference was detected between the COPD groups. Significant differences were found between the C3435 polymorphism distribution and the G2677 polymorphism distribution between reversibility positive (n:15) and negative groups (n:75) (Table 4).
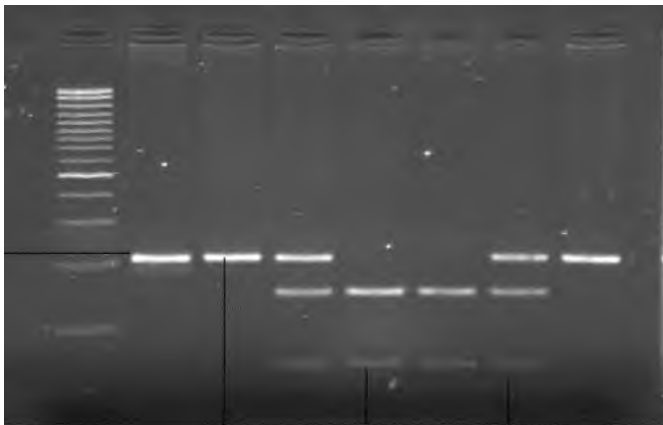
Figure 1. Agarose gel images of *MDR1* polymorphism C3435T genotypes.

DISCUSSION

P-gp protein is vital in decreasing the toxic effect of smoking and removing oxidative stress metabolites.[12] It was found that the bronchial epithelium of COPD patients has been shown to have small quantities of MDR proteins.[13] It was suggested that the *MDR1* gene may interfere with the progression of COPD by detoxification and inflammatory mechanisms. At the site of action, some multidrug resistance proteins may behave like drug efflux pumps, causing a decrease in intracellular concentrations of toxic compounds.[14] These transporters, such as P-glycoprotein and other MDR proteins, are expressed strongly
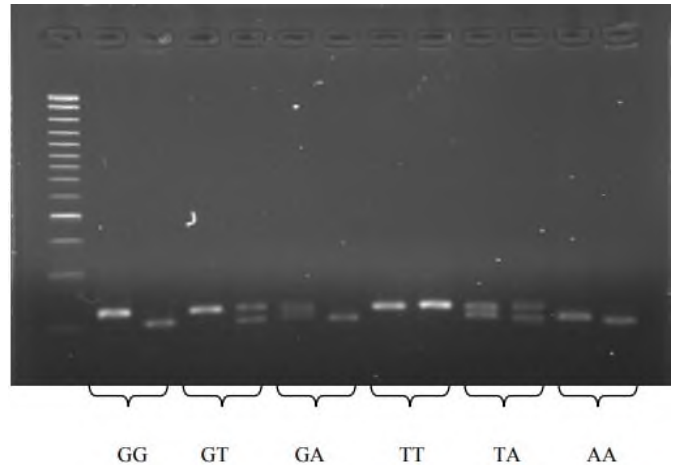
Figure 2. Agarose gel images of *MDR1* polymorphism G2677T genotypes.

in the respiratory tract. They may help prevent harmful substances from getting into the lungs, whether inside or outside the body.[15]

Other studies have also shown that the SNPs of the MDR1 gene affect how drugs are absorbed, distributed, and eliminated in the body.[16,17] The effects or clinical implications of these polymorphisms on P-gp function are often unknown. However, some of the SNPs have a functional role and can affect how drugs are metabolized in the body. The C3435T, G2677T/A, and C1236T polymorphisms have been studied for exon 26, 21, and 12, respectively, in different populations.[18,19] The importance of the *MDR1* gene polymorphisms and the alteration in the expression level of P-gp protein for respiratory diseases is still not fully understood. Still, researchers suggest that the MDR1 gene polymorphism can be clinically significant for the pathogenesis of COPD.[20] The TT genotype was detected frequently for the C3435 *MDR1* gene in COPD patients, and the *MDR1* gene C/T polymorphism is suggested to have a role in the progression of COPD.[21] We did not find significant differences in the distribution of the *MDR1* gene C3435 alleles and G2677 alleles in our study population. A silent polymorphism (the C3435T SNP) of the *MDR1* gene in exon 26 may cause protein synthesis with the same amino acid sequence but not the same structural and functional properties. Some studies have suggested that certain disease conditions may develop and worsen because of silent SNPs.[22] It is known that airflow obstruction is generally not reversible in COPD. The relationship between many factors and early reversibility in COPD was investigated. It has been shown that the proportion of eosinophils in bronchoalveolar lavage fluid and continued smoking are associated with response to bronchodilator drugs. Hemopoietic cell kinase and β2-adrenergic receptor gene polymorphisms are suggested to be associated with BDR in COPD patients.[23,24] On the other hand, the genetic determinants of BDR in COPD patients are not known. In our study, 15 of 90 COPD patients had positive

Table 1. Clinical parameters in patients with COPD severity. **FEV1:**Forced expiratory volume; **FVC:** Forced vital capacity; **MEFR:**The maximum expiratory flow rate.

	FEV1/FVC %	FEV1 (mL)	FEV1 %	FVC (mL)	FVC %	MEFR (mL)
Mild COPD	65	2590	86	3980	106	1383
Moderate COPD	61	1894	65	3083	86	958
Severe COPD	41	928	32	2246	62	352

Table 2. Distribution of C3435 polymorphism in patient group.

	Mild obstruction n=30	Moderate obstruction n=30	Severe obstruction n=30	p
C/C	8 (26.7 %)	8 (26.7 %)	6 (20 %)	>0.05
C/T	14 (46.6 %)	14 (46.6 %)	14 (46.6 %)	
T/T	8 (26.7 %)	8 (26.7 %)	10 (33.3 %)	
C	30 (50 %)	30 (50 %)	26 (43.3 %)	>0.05
T	30 (50 %)	30 (50 %)	34 (56.7 %)	

Table 3. Distribution of G2677 polymorphism in patient group.

	Mild obstruction n=30	Moderate obstruction n=30	Severe obstruction n=30	p
G/G	7 (23.3 %)	9 (30 %)	6 (20 %)	>0.05
G/T	15 (25 %)	14 (46.7 %)	13 (43.3 %)	
T/T	7 (23.3 %)	6 (20 %)	9 (30 %)	
G/A	0	1 (3.3 %)	2 (6.7 %)	
T/A	1 (1.7 %)	0	0	
G	29 (48.3 %)	33 (55 %)	27 (45 %)	>0.05
T	30 (50 %)	26 (43.3 %)	31 (51.7 %)	
A	1 (1.7 %)	1 (1.7 %)	2 (0.3 %)	

Table 4. Distribution of *MDR1* polymorphism in patient group.

Polymorphism	n	*Frequency of Allele*
MDR1 3435		
C/C	4 (26.6 %)	**C allele:** 33.3 %
C/T	2 (13.3 %)	**T allele:** 66.6 **%**
T/T	9 (60 %)	
MDR1 2677		
G/G	2 (13.3 %)	**G allele:** 26.6 %
G/T	3 (20 %)	**T allele:** 66.6 %
T/T	8 (53.3 %)	**A allele:** 6.6 %
G/A	1 (6.6 %)	
T/A	1 (6.6 %)	

reversibility tests. 2677TT (p=0.044) and 3435TT (p=0.003) alleles related to positive reversibility test.

Recent indications in the literature indicate that polymorphisms of the *MDR1* gene play an essential role in the pathogenesis and treatment of respiratory diseases.[13] In addition, in studies conducted in Turkey, it was determined that the TT genotype of the *MDR1* gene was significantly more common in COPD patients.[20,25]

A study showed that there was no significant difference between the genotypes of healthy individuals and the control group consisting of patients with chronic obstructive pulmonary disease and comorbid type 2 diabetes.[26]

The strength of this study is this issue is a point that can guide COPD treatment. A strength of our research is that it raises awareness that specific genetic variations affect people's response to bronchodilators and that bronchodilator sensitivity may differ between different types of COPD. The limitation of this study is a few patients have been included, which is insufficient to draw a clear conclusion about MDR1 genotyping's clinical relevance for treating COPD patients.

CONCLUSION

Our results suggest that bronchodilator responsiveness phenotypes in COPD patients were linked to variations in the *MDR1* C3435 and 2677 genes. Various factors may influence how COPD patients respond to bronchodilators, such as different disease subtypes, how they break down drugs, or other effects related to their genes. The following steps are to repeat this study in diverse populations, identify the specific genetic variations that affect how people respond to bronchodilators, and investigate whether bronchodilator responsiveness varies across different types of COPD. Extensive population studies with more patients are needed to investigate this.

ORCID IDs of the authors

Ersan Atahan	0000-0002-2993-243x
Buket Caliskaner Ozturk	0000-0001-5514-1108
Suat Saribas	0000-0002-4549-3887
Bulent Tutluoglu	0000-0002-1332-9927

REFERENCES

1. Mathers CD, Loncar D. Projections of global mortality and burden of disease from 2002 to 2030. *PLoS Med*. 2006;3(11):e442. doi: 10.1371/journal.pmed.0030442.

2. Global strategy for the diagnosis, management, and prevention of chronic obstructive pulmonary disease (updated 2022). GOLD. Available from: https://goldcopd.org/wp-content/uploads/2019/12/GOLD-2020-FINAL-ver1.2-03Dec19_WMV.pdf

3. Hamilton KO, Yazdanian MA, Audus KL. Contribution of efflux pump activity to the delivery of pulmonary therapeutics. *Curr Drug Metab*. 2002;3(1):1-12.

4. Lechapt-Zalcman E, Hurbain I, Lacave R, et al. MDR1-Pgp 170 expression in human bronchus. *Eur Respir J*. 1997;10(8):1837-1843.

5. Scheffer GL, Pijnenborg AC, Smit EF, et al. Multidrug resistance related molecules in human and murine lung. *J Clin Pathol*. 2002;55(5):332-339.

6. Hoffmeyer S, Burk O, von Richter O, et al. Functional polymorphisms of the human multidrug-resistance gene: multiple sequence variations and correlation of one allele with P-glycoprotein expression and activity *in vivo*. *Proc Natl Acad Sci USA*. 2000;97(7):3473-3478.

7. Cascorbi I, Gerloff T, Johne A, et al. Frequency of single nucleotide polymorphisms in the P-glycoprotein drug transporter MDR1 gene in white subjects. *Clin Pharmacol Ther*. 2001;69(3):169-174.

8. Tang K, Wong LP, Lee EJ, Chong SS, Lee CG. Genomic evidence for recent positive selection at the human MDR1 gene locus. *Hum Mol Genet*. 2004;13(8):783-797.

9. Lehmann S, Bakke PS, Eide GE, Humerfelt S, Gulsvik A. Bronchodilator reversibility testing in an adult general population; the importance of smoking and anthropometrical variables on the response to a beta2-agonist. *Pulm Pharmacol Ther*. 2006;19(4):272-280.

10. Schermer T, Heijdra Y, Zadel S, et al. Flow and volume responses after routine salbutamol reversibility testing in mild to very severe COPD. *Respir Med*. 2007;101(6):1355-1362.

11. Miller M, Ramsdell J, Friedman PJ, Cho JY, Renvall M, Broide DH. Computed tomographic scan-diagnosed chronic obstructive pulmonary disease-emphysema: Eotaxin-1 is associated with bronchodilator response and extent of emphysema. *J Allergy Clin Immunol*. 2007;120(5):1118-1125.

12. Izzotti A, Cartiglia C, Longobardi M, et al. Alterations of gene expression in skin and lung of mice exposed to light and cigarette smoke. *FASEB J*. 2004;18(13):1559-1561.

13. Milojkovic M, Milacic N, Radovic J, Ljubisavljevic S. MDR1 gene polymorphisms and P-glycoprotein expression in respiratory diseases. *Biomed Pap Med Fac Univ Palacky Olomouc Czech Repub*. 2015;159(3):341-346.

14. Ishikawa T, Hirano H, Onishi Y, Sakurai A, Tarui S. Functional evaluation of ABCB1 (P-glycoprotein) polymorphisms: High-speed screening and structure-activity relationship analyses. *Drug Metab Pharmacokinet*. 2004;19(1):1-14.

15. Schwab M, Eichelbaum M, Fromm MF. Genetic polymorphisms of the human MDR1 drug transporter. *Annu Rev Pharmacol Toxicol*. 2003;43:285-307.

16. Papp E, Gadawski I, Côté HC. Longitudinal effects of thymidine analogues on mtDNA, mtRNA and multidrug resistance (MDR-1) induction in cultured cells. *J Antimicrob Chemother*. 2008;61(5):1048-1052.

17. Israeli D, Ziaei S, Gonin P, Garcia L. A proposal for the physiological significance of mdr1 and Bcrp1/Abcg2 gene expression in normal tissue regeneration and after cancer therapy. *J Theor Biol*. 2005;232(1):41-45.

18. van der Deen M, Marks H, Willemse BW, et al. Diminished expression of multidrug resistance-associated protein 1 (MRP1) in bronchial epithelium of COPD patients. *Virchows Arch*. 2006;449(6):682-688.

19. Gümüş-Akay G, Rüstemoğlu A, Karadağ A, Sunguroğlu A. Genotype and allele frequencies of MDR1 gene C1236T polymorphism in a Turkish population. *Genet Mol Res*. 2008;7(4):1193-1199.

20. Dogan OT, Katrancioglu N, Karahan O, Sanli GC, Zorlu A, Manduz S. Frequency of the mdr-1 C>T gene polymorphism in patients with COPD. *Clinics (Sao Paulo)*. 2010;65(11):1115-1117.

21. Toru U, Ayada C, Genç O, Turgut S, Turgut G, Bulut I. MDR-1 gene C/T polymorphism in COPD: Data from Aegean part of Turkey. *Int J Clin Exp Med*. 2014;7(10):3573-3577.

22. Kimchi-Sarfaty C, Oh JM, Kim IW, et al. A "silent" polymorphism in the MDR1 gene changes substrate specificity. *Science*. 2007;315(5811):525-528.

23. Zhang X, Mahmudi-Azer S, Connett JE, et al. Association of Hck genetic polymorphisms with gene expression and COPD. *Hum Genet*. 2007;120(5):681-690.

24. Hizawa N, Makita H, Nasuhara Y, et al. Beta2-adrenergic receptor genetic polymorphisms and short-term bronchodilator responses in patients with COPD. *Chest*. 2007;132(5):1485-1492.

25. Toru U, Ayada C, Genç O, Turgut S, Turgut G, Bulut I. MDR-1 gene C/T polymorphism in COPD: Data from Aegean part of Turkey. *Int J Clin Exp Med*. 2014;7(10):3573-3577.

26. Chernetska NV, Stupnytska HY, Fediv OI. The role of MDR1 (C3435T) gene polymorphism in patients with chronic obstructive pulmonary disease associated with type 2 diabetes mellitus. *J Med Life*. 2020;13(3):349-355.

RESEARCH ARTICLE

In Silico Evaluation of ERQ Bioactive Tripeptide as an Anticancer Agent and an Inhibitor of SARS-CoV-2 Enzymes

Gozde Yilmaz[1] (ID), Sefa Celik[2] (ID), Aysen Erbolukbas Ozel[2] (ID), Sevim Akyuz[3] (ID)

[1]Istanbul University, Institute of Graduate Studies in Sciences, Istanbul, Türkiye
[2]Istanbul University, Science Faculty, Physics Department, Istanbul, Türkiye
[3]Istanbul Kultur University, Science and Letters Faculty, Physics Department, Atakoy Campus, Bakirkoy, Istanbul, Türkiye

ABSTRACT

Objective: Short peptides play a significant role in exploring drugs with higher selectivity and fewer side effects in cancer and COVID-19 therapies. This study evaluated the anticancer and anti-COVID-19 activities of Glu-Arg-Gln (ERQ) tripeptide for the first time. To discover the potentiality of the tripeptide as an anticancer and as a SARS-CoV-2 inhibitor, molecular docking analysis of ERQ tripeptide with DNA (PDB ID: 1BNA) and a variety of SARS-CoV-2 enzymes, namely. Main protease (PDB IDs: 6M03, 6LU7) and Spike glycoprotein (PDB ID: 6VXX) were performed.

Materials and Methods: To determine the binding efficiency of ERQ to target DNA and proteins, molecular docking processes were carried out using the Autodock Vina program. The sorts of bonds and interacting residues in ERQ/DNA and ERQ/protein complexes were determined.

Results: Molecular docking simulations of ERQ tripeptide against 1BNA, 6M03, 6LU7, and 6VXX were performed, and the interactions between the docked ligand and target residues were determined. The binding mechanisms of ERQ with the receptors were clarified. The binding affinities of ERQ towards the targets were predicted to be between -6.3 and -6.7 kcal/mol. ERQ showed the highest binding affinity to Spike glycoprotein (6VXX), with an estimated binding energy of -6.7 kcal/mol.

Conclusion: Molecular docking simulations revealed the potential of ERQ tripeptide as an anticancer and anti-COVID-19 agent. High binding affinity against 1BNA (-6.4 kcal/mol), 6M03 (-6.3 kcal/mol), 6LU7 (-6.6 kcal/mol), and 6VXX (-6.7 kcal/mol) indicated that ERQ could be an excellent new natural therapy for the treatment of cancer and COVID-19.

Keywords: *In silico,* Molecular docking, Glu-Arg-Gln, ERQ, Tripeptide

INTRODUCTION

Cancer is a study topic susceptible to novel techniques in developing drugs because it is a lethal disease.[1] The medications employed in conventional cancer treatment damage both healthy and cancerous cells.[2] During chemotherapy treatment, patients may have adverse effects, including depression, hair loss, and nausea.[2] As anticancer medicines, peptides with low toxicity against these side effects are essential.[3,4] Special drug carriers with peptide structures are currently being studied and developed as an alternative to conventional chemotherapy treatment approaches.[1-4] Activator protein 1 (AP-1) regulates the expression of essential oncogenes in cancer and many other cellular processes.[4,5] AP-1, which has a vital role in cancer, also plays an important role in diseases such as psoriasis, asthma, and rheumatoid arthritis[5] and has been the subject of research in

drug production due to its active roles.[5,6] Kumar et al. performed molecular docking calculations to evaluate the activity of the Glu-Glu-Arg tripeptide on the AP-1 (c-Jun:c-Fos: DNA) complex.[6] It was found that Glu-Glu-Arg has a strong affinity towards AP-1 (-9.1 kcal/mol). Thus, the Glu-Glu-Pro tripeptide was determined to be a potent anticancer candidate and can prevent the division of cancer cells.

The molecular docking method used in drug design research investigates the interaction between receptor and ligand[7], the formation of hydrogen bonds, Coulomb interactions, and van der Waals interactions that affect the ligand-receptor binding potential.[8]

DNA plays a significant role in controlling cellular functions; for this reason, it is considered an excellent target for treating genetic diseases, particularly cancer. Moreover, due to the rapid

proliferation of cancer cells, most anticancer drugs target the cell cycle. The structural changes that occur by binding of a ligand to DNA affect the biological functions of DNA, including the inhibition of transcription, replication, and DNA repair processes, thus making the ligand a potential antitumor agent.[9]

On the other hand, SARS-COV-2, main protease (M[pro]), and spike proteins are essential targets for promising anti-COVID-19 agents. In a study to determine the anthraquinone derivative's ability to prevent SARS-CoV-2 infection, Celik et al. carried out molecular docking analyses against the apo- and holo-forms of the significant protease (Mpro) and the spike glycoprotein of SARS-CoV-2 targets.[10] Molecular structure and molecular docking have yet to be published for the ERQ tripeptide. This work used molecular docking models to simulate the action of the ERQ tripeptide against DNA(1BNA), SARS-CoV-2 proteases (6M03, 6LU7), and spike glycoprotein (6VXX) to evaluate its anticancer and anti-COVID-19 properties.

MATERIALS AND METHODS

Compound Selection and Preparation

The 3D molecular structures of the SARS-CoV-2 main protease (6M03,6LU7), Spike glycoprotein (6VXX) and DNA (1BNA) were taken from the Protein Data Bank.[11]

Conformational Analysis

Using quantum chemical computations and molecular mechanics, Spartan is an effective computational modeling method for investigating organic, bioorganic, inorganic, and organometallic chemistry in academic and research fields. The Molecular Mechanics Force Field (MMFF) method[12] with Spartan06[13] program was used to determine the conformational features of ERQ (Glu-Arg-Gln) tripeptide. The determined optimized lowest energy conformer of ERQ in the gas phase by the MMFF method was taken as the initial ligand structure for molecular docking. During the molecular docking simulations, the ligand was taken as flexible.

Molecular Docking

In this study, docking simulations of ERQ tripeptide were performed using the AutoDock-Vina software program.[14] A semi-flexible docking study was carried out, where ERQ was treated as a flexible ligand by modifying its rotatable torsions, but the target DNA or protein was considered a rigid receptor. The crystal structure of DNA (PDB ID: 1BNA)[15], the crystal structures of COVID-19 main protease, in apo form (PDB ID: 6M03)[16] and in complex with N3 (PDB ID: 6LU7)[17], and the crystal structure of SARS-CoV-2 spike glycoprotein (closed state) (PDB ID: 6VXX)[18] were retrieved from protein data bank. The

DNA and protein targets were conformed to the docking by removing water molecules and adding polar hydrogens. The optimized structure of the ERQ ligand molecule in the gas phase was adapted for the docking. The partial charges of the ERQ molecule were calculated using the Geistenger method. The active sites of receptors were screened using the CAVER program[19], and then the active sites of the targets were defined within the grid size of 40Åx40Åx40Å.

RESULTS

Three-Dimensional Structure of the ERQ Tripeptide

In the first step of the study, the conformational features of the ligand were searched by the MMFF method, and all the conformers were optimized. Among the 2601 optimized conformers, the lowest energy conformer was taken as the initial structure for docking. The optimized structure of the tripeptide is shown in Figure 1. The selected bond lengths and angles from the obtained structural parameters of the ERQ tripeptide are given in Table 1.
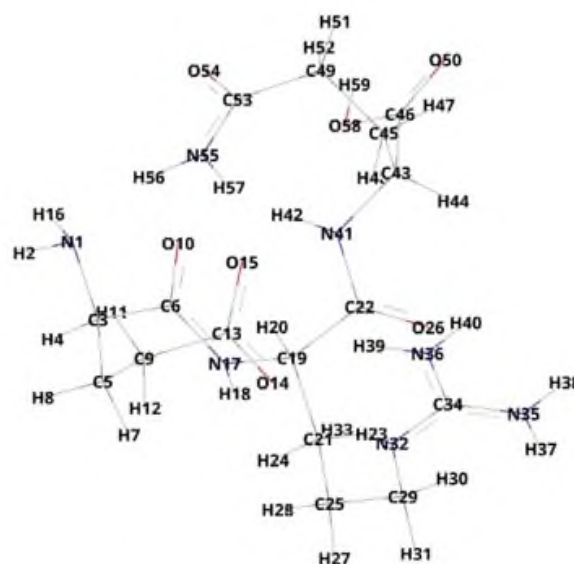
Figure 1. Optimized structure of ERQ tripeptide.

Molecular Docking Calculations

Molecular docking, an effective drug design and discovery method, reveals bimolecular interactions between the target protein and the docked ligand. To investigate anticancer and anti-COVID-19 properties of the investigated tripeptide (ERQ), it was docked in the determined binding site of DNA (1BNA), SARS-CoV-2 Mpro (6M03, 6LU7) and Spike glycoprotein (6VXX). The molecular docking results and molecular interactions are shown in Figures 2-5.

Table 1. The selected geometry parameters of ERQ tripeptide (Glu-Arg-Gln).[*]

Atoms		Atoms	
C6-O10	1.24	C6-N17-C19-C21	150.6
C13-O14	1.26	N17-C19-C21-C25	48.7
C13-O15	1.27	C19-C21-C25-C29	74.7
C22-O26	1.23	C21-C25-C29-N32	-82.4
C46-O50	1.22	C25-C29-N32-C34	154.8
C46-O58	1.35	C6-N17-C19-C22	-79.2
C53-O54	1.14	N17-C19-C22-N41	51.8
H2-N1-C3-C5	48.5	C19-C22-N41-C43	165.5
H2-N1-C3-C6	-179.1	C22-N41-C43-C46	-102.3
N1-C3-C5-C9	46.5	C22-N41-C43-C45	131.1
C3-C5-C9-C13	58.3	N41-C43-C45-C49	79.7
C3-C6-N17-C19	-175.7	C43-C45-C49-C53	-59.7

* Bond lengths in A and angles in degree (°). For atom numbering, see Figure 1.

ERQ tripeptide was docked to DNA to reveal its anticancer property. Figure 2 shows the docking results and the interactions of the tripeptide with DNA. The binding affinity (ΔG) was predicted as -6.4 kcal/mol. H- bonding is crucial in the interaction between the tripeptide and DNA bases. The ERQ tripeptide formed nine conventional hydrogen bonds with the DNA bases. These are hydrogen bond of 2.53 Å with DNA, DG2 nucleobase; hydrogen bond of 2.39 Å with DG4; hydrogen bond of 2.47 Å, with DA5; hydrogen bond of 1.91 Å with DC21; hydrogen bonds of 2.17, 2.26 and 2.46 Å with DG22; hydrogen bonds of 2.54 Å and 2.68 Å with DA6. There is also an unfavorable donor-donor interaction and a carbon-hydrogen bonding interaction with DA5 and DA6 bases with 2.03 Å and 3.74 Å longs, respectively.

The docking results of ERQ tripeptide into 6M03 are shown in Figure 3. Tripeptide forms seven conventional hydrogen bonds with the target residues. The bond lengths predicted for the hydrogen bonds between the ERQ ligand and the THR24, LEU141, ASN142, and GLY143 residues of 6M03 are 2.32, 2.59, 2.46, and 2.84 Å, respectively. Additionally, ERQ forms three conventional hydrogen bonds with GLU166 residue of 6M03, with the predicted bond lengths 2.12, 2.16, and 2.76 Å. ERQ tripeptide also involves 1.58 Å long unfavorable donor-donor interaction with HIS163, 3.53 Å long carbon-hydrogen bonding interaction with MET165, and 3.26 Å long unfavorable negative-negative interaction with GLU166.

Figure 4 displays the ERQ tripeptide's docking results into 6LU7. As seen from Figure 4, the predicted lengths of the hydrogen bonds formed between the docked ligand ERQ and the 6LU7 target residues HIS41, TYR54, ASN142, GLY143, HIS164, GLU166 are 2.49, 2.55, 2.55, 2.13, 2.8, 2.59 Å, respectively. Moreover, docking results demonstrated that ERQ forms two hydrogen bonds with both PHE140 and CYS145 residues with bond lengths of 2.34Å, 2.49 Å, and 2.93Å, 3.62Å, respectively. In addition, ERQ forms a 2.72 Å long salt bridge

interaction with GLU166 and an unfavorable donor-donor and attractive charge interactions with HIS41, at 1.77 Å and 5.58 Å bond lengths, respectively.

Figure 5 displays the results of the docking calculation for the ERQ-6VXX ligand-receptor system in which hydrogen bonding is predicted between the ERQ ligand and the GLU780, ASN1023, THR1027, LYS1028, VAL1040 residues; the corresponding hydrogen bond lengths were calculated as 2.9 Å, 2.46 Å for GLU780; 2.28 Å, 2.31 Å for ASN1023; 2.18 Å, 2.31 Å for THR1027; 2.28 Å for LYS1028; 2.71, 3.04 Å for VAL1040. Also, docking results indicate carbon-hydrogen bonds of 3.42 Å and 3.53 Å are formed through ASP1041 and PHE1042 residues. In comparison, an attractive charge interaction in a distance of 4.16 Å and an unfavorable negative-negative interaction in a distance of 4.78 Å exist between the ligand and GLU780 residue.

DISCUSSION

As we noted in the result part, the interactions resulting from DNA docking with the ERQ tripeptide were compared with similar studies in the literature. As a result of these comparisons, it was determined that the DNA nucleobases with which the ERQ tripeptide interacts in this study were the same as those in the study conducted by Demirag et al., docking analysis of the Pemetrexed molecule with DNA.[20]

A comparison of the hydrogen bonding interactions previously reported for the Pemetrexed-DNA system with those reported in this study for the ERQ-DNA system has been given here as items. i) A hydrogen bond of 2.05 Å length was reported between the Pemetrexed ligand and DG2 residue, and here we report a hydrogen bond of 2.53 Å length for the ligand ERQ and DG2 residue. ii) A hydrogen bond of 2.48 and 2.97 Å length was reported between the Pemetrexed ligand and DG4 residue,
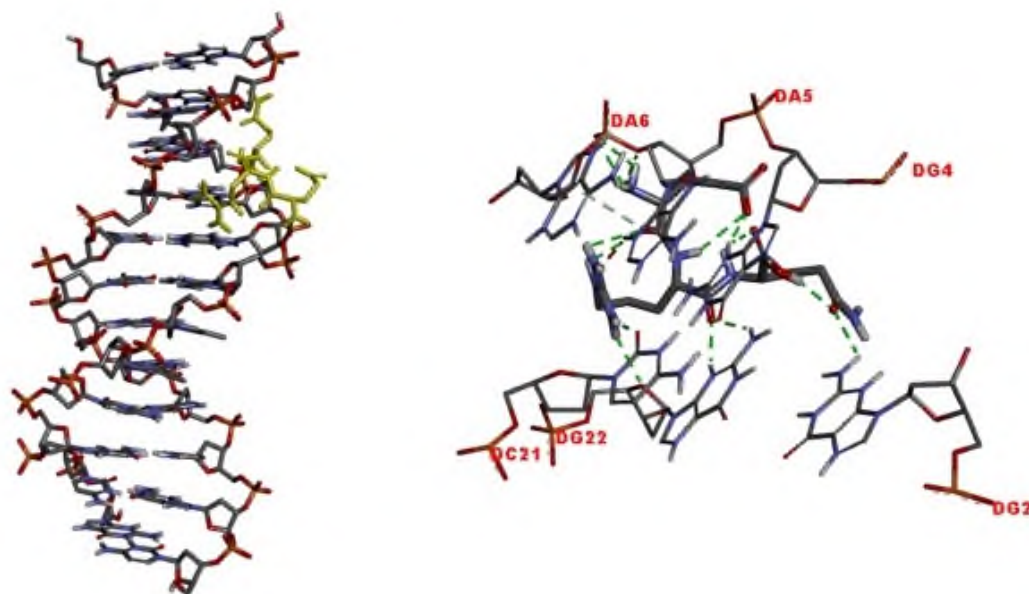
Figure 2. Molecular docking results were obtained for the ERQ-1BNA ligand-receptor system; the corresponding binding affinity is -6.4 kcal/mol.
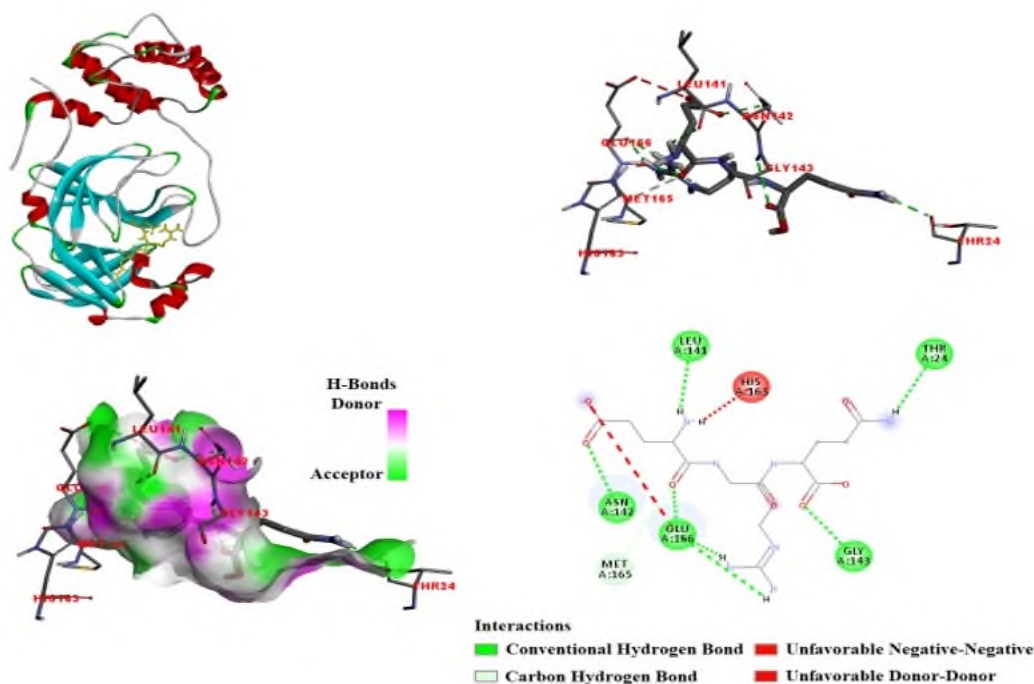
Figure 3. Molecular docking results were obtained for the ERQ-6m03 ligand-receptor system; the corresponding binding affinity is -6.3 kcal/mol.

and we report a hydrogen bond of 2.39 Å length for the ligand ERQ and DG4 residue. iii) A hydrogen bond of 2.16 Å length was reported between the Pemetrexed ligand and DA5 residue, and here we report a hydrogen bond of 2.47 Å length for the ligand ERQ and DA5 residue. iv) Hydrogen bonds of 1.91 Å and 3.03 Å length were reported between the Pemetrexed ligand

and the DT20, and DC21 residues respectively, and we report a hydrogen bond of 1.91 Å length between the ligand ERQ and DC21 residue. v) Hydrogen bonds of 2.49 Å and 3.09 Å length were reported between the Pemetrexed ligand and DG22 residue, and here we report hydrogen bonds of 2.17 Å, 2.26 Å and 2.46 Å length for the ligand ERQ and DG22 residue. The

Figure 4. Molecular docking results were obtained for the ERQ-6lu7 ligand-receptor system; the corresponding binding affinity is -6.6 kcal/mol.

Figure 5. Molecular docking results were obtained for the ERQ-6vxx ligand-receptor system; the corresponding binding affinity is -6.7 kcal/mol.

other hydrogen bonds reported for the Pemetrexed (drug)-DNA system are as follows; The H-bond contact length between the DC23 residue and the drug is 2.93 Å, the carbon hydrogen bond interaction length between the DG4 residue and the drug is 3.49 Å, the unfavorable donor-donor interaction length is 1.72 Å, and the Pi Donor hydrogen bond interaction length is 2.76 Å between the DG4 residue and the drug.[20] This similarity between the results previously reported for the Pemetrexed-DNA system

and those reported here for the ERQ-DNA system supports the reliability of our docking simulations.

Molecular docking simulations of ERQ tripeptide against 6M03 were performed and compared with similar studies. In the study conducted by Sagaama et al., a molecular docking simulation of Succinic acid (SA) with 6m03 was performed, and found that SA interacted with Ser144, Cys145, and Glu166 through hydrogen bonding interactions.[21] In another study conducted by Begum et al., tetrandrine, a bis-benzylisoquinoline alkaloid, was docked with a 6m03 receptor and binding free energy -8.91 kcal/mol was determined. Tetrandrine was highly stabilized by many non-bonded interactions.[22] Tetrandrine, bonded to the His-165 residue by hydrogen bonding interaction. The hydrophobic contacts of the tetrandrine molecule were demonstrated by Thr-25, Leu-27, His-41, Ser-46, Met-49, Asn-142, Cys-145, Glu-166, and Gln-189.

Another investigation on the relationship between aminopterin and 6M03 was carried out.[23] The binding affinity was recorded as -6.7 kcal/mol and aminopterin was bonded with THR24, THR26, ASN119, Leu141, Gly143, Cys145, and Gln189 with eight conventional hydrogen bonds, Asn142 (It was determined that it forms a carbon-hydrogen bond with a length of 3.44 Å). Additionally, pi-sigma and pi-alkyl interactions with Thr27 and Cys145, respectively, were present.[23]

The docking results on the 6m03 receptor have confirmed that the ERQ tripeptide interacts with certain residues identical to those previously reported for the 6m03 receptor in literature. This consistency supports the reliability of our docking simulations for the ERQ-6m03 ligand-receptor system. In this respect, the determined hydrogen bond lengths (2.32 Å for Thr24; 2.59 Å for Leu141; 2.46 Å for Asn142; 2.84 Å for Gly143; 2.12, 2.16 and 2.76 Å for Glu166) are remarkable. In addition, it should be noted that in the same ligand-receptor system, ERQ tripeptide forms a carbon-hydrogen bond of 3.53 Å length with the residue Met165 and involves in an unfavorable donor-donor interaction with the residue His163 (in a distance of 1.58 Å) and in an unfavorable negative-negative interaction with Glu166 (in a distance of 3.26 Å). It is believed that the main protease (M^{Pro}) amino acids HIS41, CYS44, MET49, SER144, CYS145, and GLU166 are crucial for interactions between drugs and receptors.[24]

According to the results of the comparison of ERQ tripeptide docking into 6LU7 results with similar studies in the literature: In a study conducted by Özdemir et al. in 2020, the different interactions between coumarins and the receptor's (6LU7) active site residues are shown and tabulated.[25] It is shown that one of the fluorines and the hydroxy group at position C-7 created a hydrogen bond with TYR54 and PHE140, respectively. Furthermore, a π-alkyl bond was established by one of the fluorines with HIS41. TYR54 and PHE140 have hydrogen bond lengths of 2.725 Å and 2.201 Å, respectively. And Hatada et al., (B), it was discovered that the pharmacophore's hydrogen bonding

with neighboring residues was significant for each of the five pieces.[26] The ligand's fourth portion was found to be the key component in interactions with His163, His164, and Glu166. It was also shown that dispersion interactions—like the CH/π contact with His41—provided further ligand stability. It was proposed that the ligand's fifth component may be further optimized for ligand binding to facilitate interactions with Thr25, Thr26, and Asn142 in addition to His41. Additionally, the impact of the covalent connection between the ligand and Cys145 was examined.[26] According to this study, hydrogen bonding is the primary mechanism by which His41, His163, His164, and Glu166, amino acid residues of Mpro interact with the inhibitor are shown.[26] In this study, the primary protease (MPRO) amino acids Tyr54, Asn142, Gly143, His164, Glu166, Phe140, Cys145, and His41 are the interacting amino acids. This is also compatible with the literature.

Molecular docking simulations of ERQ tripeptide against spikeglycoprotein (6VXX) were performed and compared with similar studies. In the following, these comparisons over some similar studies in the current literature are seen. In the study, in which the molecular docking analysis of cepharanthine with the residue 6vxx is given, the authors report that the cepharanthine molecule interaction with the residues Glu725 (2.69Å), Gln784 (3.52 Å), Ala1026 (4.16 Å), Asp1041 (3.11 Å), Phe1042 (3.44 Å), Lys1045 (2.64 Å) and its binding affinity is -9.7 kcal/mol.[27]

The residues Val1040, Asp1041, Leu1049, Val1068, Asn907, and Lys1038 have a significant attraction for the ligand, and they may serve as anchoring residues, as shown by Holanda et al.[28] In docked complex analysis, two residues, Arg (1039) and Asn (1023), show hydrogen bond formation with Amentoflavone with a range of 2.0 to 3.5 A, according to Joshi et al. (C), with 6VXX (Spike protein).[29] In the molecular docking simulations performed in this study, the ERQ tripeptide is involved in interaction against the receptor 6VXX through the Glu780, Asn1023, Thr1027, Val1040, Lys1028, Asp1041, and Phe1042 amino acids.

Based on the molecular docking data, we obtained in this study and also considering those previously published in relevant studies in the literature, we concluded that the amino acids through which the ligand ERQ interacts with DNA (1BNA), SARS-CoV-2 Mpro (6M03, 6LU7) and Spike glycoprotein (6VXX) are almost similar (shown in bold).

CONCLUSION

In this molecular docking study, in which the ERQ tripeptide was docked with DNA and several SARS-CoV-2 enzymes, including the Main protease and Spike glycoprotein, the ERQ tripeptide's potential as an anticancer and SARS-CoV-2 inhibitor was investigated. ERQ docked with 6vxx compound showed the highest binding affinity, demonstrating a binding energy value of -6.7 kcal/mol against the active site of Spike

glycoprotein (6VXX). It showed nine H-bonds with GLU780, ASN1023, THR1027, LYS1028, and VAL1040, two Carbon-hydrogen interactions with ASP1041 and PHE1042, as well as an attractive charge interaction, and an unfavorable negative-negative interaction with GLU780 residues. Considering these promising docking simulation outcomes with the SARS CoV-2 Spike glycoprotein (6VXX), we recommend that Glu-Arg-Gln (ERQ) tripeptide be tested to discover new natural therapies for the treatment of COVID-19. This study is a novel, effective, and time-saving in silico study of short peptides against both COVID-19 and cancer drug discovery.

Ethics Committee Approval: Ethics committee approval is not required for the study.

Peer Review: Externally peer-reviewed.

Author Contributions: Conception/Design of Study- G.Y, S.C., A.E.O., S.A.; Data Acquisition- G.Y, S.C., A.E.O., S.A. ; Data Analysis/Interpretation- G.Y, S.C., A.E.O., S.A.; Drafting Manuscript- G.Y, S.C., A.E.O., S.A.; Critical Revision of Manuscript- G.Y, S.C., A.E.O., S.A. ; Final Approval and Accountability- G.Y, S.C., A.E.O., S.A.

Conflict of Interest: Authors declared no conflict of interest.

ORCID IDs of the authors

Gozde Yilmaz	0000-0002-8000-2385
Sefa Celik	0000-0001-6216-1297
Aysen Erbolukbas Ozel	0000-0002-8680-8830
Sevim Akyuz	0000-0003-3313-6927

REFERENCES

1. Nikfar Z, Shariatinia Z. The RGD tripeptide anticancer drug carrier: DFT computations and molecular dynamics simulations. *J Mol Liq.* 2019;281:565-583.

2. Sun A, Shoji M, Lu YJ, Liotta DC, Snyder, JP. Synthesis of EF24-tripeptide chloromethyl ketone: A novel curcumin-related anticancer drug delivery system. *J Med Chem.* 2006;49(11):3153-3158.

3. Ali H, Jabeen A, Maharjan, R, et al. Furan-conjugated tripeptides as potent antitumor drugs. *Biomolecules.* 2020;10(12):1684. doi:10.3390/biom10121684

4. Lau JL, Dunn MK. Therapeutic peptides: Historical perspectives, current development trends, and future directions. *Bioorg Med Chem.* 2018;26(10):2700-2707.

5. Ye N, Ding Y, Wild C, Shen Q, Zhou J. Small molecule inhibitors targeting activator protein 1 (AP-1). *J Med Chem.* 2014;57(16):6930-6948.

6. Kumar A, Kothari J, Lokhande KB, Seethamma TN, Venkateswara Swamy K, Sharma NK. Novel antiproliferative tripeptides inhibit AP-1 transcriptional complex. *Int J Pept Res Ther.* 2021;27(4):2163-2182.

7. Fan J, Fu A, Zhang L. Progress in molecular docking. *Quant Biol.* 2019;7(2):83-89.

8. Pagadala NS, Syed K, Tuszynski J. Software for molecular docking: A review. *Biophys Rev.* 2017;9(2):91-102.

9. Gilad Y, Senderowitz H. Docking studies on DNA intercalators. *J Chem Inf Model.* 2014;54(1):96-107.

10. Celik S, Vagifli F, Akyuz S, et al. Synthesis, vibrational spectroscopic investigation, molecular docking, antibacterial and antimicrobial studies of a new anthraquinone derivative compound. *Spectrosc Lett.* 2022;55(4):259-277.

11. Protein Data Bank website. http://www.rcsb.org/pdb. Accessed November 09, 2023.

12. Halgren TA. Merck molecular force field. I. Basis, form, scope, parameterization, and performance of MMFF94. *J Comput Chem.* 1996;17(5-6):490-519.

13. Shao Y, Molnar LF, Jung Y, et al. Advances in methods and algorithms in a modern quantum chemistry program package. *Phys Chem Chem Phys.* 2006;8(27):3172-3191.

14. Trott O, Olson AJ. Autodock vina: Improving the speed and accuracy of docking with a new scoring function, efficient optimization, and multithreading. *J Comput Chem.* 2010;31:455-461.

15. Drew HR, Wing RM, Takano T, et al. Structure of a B-DNA dodecamer: Conformation and dynamics. *Proc Natl Acad Sci USA.* 1981;78(4): 2179-2183.

16. Zhao Y, Zhu Y, Liu X, et al. Structural basis for replicase polyprotein cleavage and substrate specificity of main protease from SARS-CoV-2. *Proc Natl Acad Sci USA.* 2022;119(16):e2117142119. doi:10.1073/pnas.2117142119

17. Jin Z, Du X, Xu Y, et al. Structure of Mpro from SARS-CoV-2 and discovery of its inhibitors. *Nature.* 2020;582(7811):289-293.

18. Walls AC, Park YJ, Tortorici MA, Wall A, McGuire AT, Veesler D. Structure, function, and antigenicity of the SARS-CoV-2 spike glycoprotein. *Cell.* 2020;181(2):281-292.

19. Jurcik A, Bednar D, Byska J, et al. Caver analyst 2.0: Analysis and visualization of channels and tunnels in protein structures and molecular dynamics trajectories. *Bioinformatics.* 2018;34(20):3586-3588.

20. Demirag AD, Çelik S, Akyuz S, Ozel A. Molecular docking analysis of used drugs for the treatment of cancer. *Süleyman Demirel University J Nat App Sci.* 2021;25(3):539-547.

21. Sagaama A, Brandan SA, Issa TB, Issaoui N. Searching potential antiviral candidates for the treatment of the 2019 novel coronavirus based on DFT calculations and molecular docking. *Heliyon.* 2020;6(8): e04640. doi:10.1016/j.heliyon.2020.e04640

22. Arifa Begum SK, Begum S, Bandari P, Swapna BS, Reddemma M. Tetrandrine, an effective inhibitor of COVID-19 main protease (Mpro); Insights from molecular docking and dynamics simulations. *Int J Pharm Investig.* 2023;13(4):845–851.

23. Celik S, Yilmaz G, Akyuz S, Ozel AE. Shedding light into the biological activity of aminopterin, via molecular structural, docking, and molecular dynamics analyses. *J Biomol Struct Dyn.* 2023;1-22. doi:10.1080/07391102.2023.2245493

24. Liu X, Wang XJ. Potential inhibitors against 2019-nCoV coronavirus M protease from clinically approved medicines. *J Genet Genomics.* 2020;47(2):119-121.

25. Özdemir M, Köksoy B, Ceyhan D, Bulut M, Yalcin B. *In silico*, 6LU7 protein inhibition using dihydroxy-3-phenyl coumarin derivatives for SARS-CoV-2. *J Turk Chem Soc Sect A Chem.*

2020;7(3):691-712.

26. Hatada R, Okuwaki K, Mochizuki Y, et al. Fragment molecular orbital based interaction analyses on COVID-19 main protease-inhibitor n3 complex (PDB ID:6LU7). *J Chem Inf Model.* 2020;60(7):3593-3602.

27. Celik S, Akyuz S, Ozel AE. Vibrational spectroscopic characterization and structural investigations of cepharan-thine, a natural alkaloid. *J Mol Struct.* 2022;1258:132693. https://doi.org/10.1016/j.molstruc.2022.132693

28. Holanda VN, Lima EMDA, Silva WVD, et al. Identification of 1, 2, 3-triazole-phthalimide derivatives as potential drugs against COVID-19: A virtual screening, docking and molecular dynamic study. *J Biomol Struct Dyn.* 2022;40(12):5462-5480.

29. Joshi A, Sharma V, Singh J, Kaushik V. Chemi-informatic approach to investigate putative pharmacoactive agents of plant origin to eradicate COVID-19. *Coronaviruses.* 2022;3(3):40-54.

How to cite this article

İSTANBUL UNIVERSITY PRESS

Resveratrol Dose-Dependently Protects the Antioxidant Mechanism of Hydrogen Peroxide-Exposed Healthy Cells and Lung Cancer Cells

Oznur Yurdakul[1] , Aysun Ozkan[2]

[1]Akdeniz University, Institute of Science and Technology, Biology, Antalya, Türkiye
[2]Akdeniz University, Faculty of Science, Biology Department, Antalya, Türkiye

ABSTRACT

Objective: The objective of this study was to investigate the protective effects and the underlying mechanisms of resveratrol against hydrogen peroxide (H_2O_2)-induced oxidative stress in healthy human and lung cancer cells.

Materials and Methods: The cytotoxic doses and IC_{50} values of resveratrol and hydrogen peroxide for cells were determined by the Cell Titer Blue-Viability Assay kit. The amount of malondialdehyde (MDA) was determined by fluorescence spectrophotometer. The amount of intracellular reduced glutathione level and antioxidant enzyme activities were analyzed by spectrophotometric methods.

Results: In both cells, H_2O_2 treatment alone (IC_{50} and IC_{50}) increased MDA, glutathione reductase, glutathione S-transferase, selenium-dependent glutathione peroxidase and non-selenium-dependent glutathione peroxidase activities, but glutathione levels decreased compared to the $H_2O_2^+$ resveratrol treatment. In addition, high doses of resveratrol alone (IC_{50} and IC_{70}) induced more oxidative stress in cancer cells than in healthy cells. High doses of resveratrol alone (IC_{50} and IC_{70}) also showed cytotoxic effects in cells and decreased cell viability. Resveratrol caused more cytotoxic effects in cancer cells compared to healthy cells.

Conclusion: The results of this study show that the increase in MDA level and antioxidant enzyme activity caused by high-dose resveratrol treatment reveals the prooxidant effect of resveratrol. Our results also showed an antioxidant effect by reducing oxidative stress in cells pre-incubated with low-dose resveratrol and then exposed to H_2O_2. Resveratrol has a dose-dependent biphasic (pro/antioxidant) effect on the antioxidant mechanism of cells. However, more research is needed to confirm this.

Keywords: Antioxidant enzymes, Resveratrol, Dose-dependent toxicity, Hydrogen peroxide

INTRODUCTION

Many factors, such as heat stress, transport stress, and nutrient restriction generated reactive oxygen species (ROS) cause oxidative stress. Increased ROS production causes high cellular damage when it exceeds the capacity of the cellular antioxidant system.[1-4] While low levels of ROS show beneficial effects, excessive accumulation of ROS causes various disorders, including carcinogenesis.[5] Since the lungs are exposed to oxidants of endogenous or exogenous origin (air pollutants, cigarette smoke, etc.) every day, the level of oxidative stress is very high.[6-8] Lung cancer risk can be reduced by consciously consuming antioxidant-containing foods and paying attention to nutrition. Resveratrol, also known as 3, 5, 4-trihydroxy-trans-stilbene, is a polyphenolic compound that occurs naturally in various dietary sources, including grapes and peanuts. It has been shown to possess several pharmacological properties, including anticancer and antioxidant activities.[9-13] As it is under-

stood from the studies mentioned above, it is revealed that the antiproliferative, antioxidant, prooxidant, and anticancer properties of resveratrol vary depending on the doses, and therefore it is not safe for humans. The antioxidant effect of resveratrol can change depending on the dose. At lower doses, such as nM or 5-10 μM, resveratrol acts as a potent antioxidant, while at higher doses, it may function as a pro-oxidant.[14] Human studies suggest resveratrol can be supplemented at dosages up to 5 g daily, but the most common daily doses range from 50 to 500 mg. It is important to note that resveratrol supplements have not been well-studied in people, and more high-quality research is needed to determine the most effective and safe doses.[15] Therefore, before taking resveratrol, it is advisable to consult a healthcare professional to determine the appropriate dosage for specific health benefits and to minimize potential side effects.[16] Enzymes involved in the antioxidant mechanism of living organisms can neutralize oxidants by directly acting on oxidants exceeding a certain level. In our study, the dose-dependently

effect of resveratrol on malondialdehyde (MDA) and reduced glutathione (GSH) levels, and selenium-dependent glutathione peroxidase (Se-GPx), non-selenium-dependent glutathione peroxidase (non-Se-GPx), glutathione S-transferase (GST), and glutathione reductase (GR) activities of human healthy (MRC-5) and lung cancer cells (H1299).

MATERIALS AND METHODS

Cell Culture and Chemical

H1299 and MRC-5 cell lines were purchased from ATCC (American Type Culture Collection) (Rockville, MD, USA). Resveratrol (≥99%) was purchased from Sigma-Aldrich (Germany). H1299 cell line were cultured in RPMI 1640 medium containing 10% fetal bovine serum and 1% antibiotic antimycotic solution at 37 °C within a humidity atmosphere that contained 5% CO_2. Healthy cells (MRC-5) were grown using the same conditions plus DMEM medium containing 1% amino acids.

Cell Viability Assay

10,000 cells were seeded in a monolayer in each well of a 96-well plate as part of the experiment. On the following day, the cells were treated with various doses of resveratrol (10, 15, 25, 50, 100, 150, 200, 300, 400, 500, 600, 700, 800 µM) in the medium for 24, 48, and 72 h. Since the most effective IC_{50} value was reached in 72 h resveratrol application, the hydrogen peroxide (H_2O_2) study was continued over 72 h application. The H_2O_2 concentrations applied were (25, 50, 75, 100, 150, 150, 200, 200, 250, 250, 300, 350, 400, 450, 500 µM). The resulting cytotoxicity of resveratrol and H_2O_2 on H1299, and MRC-5 cells was measured spectro-fluorometrically using the Cell Titer Blue- Viability Assay kit.[8] The reduction of cells from resozurin to resorufin was calculated by measuring the excitation at 560 nm and emission values at 590 nm in a fluorescent spectrophotometer (PerkinElmer LS55). The data obtained were the mean values derived from eight wells for each dose, and the IC10, IC_{20}, IC_{30}, IC_{50}, and IC_{70} values were calculated using linear functions. To measure the antioxidant effect of resveratrol against H_2O_2 (IC_{50} and IC_{70}) cytotoxicity, cells were pre-incubated with different concentrations of resveratrol (IC_5, IC_{10}, IC_{20}, IC_{30}) for 1 h before 72 h H_2O_2 treatments. Each concentration and control was performed five times. IC_{50} values were calculated from linear equations.

Supernatant Preparation for Chemical Parameters

For the supernatant to be used in the experiments, cells were seeded in flasks and treated with different concentrations of resveratrol (IC_{30}, IC_{50}, IC_{70}) for 72 h and a control group was seeded without resveratrol treatment. The cells in the resveratrol-treated and control flasks were trypsinized at the end of 72 h. The pellet obtained by centrifugation at 600 xg was washed 3 times with PBS (phosphate buffered saline, pH 7) solution. The homogenization buffer was prepared by mixing 300 µl buffer (100 mM K_2HPO_4 and 100 mM KH_2PO_4 solutions, pH 7), 1180 µL distilled water and 20 µL protease inhibitor cocktail (Sigma). The pellet remaining from the last wash was diluted with the homogenization buffer and transferred into Eppendorf tubes. The pellet was homogenized in a Branson Sonifier ultrasonic disintegrator for 3x15 sec on ice and centrifuged at 32,000 xg for 45 min at 4°C. The supernatant obtained was stored at -80°C until use. MDA, glutathione and enzyme measurements were performed using the supernatant obtained.

Determination of MDA Level

To evaluate the prooxidant (membrane damaging) effect of resveratrol, cells were subjected to varying doses of both resveratrol and hydrogen peroxide (at IC_{50} and IC_{70} concentrations) for a period of 72 h. To assess the antioxidant (membrane protective) effect of resveratrol, the cells were treated with the highest cytoprotective doses of resveratrol for a period of 1 h before exposure to H_2O_2 (at IC_{50} and IC_{70} concentrations) for a period of 72 h. The levels of MDA in the cells were determined using the fluorometric method.[17] The quantification of proteins was carried out using the Bradford method, with bovine serum albumin serving as a standard.[18]

Determination of Enzyme Activity

The enzymatic assays were conducted using the supernatant obtained from the samples. To determine GST activity, the method developed by Habig and Jakoby was used, with 1-chloro-2,4-dinitrophenol as a substrate.[19] Enzyme activity was quantified based on the binding of one µM of GSH per minute, corresponding to one unit of enzyme activity. GR activity was assessed by monitoring the oxidation of NADPH at 340 nm using a spectrophotometric method.[20] The reaction mixture comprised 100 mM potassium phosphate buffer (pH 7.4), 0.1 mM NADPH, oxidized glutathione (GSSG), and 1 mM EDTA. One unit of enzyme activity corresponded to the reduction of 1 µmol of GSSG per minute. Non-Se-GPx activity was measured according to the method described by Paglia and Valentine.[21] To determine Se-GPx activity, 0.25 mmol/L H_2O_2 was used as a substrate, while 0.25 mmol/L cumene H_2O_2 was used to measure total GPx.[22] By monitoring the reduction of 5,5'-dithiobis(2-nitrobenzoic) acid by NADPH in the presence of GR, spectrophotometry was utilized to determine the total GSH concentration. Then, the GSH content was calculated as nmol/mg protein.[23]

Statistical Analysis

The statistical analysis of the collected data was conducted using the IPM Spss Statistics 20 program. The intergroup eval-

uation of the results was carried out through ANOVA-Post-Hoc analysis to determine the significance level of the observed differences. Additionally, the Duncan Multiple Comparison Test was utilized to evaluate the significance of the differences.[24]

RESULTS

To demonstrate the dose-dependent prooxidant (cytotoxic) effect of resveratrol on H1299 and MRC-5 cells, the cells were treated with different doses of resveratrol at different incubation periods (Figure 1). After 24, 48, and 72-hour incubation periods, the cytotoxicity of resveratrol was found to be higher (IC$_{50}$; 200, 100, 50 µM and IC$_{70}$; 500, 300,125 µM) in H1299 cells than in MRC-5 cells (IC$_{50}$; 250, 150, 75 µM and IC$_{70}$; 700, 400, 200 µM). When H1299 and MRC-5 cells were treated with different doses of H$_2$O$_2$, a strong prooxidant, cytotoxicity increased in both cell lines due to increased H$_2$O$_2$ doses (Figure 2). As a result of cytotoxicity measurements, IC$_{50}$ and IC$_{70}$ values were determined for 72 h. These values were found to be 300 and 420 µM for H1299 cells and 200 and 300 µM for MRC-5 cells, respectively.
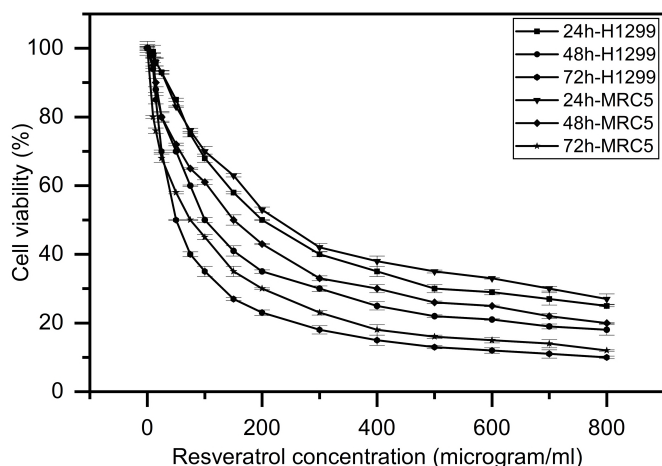

Figure 1. The dose-dependent cytotoxic effect of resveratrol in H1299 and MRC-5 cells at 24, 48 and 72 h. Values are expressed as the mean of three separate experiments. Error bars represent the standard deviation (SD) of the mean from five replications (ANOVA with Tukey's test, p<0.05).

The dose-dependent antioxidant (cytoprotective) effect of resveratrol was demonstrated by measuring the viability of cells treated with H$_2$O$_2$(IC$_{50}$ and IC$_{70}$) for 72 h after pre-incubation with low doses of resveratrol (IC$_5$, IC$_{10}$, IC$_{20}$, and IC$_{30}$). Table 1 shows the levels of H$_2$O$_2$-induced cytotoxicity in H1299 and MRC-5 cells pre-incubated with different doses of resveratrol. Maximum cytoprotective doses of resveratrol were found to be 30 µg/mL for H1299 cells and 20 µg/mL for MRC-5 cells against H$_2$O$_2$ cytotoxicity. The cytotoxic effect of H$_2$O$_2$ application after pre-incubation with resveratrol was found to be lower than the cytotoxic effect of H$_2$O$_2$ alone, which showed us the cytoprotective effect of resveratrol. From these
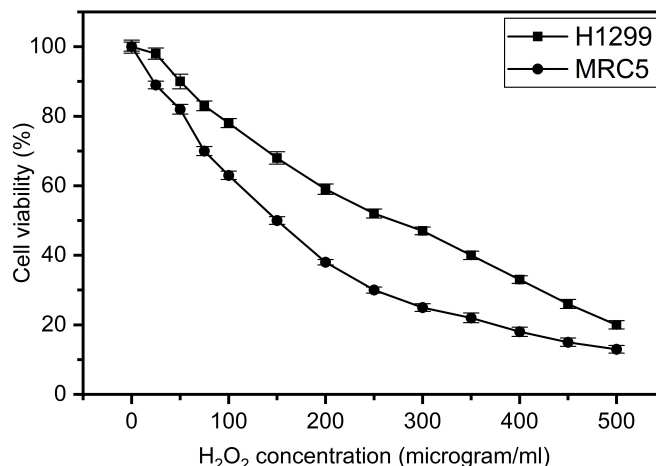
Figure 2. The dose-dependent cytotoxic effect of H$_2$O$_2$ in H1299 and MRC-5 cells. Values are expressed as the mean of three separate experiments. Error bars represent the standard deviation (SD) of the mean from five replications (ANOVA with Tukey's test, p<0.05).

results we obtained, it has been revealed that resveratrol has a dose-dependent biphasic (pro/antioxidant) effect on H1299 and MRC-5 cells.

At high concentrations, antioxidants can cause membrane damage because they act as pro-oxidants, while at lower concentrations they can protect the membrane against oxidants by showing an antioxidant effect. Oxidative stress created by pro-oxidants in the cell leads to membrane damage by lipid peroxidation and increases the MDA level. To evaluate the dose-dependent membrane-damaging and membrane-protective effects of resveratrol on H1299 and MRC-5 cells, MDA levels were assayed (Table 2). The amount of MDA obtained after exposure of H1299 cells to resveratrol at IC50 and IC70 doses was approximately 7 and 9 times higher than control cells. Similarly, MDA levels in H1299 cells exposed to IC$_{50}$ and IC$_{70}$ doses of H$_2$O$_2$, a strong oxidant, were 7 and 13 times higher, respectively, than in the control (Table 2). Here, resveratrol acts as a prooxidant depending on the dose. Resveratrol increases outer membrane permeability and membrane depolarization in cells.[25] Intracellular ROS accumulation caused significantly increased MDA levels confirmed, indicating resveratrol's prooxidant activity. On the other hand, the MDA level measured in H1299 cells exposed to low-dose resveratrol (IC$_{30}$) for one hour before 72 h of H$_2$O$_2$ (IC$_{50}$ and IC$_{70}$) administration was found to be lower than those treated with only H$_2$O$_2$. Under the same experimental conditions, the low dose of resveratrol (IC$_{20}$) for MRC-5 cells showed membrane protective effect against H$_2$O$_2$-induced membrane damage. These results indicated that the significantly reduced MDA levels were due to the antioxidant effect of resveratrol. All the results we obtained from the measurement of MDA level revealed that resveratrol has a dose-dependent biphasic effect in H1299 and MRC-5 cells by showing both membrane protective effects against H$_2$O$_2$ and damaging membrane effects.

Table 1. Protective effect of resveratrol against H_2O_2 (<IC_{50} and IC_{70}) cytotoxicity on H1299 and MRC-5 cells.

Resveratrol Concentrations H1299 cells	% Cell Viability $\pm$ S.H.	Resveratrol Concentrations MRC-5 cells	% Cell Viability $\pm$ S.H.
IC_5 Resveratrol + IC_{50} H_2O_2	45 ± 1.2	IC_5 Resveratrol + IC_{50} H_2O_2	40 ± 0.9
IC_5 Resveratrol + IC_{70} H_2O_2	39 ± 1.3	IC_5 Resveratrol + IC_{70} H_2O_2	33 ± 1.4
IC_{10} Resveratrol + IC_{50} H_2O_2	39 ± 1.3	IC_{10} Resveratrol + IC_{50} H_2O_2	45 ± 1.1
IC_{10} Resveratrol + IC_{70} H_2O_2	42 ± 1.4	IC_{10} Resveratrol + IC_{70} H_2O_2	35 ± 1.3
IC_{20} Resveratrol + IC_{50} H_2O_2	47 ± 1.2	IC_{20} Resveratrol + IC_{50} H_2O_2	57 ± 1.2
IC_{20} Resveratrol + IC_{70} H_2O_2	46 ± 1.2	IC_{20} Resveratrol + IC_{70} H_2O_2	45 ± 1.5
IC_{30} Resveratrol + IC_{50} H_2O_2	38 ± 1.4	IC_{30} Resveratrol + IC_{50} H_2O_2	34 ± 1.3
IC_{30} Resveratrol + IC_{70} H_2O_2	11 ± 1.1	IC_{30} Resveratrol + IC_{70} H_2O_2	3 ± 1.0
IC_{50} Resveratrol	50 ± 2.3	IC_{50} Resveratrol	75 ± 1.5
IC_{70} Resveratrol	125 ± 2.9	IC_{70} Resveratrol	200 ± 1.9
IC_{50} H_2O_2	51 ± 1.6	IC_{50} H_2O_2	50 ± 1.2
IC_{70} H_2O_2	31 ± 1.3	IC_{70} H_2O_2	30 ± 1.1
Control	100 ± 1.9	Control	100 ± 1.6

The glutathione system, which consists of GSH and enzymes like GPx and GR, which permit its reversible conversion (oxidation or reduction), serves as the fundamental building block for the antioxidant defense system. Reduced GSH serves as both a substrate for chemical reactions and an essential component for reducing selenolate groups found in the catalytic center of enzymes that become oxidized during the glutathione peroxidase reaction. GSH depletion in resveratrol (IC_{50} and IC_{70}) exposed cells was confirmed, which indicated the prooxidant activity of resveratrol. The changes in the GSH level in H1299 and MRC-5 cells exposed to different concentrations of resveratrol ($IC_{30}/_{20}$, IC_{50}, IC_{70}) and H_2O_2 (IC_{50} and IC_{70}) are given in Table 2. Resveratrol did not show any prooxidant effect at low doses applied to both cells. As a result of exposure of H1299 and MRC-5 cells to an IC_{50} resveratrol dose for 72 h, GSH levels decreased by 7% and 6%, compared to the control group, respectively. This is a clear sign of oxidative stress. As with resveratrol (IC_{50} and IC_{70}) administration, different doses of H_2O_2 (IC_{50} and IC_{70}), which is a strong oxidant, statistically significantly decreased the GSH level in both cells ($p<0.05$). However, as seen in Table 2, the amount of GSH in

cells pre-incubated with low dose resveratrol and then exposed to H_2O_2 was higher than the amount of GSH in cells exposed to H_2O_2 alone. Here, resveratrol protected the cells by showing antioxidant effect against H_2O_2 which is a strong oxidant.

The antioxidant defense network relies on the coordinated actions of key enzymes, including GR, GST, Se-GPx, and non-Se-GPx. GR catalyzes the reduction of oxidized glutathione (GSSG) to its active form (GSH), utilizing nicotinamide adenine dinucleotide phosphate (NADPH) as an electron donor, ensuring a continuous supply of the essential cellular antioxidant. GST, on the other hand, plays a pivotal role in detoxification by conjugating electrophilic compounds with GSH, facilitating their elimination. Se-GPx and non-Se-Px function as crucial components in the neutralization of H_2O_2 and lipid peroxides, respectively, by utilizing GSH as a co-factor. These peroxidases protect cells from oxidative damage by converting harmful ROS into less harmful substances, emphasizing their integral roles in maintaining cellular redox homeostasis and preventing oxidative stress-induced damage. On the other hand, Se-GPx (1.2-folds in H1299, 1.4-folds in MRC-5), non-Se-GPx (1.1-folds in H1299, 1.2-folds in MRC-5), GST (1.6-folds in

Table 2. Prooxidant and antioxidant effect of resveratrol on MDA and GSH levels, and Se-GSH-Px, GSH-Px, GST, and GSH-Rx activities in H1299 and MRC-5 cells.

Resveratrol Concentrations		MDA Level	GSH Level	GR	GST	Se-GPx	Non-Se-GPx
		nmol/mg	nmol/mg	mU/mg	mU/mg	µU/mg	µU/mg
		X$\pm$SE	X$\pm$SE	X$\pm$SE	X$\pm$SE	X$\pm$SE	X$\pm$SE
IC$_{30}$ Resveratrol	(H1299)	1.3 $\pm$ 0.20 [b]	59 $\pm$ 2.10 [d]	16 $\pm$ 1.9 [b]	44 $\pm$ 4.3 [ab]	520 $\pm$ 12 [ab]	679 $\pm$ 11 [b]
IC$_{50}$ Resveratrol	(H1299)	2.3 $\pm$ 0.32 [c]	53 $\pm$ 2.34 [cd]	25 $\pm$ 2.5 [bc]	64 $\pm$ 2.3 [cd]	600 $\pm$ 11 [b]	750 $\pm$ 12 [c]
IC$_{70}$ Resveratrol	(H1299)	3.0 $\pm$ 0.45 [cd]	49 $\pm$ 2.21 [c]	35 $\pm$ 2.9 [cd]	79 $\pm$ 3.3 [e]	695 $\pm$ 11 [c]	795 $\pm$ 14 [d]
IC$_{50}$ H$_2$O$_2$	(H1299)	2.5 $\pm$ 0.45 [c]	40 $\pm$ 2.33 [b]	44 $\pm$ 3.5 [de]	88 $\pm$ 3.2 [f]	714 $\pm$ 13 [c]	800 $\pm$ 14 [d]
IC$_{70}$ H$_2$O$_2$	(H1299)	4.3 $\pm$ 0.34 [e]	33 $\pm$ 2.20 [a]	56 $\pm$ 3.6 [f]	95 $\pm$ 4.1 [fg]	773 $\pm$ 12 [d]	851 $\pm$ 15 [e]
IC$_{30}$ Resveratrol + IC$_{50}$ H$_2$O$_2$ (H1299)		1.8 $\pm$ 0.25 [bc]	50 $\pm$ 2.55 [cd]	20 $\pm$ 1.2 [b]	55 $\pm$ 2.5 [bc]	528 $\pm$ 14 [ab]	660 $\pm$ 13 [a]
IC$_{30}$ Resveratrol + IC$_{70}$ H$_2$O$_2$ (H1299)		3.3 $\pm$ 0.45 [d]	40 $\pm$ 2.45 [b]	25 $\pm$ 1.0 [bc]	60 $\pm$ 2.7 [c]	595 $\pm$ 12 [b]	750 $\pm$ 14 [c]
DMSO	(H1299)	0.32 $\pm$ 0.13 [a]	58 $\pm$ 2.63 [d]	10 $\pm$ 0.9 [a]	38 $\pm$ 1.3 [a]	509 $\pm$ 12 [a]	658 $\pm$ 13 [a]
Control	(H1299)	0.33 $\pm$ 0.15 [a]	57 $\pm$ 1.58 [d]	10 $\pm$ 0.8 [a]	39 $\pm$ 2.0 [a]	506 $\pm$ 13 [a]	660 $\pm$ 14 [a]
IC$_{20}$ Resveratrol	(MRC-5)	0.8 $\pm$ 0.03 [ab]	53 $\pm$ 2.32 [cd]	11 $\pm$ 1.0 [ab]	40 $\pm$ 3.0 [b]	311 $\pm$ 12 [ab]	431 $\pm$ 10 [a]
IC$_{50}$ Resveratrol	(MRC-5)	1.4 $\pm$ 0.03 [b]	49 $\pm$ 2.38 [c]	21 $\pm$ 1.5 [bc]	53 $\pm$ 4.3 [c]	363 $\pm$ 11 [b]	481 $\pm$ 11 [b]
IC$_{70}$ Resveratrol	(MRC-5)	1.8 $\pm$ 0.04 [bc]	45 $\pm$ 2.28 [bc]	29 $\pm$ 1.3 [c]	68 $\pm$ 2.2 [e]	484 $\pm$ 11 [c]	527 $\pm$ 12 [b]
IC$_{50}$ H$_2$O$_2$	(MRC-5)	2.0 $\pm$ 0.06 [bc]	37 $\pm$ 2.29 [b]	31 $\pm$ 2.6 [cd]	72 $\pm$ 3.4 [ef]	497 $\pm$ 13 [c]	548 $\pm$ 14 [bc]
IC$_{70}$ H$_2$O$_2$	(MRC-5)	2.5 $\pm$ 0.08 [c]	30 $\pm$ 2.28 [a]	40 $\pm$ 3.1 [d]	84 $\pm$ 3.5 [fg]	553 $\pm$ 12 [cd]	601 $\pm$ 13 [c]
IC$_{20}$ Resveratrol + IC$_{50}$ H$_2$O$_2$ (MRC-5)		1.5 $\pm$ 0.03 [b]	45 $\pm$ 2.35 [bc]	14 $\pm$ 0.8 [ab]	48 $\pm$ 2.5 [c]	350 $\pm$ 14 [ab]	425 $\pm$ 12 [a]
IC$_{20}$ Resveratrol + IC$_{70}$ H$_2$O$_2$ (MRC-5)		2.0 $\pm$ 0.03 [bc]	38 $\pm$ 2.41 [b]	19 $\pm$ 0.9 [b]	52 $\pm$ 3.4 [cd]	375 $\pm$ 12 [ab]	470 $\pm$ 11 [b]
DMSO	(MRC-5)	0.29 $\pm$ 0.02 [a]	51 $\pm$ 2.43 [cd]	6 $\pm$ 0.7 [a]	30 $\pm$ 1.0 [a]	260 $\pm$ 12 [a]	405 $\pm$ 13 [a]
Control	(MRC-5)	0.26 $\pm$ 0.01 [a]	52 $\pm$ 1.40 [cd]	7 $\pm$ 0.4	29 $\pm$ 1.9 [a]	263 $\pm$ 13 [a]	400 $\pm$ 13 [a]

Results are means of eight different experiments. Values that are followed by different letters within each column are significantly different ($p \leq 0.05$). df1=2, df2=95, F=11.96. SE: Standard Error. MDA: Malondialdehyde, GSH: Reduced glutathione, Se-GPx: Selenium-dependent glutathione peroxidase, Non-Se-GPx: Non-selenium-dependent glutathione peroxidase GST: Glutathione S-transferase, GR: Glutathione reductase.

H1299, 1.8-folds in MRC-5), as well as increased GR activity (2.5-folds in H1299, 3-folds in MRC-5) was seen in IC_{50} resveratrol exposed H1299 and MRC-5 cells respectively. Also, the activity of these enzymes was found to be significantly higher in IC_{70} resveratrol-treated cells than in control cells (Table 2). As a result, high resveratrol doses like H_2O_2-induced oxidative stress in H1299 and MRC-5 cells showed an oxidative effect. Both resveratrol and H_2O_2 increased enzyme activities in cells.

On the other hand, H1299 cells, preincubated with IC_{30} resveratrol doses (the highest cytoprotective effect dose for H1299 cells against H_2O_2 cytotoxicity) for 1 h, before H_2O_2 treatment (IC_{50} and IC_{70}) for 72 h, had lower enzyme activity than non-preincubated cells (Table 2). Under the same experimental conditions, the IC_{20} dose of resveratrol for MRC-5 cells showed a protective effect against H_2O_2-induced oxidative stress. We assume that the antioxidant action of resveratrol can accompany decreasing H_2O_2-induced oxidative stress with lower doses. These findings suggest that resveratrol exhibits anticancer/antioxidant effects depending on the dose in both cells.

DISCUSSION

Lung cancer is a major cause of cancer-related mortality worldwide, with rising incidence rates globally.[26] This may be due to increased oxidative stress due to daily exposure of the lungs to oxidants from both endogenous and exogenous sources (such as air pollution and cigarette smoke).[6-8] Therefore, lung cancer cells can be selected as a model for oxidative stress studies. ROS generation is increased under oxidative stress, and antioxidant defense mechanisms like GSH, GST, GPx and GR are significantly less effective. Specifically, ROS can impair the lipid membrane by increasing its fluidity and permeability. However, appropriate doses of herbal products with antioxidant properties such as resveratrol can decrease cellular damage caused by oxidative stress.[27] Resveratrol is a natural polyphenolic compound with a well-known capacity to modulate ROS, especially hydroxyl radicals (•OH). In recent years, the scientific community has expressed considerable interest in resveratrol due to its biphasic function, which is dose-dependent. For example, in one study, while ROS play a role in muscle repair, excessive amounts of ROS over long periods of time can lead to oxidative stress. Antioxidants such as resveratrol can reduce oxidative stress, restore mitochondrial function and promote myogenesis and hypertrophy. However, resveratrol dose efficacy for muscle plasticity is unclear. Therefore, we investigated the dose-response of resveratrol on C2C12 myoblast and myotube plasticity in the presence and absence of different degrees of oxidative stress. Low resveratrol concentration (10 µM) stimulated myoblast cell cycle arrest, migration and sprouting, which were inhibited by higher doses (40-60 µM). Resveratrol did not increase oxidative capacity. In contrast, resveratrol caused loss of mitochondria, reduced cell viability and ROS production, and activated stress response pathways [Hsp70 and pSer36-p66(ShcA) proteins]. However, the deleterious effects of H_2O_2 (1000 µM) on cell migration were attenuated after preconditioning with 10 µM-resveratrol. This dose also enhanced cell motility mediated by 100 µM-H_2O_2, while higher doses of resveratrol increased H_2O_2-induced impaired myoblast regeneration and mitochondrial dehydrogenase activity. In conclusion, low doses of resveratrol promoted in vitro muscle regeneration and attenuated the effect of ROS, whereas high doses enhanced oxidative stress-induced decreased plasticity and metabolism. Thus, the effects of resveratrol depend on the dose and the degree of oxidative stress.[28] Clinical studies have reported that resveratrol can confer health benefits (both in animal and human studies) at moderate doses, while higher doses may trigger a pro-apoptotic tumoricidal effect.[14,29,30] For instance, a study showed that the resveratrol derivative produced by high-pressure treatment exhibited a proliferative inhibitory effect on cervical cancer cells.[10] It has been revealed that resveratrol exhibits many biological activities with different drug combinations at different concentrations in colorectal cancer cells.[9] When the antioxidant interaction between resveratrol (8 µg/ml) and eugenol EUG (8 mg/mL) in the carboxymethyl cellulose biodegradable film was evaluated, the combination of the two showed a synergistic antioxidant effect.[11] As noted in the studies above, scientists today focus on the dose-dependent biological effects of resveratrol, resveratrol derivatives, combinations of resveratrol with other ingredients, and encapsulated resveratrol in drug development studies. Our study explains the biphasic function (anti-/pro-oxidant) of resveratrol in a dose-dependent manner. The data we obtained showed that resveratrol has a prooxidant effect at high cell concentrations, while it protects cells pre-incubated with low concentrations of resveratrol from H_2O_2-induced oxidative stress.

In a study supporting our findings, it was observed that micromolar concentrations of trans-resveratrol reduced the MDA levels caused by t-BHP-induced oxidative stress in erythrocytes.[31] Similarly, another study found that resveratrol played a protective role in regulating oxidative damage by modulating GSH homeostasis against the environmental carcinogen $NaAsO_2$.[32] In human endothelial cells, resveratrol modulated the expression of both pro-oxidative and antioxidative enzymes, increasing mRNA expression of SOD1 and GPx1. Furthermore, pretreatment of cells with resveratrol completely prevented DMNQ-induced oxidative stress.[33] Resveratrol also demonstrated no cytotoxicity to human lymphocytes at concentrations of 10-100 µM, while inhibiting DNA damage in these cells induced by H_2O_2. Resveratrol increased the activity of GR, GST, and GPX, indicating that the modulation of antioxidant enzymes (GPX, GR, and GST) and an increase in GSH levels were responsible for resveratrol's inhibitory effect on oxidative DNA damage in human lymphocytes caused by H_2O_2.[34] In a study, the protective effects of resveratrol against H_2O_2-induced oxidative stress in bovine skeletal muscle cells (BMCs) were investigated. Pretreatment of BMCs with resveratrol before H_2O_2

exposure increased cell viability, decreased ROS and stabilized redox status compared to H_2O_2 treatment alone. H_2O_2 exposure activated sirtuin type 1 (SIRT1) and nuclear factor E2-related factor 2 (NRF2) mediated signaling pathways. Pretreatment with resveratrol did not alter SIRT1-regulated genes, but increased heme oxygenase 1 (HO-1) expression while inhibiting the up-regulation of NRF2. These results suggest that resveratrol has beneficial effects against oxidative stress.[35] In another study, the neuroprotective and antioxidant effects of resveratrol against H_2O_2 in embryonic neural stem cells were investigated. H_2O_2 treatment alone increased catalase and GPx activities, but did not change superoxide dismutase levels compared to $H_2O_2^+$ resveratrol treatment. Nitric oxide synthase activity and concomitant nitric oxide levels increased in response to H_2O_2 treatment. Conversely, nitric oxide synthase activity and nitric oxide levels were decreased in cells exposed to H_2O_2 after preincubation with resveratrol. Resveratrol also reduced H_2O_2-induced nuclear or mitochondrial DNA damage. Resveratrol decreased nitric oxide production and nitric oxide synthase activity by inducing the activity of antioxidant enzymes and reduced the potential for oxidative stress by reducing both nuclear and mitochondrial DNA damage. Therefore, it has been suggested that it may be a promising agent to protect embryonic neural stem cells.[36] In this study, the effects of resveratrol on glutamate-induced oxidative cell death were investigated. Cultured HT22 cells, an immortalized mouse hippocampal neuronal cell line, were used as an *in vitro* model. Oxidative stress and neurotoxicity in these neuronal cells were induced by exposure to high concentrations of glutamate. Resveratrol potently protected HT22 cells from glutamate-induced oxidative cell death. The neuroprotective effect of resveratrol was independent of its direct radical scavenging property, but instead depended on its ability to selectively induce mitochondrial superoxide dismutase (SOD2) expression and subsequently reduce mitochondrial oxidative stress and damage. The induction of mitochondrial SOD2 by resveratrol was mediated by activation of PI3K/Akt and GSK-3β/β-catenin signaling pathways. Taken together, the results of this study suggest that up-regulation of mitochondrial SOD2 by resveratrol represents an important mechanism for the protection of neuronal cells against oxidative cytotoxicity resulting from mitochondrial oxidative stress.[37] In our study, the involvement of antioxidant enzyme systems such as Se-dependent GRx, non-Se-GPx, GST, and GR was explored in the detoxification of ROS in H1299 and MRC-5 cells.

CONCLUSION

Based on the findings of our study, it can be suggested that high-dose resveratrol has the potential as a natural source for the production of new anticancer drugs. Our results demonstrated that high-dose resveratrol had cytotoxic effects on H1299 cells and increased membrane damage and antioxidant enzyme levels. In addition, using low-dose resveratrol to develop antioxidant drugs for healthy cells against strong oxidants will also contribute to protecting human health. Thus, dose- and time-dependent use of resveratrol may contribute to identifying new strategies for treating lung carcinoma and protecting healthy cells against prooxidants. A better understanding of the intracellular mechanisms of resveratrol will bring new strategies for producing anticancer and antioxidant drugs. More detailed studies should be conducted on phenolic compounds such as resveratrol, which show biphasic effects such as antioxidant/prooxidant in cells depending on dose and time.

ORCID IDs of the authors

Oznur Yurdakul   0000-0002-4302-0816
Aysun Ozkan   0000-0002-9403-3342

REFERENCES

1. Archile-Contreras AC, Purslow PP. Oxidative stress may affect meat quality by interfering with collagen turnover by muscle fibroblasts. *Food Res Int*. 2011;44(2):582-588.

2. Poławska E, Bagnicka AW, Niemczuk K, Lipińska JO. Relations between the oxidative status, mastitis, milk quality and disorders of reproductive functions in dairy cows—A review. *Anim Sci Pap Rep*. 2012;30(4):297-307.

3. Čáp M, Váchová L, Palková Z. Reactive oxygen species in the signaling and adaptation of multicellular microbial communities. *Oxid Med Cell Longev*. 2012;2012:976753. doi:10.1155/2012/976753

4. Descalzo AM, Sancho AM. A review of natural antioxidants and their effects on oxidative status, odor and quality of fresh beef produced in Argentina. *Meat Sci*. 2008;79(3):423-436.

5. Acharya A, Das I, Chandhok D, Saha T. Redox regulation in cancer: A double-edged sword with therapeutic potential. *Oxid Med Cell Longev*. 2010;3:702528. doi:10.4161/oxim.3.1.10095

6. Rogers LK, Cismowski MJ. Oxidative stress in the lung-The essential paradox. *Curr Opin Toxicol*. 2018;7:37-43.

7. Valavanidis A, Vlachogianni T, Fiotakis K, Loridas S. Pul-

monary oxidative stress, inflammation and cancer: Respirable particulate matter, fibrous dusts and ozone as major causes of lung carcinogenesis through reactive oxygen species mechanisms. *Int J Environ Res Public Health*. 2013;10(9):3886-3907.

8. Boukhenouna S, Wilson MA, Bahmed K, Kosmider B. Reactive oxygen species in chronic obstructive pulmonary disease. *Oxid Med Cell Longev*. 2018;5730395. doi:10.1155/2018/5730395.

9. Amintas S, Dupin C, Boutin J, et al. Bioactive food components for colorectal cancer prevention and treatment: A good match. *Crit Rev Food Sci Nutr*. 2023;63(23):6615-6629.

10. Sugahara Y, Ohta T, Taguchi Y, et al. Resveratrol derivative production by high-pressure treatment: proliferative inhibitory effects on cervical cancer cells. *Food Nutr Res*. 2022;66. doi:10.29219/fnr.v66.7638

11. Aminzare M, Moniri R, Hassanzad Azar H, Mehrasbi MR. Evaluation of antioxidant and antibacterial interactions between resveratrol and eugenol in carboxymethyl cellulose biodegradable film. *Food Sci Nutr*. 2022;10(1):155-168.

12. Wijekoon C, Netticadan T, Siow YL, et al. Potential associations among bioactive molecules, antioxidant activity and resveratrol production in vitis vinifera fruits of North America. *Molecules*. 2022;27(2):336. doi:10.3390/molecules27020336.

13. Yi J, He Q, Peng G, Fan Y. Improved water solubility, chemical stability, antioxidant and anticancer activity of resveratrol via nanoencapsulation with pea protein nanofibrils. *Food Chem*. 2022;377:131942. doi:10.1016/j.foodchem.2021.131942.

14. Mukherjee S, Dudley JI, Das DK. Dose-dependency of resveratrol in providing health benefits. *Dose Response*. 2010;8(4):478-500.

15. Zhang L-X, Li C-X, Kakar MU, et al. Resveratrol (RV): A pharmacological review and call for further research. *Biomed Pharmacother*. 2021;143:112164. doi:10.1016/j.biopha.2021.112164.

16. Salehi B, Mishra AP, Nigam M, et al. Resveratrol: A double-edged sword in health benefits. *Biomedicines*. 2018;6(3):91. doi:10.3390/biomedicines6030091

17. Wasowicz W, Nève J, Peretz A. Optimized steps in fluorometric determination of thiobarbituric acid-reactive substances in serum: Importance of extraction pH and influence of sample preservation and storage. *Clinical Chem*. 1993;39(12):2522-2526.

18. Bradford MM. A rapid and sensitive method for the quantitation of microgram quantities of protein utilizing the principle of protein-dye binding. *Anal Biochem*. 1976;72:248-254.

19. Habig WH, Jakoby WB. Assays for differentiation of glutathione S-transferases. *Methods Enzymol*. 1981;77:398-405.

20. Carlberg I, Mannervik B. Glutathione reductase. *Methods Enzymol*. 1985;113:484-490.

21. Paglia DE, Valentine WN. Studies on the quantitative and qualitative characterization of erythrocyte glutathione peroxidase. *J Lab Clin Med*. 1967;70(1):158-169.

22. Lawrence RA, Burk RF. Glutathione peroxidase activity in selenium-deficient rat liver. *Biochem Biophys Res Commun*. 1976;71(4):952-958.

23. Beutler E. Glutathione peroxidase. In: Red cell metabolism: A manual of biochemical methods. *Grune & Stratton*. 1975:71-73.

24. SPSS. IBM SPSS Statistics for Windows. IBM Corp.

25. Lee W, Lee DG. Resveratrol induces membrane and DNA disruption via pro-oxidant activity against *Salmonella typhimurium*. *Biochem Biophys Res Commun*. 2017;489(2):228-234.

26. Bade BC, Dela Cruz CS. Lung cancer 2020: Epidemiology, etiology, and prevention. *Clin Chest Med*. 2020;41(1):1-24.

27. Sharifi-Rad M, Anil Kumar NV, Zucca P, et al. Lifestyle, oxidative stress, and antioxidants: Back and Forth in the pathophysiology of chronic diseases. *Front Physiol*. 2020;11:694. doi:10.3389/fphys.2020.00694

28. Bosutti A, Degens H. The impact of resveratrol and hydrogen peroxide on muscle cell plasticity shows a dose-dependent interaction. *Sci Rep*. 2015;5(1):8093. doi:10.1038/srep08093

29. Yang L, Yang L, Tian W, et al. Resveratrol plays dual roles in pancreatic cancer cells. *J Cancer Res Clin Oncol*. 2014;140(5):749-755.

30. Singh CK, Ndiaye MA, Ahmad N. Resveratrol and cancer: Challenges for clinical translation. *Biochim Biophys Acta*. 2015;1852(6):1178-1185.

31. Pandey KB, Rizvi SI. Protective effect of resveratrol on formation of membrane protein carbonyls and lipid peroxidation in erythrocytes subjected to oxidative stress. *Appl Physiol Nutr Metab*. 2009;34:1093-1097.

32. Chen C, Jiang X, Zhao W, Zhang Z. Dual role of resveratrol in modulation of genotoxicity induced by sodium arsenite via oxidative stress and apoptosis. *Food Chem Toxicol*. 2013;59:8-17.

33. Spanier G, Xu H, Xia N, et al. Resveratrol reduces endothelial oxidative stress by modulating the gene expression of superoxide dismutase 1 (SOD1), glutathione peroxidase 1 (GPx1) and NADPH oxidase subunit (Nox4). *J Physiol Pharmacol*. 2009;60(4):111-116.

34. Yen GC, Duh PD, Lin CW. Effects of resveratrol and 4-hexylresorcinol on hydrogen peroxide-induced oxidative DNA damage in human lymphocytes. *Free Radic Res*. 2003;37(5):509-514.

35. Zhang X, Liu X, Wan F, et al. Protective effect of resveratrol against hydrogen peroxide-induced oxidative stress in bovine skeletal muscle cells. *Meat Science*. 2022;185:108724. doi:10.1016/j.meatsci.2021.108724

36. Konyalioglu S, Armagan G, Yalcin A, Atalayin C, Dagci T. Effects of resveratrol on hydrogen peroxide-induced oxidative stress in embryonic neural stem cells. *Neural Regen Res*. 2013;8(6):485-495.

37. Fukui M, Choi HJ, Zhu BT. Mechanism for the protective effect of resveratrol against oxidative stress-induced neuronal death. *Free Radic Biol Med*. 2010;49(5):800-813.

How to cite this article

İSTANBUL UNIVERSITY PRESS

RESEARCH ARTICLE

Induction of Apoptosis through Oxidative Stress Caused by *Rubus tereticaulis* Leaves Extracts in A549 Cells

Gamze Nur Oter[1,2] , Ezgi Durmus[3,5] , Ali Sen[4] , Abdurrahim Kocyigit[5]

[1]Istanbul University, Institute of Health Sciences, Department of Medical Biochemistry, Istanbul, Türkiye
[2]Istinye University, Faculty of Medicine, Department of Medical Pathology, Istanbul, Türkiye
[3]Bezmialem Vakıf University, Institute of Health Sciences, Department of Medical Biochemistry, Istanbul, Türkiye
[4]Marmara University, Faculty of Pharmacy, Department of Pharmacognosy, Istanbul, Türkiye
[5]Bezmialem Vakif University, Faculty of Medicine, Department of Medical Biochemistry, Istanbul, Türkiye

ABSTRACT

Objective: Plants have been used for medicinal purposes since the beginning of human history and form the basis of modern medicine, and they are also the source of most chemotherapeutic drugs for cancer treatment. This study aims to investigate for the first time the cytotoxic and apoptotic effects of the active ethanol (RTE) and chloroform (RTC) extracts of *Rubus tereticaulis* leaves in the A549 non-small-cell lung cancer cell line.

Materials and Methods: A549 cells were treated with RTE and RTC individually. The MTT assay was used to quantitatively detect RTE and RTC's cytotoxic effects. The fluorescent signal indicator H2DCF-DA was used to detect cellular reactive oxygen species (ROS) production. Apoptosis was evaluated by fluorescence microscope after acridine orange/ethidium bromide fluorescent staining, annexin V-FITC and immunoblotting analyses, immunofluorescence, and imaging.

Results: Both RTE and RTC induced cytotoxicity in A549 cells in a dose-dependently, which was accompanied with induced ROS accumulation. Both early and late apoptotic cells detected by flow cytometry were increased in the RTE- and RTC-treated cells. In addition, the results show RTC to have higher cytotoxic and apoptotic effects and increased ROS-generation capacity than RTE. Therefore, the polarity of the solvent used to exert the anticancer effect of *R. tereticaulis* leaves is crucial.

Conclusion: This is the first anti-cancer activity study on *R. tereticaulis*. The results suggest *R. tereticaulis* leaves to have an anti-cancer effect on lung cancer cells through ROS-mediated apoptosis and RTC to be an effective therapeutic/adjuvant strategy in cancer treatment.

Keywords: Lung cancer, Anti-cancer effect, Oxidative stress, *Rubus tereticaulis*, Apoptosis

INTRODUCTION

One of the leading causes of cancer-related deaths worldwide is lung cancer. Lung cancer affects 1.8 million people worldwide each year and claims 1.6 million lives. Non-small-cell lung cancer (NSCLC) and small-cell lung cancer (SCLC) are the two main kinds of lung cancer and respectively cause approximately 85% and 15% of all newly discovered lung cancers.[1,2]

The best course of treatment for a patient with lung cancer depends on the stage at which they are discovered to have this dreadful disease. It typically entails surgical resection followed by chemotherapy and/or radiotherapy.[3] The main treatments for lung cancer involve chemotherapeutic medications such as paclitaxel, 5-fluorouracil (5-FU), docetaxel, cisplatin, and gemcitabine. The effectiveness of many chemotherapeutic treatments has been significantly reduced in lung cancer due to the emergence of drug resistance strains.[4-6] Additionally, the chemotherapeutic approach to treating lung carcinomas frequently results in serious off-target side effects. In order to replace the widely used chemotherapeutics, a worldwide push has occurred for researching alternative medicines with higher tolerance profiles, such as natural products.

Many cancer cells have a prolonged increase in the creation of intrinsic reactive oxygen species (ROS) during malignant transformation, which sustains the oncogenic phenotype and promotes tumor growth. Redox adaptation enables cancer cells to increase survival and build resistance to anti-cancer medicines by upregulating anti-apoptotic and antioxidant chemicals.[7]

Plants have long been employed for their numerous health

advantages. Around 80%-85% of people globally rely on conventional plant-based medicines for their medical requirements. Many plant extracts, isolated chemicals, and their equivalents have been employed as powerful anticancer medications, and research into the medicinal qualities of substances derived from plants has grown in popularity.[8] The antioxidant, anti-cancer, antibacterial, antiviral, and anti-inflammatory effects of phenolic compounds found in plants are well documented.[9] Research on medicinal plants and their polyphenol-rich extracts is crucial. As a result, the need exists for new products with fewer negative effects than those currently in use.

The genus Rubus is a member of the Rosaceae family that has 740 species growing naturally in the world, with 10 taxa in Turkey.[10] *Rubus* species are used internally or externally in traditional folk medicine to treat various diseases.[11] Flavonoids (e.g., quercetin, kaempferol) and phenolic acids (e.g., caffeic acid, chlorogenic acid) have been found in phytochemical investigations of *Rubus* species. The presence of catechins, pectins, carboxylic acids, anthocyanins, vitamin C, and saturated as well as unsaturated fatty acids has also been shown in prior investigations.[12-14] Only two previous studies by some of this team's researchers are found on the phytochemical content and bioactivity (i.e., antioxidant, anti-inflammatory, anticolitis, and wound healing activities) of *Rubus tereticaulis*. One of these studies reported *R. tereticaulis* ethanol extract to contain quinic acid, 5-caffeoylquinic acid, quercetin pentoside, quercetin glucoside, quercetin-3-O-β-D-glucuronide, kaempferol-3-O-β-D-glucuronide, and kaempferol rutinoside. In addition, the total phenol and flavonoid amounts in this species were calculated and revealed to show antioxidant, anti-inflammatory, and anticolitis activity. The compound responsible for these activities has been shown to be quercetin-3-O-β-D-glucuronide, which is the major compound in the extract, along with other phenolic compounds.[14] The second study reported *R. tereticaulis* to show wound healing activity.[15]

The aim of this study is to investigate for the first time the cytotoxic and apoptotic effects of *R. tereticaulis* leaves' active ethanol (RTE) and chloroform (RTC) extracts in the A549 lung cancer cell line.

MATERIALS AND METHODS

Plant Material and Extraction

R. tereticaulis leaves in the flowering period were collected from the Şile region of Türkiye's Istanbul province on June 15, 2016 and identified by Dr. Ahmet Dogan. Voucher specimens were kept in the herbarium of the Marmara University Faculty of Pharmacy (MARE No. 18573). RTE and RTC extracts from the *R. tereticaulis* leaves had been obtained in the previously reported study[14] and stored at 4° C until analysis.

Cell Culture

The A549 cells was purchased from the American Type Culture Collection (ATCC, USA), maintained in DMEM/F12K, and supplemented with 10% fetal bovine serum (FBS), 1% 100 units/mL of penicillin, and 1% 100 μg/mL of streptomycin. The cells were cultured in a humidified atmosphere of 5% CO_2 at 37 °C. The cells were grown in 75 cm^2 culture bottles.

The study uses the RTE and RTC extracts as experimental groups. Before the cell culture studies, the extracts were dissolved in a 1% dimethyl sulfoxide solution and then diluted with 1X phosphate buffer saline (PBS). The control group is A549 cells exposed to the 0.1% (v/v) dimethyl sulfoxide solution that had not been treated with any extract.

Cell Viability Assay

The 3-(4,5-dimethyl-2-thiazolyl)-2,5-diphenyltetrazolium bromide (MTT) test (Sigma) was used to assess cellular metabolic activity in a 96-well plate. The A549 cells were plated in wells at a density of 5 x 10^4 cells each, with the cells then treated with increasingly greater concentrations (25-600 μg/mL) of the RTE and RTC samples at 37 °C for 48 h. After incubation, 10 μL of the MTT solution (5 mg/mL in sterile PBS) and 100 mL of fresh DMEM were added to each well and incubated 4 h. The dimethyl sulfoxide (DMSO) solution was then added to 100 μL of a dissolving buffer and incubated for 15 min at room temperature. The optical density was read at 570 nm on a microplate reader to ascertain the MTT reaction in cells (Varioskan Flash Spectral Scanning Multimode Reader, Thermo Scientific). Cell viability was calculated as a percentage of the controls.[16]

Measuring ROS Levels

The fluorescent signal indication 2,7 dichlorodihydrofluorescein diacetate was used to measure intracellular ROS generation (H2DCF-DA). After being oxidized by ROS in the media, the colorless H_2DCF-DA transforms into green luminous dichlorofluorescein (DCF). A fluorescent link is found between elevated ROS levels and the fluorescence that is released.[17]

After 24 h of incubation, 1x10^4 cells seeded on 96 opaque black plates were given RTC and RTE. These were then incubated for 48 h in accordance with the experimental groups. The media were aspirated and given three washings in 1xPBS following incubation. An incubator was filled with 100 μl of 10 μM H2DCF-DA produced in ddH$_2$O, and the mixture was then incubated at 37 °C. A fluorescence plate reader equipped with an Ex:488nm/Em:525nm laser was used to measure the DCF fluorescence intensity that resulted during incubation (Varioskan Flash Multimode Reader, Thermo Scientific). MTT was compared to the control group with 0.1% DMSO added, and the results were determined using the ratio of ROS:MTT.[16]

Dual Acridine Orange/Ethidium Bromide (AO/EB) Staining

The dyes AO/EB are unique to DNA. McGahon et al. invented the dual AO/EB staining method,[18] which allows one to distinguish among viable, apoptotic (early or late stages), and necrotic cells by combining the differential uptake of fluorescent DNA binding dyes of AO and EB with the morphological feature of the chromatin condensation in the stained nucleus. Both live and nonviable organisms absorb the acridine orange, which then either intercalates into double-stranded nucleic acids (mostly DNA) or binds to single-strand nucleic acids to produce red fluorescence (RNA). Ethidium bromide only enters nonviable cells and intercalates into DNA to produce red fluorescence. A viable cell would therefore have an orange cytoplasm and a uniform bright green nucleus. An early apoptotic cell, whose membranes are still intact but have begun to cleave its DNA, would still have a green nucleus but exhibit bright green patches of condensed chromatin. A late apoptotic cell would exhibit bright orange areas of condensed chromatin in the nucleus (EB predominates over AO). A necrotic cell would have a uniform bright orange nucleus. When stimulated at 480–490 nm by living cells, AO diffuses into dsDNA and distributes green fluorescence. In a nutshell, 6-well plates were seeded with 2×10^5 cells/well and incubated for 24 h. After that, another 24 h of incubation occurred with the addition of RTC and RTE below the IC_{50} values. After being treated with RTC and RTE, the cells were taken out and cleaned with PBS before being stained with a 1:1 mixture of AO/EB (100 µg/mL; CAT: 235474/E8751-Sigma Aldrich, USA). Using a fluorescent microscope, the incidence of apoptotic chromatin condensation was measured and scored for three replicate samples, each containing one hundred cells (Leica DM 1000, Solms, Germany).

Annexin V-FITC Analysis

For the purpose of detecting apoptosis, the manufacturer's instructions for the Annexin V-FITC staining kit (eBioscience, Thermo Fisher Scientific, USA) were followed. In brief, the A549 cells were seeded onto six-well plates at a density of 1.5 x 10^5 cells per well and left to adhere overnight before being treated for 24 h with IC_{50} doses of RTC and RTE. The trypsin-digested cells were centrifuged for five minutes at 200× rpm. Resuspended in 100 µL Annexin V-FITC labeling solution, the cell pellet was then incubated at 15–20°C for 10–15 min. Immediately after, it was analyzed using flow cytometry (Becton Dickinson, FACS Canto II) at 525 nm for emission and 488 nm for excitation.

Immunoblotting Analysis

The A549 cells were seeded on 6-well plates at 1.5×10^5 per well, and the plates were cultured for a full day. Then, based on their IC_{50} values, they received treatment with RTC and RTE. The NP-40 cell lysis buffer (2 mM Tris-HCl pH 7.5, 150 mM NaCl, 10% glycerol, and 0.2% NP-40 plus a protease inhibitor cocktail) was used to harvest and prepare the cells after 24 h of incubation. The cells were centrifuged at 14,000× rpm (Beckman Coulter, Krefeld, Germany) for 10 min at 4°C. Next, the cytosolic fraction was made from the final supernatant. The Bradford protein assay method was used to calculate the supernatant's protein concentration. Proteins from cellular supernatants were separated on 8%-10% polyacrylamide gels and then moved using the trans-blot SD semipermeable electrophoretic transfer cell to a nitrocellulose membrane (Bio-Rad, Hercules, CA). The membrane was blocked using Tris-HCl-buffered saline with Tween 20 (TBST) and 5% nonfat milk. Following an overnight incubation at 4°C, the primary antibodies caspase-3 (1:1000 dilution), PARP (1:500 dilution) were employed. To standardize protein levels, β-actin (1:2000 dilution) was also blotted for all samples. The membrane was cleaned with TBST and then incubated for an additional hour with secondary antibodies conjugated with horseradish peroxidase (Cell Signaling Technology, Danvers, MA). Pierce ECL Western staining substrate (Thermo Scientific) was used to visualize immunolabelled proteins, and an imaging system (Vilber Lourmat Sté, Collégien, France) was used to acquire the images.

Immunofluorescence and Imaging

The A549 cells were fixed in 4% buffered formalin after being treated with the RTC and RTE extracts for 48 h. PBS was then used as a washing medium. Cells were permeabilized using 0.3% Triton X-100 in PBS, blocked with goat serum in PBS, and then treated for 1 h at 37°C with caspase-3 (1:100). Alexa fluor was then used as the secondary antibody and allowed to sit at room temperature for 30 min. A Zeiss fluorescence microscope was used to observe the cells following their mounting with 4',6-diamidino-2-phenylindole (DAPI) for nucleus staining.

Statistical Analysis

Statistical analysis was done with GraphPad Prism 8. Data are expressed as mean ± standard deviation. Data were analyzed with the two-way analysis of variance (ANOVA) test. Significance changes with different p values (** $p < 0.01$, *** $p < 0.001$, **** $p < 0.0001$).

RESULTS

Cell Viability Assessment

The MTT results show a marginally higher viability in the A549 cells treated with RTC and RTE at low dosages (25-50 µg/mL) compared to the control (Figure 1A). This outcome was
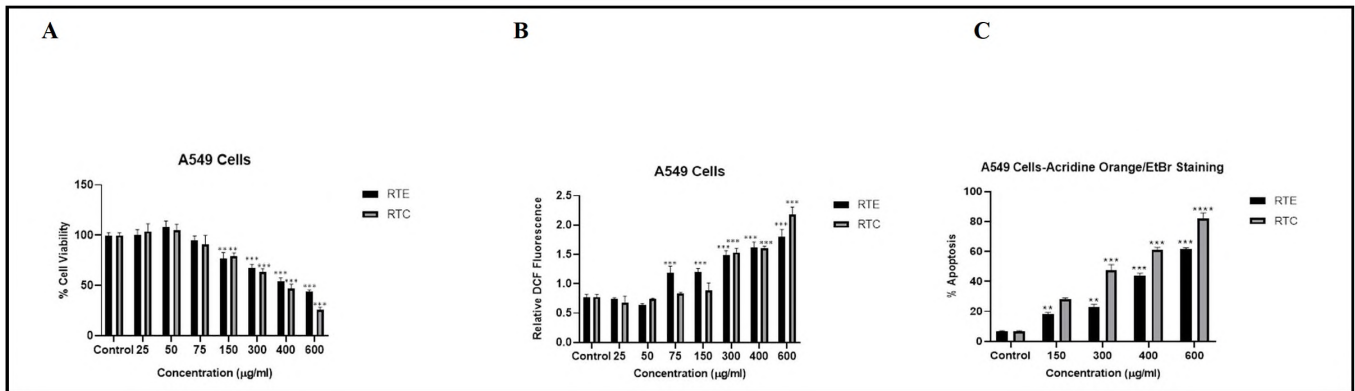
Figure 1. Effect of *R. tereticaulis* leaves' active ethanol (RTE) and chloroform (RTC) extracts on cell viability of A549, change in the amount of intracellular ROS and apoptotic effects in the cell. **(A)** Effects of RTC and RTE on A549 cell viability in a dose-dependent manner (**p<0.01 and *** p<0.001). **(B)** Dose-dependent effects of RTC and RTE on the amount of intracellular ROS in A549 cells (*** p<0.001). **(C)** Dose-dependent apoptotic effects of RTC and RTE in A549 cells (**p<0.01, *** p<0.001 and ****p<0.0001).

anticipated. When comparing the cells to those in the control group, a statistically significant decline was seen in the viability of the A549 cells that had been treated with 150, 300, 400 and 600 µg/mL each of RTC and RTE ($p < 0.001$). RTC was found to be more cytotoxic than RTE against A549 cells. The RTC and RTE extracts inhibited proliferation of the A549 cells at the IC_{50} values of 395 and 480 µg/mL, respectively.

ROS Generation Assessment

RTC and RTE had slight antioxidative effects on ROS levels in the A549 cells when compared to the control at the same low dosages (25–50 µg/mL). RTC and RTE demonstrated a prooxidant effect at high concentrations (50-600 µg/mL), whereas they demonstrated an antioxidant effect at doses (25-50 µg/mL; Figure 1B). While a statistically significant increase had occurred in the quantity of intracellular ROS in the A549 cells treated with 75 µg/mL and 150 µg/mL of RTE compared to the control group ($p < 0.001$), no such statistically significant increase was seen in the A549 cells treated with the same doses of RTC (Figure 1B). When comparted to the control group, the A549 cells treated with 300, 400, and 600 µg/mL each of RTC and RTE showed a statistically significant increase in the amount of intracellular ROS ($p < 0.001$). In particular, the amount of intracellular ROS in cells treated with 600 µg/mL of RTC dramatically increased in comparison to the levels of intracellular ROS in the control cells and those treated with RTE.

Apoptosis Assessment

As a result of apoptosis, many cellular structures and organelles are damaged or destroyed. The study has evaluated the apoptotic effects of RTC and RTE using different methods such as

AO/EB double staining and Annexin V-FITC. The A549 cells treated with different concentrations (150-600 µg/mL) of RTC and RTE showed the morphological features of apoptosis. According to the dual AO/EB staining, increasing the RTC and RTE doses decreased the live cell rates and increased apoptotic cell rates (Figures 1C, 2 and 3). In particular, the live cell rates of A549 cells treated with 400 and 600 µg/mL of RTC decreased more and the apoptotic cell rates increased more compared to the other groups ($p < 0.0001$; Figure 3). Additionally, the annexin V-FITC results support the AO/EB data (Figure 4).

Western Blotting Results

Increased levels of cleaved caspase-3 and cleaved PARP were detected in the A549 cells after 48 h of RTC and RTE treatment (Figure 5). RTC was determined to have a stronger apoptotic effect compared to RTE ($p < 0.001$; Figures 5B and 5C).

Direct Immunofluorescence Results

In order to investigate the apoptotic effect of *Rubus* extracts on A549 cells, this study exposed the A549 cells to various doses (400 and 600 µg/mL) of RTE and RTC extracts for 48 h. Caspase-3 levels of the cells were analyzed by immunofluorescence staining. While apoptosis in the cells increased significantly compared to the control group after applying 600 µg/mL of RTC, no significant difference was observed in the group that was applied RTE (Figures 6 and 7).

DISCUSSION

Many chemotherapy therapies no longer work as well as they once did because of the development of drug resistance in
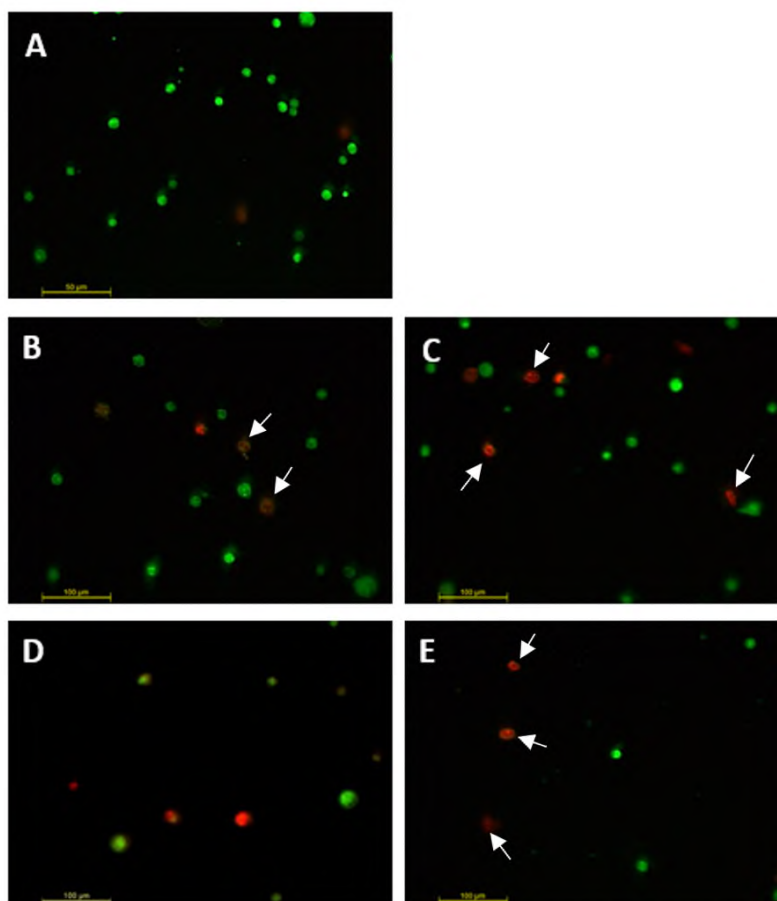
Figure 2. Detection of dose-dependent apoptotic effects of *R. tereticaulis* leaves' active chloroform (RTC) extracts in A549 cells with AO/EB dye. **A)** Control, **B)** 150 µg/mL, **C)** 300 µg/mL, **D)** 400 µg/mL, **E)** 600 µg/mL. Magnification: 20X. Arrows indicated the apoptotic cells.

lung cancer.[4-6] Furthermore, the chemotherapeutic method of treating lung carcinomas frequently results in substantial off-target adverse effects. The trend toward medications made from plants has begun due to their lack of negative side effects and their high levels of phenolic compounds (e.g., flavonoids, phenolic acids).[19] This study focused on the anticancer activity of *R. tereticaulis*, which a previous study on lung cancer had shown to have high phenolic and flavonoid content.[14]

The cytotoxic effect of the ethanol and chloroform extracts of *R. tereticaulis* on human lung cancer cells was investigated by MTT assay after 48 h of incubation with RTE and RTC extracts; 50% of the cells were inhibited at the concentrations of 395 and 480 µg/mL for the respective RTC and RTE extracts. No study in the literature has been found regarding the anticancer activity of *R. tereticaulis*, not only against lung cancer cell line but also against any other cancer line. However, well-known *Rubus* species such as *R. coreanum, R. adenotrichos, R. occidentalis,* and *R. fairholmianus* have all shown anti-cancer effects in previous studies. Two different studies have shown *R. coreanum* ethanolic extracts and *R. coreanus* to have cytotoxic effect on HT-29 colon cancer cells.[20,21] In addition, *R. occidentalis* has been shown to have activity against a number of cancer types

such as esophageal, colorectal, epidermal, and breast cancer in both *in vitro* and *in vivo* studies.[22] These results are in line with those of the current study and confirm the anticancer activity of the *Rubus* species. Although many studies are found to have reported the cytotoxic effects of the *Rubus* species, the cellular mechanisms underlying their effects have not been sufficiently elucidated. This study presents for the first time the half-maximal inhibitory concentrations of the ethanol and chloroform extracts of *R. tereticaulis* on A549 cells.

During malignant transformation, many cancer cells produce an excessive amount of intrinsic ROS, which encourages tumor growth.[20] Cancer cells can boost their survival rate and develop resistance to anti-cancer medications as a result of redox adaptation, which controls anti-apoptotic and antioxidant molecules.[7] Additionally, a growing body of proof is found showing ROS to play a crucial role in both other cells and inflammatory cells when inducing apoptosis.[23] Natural antioxidants at high doses are well-known for exhibiting pro-oxidant activity and to produce ROS via the Fenton reaction. Higher concentrations of antioxidant molecules, particularly in cancer cells, induce DNA damage and apoptosis through their pro-oxidant activity.[24] One previous study found bioactive compounds iso-
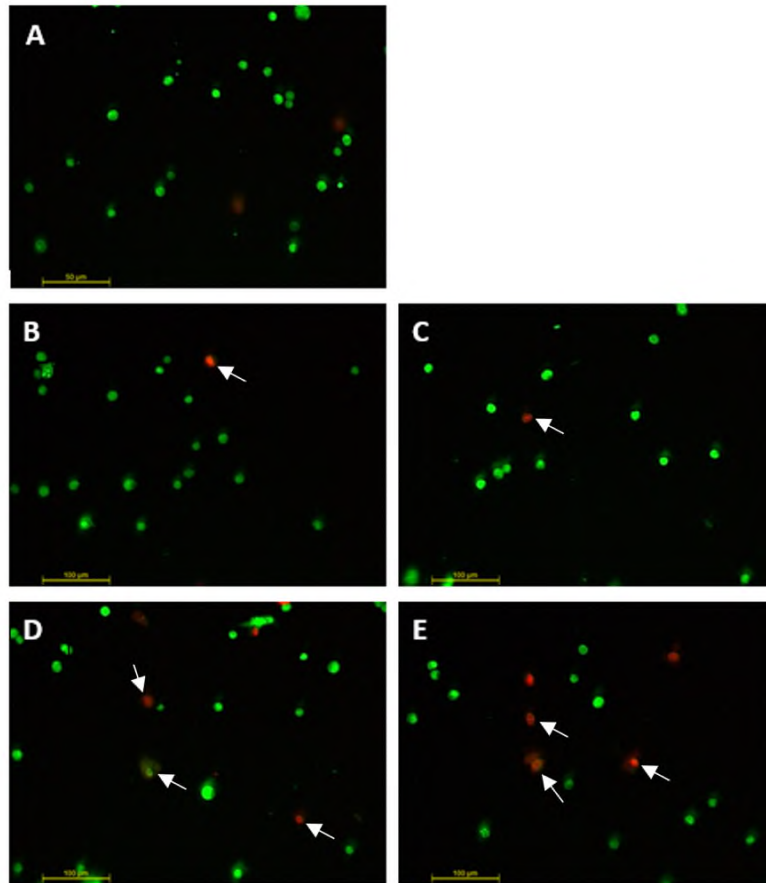
Figure 3. Detection of dose-dependent apoptotic effects of *R. tereticaulis* leaves' active ethanol (RTE) extracts in A549 cells with AO/EB dye. **A)** Control, **B)** 150 µg/mL, **C)** 300 µg/mL, **D)** 400 µg/mL, **E)** 600 µg/mL. Magnification: 20X. Arrows indicated the apoptotic cells.

Figure 4. Annexin-V-FITC dual staining to assess the apoptotic activity of *R. tereticaulis* leaves' active ethanol (RTE) and chloroform (RTC) extracts on A549 cells. Cells were treated with different concentrations RTC and RTE for 24 h, stained with Annexin- V/PI, and measured by a flow cytometry. **A)** RTC- Control, **B)** RTC- 300 µg/mL, **C)** RTC- 600 µg/mL, **D)** RTE- Control, **E)** RTE- 300 µg/mL, **F)** RTE- 600 µg/mL.

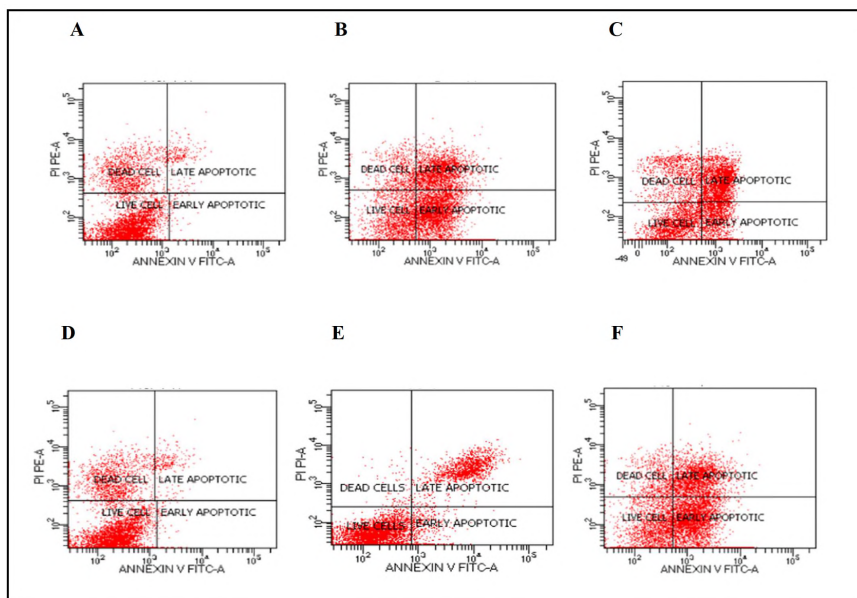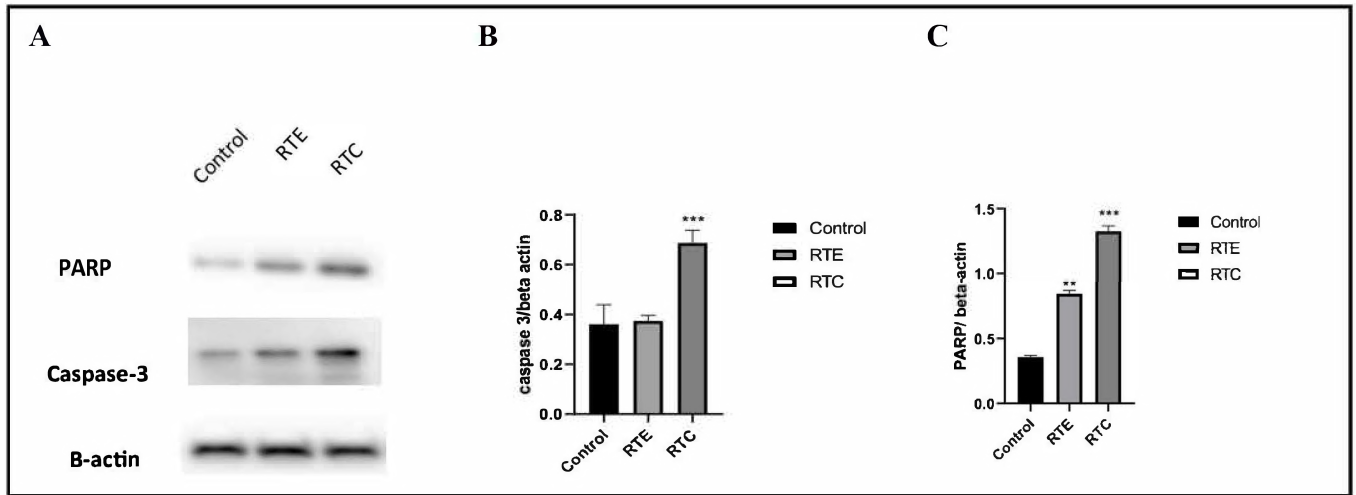**Figure 5.** Examination of apoptotic proteins after 24-hour *R. tereticaulis* leaves' active ethanol (RTE) and chloroform (RTC) extracts application to A549 cells. **A)** Immunopositive bands for caspase-3 and PARP, **B)** Graphic indicates cleaved PARP normalization, **C)** Graphic indicates cleaved caspase-3 normalization. **p<0.01 and *** p<0.001.
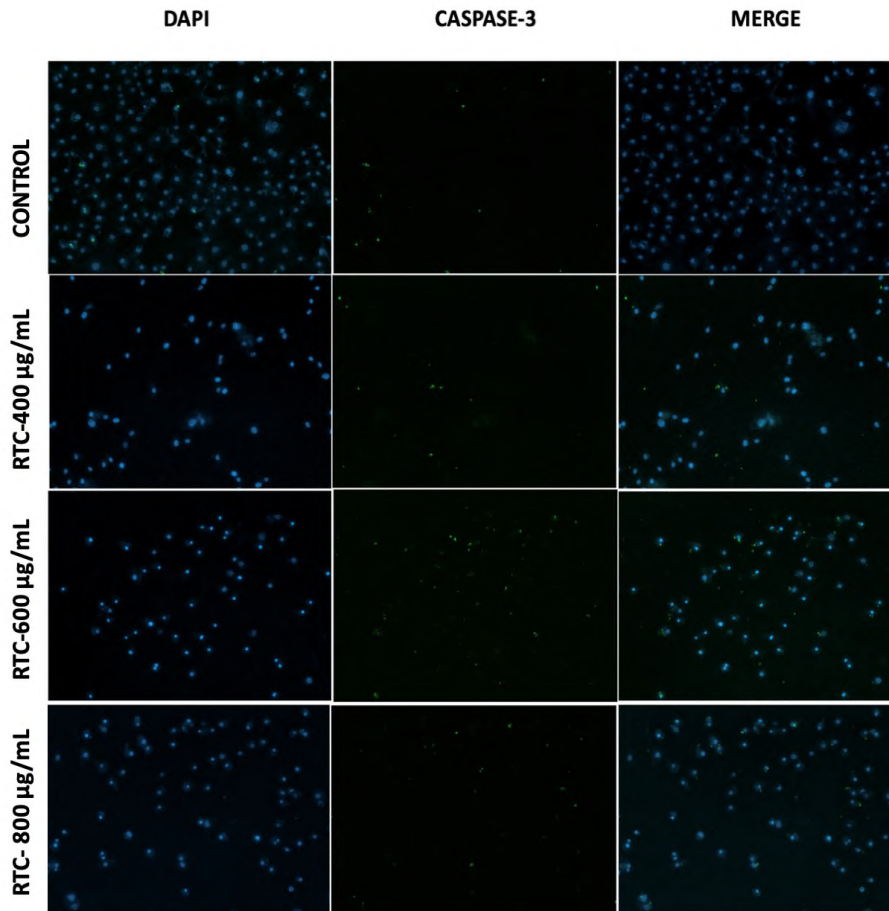
Figure 6. Fluorescence microscope images of A549 cells which were subjected to immunofluorescence detection (10x) after *R. tereticaulis* leaves' active chloroform (RTC) extracts.
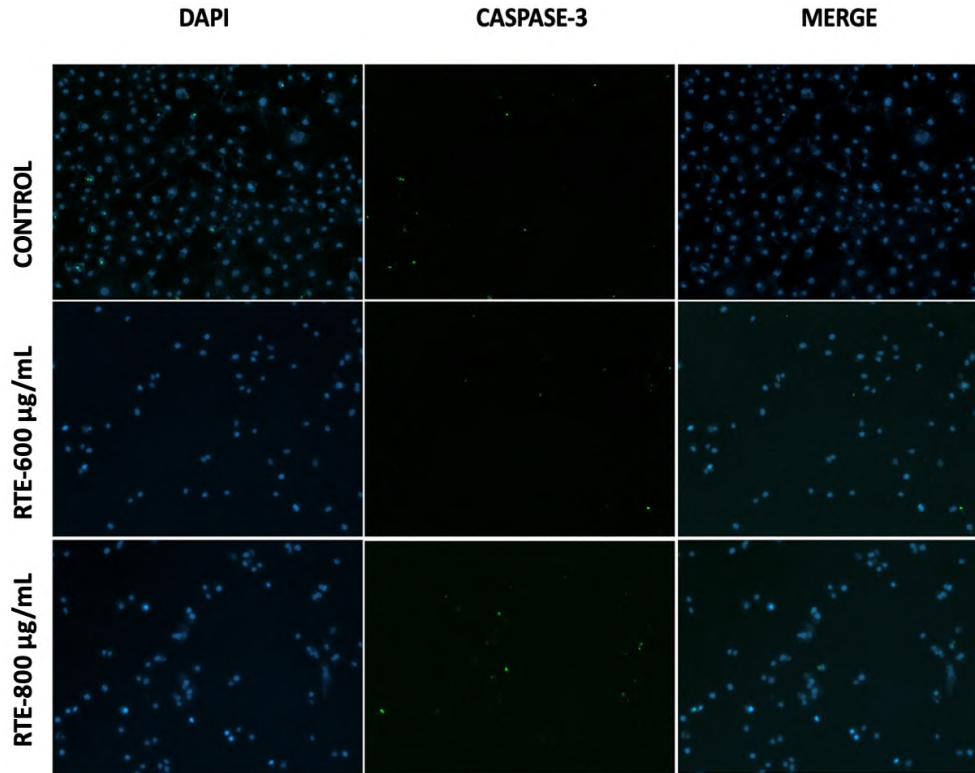
Figure 7. Fluorescence microscope images of A549 cells which were subjected to immunofluorescence detection (10x) after *R. tereticaulis* leaves' active ethanol (RTE) extracts.

lated from *R. fairholmianus* to exert anti-cancer effects by increasing ROS production in MCF-7 breast cancer cells.[25] The current study has shown for the first time the cytotoxic effect of RTC and RTE treatment on A549 cells to be dependent on their pro-oxidant properties. According to this investigation's findings, RTE and RTC treatment of A549 cells has resulted in a decrease in the amount of ROS at lower concentrations while resulting in an increase at higher concentrations.

To date, very few studies have been conducted to elucidate the apoptotic effect of the *Rubus* species on cancer cells; nor has research yet been conducted to elucidate the apoptotic mechanism of *R. tereticaulis* in either cancer or normal cells. During apoptosis, biochemical events occur such as caspase activation in the cell and DNA and protein degradation, as well as some changes to membrane structure. Caspases in particular, which are activated during the caspase phase, take part in breaking down many proteins, nuclei, and cytoskeletons.[26,27] There are some studies that have shown the *Rubus* species' effect on apoptosis signal transduction pathways, but these are limited.[21,25,28] In fact, no studies are found based on *R. tereticaulis*. The present study has reported the treatment of around IC_{50} doses of the RTE and RTC extracts to induce apoptosis significantly compared to the non-treatment group. Morphological, biochemical, and molecular changes related to apoptosis in cells can be measured by different methods. This study analyzed apoptosis

using dual AO/EB staining, annexin V-FITC and immunoblotting analyses, immunofluorescence, and imaging. Apoptotic, necrotic, and living cells can be distinguished by these methods. The results of the current study reveal RTC and RTE at IC_{50} doses to increase apoptosis in A549 cancer cells, with RTC inducing more apoptosis than RTE. Consequently, the mechanisms underlying the cytotoxic and apoptotic activity of the different *Rubus* extracts have been clarified as a result of the evidence for the generation of intracellular ROS and apoptosis. Further studies should be conducted to elucidate the signal transduction pathways underlying these impacts. Additionally, RTC may have had a slightly stronger apoptotic and ROS generative impact than RTE due to being prepared with a different solvent. This may also be due to RTC containing more apolar compounds with cytotoxic activity than RTE.[29]

Recent data have shown inflammation to be closely associated with tumors and to be a critical component of cancer progression.[30] Epidemiologic evidence has also revealed approximately 25% of all human cancers worldwide to be associated with chronic inflammation, chronic infection, or both.[31] The use of anti-inflammatory agents can improve patients' prognoses by reducing the incidence and recurrence of various cancers.[32] Naturally derived agents with anti-inflammatory activity have also been reported to have anti-cancer activity.[33] Therefore, conducting research is important on medicinal plants

whose anti-inflammatory and antioxidant activity have already been investigated. Previous studies have revealed RTE and RTC to show antioxidant and anti-inflammatory activity due to their phenolic and flavonoid contents. In addition, the major compound of RTE that has antioxidant and anti-inflammatory activity was revealed to be quercetin-3-O-β-D-glucuronide.[14] Some studies have suggested that natural phenolic compounds with pro-oxidant and anti-inflammatory properties may be promising anticancer agents against lung cancer.[34,35] Thus, the phenolic compounds in RTE and RTC that have pro-oxidant and anti-inflammatory activity may be responsible for the anticancer activity. In addition, quercetin glucuronides have been shown to have cell cycle arresting and apoptosis-inducing effects against the human lung cancer cell line NCI-H209.[36] Therefore, one can argue that quercetin-3-O-β-D-glucuronide, which has been shown to have antioxidant and anti-inflammatory activity in previous studies and is the major compound in RTE, is also significantly responsible for RTE's anticancer activity.

CONCLUSION

The present results have demonstrated *R. tereticaulis* extracts, especially RTC, to be able to be a potential therapeutic agent for human lung cancer treatment. However, *in vivo* studies are needed to fully demonstrate RTC's anticancer effect against lung cancer.

ORCID IDs of the author

Gamze Nur Oter	0000-0002-7063-3984
Ezgi Durmus	0000-0002-0760-497X
Ali Sen	0000-0002-2144-5741
Abdurrahim Kocyigit	0000-0003-2335-412X

REFERENCES

1. Hirsch FR, Scagliotti GV, Mulshine JL, et al. Lung cancer: current therapies and new targeted treatments. *Lancet*. 2017;389(10066):299-311.

2. Oser MG, Niederst MJ, Sequist LV, Engelman JA. Transformation from non-small-cell lung cancer to small-cell lung cancer: Molecular drivers and cells of origin. *Lancet Oncol*. 2015;16(4):e165-e172. doi:10.1016/S1470-2045(14)71180-5

3. Zappa C, Mousa, SA. Non-small cell lung cancer: Current treatment and future advances. *Transl Lung Cancer Res*. 2016;5(3):288. doi:10.21037/tlcr.2016.06.07

4. Li N, Mai Y, Liu Q, Gou G, Yang J. Docetaxel-loaded D-α-tocopheryl polyethylene glycol-1000 succinate liposomes improve lung cancer chemotherapy and reverse multidrug resistance. *Drug Deliv Transl Res*. 2021;11:131-141.

5. Lynch TJ, Kass F, Elias AD, et al. Cisplatin, 5-fluorouracil, and etoposide for advanced non-small cell lung cancer. *Cancer*. 1993;71(10):2953-2957.

6. Zhang M, Li M, Du L, Zeng J, Yao T, Jin Y. Paclitaxel-in-liposome-in-bacteria for inhalation treatment of primary lung cancer. *Inter J Pharm*. 2020;578:119177. doi: 10.1016/j.ijpharm.2020.119177

7. Storz P. Mitochondrial ROS–radical detoxification, mediated by protein kinase D. *Trends Cell Bio*. 2007;17(1):13-18.

8. Prakash O, Kumar A, Kumar P, Ajeet. Anticancer potential of plants and natural products. *Am J Pharmacol Sci*. 2013;1(6):104-115.

9. Hyun TK, Kim HC, Ko YJ, Kim JS. Antioxidant, α-glucosidase inhibitory and anti-inflammatory effects of aerial parts extract from Korean crowberry (*Empetrum nigrum* var. *japonicum*). *Saudi J Bio Sci*. 2016;23(2):181-188.

10. George BP, Abrahamse H. Traditional uses and bioactivities of common *Rubus* species with reference to cancer: A mini-review. *Phyto:Pot Ther Appl*. 2021;259-270.

11. Tuzlacı E. *Türkiye Bitkileri Geleneksel İlaç Rehberi (Turkey's Plants Traditional Medicine Guide)*, First ed. İstanbul: İstanbul Tıp Kitabevleri Press; 2016.

12. Gudej J, Tomczyk M. Determination of flavonoids, tannins and ellagic acid in leaves from *Rubus* L. species. *Arch Pharm Res*. 2004;(27):1114-1119.

13. Wolniak M, Tomczykowa M, Tomczyk M, Gudej J, Wawer I. Antioxidant activity of extracts and flavonoids from *Bidens tripartita*. *Acta Poloniae Pharm*. 2007; 64(5): 441-447.

14. Sen A, Ozbeyli D, Teralı K, et al. Protective effects of *Rubus tereticaulis* leaves ethanol extract on rats with ulcerative colitis and bio-guided isolation of its active compounds: A combined *in silico*, *in vitro* and *in vivo* study. *Chemico-Bio Inter*. 2023;369:110263. doi:10.1016/j.cbi.2022.110263

15. Aksoy H, Demirbag C, Sen A, et al. Evaluation of biochemical parameters in *Rubus tereticaulis* treated rats and its implications in wound healing. *Mol Cell Biochem*. 2020; 472:67-78.

16. Kocyigit A, Guler EM, Karatas E, Caglar H, Bulut H. Dose-dependent proliferative and cytotoxic effects of melatonin on human epidermoid carcinoma and normal skin fibroblast cells. *Mut Res Genet Toxico Envir Mutag*. 2018;829:50-60.

17. Wu T, Qiang L, Chen FH, et al. LFG-500, a newly synthesized flavonoid, induced a reactive oxygen species-mitochondria-mediated apoptosis in hepatocarcinoma cells. *Bio Preven Nutr*. 2011;1(2):132-138.

18. Mcgahon AJ, Martin SJ, Bissonnette RP, et al. The end of the (cell) line: Methods for the study of apoptosis *in vitro*. *Method Cell Biol*. 1995;46:153-185.

19. Wen T, Song L, Hua S. Perspectives and controversies regarding the use of natural products for the treatment of lung cancer. *Cancer Med*. 2021;10(7):2396-2422.

20. Zhao X, Song J, Lee JH, Kim SY, Park KY. Antioxidation and cancer cell (HT-29) antiproliferation effects of *Rubus coreanus* Miquel bamboo salt. *J Cancer Prev.* 2010; 15(4):306-312.

21. Kim EJ, Lee YJ, Shin HK, Park JHY. Induction of apoptosis by the aqueous extract of Rubus coreanum in HT-29 human colon cancer cells. *Nutrition.* 2005;21(11-12):1141-1148.

22. Saikolappan S, Kumar B, Shishodia G, Koul S, Koul HK. Reactive oxygen species and cancer: A complex interaction. *Cancer Lett.* 2019;452:132-143.

23. Simon HU, Haj-Yehia A, Levi-Schaffer F. Role of reactive oxygen species (ROS) in apoptosis induction. *Apoptosis.* 2000;5:415-418.

24. Kocyigit A, Koyuncu I, Taskin A, Dikilitas M, Bahadori F, Turkkan B. Antigenotoxic and antioxidant potentials of newly derivatized compound naringenin-oxime relative to naringenin on human mononuclear cells. *Drug Chem Toxicol.* 2016;39(1):66-73.

25. George BP, Abrahamse H. Increased oxidative stress induced by rubus bioactive compounds induce apoptotic cell death in human breast cancer cells. *Oxid Med Cell Longev.* 2019;6797921. doi:10.1155/2019/6797921

26. Lavrik IN, Golks A, Krammer PH. Caspases: Pharmacological manipulation of cell death. *J Clinic Inves.* 2005;115(10):2665-2672.

27. Galluzzi L, Maiuri MC, Vitale I, et al. Cell death modalities: Classification and pathophysiological implications. *Cell Death Differ.* 2007;14(7):1237-1243.

28. Plackal Adimuriyil George B, Tynga IM, Abrahamse H. *In vitro* antiproliferative effect of the acetone extract of *Rubus fairholmianus* gard. Root on human colorectal cancer cells. *BioMed Res Inter.* 2015;2015:165037. doi:10.1155/2015/165037

29. Erel SB, Demir S, Nalbantsoy A, et al. Bioactivity screening of five *Centaurea* species and *in vivo* anti-inflammatory activity of *C. athoa. Pharm Biol.* 2014;52(6):775-781.

30. Coussens LM, Werb Z. Inflammation and cancer. *Nature.* 2002;420(6917):860-867.

31. Morrıson WB. Inflammation and cancer: A comparative view. *J Vet Int Med.* 2012; 26(1):18-31.

32. Rayburn ER, Ezell SJ, Zhang R. Anti-inflammatory agents for cancer therapy. *Mol Cell Pharm.* 2009;1(1):29-43.

33. Kawamori T, Lubet R, Steele VE, et al. Chemopreventive effect of curcumin, a naturally occurring anti-inflammatory agent, during the promotion/progression stages of colon cancer. *Cancer Res.* 1999;59(3):597-601.

34. Muller AG, Sarker SD, Saleem IY, Hutcheon GA. Delivery of natural phenolic compounds for the potential treatment of lung cancer. *DARU J Pharma Sci.* 2019;27: 433-449.

35. Amararathna M, Johnston MR, Rupasinghe HPV. Plant polyphenols as chemopreventive agents for lung cancer. *Inter J Mol Sci.* 2016;17(8):1352. doi:10.3390/ijms17081352

36. Murakami A, Ashida H, Terao J. Multitargeted cancer prevention by quercetin. *Cancer Lett.* 2008;269(2):315-325.

How to cite this article

Investigating the Involvement of Fibroblast Growth Factors in Adipose Tissue Thermogenesis

Serkan Kir[1] iD

[1] Koç University, Faculty of Sciences, Department of Molecular Biology and Genetics, Istanbul, Türkiye

ABSTRACT

Objective: Thermogenesis in white and brown adipose tissues can be induced by various stimuli, including cold exposure, β-adrenergic stimulation, and tumor growth. Fibroblast growth factor (FGF) 21 has emerged as an important mediator of thermogenesis. This study investigated the involvement of other FGF family members in the regulation of adipose tissue thermogenesis.

Materials and Methods: Mice were exposed to cold and administrated a β-adrenergic agonist (CL-316,243) to stimulate a thermogenic response in adipose tissues. Stromavascular fractions isolated from white and brown adipose tissues were cultured and differentiated into primary adipocytes. These cells were treated with recombinant FGFs. Changes in the expression levels of thermogenic genes and FGFs were determined by real-time quantitative PCR.

Results: Cold exposure stimulated thermogenic gene expression in the adipose tissue, which was accompanied by the upregulation of certain FGFs. *Ffg9* and *Fgf21* were prominently induced in white and brown adipose tissues. β-adrenergic stimulation also upregulated thermogenic genes in adipocytes. *Fgf21* was identified as the main responder to the β-adrenergic pathway. The administration of recombinant FGFs to cultured primary white and brown adipocytes induced thermogenic genes, including *uncoupling protein-1 (Ucp1)*. FGF2, FGF9, and FGF21 triggered the most significant *Ucp1*-inducing effects in these cells.

Conclusion: FGF21 is as a prominent inducer of thermogenesis in adipose tissue and a promising therapeutic target against cardiovascular and metabolic diseases. FGF2 and FGF9 potently promote thermogenic gene expression in adipocytes. Therefore, their therapeutic targeting should be considered to enhance energy metabolism in adipose tissues.

Keywords: Adipose tissue thermogenesis, Browning, Fibroblast growth factors, FGF2, FGF9, FGF21

INTRODUCTION

Nonshivering thermogenesis involves the generation of heat by brown adipose tissue and is an important response to cold exposure. Brown fat contributes to the maintenance of body temperature in rodents and human infants.[1,2] Recently, the activation of adipose depots by cold exposure has been described in human adults.[3-5] In addition, white adipose tissue has been shown to acquire thermogenic capacity in response to various stimuli, including cold exposure, β-adrenergic stimulation, and tumor growth.[1,6,7] This process is referred to as "browning" and is associated with the increased expression of Uncoupling Protein 1 (UCP1). This protein is localized to the mitochondrial inner membrane and facilitates proton leakage. UCP1 uncouples ATP generation from the proton gradient, which results in enhanced oxidative metabolism and heat generation.[8] The upregulation of *Ucp1* expression is an important marker of adipose tissue browning and thermogenic activity.[9] In addition, the thermogenic program in adipocytes involves increased levels of genes such as *Cidea, Dio2,* and *Pgc1a*.[10] Importantly, *Pgc1a* is a transcriptional regulator, which is responsible for inducing the expression of thermogenic genes.[9]

Fibroblast growth factor (FGF) 21 has previously been described as a prominent inducer of browning in the white adipose tissue of rodents.[11-13] The expression of this protein is stimulated in adipose tissues in response to cold exposure or through β-adrenergic stimulation.[14] Treatment of adipocytes with recombinant FGF21 protein upregulated *UCP1* and other thermogenesis-related genes.[15] The genetic deletion of FGF21 in mice impaired heat generation in response to cold exposure and β-adrenergic stimulation.[15,16] However, the long-term cold adaptation in mice did not require FGF21, which suggests the potential contribution of other factors.[17] FGF21 is

a member of the FGF family that is made up of 18 proteins, which exhibit varying expression profiles in different tissues. These include FGF1–FGF10 and FGF16–FGF23. FGF homologous factors, FGF11- FGF14, are not considered FGF family members because these proteins do not activate FGF receptors (FGFRs).[18] FGF proteins play diverse roles in pathophysiology, ranging from angiogenesis and wound healing to embryonic development.[19] Some of these factors have been associated with the regulation of various aspects of glucose and energy metabolism.[19,20]

In this study, we explored the involvement of different FGF family members in the regulation of adipose tissue thermogenesis. We examined the expression levels of FGFs in the brown and white adipose tissue of mice and their regulation in response to cold exposure and β-adrenergic stimulation. The FGFs that were expressed in adipose tissues at detectable levels (FGF1, FGF2, FGF7, FGF9, FGF10, FGF16, FGF17, FGF18, FGF21, and FGF22) were also tested in the primary white and brown adipocytes for their ability to stimulate thermogenic gene expression.

MATERIALS AND METHODS

Reagents

Recombinant proteins FGF1, FGF2, FGF7, FGF9, FGF10, FGF16, FGF17, FGF18, FGF21, and FGF22 were purchased from R&D Systems, and the β-adrenergic agonist CL-316,243 (C5976) was obtained from Sigma.

Mice

C57BL/6 male mice were used for all experiments, which were performed at the KUTTAM Animal Research Facility of Koç University. These 8–12-week-old mice were provided ad libitum access to standard rodent chow diet and water. For temperature-controlled experiments, the mice were placed under thermoneutral conditions (30°C) for 24 h to acclimate. The cold exposure group was transferred to 4°C for 6 h. The mice were individually housed to prevent huddling under the cold conditions. Mice were administered CL-316,243 intraperitoneally (1 mg/kg body weight) and sacrificed after 6 h. All animal protocols were reviewed and approved by the Institutional Animal Care and Use Committee of Koç University (permit number: 2024, HADYEK.003). All experiments were conducted in accordance with institutional policies and animal care ethics guidelines.

Primary White Adipocyte Culture

Stromavascular fractions of inguinal fat depots were isolated from mice that were 30–35 days old. The detailed procedure has been previously described.[6] Cells were maintained in an adipocyte culture medium composed of Dulbecco's Modified Eagle Medium/Nutrient Mixture F-12 (DMEM/F12)-glutamax (Invitrogen), penicillin/streptomycin (Invitrogen), and 10% fetal bovine serum (FBS). The cells were differentiated into primary white adipocytes by the addition of a differentiation cocktail containing 0.5 mM isobutylmethylxanthine (Sigma), 5 µg/mL insulin (Sigma), 1 µM dexamethasone (Sigma), and 1 µM rosiglitazone (Sigma) for 2 days. In the 4 days that followed, the adipocyte culture medium was supplemented with 5 µg/mL insulin and 1 µM rosiglitazone. During the next 2 days, the cells were maintained in the adipocyte culture medium, treated with the recombinant FGF proteins for 24 h, and then harvested 8 days after the initiation of differentiation.

Primary Brown Adipocyte Culture

Stromavascular fractions of interscapular brown fat depots were isolated from newborn mice that were 2–4 days old. The detailed procedure thereof has been previously described.[6] Cells were maintained in an adipocyte culture medium composed of DMEM/F12-glutamax (Invitrogen), penicillin/streptomycin (Invitrogen), and 10% FBS. The cells were differentiated into primary brown adipocytes by the addition of a differentiation cocktail containing 0.5 mM isobutylmethylxanthine (Sigma), 125 µM indomethacin (Sigma), 5 µM dexamethasone (Sigma), 0.02 µM insulin (Sigma), 1 nM T3 (Sigma), and 1 µM rosiglitazone (Sigma) for 2 days. The adipocyte culture medium was then supplemented with 0.02 µM insulin, 1 nM T3, and 1 µM rosiglitazone for a further 2 days. Cells maintained in the adipocyte culture medium were treated with recombinant FGF proteins for 24 h and then harvested 8 days after the initiation of differentiation.

Gene Expression Analysis (RT-qPCR)

Total RNA was isolated and used to perform reverse transcription reactions and real-time quantitative PCR (RT-qPCR) reactions, as previously described.[21] The ΔCt method was used to calculate the relative mRNA expression levels, which were normalized to cyclophilin. The RT-qPCR primer sets used in the study are presented in Table 1.

Statistical Analysis

Statistical analysis was conducted using a two-tailed and unpaired t-test for the comparison of two groups and a one-way analysis of variance (ANOVA) for the comparison of multiple groups. ANOVA comparisons were corrected using Tukey's post-hoc test. Values were presented as the mean ± standard error of the mean. Error bars represent deviation between biological replicates. Differences with a P value less than 0.05 were regarded as statistically significant.

Gene	Forward (5'-3')	Reverse (5'-3')
Cyclo	GGAGATGGCACAGGAGGAA	GCCCGTAGTGCTTCAGCTT
Ucp1	AAGCTGTGCGATGTCCATGT	AAGCCACAAACCCTTTGAAAA
Dio2	TCCTAGATGCCTACAAACAGGTTA	CGGTCTTCTCCGAGGCATAA
Cidea	GGTTCAAGGCCGTGTTAAGG	CGTCATCTGTGCAGCATAGG
Pgc1a	AGACAAATGTGCTTCGAAAAAGAA	GAAGAGATAAAGTTGTTGGTTTGGC
Ap2	AGTGAAAACTTCGATGATTACATGAA	GCCTGCCACTTTCCTTGTG
Fgf1	ACACCGAAGGGCTTTTATACG	GTGTAAGTGTTATAATGGTTTTCTTCCA
Fgf2	CAACCGGTACCTTGCTATGA	TCCGTGACCGGTAAGTATTG
Fgf7	AAGGGACCCAGGAGATGAAG	ACTGCCACGGTCCTGATTT
Fgf9	CTATCCAGGGAACCAGGAAAGA	CAGGCCCACTGCTATACTGATAAA
Fgf10	GCGGGACCAAGAATGAAGA	AGTTGCTGTTGATGGCTTTGA
Fgf16	GGCCTGTACCTAGGAATGAATGA	TTCCCGGAAAACACATTCAC
Fgf17	GGCAAATCCGTGAATACCA	CTGCTGCCGAATGTATCTGT
Fgf18	TGCTGTGCTTCCAGGTTCA	GGATGCGGAAGTCCACATT
Fgf21	CCTCTAGGTTTCTTTGCCAACAG	AAGCTGCAGGCCTCAGGAT
Fgf22	GTGGGCACTGTGGTGATCA	GCGATTCATGGCCACATAGA

RESULTS

Cold Exposure Stimulated the Expression of Thermogenic Genes and FGFs, Including *Fgf9* and *Fgf21*, in Adipose Tissues

We investigated the transcriptional changes that occurred in the adipose tissue in response to cold exposure and assessed the FGF expression levels. For this purpose, mice were exposed to thermoneutral conditions (30°C) for 24 h, and a group of them was transferred to 4°C for 6 h as the cold exposure group. Epididymal white adipose tissue (eWAT) and inguinal white adipose tissue (iWAT), which represent visceral and subcutaneous fat depots, respectively, were collected, as well as the interscapular brown adipose tissue (iBAT). The thermogenesis-inducing effect of cold exposure was confirmed by the increased expression of *Ucp1* and other thermogenic genes, including *Dio2, Cidea*, and *Pgc1a*, while *Ap2* expression was evaluated as an adipose tissue-specific marker gene. The up-and down-regulation of the FGFs was investigated in these tissues.

We found that adipose tissue expressed the following FGFs: F*gf1, Fgf2, Fgf7, Fgf9, Fgf10, Fgf16, Fgf17, Fgf18, Fgf21*, and *Fgf22*. In the eWAT depots, mRNA levels of *Ucp1, Dio2*, and *Cidea* were induced by cold exposure compared to thermoneutrality (Figure 1A). *Fgf1* and *Fgf16* expression were stimulated in this tissue, whereas *Fgf2* and *Fgf7* were downregulated (Figure 1B). iWAT tissue responded to cold exposure robustly as the expression of all thermogenic genes was significantly stimulated (Figure 1C). In this tissue, *Fgf9* and *Fgf21* were upregulated, whereas *Fgf2, Fgf17*, and *Fgf18* were downregulated (Figure 1D). *Ucp1* and *Dio2* were induced by cold exposure in iBAT, and the expression of *Fgf1, Fgf9, Fgf18*, and *Fgf21* was also stimulated (Figures 1E and 1F). All other FGFs were downregulated in this tissue upon cold exposure (Figure 1F). These results demonstrate that cold exposure stimulated ther-

mogenic activity in adipose tissues, which was accompanied by the upregulation of certain FGFs. In the iWAT and iBAT depots, the expression of *Ffg9* and *Fgf21* was prominently induced.

β-Adrenergic Activation Upregulated Thermogenic Genes and *Fgf21* in Adipose Tissues

We next investigated the influence of β-adrenergic stimulation on adipose tissue gene expression. Mice that were housed at room temperature were administered the β-adrenergic agonist CL-316,243 and sacrificed after 6 h. We assessed the expression of thermogenic genes and FGFs in the adipose tissues. *Ucp1, Dio2*, and *Pgc1a* were robustly upregulated in eWAT upon β-adrenergic stimulation (Figure 2A). This was accompanied by a mild effect on *Fgf7* expression and a marked increase in *Fgf21* mRNA levels (Figure 2B); however, the expression of *Fgf1* and *Fgf7* was reduced (Figure 2B). The same thermogenic genes were also induced in iWAT, where *Fgf21* was dramatically upregulated (Figures 2C and 2D), and *Fgf1, Fgf2*, and *Fgf7* were downregulated (Figure 2D). iBAT responded to the β-adrenergic agonist with significantly increased levels of *Dio2* and *Pgc1a* (Figure 2E). The expression of *Fgf21* was robustly induced with milder increases in *Fgf17, Fgf18*, and *Fgf22* (Figure 2E). These results indicate that β-adrenergic stimulation upregulates the thermogenic gene expression in adipose tissues, particularly in eWAT and iWAT. *Fgf21* was identified as the main responder to the β-adrenergic pathway.

FGF2, FGF9, and FGF21 were the Most Prominent Inducers of Thermogenic Gene Expression in Adipocytes

To investigate the potential impact of FGFs on the regulation of thermogenic gene expression, we utilized primary white and brown adipocytes isolated from mice. Briefly, stromavascular
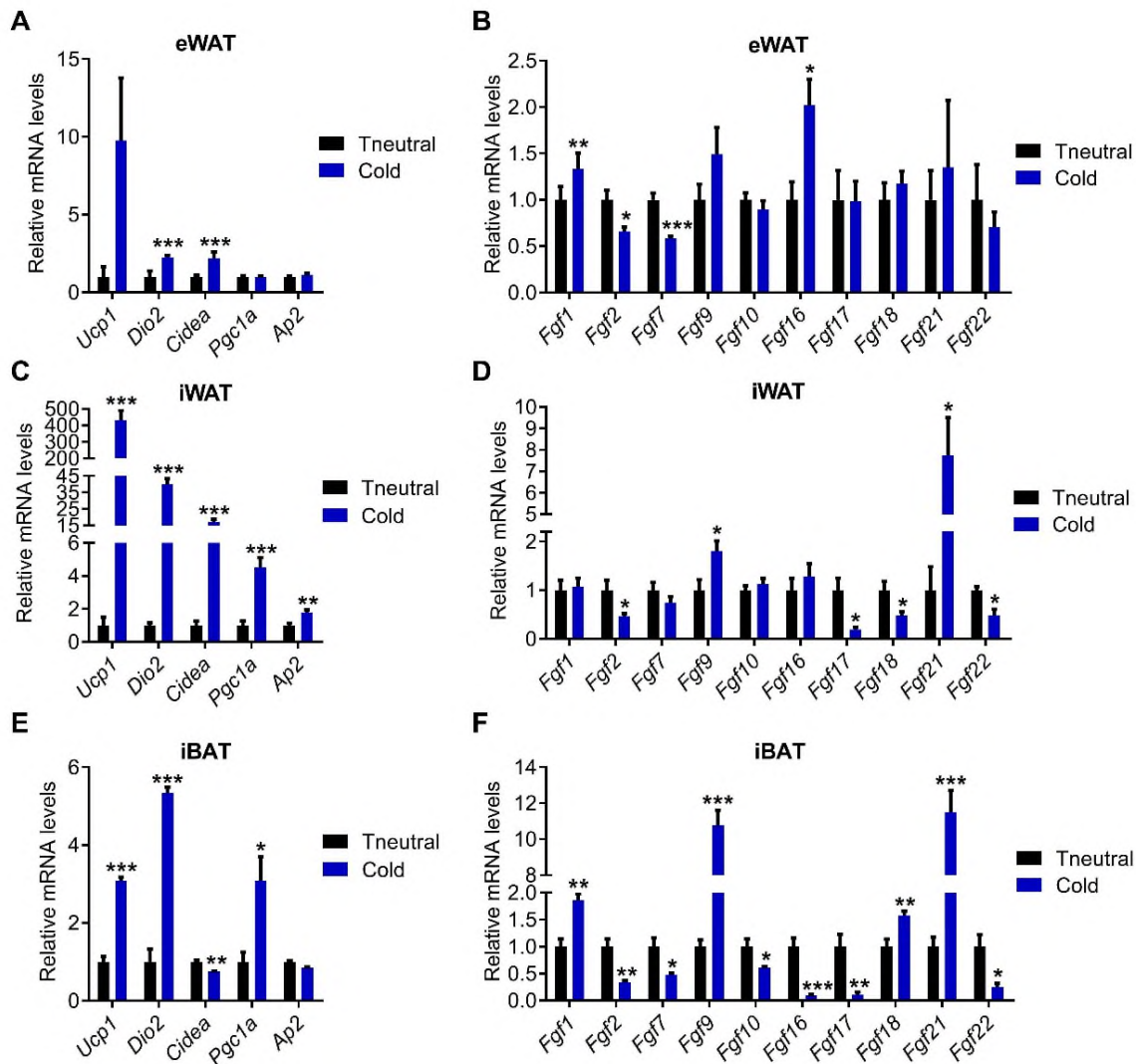
Figure 1. Cold exposure stimulates the expression of thermogenic genes and FGFs, including *Fgf9* and *Fgf21*. Mice were placed under thermoneutrality (30°C; Tneutral) for 24 h. One group was exposed to cold (4°C) for 6 h. eWAT (**A** and **B**), iWAT (**C** and **D**) and iBAT (**E** and **F**) tissues were collected and gene expression was tested by RT-qPCR (n = 5). Values are mean ± SEM. * $p < 0.05$, ** $p < 0.01$ and *** $p < 0.001$ versus Tneutral.

fractions prepared from iWAT and iBAT depots were cultured and differentiated into white and brown adipocytes, respectively, through the administration of a differentiation-inducing cocktail. After 7 days, the fully differentiated adipocytes were treated with recombinant FGFs for 24 h, and changes in their gene expression were studied. In the white adipocytes, *Ucp1* mRNA was significantly upregulated by FGF2, FGF9, and FGF21 treatment (Figure 3A). *Dio2* was upregulated by FGF9 and FGF17 treatment, while *Cidea* was induced by FGF16 and FGF21 treatment (Figure 3A). In the brown adipocytes, *Ucp1* mRNA was significantly upregulated by FGF2, FGF9, FGF17, and FGF21 treatment, while *Cidea* was induced by FGF9, FGF16, and FGF21 treatment (Figure 3B). These results suggest that FGF2, FGF9, and FGF21 triggered the most significant *Ucp1*-inducing effects in the primary adipocytes.

DISCUSSION

FGF21 has emerged as an important therapeutic target in cardiovascular and metabolic diseases.[22] In addition to FGF19 and FGF23, FGF21 is a member of the FGF subfamily, whose members function as hormones because of their reduced affinity toward heparan sulfate that is found in the extracellular matrix.[23] Heparan sulfate is required for the binding of FGFs to FGFRs.[24] However, for the endocrine FGFs, this function is performed by the Klotho and β-klotho coreceptors.[20] Previous studies have demonstrated that FGF21 is highly induced upon cold exposure or through β-adrenergic stimulation and that FGF21 stimulated adaptive thermogenesis in adipocytes by the upregulation of UCP1 and other thermogenic genes.[14,15] The findings presented in this study confirmed the cold exposure and β-adrenergic
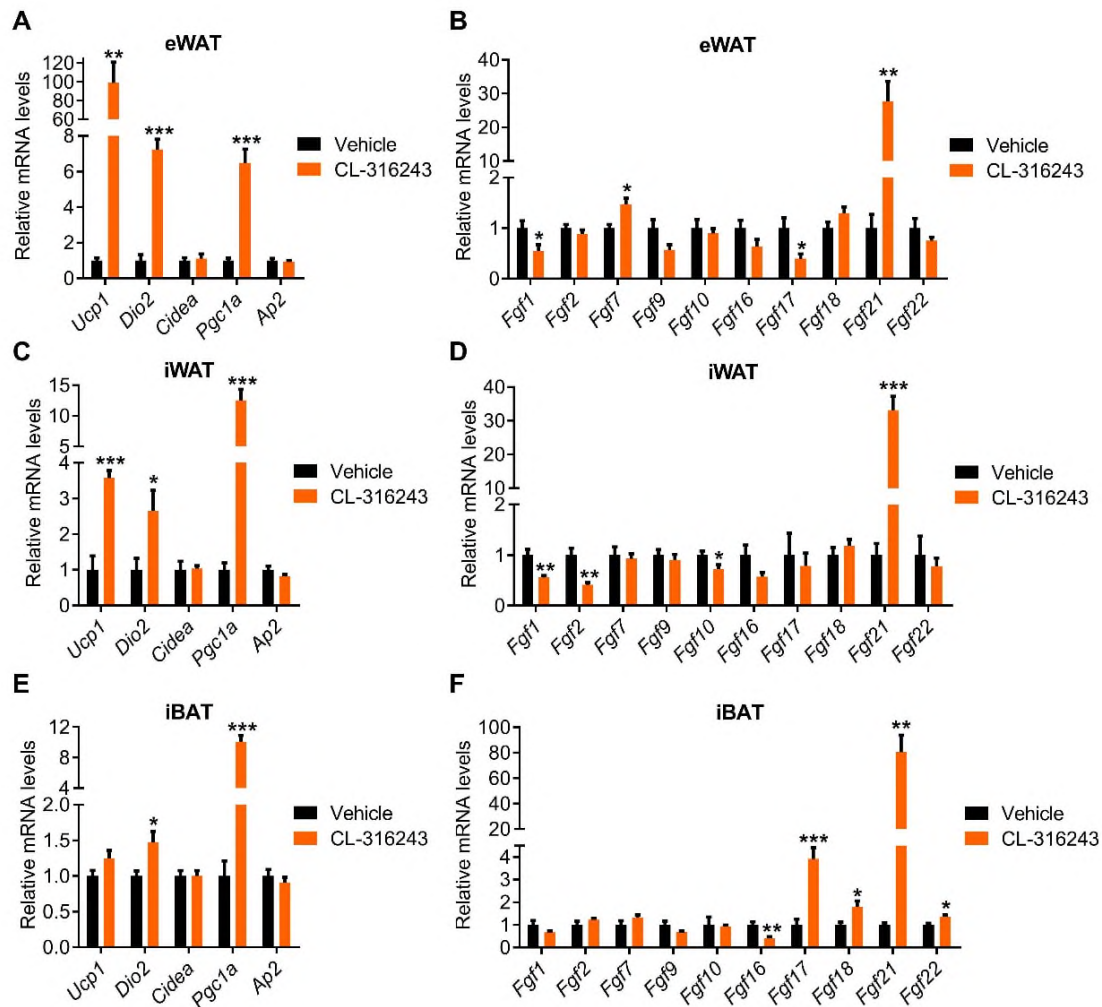
Figure 2. β -adrenergic stimulation induces the expression of thermogenic genes and FGFs, including *Fgf17* and *Fgf21*. Mice received intraperitoneal injections of CL-316,243 (1 mg/kg body weight) and sacrificed 6 h later. eWAT (**A** and **B**), iWAT (**C** and **D**) and iBAT (**E** and **F**) tissues were harvested and gene expression was tested by RT-qPCR (n = 5). Values are mean ± SEM. * $p < 0.05$, ** $p < 0.01$ and *** $p < 0.001$ versus vehicle.

pathway-dependent regulation of FGF21 and further confirmed the potency of this protein to upregulate thermogenic genes. Previously, FGF21-related improvements in glucose and energy metabolism were partly attributed to the thermogenic and browning-inducing effects of this hormone.[12,25] The autocrine functions of FGF21 in adipose tissue have been found to be relevant for the induction of thermogenic gene expression.[16] However, FGF21 likely stimulates energy metabolism via mechanisms that are independent of UCP1-mediated thermogenesis, and the long-term adaptation to cold exposure may not require FGF21.[17,26] Various therapeutic agents targeting FGF21 have been developed and tested in preclinical and clinical studies to treat hepatic lipid accumulation and systemic insulin resistance.[12] Particularly, FGF21 analogs have demonstrated efficacy in reversing the fat content in the liver. However, side effects are associated with these drugs, which have been observed in clinical trials, and FGF21-induced bone loss has been

reported in rodent models, thus raising safety concerns regarding the use of these therapeutics.[12,27]

Previous studies have indicated that FGF2 and FGF9 negatively influence the browning program of adipocytes.[28,29] FGF9 expression was reported to be suppressed in adipose tissue in response to cold stress.[28] In contrast, our study detected significantly upregulated levels of *Fgf9* in iWAT and iBAT tissues upon cold exposure, and FGF9 treatment of fully differentiated adipocytes activated the thermogenic gene expression. In agreement with the results presented here, a recent study demonstrated that FGF9 expression in adipose tissue was upregulated by exposure to cold conditions, and FGF9 promoted UCP1 expression in adipocytes. FGF9 expression is positively correlated with UCP1 levels in human neck fat biopsies. BAT-specific deletion of FGF9 caused impaired cold tolerance, which suggests an important role of this protein in BAT thermogenesis.[30] Previously, whole-body FGF2 disruption was
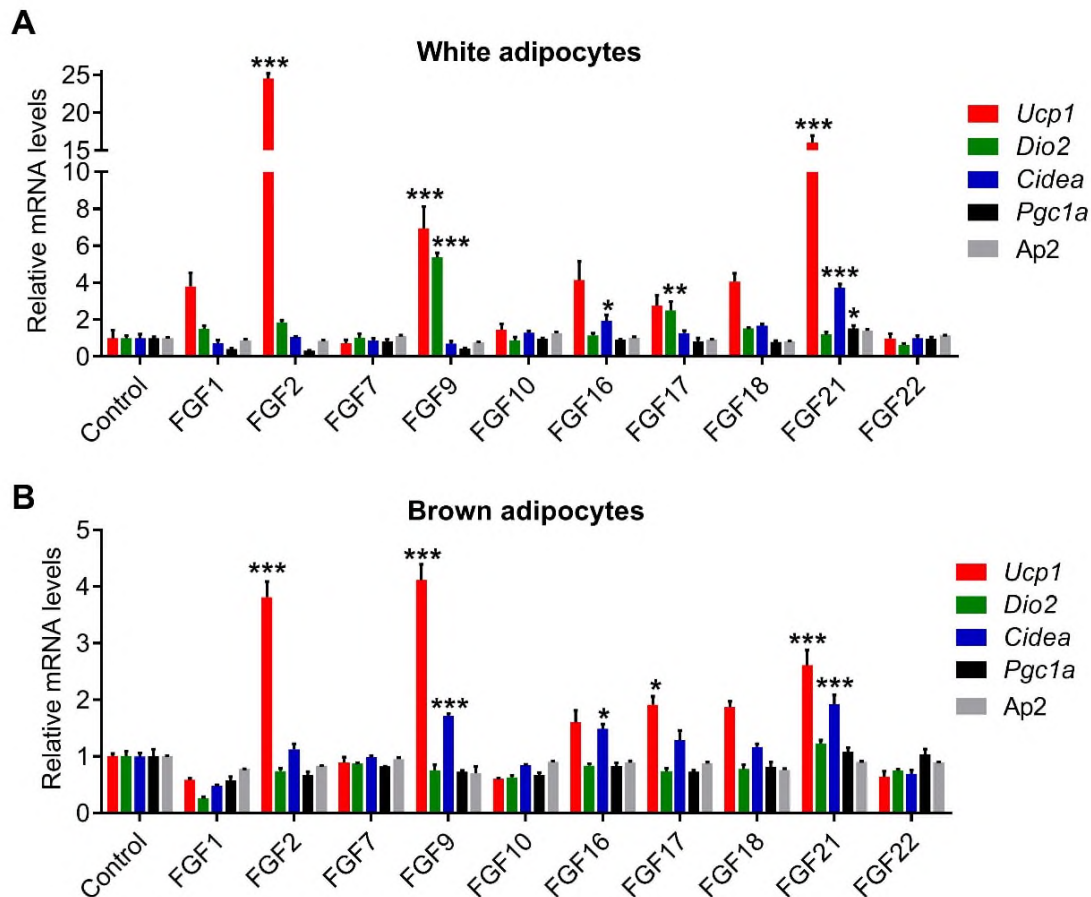
Figure 3. Thermogenic gene expression in adipocytes is induced by FGFs, including FGF2, FGF9 and FGF21. White (**A**) and brown (**B**) adipocytes were fully differentiated and treated with various FGFs (250 ng/ml) for 24 h. Gene expression was tested by RT-qPCR (n = 3). * $p < 0.05$, ** $p < 0.01$ and *** $p < 0.001$ versus control.

revealed to enhance thermogenic capacity in the adipose tissue of mice, whereas the administration of exogenous FGF2 suppressed UCP1 expression in the adipocytes.[29] However, we found that FGF2 administration robustly induced UCP1 expression in the adipocytes, and FGF2 triggered a more potent effect in white adipocytes compared with that of FGF9 and FGF21. Adipocyte-specific FGF2 deletion studies are required to ascertain the function of this protein in adipose tissue thermogenesis.

Unlike FGF21, FGF2 and FGF9 are nonendocrine FGFs that induce cell proliferation.[20] Therefore, any therapeutic strategy utilizing FGF2 and FGF9 to promote adipose tissue thermogenesis and energy metabolism is limited by undesirable mitogenic effects and reduced tissue penetration. However, paracrine FGFs have previously been converted into hormonal factors by substituting the C-terminal tails with the tails of endocrine FGFs.[31,32] These chimeric factors can be generated as pharmacological agents to overcome the limitations associated with the therapeutic use of FGF2, FGF9, and FGF21 and utilize the remarkable thermogenesis-inducing effects of these FGFs.

CONCLUSION

In this study, we investigated the transcriptional regulation of FGFs in response to cold exposure and through β-adrenergic stimulation and assessed the potential of these proteins to stimulate the expression of thermogenic genes in primary adipocytes. Most FGFs were differentially expressed upon these stimuli, and FGF9 and FGF21 exhibited the greatest changes. FGF21 has been recognized as a prominent inducer of adipose tissue thermogenesis, and the findings presented here support this notion. Moreover, FGF21 is a promising target for the development of therapeutics against cardiovascular and metabolic diseases. Our results further reveal that FGF2 and FGF9 potently promote thermogenic gene expression in adipocytes, and therefore, their therapeutic targeting should be considered to enhance energy metabolism in adipose tissue.

ORCID IDs of the author

Serkan Kir   0000-0001-8722-9913

REFERENCES

1. Peirce V, Carobbio S, Vidal-Puig A. The different shades of fat. *Nature*. 2014;510(7503):76-83.

2. Lidell ME. Brown adipose tissue in human infants. *Handb Exp Pharmacol*. 2019;251:107-123.

3. Virtanen KA, Lidell ME, Orava J, et al. Functional brown adipose tissue in healthy adults. *N Engl J Med*. 2009;360(15):1518-1525.

4. Cypess AM, White AP, Vernochet C, et al. Anatomical localization, gene expression profiling and functional characterization of adult human neck brown fat. *Nature Med*. 2013;19(5):635-639.

5. van Marken Lichtenbelt WD, Vanhommerig JW, Smulders NM, et al. Cold-activated brown adipose tissue in healthy men. *N Engl J Med*. 2009;360(15):1500-1508.

6. Kir S, White JP, Kleiner S, et al. Tumour-derived PTH-related protein triggers adipose tissue browning and cancer cachexia. *Nature*. 2014;513(7516):100-104.

7. Petruzzelli M, Schweiger M, Schreiber R, et al. A switch from white to brown fat increases energy expenditure in cancer-associated cachexia. *Cell Metab*. 2014;20(3):433-447.

8. Kir S, Spiegelman BM. Cachexia and brown fat: A burning issue in cancer. *Trends Cancer*. 2016;2(9):461-463.

9. Cohen P, Spiegelman BM. Brown and beige fat: Molecular parts of a thermogenic machine. *Diabetes*. 2015;64(7):2346-2351.

10. Kir S, Komaba H, Garcia AP, et al. PTH/PTHrP receptor mediates cachexia in models of kidney failure and cancer. *Cell Metab*. 2016;23(2):315-323.

11. Cuevas-Ramos D, Mehta R, Aguilar-Salinas CA. Fibroblast growth factor 21 and browning of white adipose tissue. *Front Physiol*. 2019;10:37. doi:10.3389/fphys.2019.00037

12. Szczepanska E, Gietka-Czernel M. FGF21: A Novel regulator of glucose and lipid metabolism and whole-body energy balance. *Horm Metab Res*. 2022;54(4):203-211.

13. Lu W, Li X, Luo Y. FGF21 in obesity and cancer: New insights. *Cancer Lett*. 2021;499:5-13.

14. Chartoumpekis DV, Habeos IG, Ziros PG, Psyrogiannis AI, Kyriazopoulou VE, Papavassiliou AG. Brown adipose tissue responds to cold and adrenergic stimulation by induction of FGF21. *Mol Med*. 2011;17(7-8):736-740.

15. Fisher FM, Kleiner S, Douris N, et al. FGF21 regulates PGC-1alpha and browning of white adipose tissues in adaptive thermogenesis. *Genes Dev*. 2012;26(3):271-281.

16. Abu-Odeh M, Zhang Y, Reilly SM, et al. FGF21 promotes thermogenic gene expression as an autocrine factor in adipocytes. *Cell Rep*. 2021;35(13):109331. doi:10.1016/j.celrep.2021.109331

17. Keipert S, Kutschke M, Ost M, et al. Long-term cold adaptation does not require FGF21 or UCP1. *Cell Metab*. 2017;26(2):437-446 e5. doi:10.1016/j.cmet.2017.07.016

18. Beenken A, Mohammadi M. The FGF family: Biology, pathophysiology and therapy. *Nat Rev Drug Discov*. 2009;8(3):235-253.

19. Hui Q, Jin Z, Li X, Liu C, Wang X. FGF family: From drug development to clinical application. *Int J Mol Sci*. 2018;19(7):1875. doi:10.3390/ijms19071875

20. Li X. The FGF metabolic axis. *Front Med*. 2019;13(5):511-530.

21. Bilgic SN, Domaniku A, Toledo B, et al. EDA2R-NIK signalling promotes muscle atrophy linked to cancer cachexia. *Nature*. 2023;617(7962):827-834.

22. Tan H, Yue T, Chen Z, Wu W, Xu S, Weng J. Targeting FGF21 in cardiovascular and metabolic diseases: From mechanism to medicine. *Int J Biol Sci*. 2023;19(1):66-88.

23. Dolegowska K, Marchelek-Mysliwiec M, Nowosiad-Magda M, Slawinski M, Dolegowska B. FGF19 subfamily members: FGF19 and FGF21. *J Physiol Biochem*. 2019;75(2):229-240.

24. Harmer NJ. Insights into the role of heparan sulphate in fibroblast growth factor signalling. *Biochem Soc Trans*. 2006;34(Pt 3):442-445.

25. Kwon MM, O'Dwyer SM, Baker RK, Covey SD, Kieffer TJ. FGF21-mediated improvements in glucose clearance require uncoupling protein 1. *Cell Rep*. 2015;13(8):1521-1527.

26. Keipert S, Lutter D, Schroeder BO, et al. Author Correction: Endogenous FGF21-signaling controls paradoxical obesity resistance of UCP1-deficient mice. *Nat Commun*. 2021;12(1):1804. doi:10.1038/s41467-021-22119-x

27. Charoenphandhu N, Suntornsaratoon P, Krishnamra N, et al. Fibroblast growth factor-21 restores insulin sensitivity but induces aberrant bone microstructure in obese insulin-resistant rats. *J Bone Miner Metab*. 2017;35(2):142-149.

28. Sun Y, Wang R, Zhao S, et al. FGF9 inhibits browning program of white adipocytes and associates with human obesity. *J Mol Endocrinol*. 2019;62(2):79-90.

29. Li H, Zhang X, Huang C, et al. FGF2 disruption enhances thermogenesis in brown and beige fat to protect against adiposity and hepatic steatosis. *Mol Metab*. 2021;54:101358. doi:10.1016/j.molmet.2021.101358

30. Shamsi F, Xue R, Huang TL, et al. FGF6 and FGF9 regulate UCP1 expression independent of brown adipogenesis. *Nat Commun*. 2020;11(1):1421. doi:10.1038/s41467-020-15055-9

31. Goetz R, Ohnishi M, Kir S, et al. Conversion of a paracrine fibroblast growth factor into an endocrine fibroblast growth factor. *The J Biol Chem*. 2012;287(34):29134-29146.

32. Zhao L, Niu J, Lin H, et al. Paracrine-endocrine FGF chimeras as potent therapeutics for metabolic diseases. *EBioMedicine*. 2019;48:462-477.

How to cite this article

İSTANBUL
UNIVERSITY
— P R E S S —

Investigating the Antioxidant Capacity of Lunasin Expressed in *Aspergillus oryzae*

Elif Karaman[1] (ID), Cem Albayrak[1] (ID), Serdar Uysal[1] (ID)

[1]Bezmialem Vakif University, Beykoz Institute of Life Sciences and Biotechnology, Istanbul, Türkiye

ABSTRACT

Objective: Lunasin is a bioactive protein that possesses anti-carcinogenic, anti-inflammatory, and antioxidant properties. Traditional isolation methods are resource-intensive, and chemical synthesis faces cost and environmental issues. This study aims to achieve cost-effective lunasin expression in *Aspergillus oryzae* with a focus on exploring its antioxidant properties *in vitro*.

Materials and Methods: The expression vector carrying four lunasin sequences fused with amylase and an 8xHis-tag was introduced into *pyrG* auxotrophic *A. oryzae*. Subsequently, the recombinant protein was purified using metal affinity chromatography. The study uses sodium dodecyl sulfate-polyacrylamide gel electrophoresis (SDS-PAGE), western blot analyses, and size-exclusion chromatography to evaluate the composition and purity of the protein, a linoleic acid assay to demonstrate the inhibitory effect on lipid peroxidation, and the 2,2'-azinobis-[3-ethylbenzothiazoline-6-sulfonic acid] ABTS) assay to evaluate the radical scavenging activity.

Results: SDS-PAGE and western blot analyses confirmed sustained lunasin expression in *A. oryzae*, appearing in both fusion and non-fusion forms. Yields were 5.8 mg/L for non-fusion and 4 mg/L for fusion lunasin expression. Moreover, 0.1 µM non-fusion lunasin surpassed α-tocopherol and butylated hydroxyanisole (BHA; $p < 0.05$) in reducing lipid peroxidation at 4 and 72 h. Unlike the fusion lunasin, the non-fusion lunasin displayed concentration- and time-independent inhibitory effects on linoleic acid peroxidation as well as significant ABTS scavenging activity ($p < 0.05$).

Conclusion: The study has shown for the first time *A. oryzae* to efficiently express and secrete both fusion and non-fusion lunasin proteins in a soluble form, with the non-fusion lunasin exhibiting superior antioxidant effectiveness compared to the fusion lunasin. The findings underscore *A. oryzae*'s potential as a promising host for producing functional lunasin with antioxidant properties, opening avenues for broader applications in biotechnology and bioactive peptides.

Keywords: Lunasin, *Aspergillus oryzae,* Antioxidant, Biotechnology

INTRODUCTION

Lunasin is a bioactive peptide predominantly found in soybeans and various natural plant products such as quinoa and wheat and has garnered considerable research attention. It features a cell adhesion motif facilitating binding to the extracellular membrane and a negatively charged carboxyl region that interacts with nuclear histone molecules, inhibiting their acetylation.[1,2] These characteristics make lunasin a remarkable bioactive protein with anti-carcinogenic, anti-inflammatory, cholesterol-lowering, and antioxidant properties.[3-10]

Dietary components are increasingly being recognized for their potential as health-promoting substances in chronic diseases, cancer included.[9] The World Health Organization (WHO) reported over two million new cancer cases in 2024, with projections indicating a surge to 29.4 million annual cases

by 2040.[11] Lunasin demonstrates anti-carcinogenic effects on multiple cancers, including lung, colon, leukemia, melanoma, and breast cancer. Its mechanisms involve inhibiting histone acetylation, blocking integrin signaling, inducing cell cycle arrest, and promoting apoptosis. In leukemia, lunasin acts as a chemoprotective by interrupting the cell cycle at the G2 level, increasing caspase enzymes, and triggering apoptosis.[12] Lunasin exhibits antimitotic properties akin to widely-used anti-cancer drugs such as paclitaxel by binding to chromatin and hindering the formation of kinetochore complexes, thereby inducing mitotic disruption and subsequent cell lysis. Additionally, lunasin prevents tumor cell metastasis by adhering to the extracellular matrix.[1,13] Lunasin also acts as an anti-inflammatory agent in rheumatoid arthritis by reducing synovial cell proliferation and cytokine levels through the inhibition of interleukin-6, interleukin-8, and matrix metalloproteinase-3, along with

suppressing nuclear factor kappa B (NF-κB) activity.[14] As a cholesterol-lowering agent, lunasin directly inhibits 3-hydroxy-3-methyl-glutaryl-CoA reductase, thus lowering low-density lipoprotein and cholesterol levels.[15] As an antioxidant, lunasin additionally inhibits apoptosis induced by free radicals, regulates apoptotic Bax and Bcl-2 molecules, and stimulates dendritic and natural killer immune cells.[16]

Lunasin is emerging as a notable bioactive peptide with biological activities, making it a promising candidate for addressing various health concerns, including cancer, obesity, cardiovascular, and immune-related disorders. Moreover, several nutritional supplements containing lunasin (e.g., LunaRichX®, LunasinXP®, Carefast FSP100, LunaCell™) have been developed to harness its beneficial properties.[9] However, obtaining adequate quantities of lunasin from natural sources presents obstacles, highlighting the necessity for developing reliable production methodologies in order to meet the demand for research and biotechnological applications.

Lunasin is a 43-amino acid peptide and was initially isolated from soybeans in 1987.[17] Traditional methods for isolating lunasin from soybeans pose challenges that require substantial raw materials and intricate time-consuming processes while only yielding variable results. Similarly, while chemical synthesis methods are an alternative, these face rising costs, present complexities for large-scale production, and raise environmental concerns related to chemical usage.[2,5,9]

This study aims to achieve a cost-effective and high-yield expression of lunasin in the *Aspergillus oryzae (A. oryzae)* microorganism along with conducting *in vitro* investigations into its antioxidant properties. *A. oryzae* is a filamentous fungus that has been approved by the Food and Drug Administration (FDA) with the status of being Generally Recognized as Safe.[18,19] *A. oryzae* is known for its robust secretion mechanisms attributed to its larger genome size compared to other *Aspergillus* species, primarily due to its genes encoding secretory hydrolases. This secretion system enables large-scale production of heterologous proteins. Widely utilized in industrial-scale protein production, this expression system relies on auxotrophic nutritional markers such as pyrG, high-yield promoter genes, and efficient transformation. Furthermore, *A. oryzae* offers advantages such as cost-effective media and resistance to diverse environmental conditions.[18] With its pivotal role in fermentation technology, *A. oryzae* has emerged as an optimal choice for lunasin production.

MATERIALS AND METHODS

Strains, Materials and Reagents

Competent *Escherichia coli (E. coli)* TOP10 cells (#C404010, Thermo Fisher Scientific, MA, USA) were employed for gene subcloning and plasmid replication prior to expression of the proteins in *pyrG* auxotrophic *A. oryzae*. *E. coli* cells carrying plasmids were cultured in Luria-Bertani (LB) medium (1% tryptone, 0.5% yeast extract, and 1% NaCl) with 100 g/mL of ampicillin. The *pyrG* auxotrophic *A. oryzae* used in this study was derived from the *A. oryzae* RIB40 strain (#42149, American Type Culture Collection, VA, USA) in a previous study.[20] A DPY medium containing 2% dextrin, 1% polypeptone, 0.5% yeast extract, 0.5% KH_2PO_4, and 0.05% $MgSO_4.7H_2O$ (pH 5.5) was used to cultivate *A. oryzae*. The *pyrG* auxotrophic *A. oryzae* was cultured in the DPY medium enhanced with 20 mM uridine and 0.2% uracil. Chemicals, reagents, and the ingredients of the cultivation media for *E. coli* and *A. oryzae* were purchased from Sigma (MO, USA) and Biofroxx (Germany).

The plasmid isolation kit (12143) was purchased from Qiagen (VLC, CA). Restriction enzymes were purchased from New England Biolabs (MA, USA), while Yatalase (T017) was purchased from Takara Bio Inc. (Japan). The nickel resin (HisPur™ Ni-NTA Resin) and the dialysis membrane (68035, 3.5k MWCO) were purchased from Thermo Fisher Scientific (MA, USA). The protein ladder (24052) was purchased from Intron Biotechnology (South Korea). The nitrocellulose membrane (Amersham™ Protran® Premium, 10600003) and Superdex 75 Increase 10/300 GL column were purchased from GE Healthcare (IL, USA). The HRP-conjugated anti-6xHis-tag® antibody (ab1269) was purchased from Abcam (Cambridge, UK). The chemiluminescence detection kit (Western Bright™ Sirius, K-12043-D10) was purchased from Advansta (CA, USA). 96-well enzyme-linked immunosorbent assay (ELISA) plates (514201) were purchased from NEST Biotechnology Co., Ltd. (China). Linoleic acid (90150) was purchased from Cayman Chemical (MI, USA). Butylated hydroxyanisole (BHA; B1253), α-tocopherol (T3251), 2,2-azinobis-[3-ethylbenzothiazoline-6-sulfonic acid] (ABTS) diammonium salt, and 6-hydroxy-2,578-tetramethylchroman-2-carboxylic acid (Trolox; 238813) was purchased from Sigma (MO, USA).

Designing the Lunasin Expression Vectors

The lunasin protein sequence (amino acids 22-64) was derived from the 2S seed storage albumin protein (UniProtKB-P19594). The expression vector was constructed using the *pUC57* commercial vector, which includes the amylase promoter, signal sequence, terminator, and *pyrG* gene. The expression vector containing four repetitive lunasin sequences fused with amylase (UniprotKB-P0C1B3) was designed to produce lunasin (Figure 1), with the sequences separated by GGGS linker sites. The tobacco etch virus (TEV) recognition site (ENLYFQS) distinguished fungal amylase from the initial lunasin sequence, and an 8xHis-tag was added to the C-terminus for efficient detection and purification of the recombinant lunasin protein. The designed construct was optimized for *A. oryzae*, and its nucleotide sequence was synthesized by GenScript Biotech PTE. LTD. (NJ, USA).
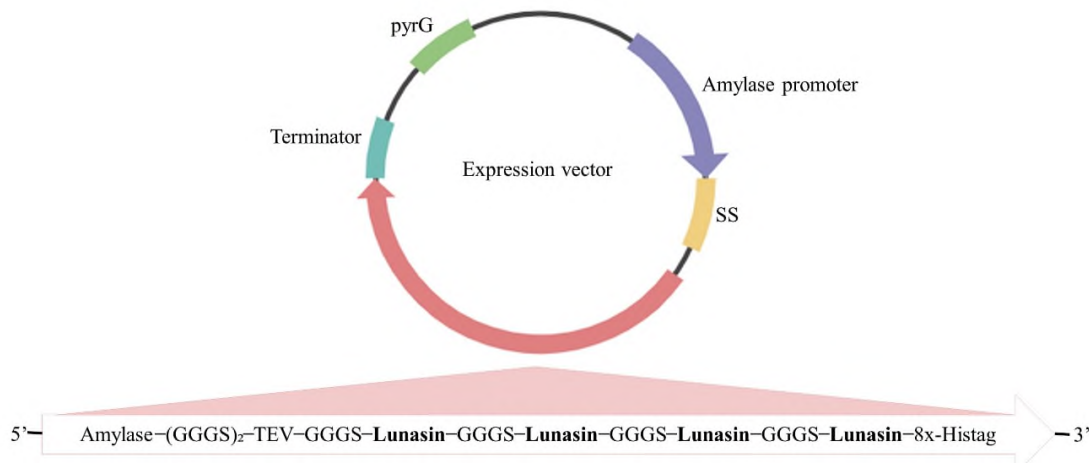
Figure 1. Illustration of expression vector containing the amylase promoter, signal sequence (SS), amylase-encoding gene, TEV recognition site, 4 tandem repetitive lunasin sequences, terminator, and *pyrG* gene. GGGS sequences served as the linker.

Transformation and Expression of Lunasin in *A. oryzae*

The expression vector was amplified in *E. coli*, purified, and digested using *EcoRI* and *HindIII* restriction enzymes. The linearized vector was then transformed into *pyrG* auxotrophic *A. oryzae* via protoplast-mediated transformation.[21] In brief, *pyrG* auxotrophic *A. oryzae* was cultivated on the DPY medium containing uracil and uridine at 30°C and 180 rpm. After an overnight incubation, the mycelia were lysed for 4 h at 30°C and 80 rpm using a lysis solution (50 mM malate buffer, 0.6 M $(NH_4)_2SO_4$, pH 5.5) with 1% Yatalase. Spheroplasts were washed with a solution containing 50 mM $CaCl_2$ and 1.2 M sorbitol. Following the combination of the linearized expression vector with the resulting spheroplasts and polyethylene glycol 4000 (PEG4000), the mixture was spread on minimal agar media and incubated at 30°C for 5-7 days. The control group received no insert DNA treatment.

To identify the recombinant colonies capable of expressing lunasin, multiple randomly selected transformant colonies were inoculated into 15 mL of the DPY medium. Following an overnight incubation at 30°C and 180 rpm, each preculture was diluted (1:10) into 75 mL of a DPY medium containing 4% dextrin. The incubation was then carried out at 30°C and 180 rpm for five days. Sodium dodecyl-sulfate polyacrylamide gel electrophoresis (SDS-PAGE) analysis was performed on the culture samples obtained on the third and fifth days of expression.

Purification of Lunasin Proteins

The aqueous phase of the expression culture was collected by filtering using Whatman filter paper to eliminate fungal cells after five days of incubation at 30 °C and 180 rpm. For purification, the resulting sample was loaded onto a nickel-nitrilotriacetic acid (Ni-NTA) affinity column utilizing HisPur™ Ni-NTA resin. After washing the column with the washing solution (50 mM NaH_2PO_4 and 500 mM NaCl (pH 7.4)), the 8xHis-tagged recombinant proteins were eluted with the elution solution (50 mM NaH_2PO_4, 300 mM NaCl, and 200 mM imidazole (pH 7.4)). Imidazole was removed by dialyzing the eluted protein solutions against a phosphate-buffered saline (PBS) buffer (137 mM NaCl, 2.7 mM KCl, 10 mM Na2HPO4, and 1.8 mM KH2PO4 [pH 7.4]). SDS-PAGE (12%) was used to evaluate the purity of the protein samples obtained from the purification processes. A Bradford assay was employed to determine the concentration of pure recombinant proteins at 595 nm, with bovine serum albumin serving as the protein standard.

Size-exclusion chromatography was performed to assess the composition and purity of the dialyzed recombinant proteins. The samples were fed into a Superdex 75 Increase 10/300 GL column at room temperature via the ÄKTA pure chromatography system. The column was pre-equilibrated using PBS (pH 7.4) prepared in accordance with manufacturer's instructions. The PBS buffer (pH 7.4) was employed as a wash and elution buffer, with the flow rate maintained at 0.5 mL/min.

Western Blot

Expression and purification protein samples were separated using 12% SDS-PAGE and then transferred to a nitrocellulose membrane. 24 mM Trizma® base, 192 mM glycine, and 20% methanol were used as the transfer solution. 10 mM Tris-HCl (pH 7.4), 0.9% NaCl, and 0.2% Tween® 20 Detergent were used as the wash solution. Following overnight blocking using the wash solution supplemented with 5% nonfat milk powder, the membrane was washed three times. The membrane was then blotted with HRP-conjugated anti-6xHis-tag® antibody (1:5,000) for 2 h at room temperature. The 8xHis-tag lunasin proteins were coupled with the HRP-anti-His antibody and detected using a chemiluminescence western blotting detection kit in accordance with manufacturer's instructions.

Linoleic Acid Peroxidation Assay

A linoleic acid assay[22] was employed to demonstrate the *in vitro* inhibitory effect of purified lunasin proteins on lipid peroxidation. 50 mM linoleic acid was prepared in 100% ethanol. In a glass tube, 1 mL of 0.1 M sodium phosphate buffer (pH 7.0), 1 mL of 50 mM linoleic acid, and 0.5 mL of dH_2O were mixed. After adding the dialyzed lunasin protein sample, the mixture was kept for 72 h at 40 °C. The tubes were closed tightly and kept away from light. BHA (10 µM) and α-tocopherol (1 µM) served as control groups. In all control and test groups, samples to be tested were added to the mixture at equal total volumes. For the measurements, samples from the mixture in the glass tubes were withdrawn at 4, 24, 48, and 72 h and combined with 2.35 mL of 75% ethanol, 50 µL of 30% ammonium thiocyanate, and 50 µL of 20 mM $FeCl_2$ (freshly prepared in 3.5% HCl). The absorbance of the samples was measured at 500 nm after exactly 3 min. The control group contained only linoleic acid with no additional compound.

ABTS Radical Scavenging Activity Assay

To evaluate the radical scavenging activity of purified lunasin proteins, a modified ABTS assay was employed.[22] A 7 mM ABTS stock solution was prepared in dH_2O and mixed with 2.45 mM potassium persulfate at a total volume of 10 mL. The reaction was kept at room temperature in the dark for 16 h to obtain ABTS radicals. Following the incubation, the ABTS radical solution was diluted in a 5 mM PBS buffer (pH 7.4) until the absorbance was 0.7 at 734 nm. 10 µL of the purified lunasin protein to be tested were loaded alongside the standard samples into wells on the ELISA plate, and 190 µL of diluted ABTS radical solutions were added to the samples. The absorbance of colored mixtures was measured every min for 10 min. The percentage of decolorization based on the observed absorbance after 7 min was determined as follows:

$$\%decolarization = \frac{(Control\ absorbance - Sample\ absorbance)}{(Control\ absorbance)} \times 100 \quad (1)$$

Trolox (standard) was prepared at a concentration of 2 mM, and its repeated dilutions in the 5 mM PBS buffer (pH 7.4) were performed to generate the standard curve. The Trolox equivalent antioxidant capacity (TEAC) was calculated by dividing the gradient of the concentration-dependent absorbance plot for lunasin by the gradient of the Trolox plot.

Statistical Analysis

The results were evaluated using the program SPSS Statistics (ver. 28.0.0.0, IBM). Statistical analyses of the acquired data were conducted for the linoleic acid peroxidation assay using the Kruskal-Wallis H and Mann Whitney U tests, with $p <$ 0.05 being considered statistically significant. Multiple comparisons were performed using the Kruskal-Wallis H test. The data acquired for the ABTS radical scavenging activity assay were statistically evaluated using Student's t-tests, again with $p < 0.05$ being considered statistically significant.

RESULTS

Expression of Lunasin in *A. oryzae*

The study has employed an expression vector carrying the *pyrG* gene to successfully incorporate the lunasin gene into the *pyrG* auxotrophic *A. oryzae* genome via gene replacement. Following transformation, several colonies were randomly selected for expression tests to determine the colonies expressing the recombinant protein in small flask volumes. Following a 5-day incubation period, the SDS-PAGE analysis conclusively demonstrated the sustained expression of the recombinant protein in *A. oryzae* (Figure 2). *A. oryzae* was observed in the SDS-PAGE analyses to express the lunasin protein in two distinct manners: an amylase fusion (shown with a band measuring approximately 72 kDa in Figure 2A) and without being fused with amylase (shown with a band measuring approximately 14 kDa in Figure 2B). Non-fusion lunasin was released into the culture medium following its separation from the amylase as a result of self-cleavage.

Purification of Recombinant Lunasin Proteins

A. oryzae efficiently expressed and secreted both fusion and non-fusion lunasin proteins in soluble form alongside the fungal amylase as a product of *A. oryzae* secretion into the culture medium. After filtration of the expression culture medium, recombinant lunasin proteins were purified under native conditions. The expressed 8xHis-tagged recombinant lunasin proteins were effectively separated from the host proteins using a metal affinity chromatography column. After purification, the analyzed eluted samples consistently displayed protein bands with a molecular weight of approximately 72 kDa for the fusion lunasin and approximately 14 kDa for the non-fusion lunasin in SDS-PAGE, as shown in Figures 3A and 4A. After the metal affinity chromatography, the fractions harboring lunasin proteins were concentrated, and the purity of Lunasin proteins was validated through western blot analysis using the HRP-conjugated anti-6xHis-tag® antibody for the detection. This confirmed the successful expression and purification of lunasin proteins by *A. oryzae*, as shown in Figures 3 and 4.

Size exclusion chromatography was employed to achieve a high level of purity and to evaluate structural stability of the purified lunasin proteins. Both recombinant lunasin variants eluted in a single peak on the chromatograms, as shown in Figures 3 and 4, indicating their stability. The purified fusion lunasin demonstrated a yield of 4 mg per liter of culture medium,
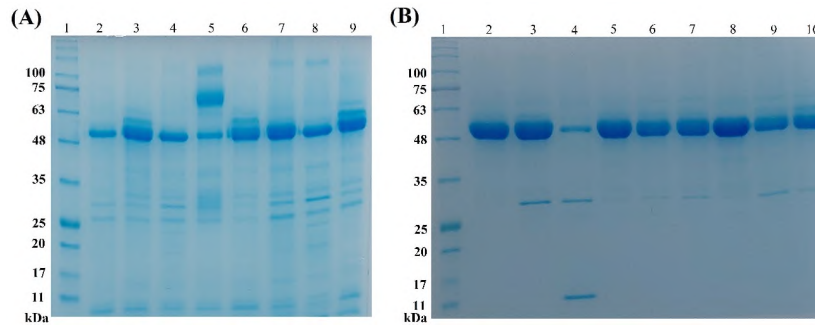
Figure 2. Protein expression tests on a small scale using sodium dodecyl sulfate polyacrylamide gel electrophoresis (SDS-PAGE) examination of multiple transformed colonies. **(A)** SDS-PAGE analysis of fusion lunasin. Lane 1: Gangnam-Stain Protein Ladder. Lane 2–4, 6–9: the colonies not expressing recombinant protein. Lane 5: the colony expressing fusion lunasin (~72 kDa). **(B)** SDS-PAGE analysis of non-fusion lunasin. Lane 1: Gangnam-Stain Protein Ladder. Lanes 2, 3, 5–10: the colonies not expressing recombinant protein. Lane 4: the colony expressing recombinant non-fusion lunasin protein (~14 kDa).

Figure 3. SDS-PAGE examination **(A)** and Western blot analysis **(B)** of purification samples of His-tagged fusion lunasin with the Ni-NTA column. Lanes 1: Gangnam-Stain Protein Ladder. Lanes 2: the culture medium of the colony expressing the fusion lunasin. Lanes 3: the wash solutions collected from the Ni-NTA column. Lanes 4: the eluted sample containing fusion lunasin. **(C)** Size exclusion chromatography purification chromatogram on a Superdex 75 Increase 10/300 GL column. The peak indicates the purified fusion lunasin.
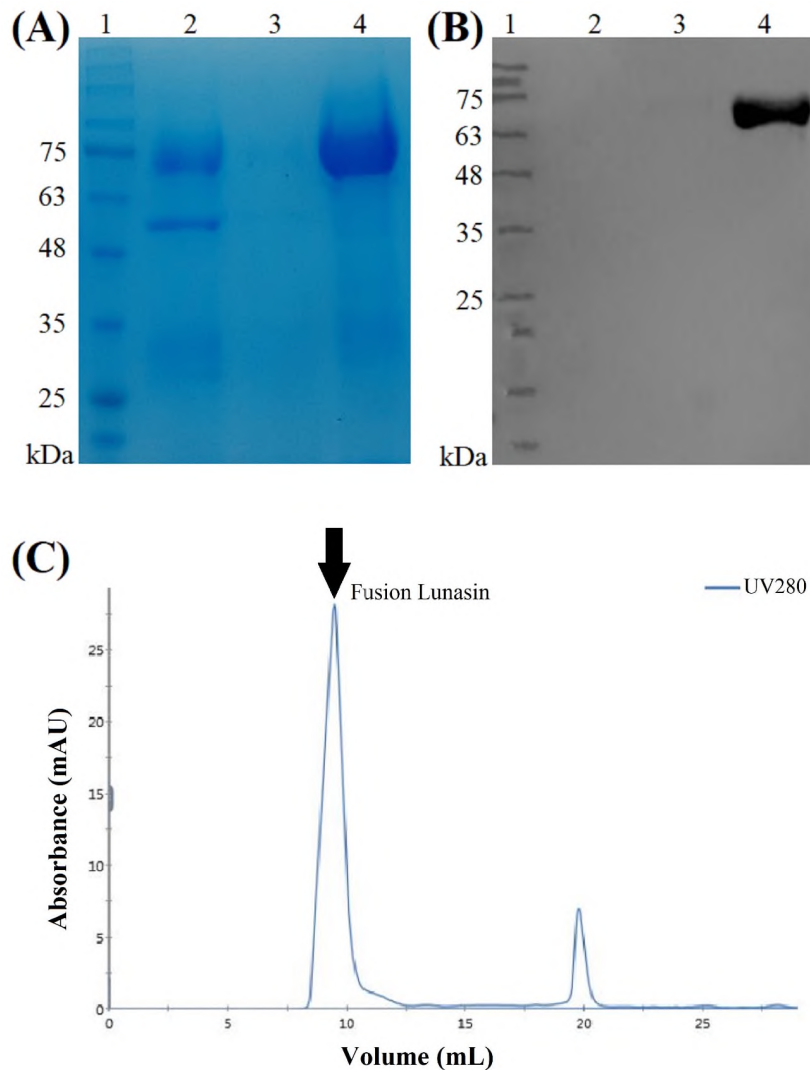
Figure 4. SDS-PAGE examination **(A)** and Western blot analysis **(B)** of purification samples of His-tagged non-fusion lunasin with the Ni-NTA column. Lanes 1: Gangnam-Stain Protein Ladder. Lanes 2: the culture medium of the colony expressing the non-fusion lunasin. Lanes 3: the wash solutions collected from the Ni-NTA column. Lanes 4: the eluted sample containing non-fusion lunasin. **(C)** Size exclusion chromatography purification chromatogram on a Superdex 75 Increase 10/300 GL column. The peak indicates the purified non-fusion lunasin.
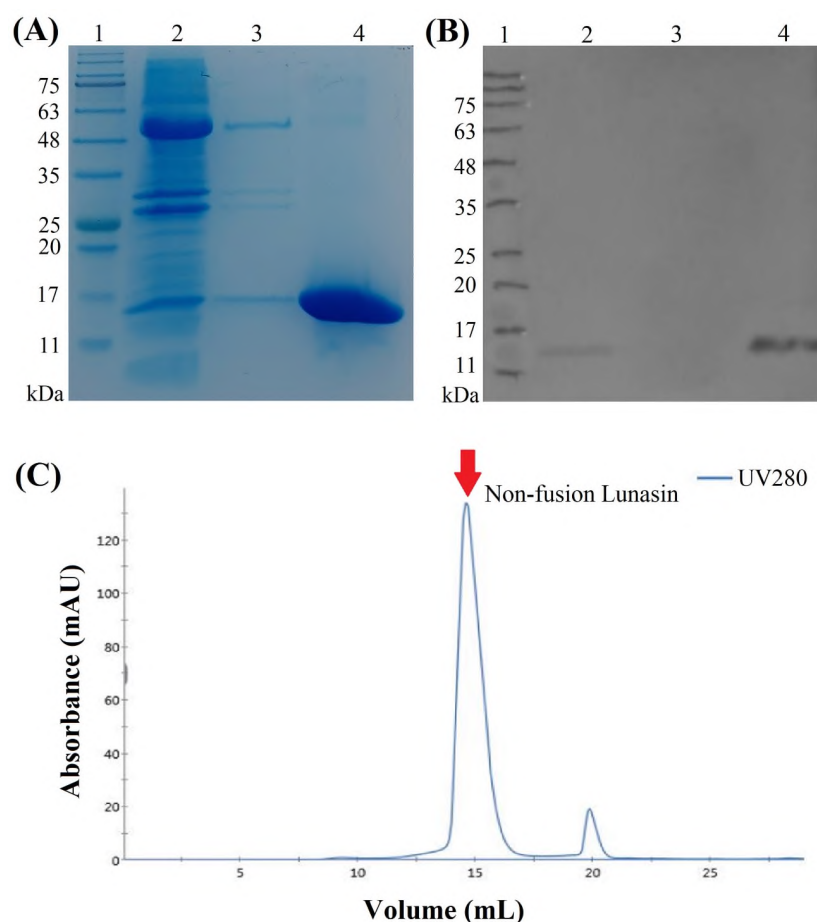
whereas the non-fusion lunasin exhibited a yield of 5.8 mg per liter of culture medium.

Inhibitory Inhibition of Linoleic Acid Peroxidation

The linoleic acid inhibition assay measures the oxidation of ferrous ions into ferric ions, resulting in the formation of a colored complex. Therefore, the study investigated the *in vitro* peroxidation levels triggered by ferrous ions in the presence of ferrous chloride.

The antioxidant capacity of the purified fusion and non-fusion lunasin proteins was evaluated through their inhibition of lipid peroxidation in linoleic acid over a 72-hour period. Inhibition activities were assessed at different concentrations (0.1, 1, and 10 μM) and compared to standard compounds known for their significant antioxidant capacity.

Figure 5A illustrates the time course of linoleic acid oxidation in the presence and absence of non-fusion lunasin at varying concentrations. At 10 μM, non-fusion lunasin showed no noticeable inhibitory effect. However, 1 μM of non-fusion lunasin induced a slight, albeit statistically insignificant, decrease in peroxidation. Notably, 0.1 μM non-fusion lunasin exhibited a significant inhibition of lipid peroxidation at both the 4 h and 72 h time points after being introduced into the linoleic acid reaction mixture ($p < 0.05$).

Figure 5B shows the assessment of the inhibitory effect of 0.1 μM non-fusion lunasin in comparison with standard compounds at the time points of 4 h, 24 h, 48 h, and 72 h. At a concentration of 0.1 μM, the non-fusion lunasin exhibited a substantial reduction in absorbance at both the 4 h and 72 h time points, signifying a superior inhibitory effect when compared with -tocopherol and BHA ($p < 0.05$).

ABTS Radical Scavenging Activity of Lunasin

The antioxidant capacity of lunasin proteins was also evaluated utilizing the ABTS assay, which involves the chemical generation of ABTS radicals through the reaction between ABTS and
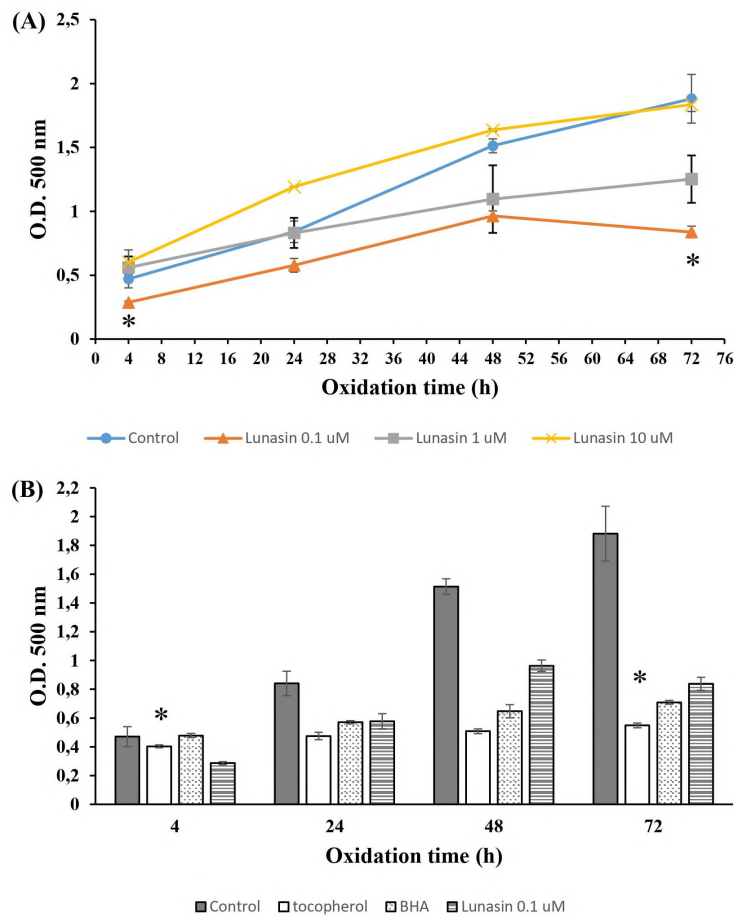
Figure 5. Inhibitory effect of the purified non-fusion lunasin on lipid peroxidation. **(A)** Lipid peroxidation inhibitory activity of non-fusion lunasin at concentrations of 0.1 µM, 1 µM, and 10 µM for the periods of 4, 24, 48, and 72 h. **(B)** Inhibitory effect of 0.1 µM non-fusion lunasin compared to standards (1 µM α-tocopherol and 10 µM BHA). Each value displays the mean and standard deviation in error bars. * Statistically different ($P < 0.05$).

potassium persulfate. This assay quantifies a substance's antioxidant capability for scavenging ABTS radicals, leading to a reduction in absorbance as a result of hydrogen atom donation. Consequently, the concentration of the antioxidant is inversely proportional to the measured absorbance.

The percentage inhibition of ABTS radicals (% decolorization) was determined as a function of concentration and time, normalized against the reactivity of Trolox as a standard. A calibration curve was constructed based on the % decolorization of Trolox against varying Trolox concentrations at 7 min. The TEAC value for non-fusion lunasin was calculated, representing its antioxidant capacity in comparison to Trolox's at 7 min. The unit of activity, known as TEAC, signifies the concentration of one unit of Trolox that matches the antioxidant capacity of one unit of the tested substance at a specific time point. The non-fusion lunasin demonstrated significant ABTS scavenging activity ($p < 0.05$), while the fusion lunasin did not exhibit

a comparable effect. Additionally, the ABTS assay parameter exhibited a robust level of reliability, as indicated in Table 1.

DISCUSSION

Lunasin is currently produced through natural sources, chemical synthesis, and recombinant methods. The yields for lunasin from plant sources vary based on origin and methods used.[23] Cost-effective industrial production is essential due to high production costs. Lunasin has been the subject of 25 worldwide patents since its discovery. Interestingly, three of these patents address its recombinant expression in different microorganisms, namely *E. coli* (CN103819546A), *Pichia pastoris (P. pastoris)* (CN105647960A), and CHO-S mammalian cells (CN107574172).[9] These studies showed lunasin being expressed in fusion form in order to protect it from proteolytic degradation and increase its solubility. The present

Table 1. Formula and R^2 values of curves representing % decolorization values after 7 min incubation. The TEAC value of non-fusion lunasin was determined in comparison with Trolox. n + SD =3, each performed in triplicate.

Sample	Formula	R^2 value	TEAC value $(\mu M)^{\alpha}$
Trolox	y = 0.0734x + 0.2554	0.9993	-
Non-fusion lunasin	y = 0.333x + 9.3123	0.9943	4.450±0.093

$^{\alpha}$ n + SD =3, each performed in triplicate.

study has for the first time successfully produced lunasin in two forms in *A. oryzae*, with final yields of 4 mg/L for fusion lunasin and 5.8 mg/L for non-fusion lunasin. The study stands apart from others by demonstrating for the first time the production of functional lunasin as a non-fusion compound utilizing a microorganism suitable for industrial-scale production.

Liu et al.[24] achieved soluble expression of His-tagged lunasin in *E. coli*, yielding biologically active lunasin at 4.73 mg/L. Kyle et al.[25] overexpressed His-tagged lunasin in *E. coli* using the Clostridium thermocellum cipB domain as a fusion partner, achieving a final yield of 210 mg/L. Setrerrahmane et al.[26] explored a cost-effective strategy in *E. coli* to obtain a purified protein yield of 75 mg/L. Tian et al.[27] used a fusion tag strategy with the TEV protease cleavage mechanism in *E. coli*, achieving an approximate yield of 86 mg/L after cleavage. Zhu et al.[28] expressed tandem-repeated lunasin units in *P. pastoris*, obtaining 0.24 mg/mL of purified proteins. The separated lunasin analogs showed dose-dependent reduction in inflammatory response in lipopolysaccharide-stimulated RAW 246.7 cells, which suggests an industrial strategy for lunasin use.[28]

Lunasin has been proven to ameliorate vascular endothelial cell damage by regulating the apoptotic pathway induced by free radicals.[16] Jeong et al.'s[29] study discovered lunasin to protect DNA from oxidation by chelating ferrous ions. Additionally, they noted lunasin to decrease the formation of intermediate products in lipid peroxidation, thereby reducing the free radical burden.[29] Another study conducted by Hernandez-Ledesma et al.[22] demonstrated lunasin to inhibit the oxidation of linoleic acid, leading to a substantial reduction in reactive oxygen species production in macrophages in a dose-dependent manner. The present study has examined the inhibitory effect of non-fusion and fusion lunasin expressed in *A. oryzae* with regard to lipid peroxidation as a measure of antioxidant capacity under stable environmental conditions. Remarkably, the results suggest the substantial inhibitory activity of non-fusion

lunasin on linoleic acid peroxidation to be independent of both concentration and time. This result is believed to be attributed to the redox state of non-fusion lunasin expressed in *A. oryzae* at the tested time points.

Lunasin is known for its histone-binding ability at the C-terminal end and shares homology with conserved regions in chromatin binding proteins.[1,13,30] Similar to other chromatin binding proteins, lunasin exhibits a dynamic equilibrium between oxidized and reduced secondary structural forms. Aleksis et al.'s[30] study utilized NMR techniques on lunasin and its truncated N-terminal variant expressed in *E. coli* and revealed the oxidized form to exhibit enhanced stability compared to the reduced form. Depending on environmental conditions, lunasin can exist in a reduced form with free cysteine thiols or in an oxidized form featuring an intramolecular disulfide bond.[30]

Unlike the non-fusion lunasin in the current study, the fusion lunasin exhibited no significant inhibitory effect on linoleic acid peroxidation. The fusion of lunasin with amylase is believed to be able to potentially result in the modification of its redox properties or the weakening of its interaction with lipid molecules by affecting flexibility. This could be attributed to the structural complexity introduced by the fusion protein itself. As a result, the antioxidant efficacy of fusion lunasin has been determined to be less robust compared to its non-fused lunasin. The results of the antioxidant effects on lipid peroxidation for both the fusion lunasin and non-fusion lunasin are supported by the outcomes of the free radical scavenging activity. Alves de Souza et al.[31] investigated conformational differences between the oxidized and reduced forms of lunasin, highlighting the structural heterogeneity that imparts flexibility in binding to various partners. Consequently, the redox properties of lunasin, particularly its cysteine bond, play a crucial role in its interaction with other molecules and antioxidative activity. Furthermore, the time- and environment-dependent nature of the disulfide bond formation affects the stabilization of the redox state and consequently the antioxidative activity due to the ab-

sence of a stable tertiary structure. Additionally, the abundance of hydrophilic regions, combined with the presence of an aspartic acid end, not only enhances flexibility but also induces structural instability through electrostatic attractions.[31]

CONCLUSION

In conclusion, the study has successfully demonstrated for the first time the efficient expression and secretion of lunasin proteins in a soluble form using *A. oryzae*. Self-cleavage led to the release of non-fusion lunasin into the culture medium after separation from the amylase. The outcomes derived from the assays measuring linoleic acid peroxidation and radical scavenging activity distinctly emphasize the enhanced antioxidant efficacy of the non-fusion lunasin when compared to the fusion lunasin. This innovative approach has not only achieved a cost-effective and high-yield expression of lunasin but has also provided valuable insights into its antioxidant properties through in vitro investigations. The findings underscore the potential *A. oryzae* has as a promising host organism for producing functional lunasin with antioxidant capabilities, thus paving the way for further applications in the fields of biotechnology and bioactive peptides.

ORCID IDs of the author

Elif Karaman   0000-0001-6244-4668
Cem Albayrak   0000-0002-4496-4237
Serdar Uysal   0009-0003-7471-353X

REFERENCES

1. Galvez AF, de Lumen BO. A soybean cDNA encoding a chromatin-binding peptide inhibits mitosis of mammalian cells. *Nat Biotechnol*. 1999;17(5):495-500.

2. Hernández-Ledesma B, Hsieh CC, Dia V, de Mejia EG, de Lumen BO. In: Soybean and Health. Lunasin, a cancer preventive seed peptide. Soybean and health: 2011:145-166.

3. Gonzalez de Mejia EG, Dia VP. Lunasin and lunasin-like peptides inhibit inflammation through suppression of NF-κB pathway in the macrophage. *Peptides*. 2009; 30(12): 2388-2398.

4. Hsieh CC, Hernández-Ledesma B, Jeong HJ, Park JH, de Lumen BO. Complementary roles in cancer prevention: Protease inhibitor makes the cancer preventive peptide lunasin bioavailable. *PloS One*. 2010;5(1):e8890. doi:10.1371/journal.pone.0008890.

5. Hernández-Ledesma B, de Lumen BO, Hsieh, CC. 1997-2012: fifteen years of research on peptide Lunasin. In: Bioactive Food Peptides in Health and Disease. London, England: InTech Open: 2013: 3-22. doi:10.5772/52368.

6. Chang HC, Lewis D, Tung CY, et al. Soypeptide lunasin in cytokine immunotherapy for lymphoma. *Cancer Immunol Immunother*. 2014;63:283-295.

7. Fernández-Tomé S, Ramos S, Cordero-Herrera I, Recio I, Goya L, Hernández-Ledesma B. *In vitro* chemo-protective effect of bioactive peptide lunasin against oxidative stress in human HepG2 cells. *Food Res Inter*. 2014;62:793-800.

8. García-Nebot MJ, Recio I, Hernández-Ledesma B. Antioxidant activity and protective effects of peptide lunasin against oxidative stress in intestinal Caco-2 cells. *Food Chem Toxicol*. 2014;65:155-161.

9. Fernández-Tomé S, Hernández-Ledesma B. Current state of art after twenty years of the discovery of bioactive peptide lunasin. *Food Res Inter*. 2019;116:71-78.

10. Kaufman-Szymczyk A, Kaczmarek W, Fabianowska-Majewska K, Lubecka-Gajewska K. Lunasin and its epigenetic impact in cancer chemoprevention. *Inter J Mol Sci*. 2023;24(11):9187. doi: 10.3390/ijms24119187

11. World Health Organization. WHO report on cancer: Setting priorities, investing wisely and providing care for all. *World Health Organization*. 2020 https://iris.who.int/handle/10665/330745. License: CC BY-NC-SA 3.0 IGO.

12. Vuyyuri SB, Shidal C, Davis KR. Development of the plant-derived peptide lunasin as an anticancer agent. *Curr Opin Pharmacol*. 2018;41:27-33.

13. Galvez AF, Chen N, Macasieb J, Ben O. Chemopreventive property of a soybean peptide (lunasin) that binds to deacetylated histones and inhibits acetylation. *Cancer Res*. 2001;61(20):7473-7478.

14. Jia S, Zhang S, Yuan H, Chen N. Lunasin inhibits cell proliferation via apoptosis and reduces the production of proinflammatory cytokines in cultured rheumatoid arthritis synovial fibroblasts. *BioMed Res Inter*. 2015;346839. doi:10.1155/2015/346839

15. Galvez AF. U.S. Patent No. 7,731,995. Washington, DC: U.S. Patent and Trademark Office, 2010.

16. Gu L, Ye P, Li H, et al. Lunasin attenuates oxidant-induced endothelial injury and inhibits atherosclerotic plaque progression in *ApoE-/-* mice by up-regulating heme oxygenase-1 via PI3K/Akt/Nrf2/ARE pathway. *FASEB J*. 2019;33(4):4836-4850.

17. Odani S, Koide T, Ono T. Amino acid sequence of a soybean (Glycine max) seed polypeptide having a poly (L-aspartic acid) structure. *J Biol Chem*. 1987;262(220):10502-10505.

18. He B, Tu Y, Jiang C, Zhang Z, Li Y, Zeng B. Functional genomics of *Aspergillus oryzae*: Strategies and progress. *Microorganisms*. 2019;7(103):1-13.

19. Ntana F, Mortensen UH, Sarazin C, Figge R. Aspergillus: A powerful protein production platform. *Catalysts*. 2020;10(9):1064. doi: 10.3390/catal10091064

20. Karaman E, Eyupoglu AE, Mahmoudi Azar L, Uysal S. Large-scale production of anti-RNase A VHH expressed in *pyrG* auxotrophic *Aspergillus oryzae. Curr Issues Mol Biol.* 2023;45(6):4778-4795.

21. Sakai K, Kinoshita H, Nihira, T. Heterologous expression system in *Aspergillus oryzae* for fungal biosynthetic gene clusters of secondary metabolites. *Appl Microbiol Biotechnol.* 2012;93(5):2011-2022.

22. Hernández-Ledesma B, Hsieh CC, de Lumen BO. Antioxidant and anti-inflammatory properties of cancer preventive peptide Lunasin in RAW 264.7 macrophages. *Biochem Biophys Res Commun.* 2009;390(3):803-808.

23. Gonzalez de Mejia E, Vásconez M, de Lumen BO, Nelson R. Lunasin concentration in different soybean genotypes, commercial soy protein, and isoflavone products. *J Agric Food Chem.* 2004;52(19):5882-5887.

24. Liu CF, Pan TM. Recombinant expression of bioactive peptide lunasin in *Escherichia coli. Appl Microbiol Biotechnol.* 2010;88(1):177-186.

25. Kyle S, James KA, McPherson MJ. Recombinant production of the therapeutic peptide lunasin. *Microb Cell Fact.* 2012;29:11-28.

26. Setrerrahmane S, Zhang Y, Dai G, Lv J, Tan S. Efficient production of native lunasin with correct N-terminal processing by using the pH-induced self-cleavable Ssp DnaB mini-intein system in *Escherichia coli. Appl Biochem Biotechnol.* 2014;174(2):612-622.

27. Tian Q, Zhang P, Gao Z, Li H, Bai Z, Tan S. Hirudin as a novel fusion tag for efficient production of lunasin in *Escherichia coli. Prep Biochem Biotechnol.* 2017;47(6):619-626.

28. Zhu Y, Nadia E, Yao Y, Shi Z, Ren G. Tandem repeated expression of lunasin gene in *Pichia pastoris* and its anti-inflammatory activity in vitro. *J Biosci Bioeng.* 2018;126(1):1-8.

29. Jeong JB, De Lumen BO, Jeong HJ. Lunasin peptide purified from *Solanum nigrum L.* protects DNA from oxidative damage by suppressing the generation of hydroxyl radical via blocking fenton reaction. *Cancer Lett.* 2010;293(1):58-64.

30. Aleksis R, Jaudzems K, Muceniece R, Liepinsh E. Lunasin is a redox sensitive intrinsically disordered peptide with two transiently populated α-helical regions. *Peptides.* 2016;85:56-62.

31. Alves de Souza SM, Fernandes TVA, Kalume DE, T R Lima LM, Pascutti PG, de Souza TLF. Physicochemical and structural properties of lunasin revealed by spectroscopic, chromatographic and molecular dynamics approaches. *Biochim Biophys Acta Proteins Proteom.* 2020;1868(8):140440. doi:10.1016/j.bbapap.2020.140440

How to cite this article

İSTANBUL UNIVERSITY PRESS

RESEARCH ARTICLE

Radiofrequency Electromagnetic Field Exposure Amplifies the Detrimental Effects of Fetal Hyperglycemia in Zebrafish Embryos

Derya Cansiz[1] ⓘ, Merih Beler[2] ⓘ, Gizem Egilmezer[2] ⓘ, Semanur Isikoglu[2] ⓘ, Zulal Mizrak[2] ⓘ,
Ismail Unal[2] ⓘ, Selcuk Paker[3] ⓘ, Ahmet Ata Alturfan[4] ⓘ, Ebru Emekli-Alturfan[5] ⓘ

[1]Istanbul Medipol University, School of Medicine, Biochemistry Department, Istanbul, Türkiye
[2]Marmara University, Institute of Health Sciences, Istanbul, Türkiye
[3]Istanbul Technical University, Faculty of Electrical and Electronic Engineering, Istanbul, Türkiye
[4]Istanbul University-Cerrahpaşa, School of Medicine, Biochemistry Department, Istanbul, Türkiye
[5]Marmara University, Faculty of Dentistry, Department of Biochemistry, Istanbul, Türkiye

ABSTRACT

Objective: Radiofrequency electromagnetic field (RF-EMF) exposure during the embryonic period can cause defects in the development of the fetus. The study's aim is to evaluate the effects of RF-EMF on the lipid accumulation, oxidant-antioxidant system parameters, locomotor activities, and gene expressions of insulin and leptin as genes related to insulin resistance in fetal hyperglycemia-induced zebrafish embryos.

Materials and Methods: The study exposed zebrafish embryos to RF-EMF (60 min) and glucose (5%) every day until 96 hours post fertilization (hpf). The study measured lipid peroxidation (LPO), superoxide dismutase, nitric oxide (NO), glutathione *S*-transferase (GST), and glutathione (GSH) levels to observe the oxidative stress status. The study monitored the development of the zebrafish embryos under a microscope, performed a locomotor activity analysis, measured acetylcholinesterase activity, and conducted oil red O staining to determine lipid accumulation. The study used reverse transcription polymerase chain reactions (RT-PCRs) to determine the expressions of *ins* and *lepa* by using RT-PCR.

Results: Both the glucose and RF-EMF applications decreased locomotor activity and increased the LPO and NO levels as oxidative damage indicators. Applying RF-EMF alone increased GST and GSH levels, while applying RF-EMF and glucose showed a decrease in the antioxidant defense systems. *ins* expression increased in the glucose and RF-EMF groups, while *lepa* expression increased in the glucose group and decreased in the RF-EMF group.

Conclusion: The harmful effects of hyperglycemia and RF-EMF exposure during the fetal period on embryo development need to be supported by studies to confirm the changes the current study has identified at the gene and protein levels.

Keywords: Radiofrequency electromagnetic field, Zebrafish embryos, Fetal hyperglycemia, Insulin resistance

INTRODUCTION

Despite the benefits of using radiofrequency electromagnetic fields (RF-EMF) through different sources (e.g., wi-fi, mobile phones, television), the negative effects of RF-EMF exposure are a matter of concern, as RF-EMF exposure has also been associated with undesirable effects on cell components, causing differentiation and abnormalities in cell proliferation, DNA damage, cancer, and birth defects.[1] EMFs are classified based on their respective frequencies, with low frequency EMFs being below 300 Hz, intermediate frequency EMFs occurring between 300 Hz-10 MHz , and high frequency EMFs ranging between 10 MHz-3 GHz. Mobile phones emit high-frequency RF-EMFs.[1]

EMFs have a high penetrating capacity, and the electrons they emit have the ability to move macromolecular ions and charged particles. Consequently, they can have devastating effects on the body.[2,3] Many devices used daily (e.g., computers, televisions, radios, mobile phones) cause the formation of magnetic fields. Daily exposure to the radio waves that mobile phones emit has been associated with infertility, congenital anomalies, and stillbirths.[4,5] In addition to all these, exposure to RF-EMF during pregnancy adversely affects fetal development, through studies on this subject have not been conclusive.[4-6]

Hyperglycemia in pregnancy is called gestational diabetes and causes excess glucose transport from the mother to the fetus through the placenta. As a result, it frequently increases

the risk of developing metabolic disorders such as fetal macrosomia, excess weight, insulin resistance, and type 2 diabetes.[7] The mechanism underlying the relationship between fetal exposure to maternal hyperglycemia and increased disease risk in adulthood has not yet been elucidated. Functional changes occurring in the target tissues of diabetes (e.g., adipose tissue) have been suggested to play an important role in epigenetic mechanisms. Zebrafish embryos subjected to glucose represent an effective model for fetal hyperglycemia associated with gestational diabetes.[7]

High RF-EMF causes membrane depolarization, changes in calcium ion diffusion, and nerve and muscle stimulation. A fetus has many stem cells and the fetus' immunity has not yet developed. Environmental exposure to such things as RF-EMFs cause changes in gene expression in stem cells (e.g., HSP70). This situation causes the development of oxidative stress, disrupting the oxidant-antioxidant balance in the organism. Moreover, once the antioxidant system is disrupted, the organism cannot provide adequate defense against RF-EMF exposure, resulting in increased oxidative stress.[1]

Zebrafish have a 71% genetic similarity to humans and are an important experimental model for developmental biology, human genetics, and diseases. Due to external fertilization and the optical transparency of their embryos, their embryonic development can be easily observed live under a microscope. These factors facilitate the use of zebrafish embryos in genetic, toxicological, and many other studies. In addition to being widely used for developmental biology and toxicology studies, zebrafish have also been frequently used in researching metabolic diseases in recent years.[8] The pancreas of zebrafish embryos completes its development between 48-72 hours post fertilization (hpf). The energy required for the cell divisions occurring during embryogenesis is provided through the use of maternal glycogen stores.[9] As the size of the yolk decreases toward 96 hpf, the energy needs of the zebrafish embryo are met by gluconeogenesis.[10] However, increased glucose flow to the fetus as a result of maternal hyperglycemia or various environmental exposures during the embryonic period may cause various defects in embryonic development.[11] No study is found in the literature to have examined the effects of glucose and RF-EMF exposure during the embryonic period on embryonic development or on the genes that play a key role in insulin resistance. Based on this, the current study aim of the study is to determine the effects RF-EMF has on gene expressions related to the development of insulin resistance in fetal hyperglycemia-induced zebrafish embryos. The research also aims to determine the effects of glucose and RF-EMF exposures on lipid accumulation and oxidant-antioxidant system parameters and examines acetylcholinesterase (AChE) activity and locomotor activities in relation to behavioral and developmental impairments.

MATERIALS AND METHODS

Zebrafish Care

Wildtype AB/AB strain zebrafish were maintained under apparently disease-free conditions. Husbandry and egg laying were carried out in accordance with the protocols approved by the Marmara University Institutional Animal Care and Use Committee. Fish were kept in an aquarium rack system (Zebtec, Tecniplast, Italy) at a temperature of 27 ± 1 ºC on a 14/10 h light/dark cycle and fed twice a day with live Artemia as well as flake fish food. Following natural spawning, fertilized embryos were collected and staged according to their development and morphology.[12] These were then included in the experiments. 100 embryos from each group were used for the biochemical parameters, 40 embryos for the reverse transcription polymerase chain reaction (RT-PCR) analyses, and 20 embryos for the oil red O method.

RF-EMF and Glucose Exposure

Zebrafish embryos at 0–2 hpf were divided into four groups: control, RF-EMF-exposed group (EMF), 5% glucose-exposed group (G), and both EMF- and 5% glucose-exposed group (EMF+G). EMF exposure was applied for 60 min once a day at 0-2, 24, 48, 72, and lastly 96 hpf. For this exposure, the study used a special exposure system installed by the Istanbul Technical University Faculty of Electronics. The 5% glucose exposure was applied at 0-2, 24, 48, and 72 hpf. Embryos were maintained in E3 medium (15 mM NaCl, 0.5 mM KCl, 1.0 mM MgSO$_4$, 0.15 mM KH$_2$PO$_4$, 0.05 mM Na$_2$HPO$_4$, 1.0 mM CaCl$_2$, 0.7 mM NaHCO$_3$, pH 7.2) throughout their exposure period.

Locomotor Activity Analysis

At the end of 96 hpf, behavioral analyses were performed with 10 randomly selected embryos from each group. The embryos were placed one by one in a petri dish with a diameter of 20 cm. The tail was then stimulated laterally with a sharp object, and this process was recorded with a camera. Next, the camera recordings were analyzed using the semi-automated system, and numerical data was obtained from the images.[13] The results of these analyses provided measurements for the average speed, total distance, and exploration rate parameters.

Biochemical Analyses

For each group, 10% homogenates were prepared in three replicates using physiological saline for biochemical analyses from the pools of zebrafish embryos. The supernatant was separated for analysis. Lowry's method was used for determining total protein,[14] Yagi's method for lipid peroxidation (LPO),[15] Mi-

randa's method for nitric oxide (NO),[16] Habig's method for glutathione s-transferase (GST),[17] Mylorie's method for superoxide dismutase (SOD),[18] Ellman's method for AChE,[19] and Beutler's method for glutathione (GSH).[20] Protein levels were measured to present biochemical data as values per mg of protein.

RT-PCR Analysis

Three biological replicates were made from each pool of zebrafish embryos, with each replication consisting of 40 embryos. These were homogenized with a 350 µL lysis buffer. The RNeasy Mini Kit and the QIAcube RNeasy kit (Qiagen, Hilden, Germany) were used to isolate the RNA from the embryos. The BlasTaq™ 2X qPCR MasterMix kit (Applied Biological Materials Inc. (abm) , Richmond, Canada) was used to perform the RT-PCRs. Beta-actin (*actb1*) is a housekeeping gene and is used as a reference gene. Expressions for the *lepa* and *ins* genes were determined through the RT-PCR analyses (Table 1). Relative transcription levels were calculated based on the normalization of values using the housekeeping gene.[21]

Table 1. Forward and reverse primers used in the study.

Genes	Primers (forward/reverse)
actb1	5′-AAGCAGGAGTACGATGAGTCTG-3′
	5′-GGTAAACGCTTCTGGAATGAC-3′
ins	5′-GCTCTGTTGGTCCTGTTGGT-3′
	5′-GGGCAGATTTAGGAGGAAGG-3′
lepa	5′-CTCCAGTGACGAAGGCAACTT-3′
	5′-GGGAAGGAGCCGGAAATGT-3′

Oil Red O Methods

At 96 hpf, the embryos were subjected to the following procedures for oil red O (ORO) staining. All embryos were fixed in 4% paraformaldehyde overnight. After fixation, embryos (10-15 embryos for each microcentrifuge tub) were transferred to a 1.5 mL microcentrifuge tube and washed three times (5 min each) with 1X phosphate buffered saline/0.5% Tween-20 (PBS-Tween). After PBS-Tween removal, the embryos were then stained with a mixture of 300 µL of 0.5% ORO and 200 µL of distilled water in 100% isopropyl alcohol for 15 min. The embryos were then washed three times in 1X PBS-Tween and twice in 60% isopropyl alcohol for 5 min each. Lastly, the embryos were then washed in PBS-Tween and fixed in 4% paraformaldehyde for 10 min. Embryos were mounted in glycerol before imaging, and ORO staining of the embryos was recorded under a Zeiss Sterio Discovery V8 microscope.[22]

Statistical Analysis

GraphPad 9 was used to evaluate the differences among the groups. First, one-way analysis of variance (ANOVA) was applied, followed by Tukey's multiple comparison test. A value of $p < 0.05$ is considered statistically significant.

RESULTS

Results of Morphological Analysis and ORO Staining

Embryonic development was observed under a microscope to monitor the malformations that had occurred as a result of the experimental exposures at 24, 48, 72, and 96 hpf. Scoliosis was observed in zebrafish embryos given a 5% glucose solution at 48 hpf. At 72 hpf, scoliosis was detected in the G and EMF+G groups, while cardiac edema was detected in the EMF and G groups. Eye development retardation was also detected in the EMF, G, and EMF+G groups. Head hemorrhage was seen in the G group, and yolk edema was seen in the G and EMF+G groups. Scoliosis, yolk edema, delay in eye development, and cardiac edema were observed in all exposure groups at 96 hpf (Figure 1). ORO stain was used to detect lipid accumulation in the zebrafish embryos, an increase in lipid accumulation in the liver being found at 96 hpf in the EMF and EMF+G groups (Figure 2).

Results of Locomotor Activity

The study has found average speed, total distance, and exploration rate to have decreased in all groups compared to the control. Furthermore, all locomotor parameters were lower in the EMF+G group compared to the G group (Figures 3a-c).

Results of Biochemical Analysis

As a result of the 5% glucose and RF-EMF exposures, lipid peroxidation levels were seen to have increased significantly in the EMF, G, and EMF+G groups compared to the control group. LPO increased significantly in the G group compared to the EMF group (Figure 4a). In addition, NO levels had increased significantly in the EMF, G, and EMF+G groups compared to the control group. Furthermore, NO levels were significantly lower in the EMF+G group than in the EMF group (Figure 4b). Compared to the control group, GST activities had increased significantly in the EMF and EMF+G groups. Compared to the G group, GST activities had again increased significantly in the EMF and EMF+G groups (Figure 4c). SOD activities declined significantly in the EMF and EMF+G groups compared to the control group. SOD activity also decreased significantly in the EMF and EMF+G groups compared to the G group (Figure 4d). When compared to the control, AChE activities were found to have significantly decreased in the EMF, G, and EMF+G groups. AChE activity was also seen to have decreased in the EMF and EMF+G groups compared more than in the G group (Figure 4e). GSH levels were higher in the EMF group compared to the control group. The EMF group showed a
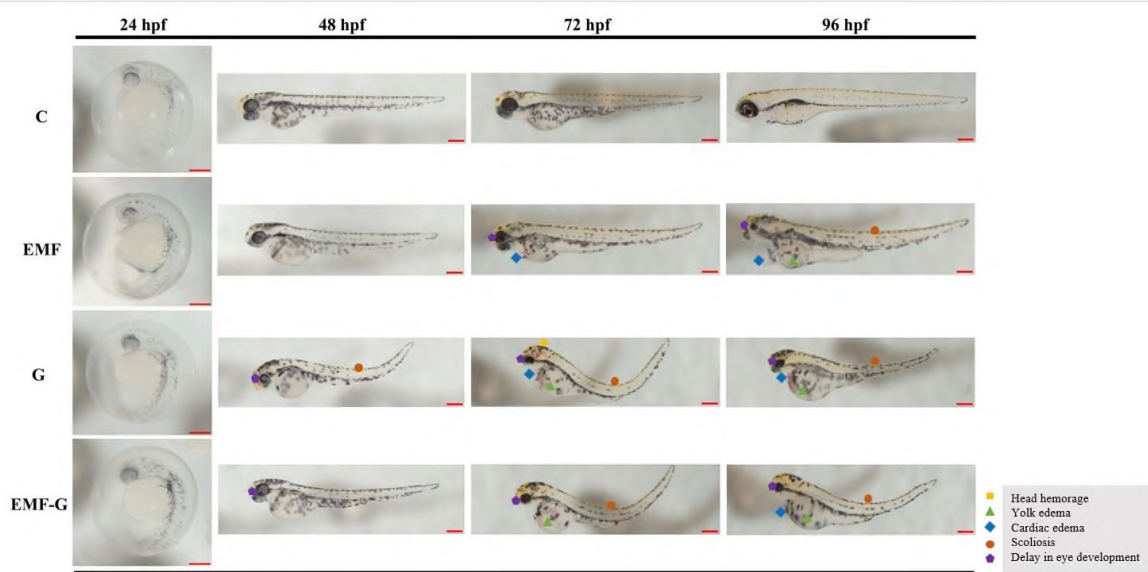
Figure 1. Effects of RF-EMF and 5% glucose exposure on embryonic development. Representative figures of zebrafish embryos at 24, 48, 72 and 96 hpf: A Zeiss Sterio Discovery V8 microscope was used for measurements. 6.3X magnification was used for embryos in the chorion and 3.2X magnification was used for hatching embryos. Scale bar: 500µm.

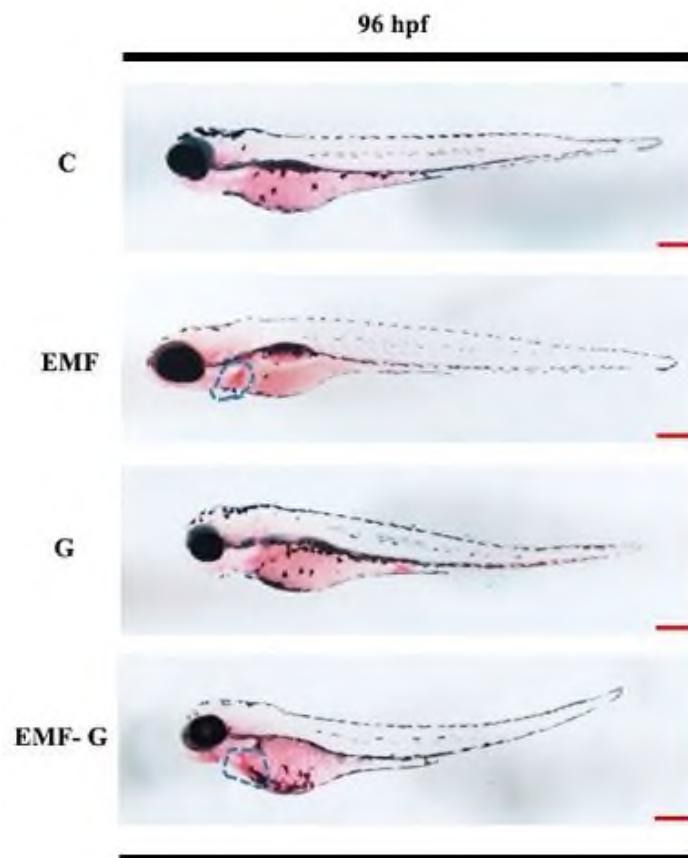**Figure 2.** Comparison of lipid accumulations of the groups with oil red O staining. Representative figures of zebrafish embryos at 24, 48, 72 and 96 hpf; A Zeiss Sterio Discovery V8 microscope was used for measurements. 3.2X magnification was used for embryos. Scale bar: 500µm.
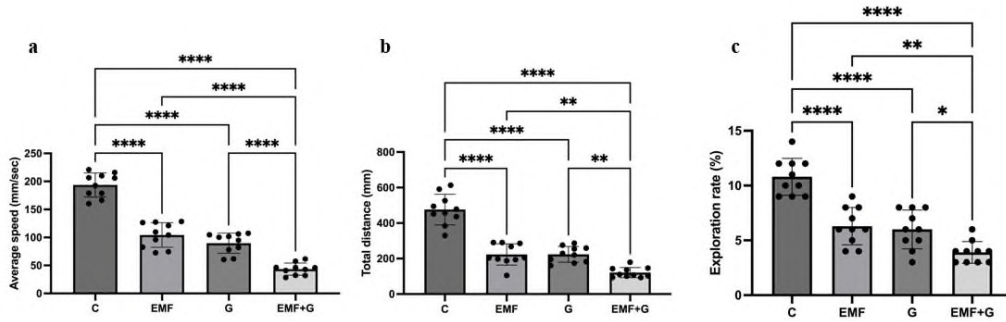
Figure 3. Bar graph presentation of the locomotor activity: a) Average speed analysis results of the groups; b) Total distance measurement results of the groups; and c) Exploration rates of the groups. Data are expressed as *Mean ± SD (n = 10)*. * $p < 0.05$; ** $p < 0.01$; **** $p < 0.0001$.
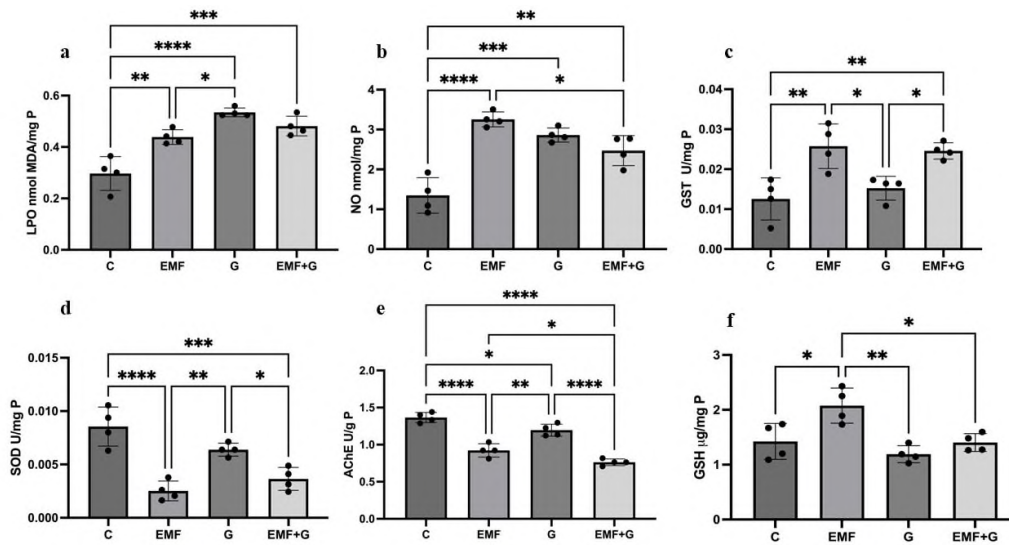

Figure 4. Bar graph presentation of the comparison of the biochemical parameters of the groups': a) lipid peroxidation (LPO) levels; b) nitric oxide (NO) levels; c) glutathione S-transferase (GST) levels; d) superoxide dismutase (SOD) levels; e) acetylcholinesterase (AChE) activities; and f) glutathione (GSH) levels. The data from the four independent experiments are expressed as *Mean ± SD (n = 4, 4 biological replicates for each group, 50 embryos per pool)*; * $p < 0.05$; ** $p < 0.01$; *** $p < 0.001$; **** $p < 0.0001$.

greater increase in GSH levels compared to the G group, while the EMF+G group showed no statistical difference. GSH levels had declined more in the EMF+G group compared to the EMF group (Figure 4f).

Results of RT-PCR Analysis

The RT-PCR analysis was performed to determine the *lepa* and *ins* mRNA expression levels as a result of RF-EMF and 5% glucose exposure. As a result of these analyses, *lepa* expression levels were lower in the EMF and EMF+G groups compared to the control, while these levels increased significantly in the G group (Figure 5a). *ins* expression levels were higher in the EMF, G, and EMF+G groups compared to the control. Furthermore, INS expression levels were lower in the EMF and EMF+G groups compared to the G group (Figure 5b).

DISCUSSION

During the fetal period, exposure to various stress factors can lead to various defects in fetuses, whose metabolic development is inadequate. Exposure to various environmental factors (e.g., radiation, heavy metals, air pollution) increase the risk of developing various diseases during prenatal and early infancy when rapid development occurs.[23]

The present study has examined the effect of RF-EMF exposure on glucose-exposed zebrafish embryos as a model of fetal hyperglycemia. In order to evaluate whether RF-EMF exposure may have an effect on gene expressions related to the development of insulin resistance, the study determined the mRNA expressions of insulin and leptin and performed an oil red O staining to determine lipid accumulation. Developmental parameters, oxidant-antioxidant status, and locomotor activity
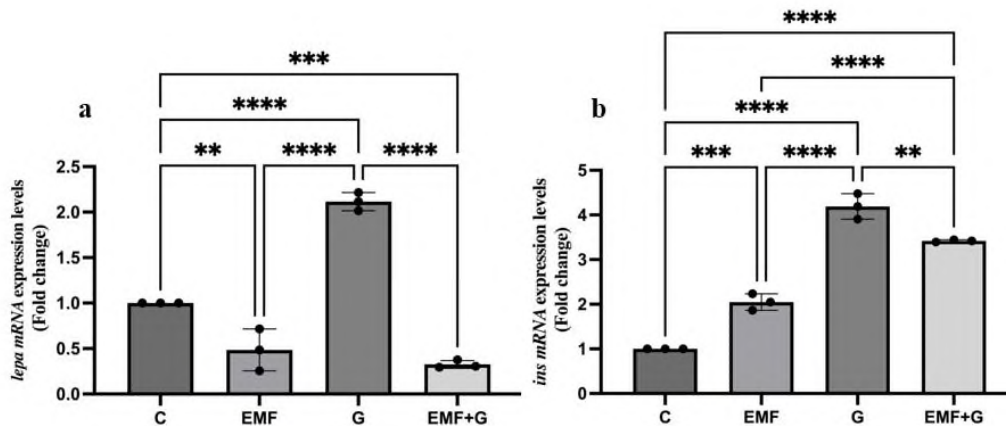
Figure 5. Bar graph presentation of the fold change of the RT-PCR-quantified transcripts of a) *lepa* and b) *ins*. All RT-PCR results are expressed as changes from their respective controls after being normalized to the housekeeping gene *actb1*. Three studies ($n = 3$; 3 biological replicates for each group, 50 embryos per pool) were used to calculate the average values. Data presented are expressed as *Mean ± SD*. **$p < 0.01$; ***$p < 0.001$; ****$p < 0.0001$.

were also assessed to find out how these exposures affected normal embryonic development.

According to the Pedersen hypothesis, an increase in glucose flow to the fetus causes fetal hyperinsulinemia, which may cause changes in the development and growth of the fetus.[11] The 5% glucose exposure-induced hyperglycemia model in zebrafish embryos revealed defects in eye development.[24] Another study found that zebrafish embryos that had been exposed to glucose developed scoliosis and edema.[25] Consistent with these studies, edema, scoliosis, and retardation in eye development were determined in the groups exposed to RF-EMF and glucose.

The present study assessed LPO levels to detect oxidative stress status. According to the results, 5% glucose and RF-EMF exposure have been revealed to lead to an increase in oxidative stress. Furthermore, lipid accumulation was observed in the liver of the RF-EMF-applied groups as a consequence of staining with oil red O. Guru and Arockiaraj performed oil red o staining to observe lipid accumulation in the fetal hyperglycemia model induced by bisphenol A in zebrafish embryos and identified lipid accumulation in the abdominal area.[26] The accumulation of specific lipid metabolites and increased lipid levels within the cell are related to hyperglycemia.[27] Hyperglycemia can damage vascular structures by stimulating oxidative stress, interfering with NO production, and triggering the formation of lipid-containing foam cells by macrophages.[28] As a result of the disruption in the integrity of the endothelial structure, lipid accumulation accelerates.[28] Kaplan et al. revealed an increase in NO and LPO levels in zebrafish embryos that had been administered 5% glucose.[7] In light of this information, the increase in LPO and NO levels in this study's exposure groups may be associated with lipid accumulation and hyperglycemia.

Kaplan et al. demonstrated an increase in GST activities in the fetal hyperglycemia model they created regarding zebrafish embryos.[7] While GST activity in the present study did not

change significantly in the group given only 5% glucose, increased GST activity was observed in the RF-EMF groups, which may be related to the increased LPO in these groups. The GST enzyme is effective in xenobiotic detoxification. This enzyme aims to prevent cellular damage by conjugating the reactive species created by Phase I enzymes with glutathione.[29] In both RF-EMF groups, glucose exposure caused a decrease in GSH and GST activities. This demonstrates that glucose exposure suppresses the elements of the antioxidant defense system that activate under increased oxidative stress in the case of RF-EMF exposure. A significant decrease in SOD activity was observed to have occurred in the group that was administered 5% glucose.[11] Consistent with the findings of Hansen et al., the decrease observed in SOD activity in the glucose and RF-EMF groups in the present study is an indicator of the decreased antioxidant defense system in the face of increasing oxidative stress in these groups and supports the findings regarding the disruption of embryonal development in these groups.

Aerobic organisms need oxygen to survive. While a large portion of oxygen molecules turn into water in the electron transport chain, a very small portion may cause radical formation. The increases in *ins* mRNA levels and in LPO and GST activity in this study may be indicators of oxidative stress formation. Increased oxidative stress and mitochondrial dysfunction have been reported in the glucose-induced hyperglycemia model in zebrafish.[25] The glucose-stimulated increase in insulin mRNA expression in the present study was accompanied by increased LPO (an indicator of oxidative stress), as well as the stimulation of antioxidant defense systems in response to this situation. Mitochondrial dysfunction that develops as a result of hyperglycemia can cause a disruption in the electron transport chain and ROS formation. Although this situation was observed in both the RF-EMF and glucose groups, the increase in insulin gene expression was much more pronounced in the glucose group. On the other hand, when glucose was administered to

the RF-EMF group, an increase in insulin gene expression was detected, which was expected.

Torres-Ruiz et al. discovered RF-EMF exposure to cause a decrease in AChE activity as well as locomotor activity in zebrafish embryos.[30] In the present study, locomotor activity decreased in all exposure groups, with the G group showing an increase in AChE enzyme activity, which hydrolyzes acetylcholine, while the EMF and EMF+G groups showed a decrease.

In the present study, *ins* mRNA expression increased in all exposure groups compared to the control. Furthermore, *lepa* mRNA expression increased in the glucose group compared to the control group while decreasing in the EMF and EMF+G groups. Insulin is one of the most important hormones for ensuring glucose control. Therefore, the present study analyzed the expressions of the *ins* and *lepa* genes to understand how these two hormones act in case of EMF exposure in a fetal hyperglycemia model, as well as to evaluate whether EMF exposure affects the gene expressions related to the development of insulin resistance that may develop in fetal hyperglycemia. The increase in *ins* mRNA levels in the present study indicates that RF-EMF exposure during the fetal period may affect glucose hemostasis. Glucose is known to stimulate the accumulation of insulin mRNA. In accordance with this information, the study found increased insulin mRNA levels in the glucose-exposed groups.[31] Consistent with the current study, Kaplan et al. reported an increase in *ins* mRNA levels in their hyperglycemia model induced with 5% glucose.[7] Meo and Rubeaan's study revealed fasting blood glucose and insulin resistance to increase in Wister Albina rats that were exposed to mobile phone radiation for more than 15 minutes a day over three months.[32]

Leptin hormone is important in energy homeostasis and regulates the hunger and satiety mechanism.[33] The current study detected a decrease in *lepa* mRNA levels. Leptin levels have been positively correlated with body fat, with obese subjects being more hyperleptinemic than lean subjects.[34] Reduced leptin mRNA levels through RF-EMF exposure may be related to the lipid accumulation observed in these groups. However, in order to support these findings, the changes this study has identified in insulin and leptin expressions at the gene level need to be confirmed at the protein level.

CONCLUSION

Hyperglycemia in a mother during pregnancy increases glucose flow to the fetus, which can cause ROS accumulation and lipid accumulation in addition to developmental disorders. This study's results have shown that, in cases of fetal hyperglycemia, RF-EMF exposure increases the harmful effects caused by glucose exposure on zebrafish embryo development. In addition, this study supports the suitability of the zebrafish embryo for studies on fetal hyperglycemia and exposure to environmental factors, including RF-EMF.

ORCID IDs of the author

Derya Cansiz	0000-0002-6274-801X
Merih Beler	0000-0002-3828-4630
Gizem Egilmezer	0000-0002-1231-5232
Semanur Isikoglu	0009-0003-9779-2867
Zulal Mizrak	0009-0004-7647-7267
Ismail Unal	0000-0002-8664-3298
Selcuk Paker	0000-0002-1769-1835
Ahmet Ata Alturfan	0000-0003-0528-9002
Ebru Emekli-Alturfan	0000-0003-2419-8587

REFERENCES

1. Kashani ZA, Pakzad R, Fakari FR, et al. Electromagnetic fields exposure on fetal and childhood abnormalities: Systematic review and meta-analysis. *Open Med (Wars)*. 2023;18(1):20230697. doi:10.1515/med-2023-0697

2. Scientific Committee on Emerging Newly Identified Health Risks. Opinion on potential health effects of exposure to electromagnetic fields. *Bioelectromagnetics*. 2015;36(6):480–484.

3. Leszczynski D, Joenväärä S, Reivinen J, Kuokka R. Non-thermal activation of the hsp27/p38MAPK stress pathway by mobile phone radiation in human endothelial cells: molecular mechanism for cancer- and blood-brain barrier-related effects. *Differentiation*. 2002;70(2-3):120–129.

4. Larsen AI, Olsen J, Svane O. Gender-specific reproductive outcome and exposure to high-frequency electromagnetic radiation among physiotherapists. *Scand J Work Environ Health*. 1991;17(5):324-329.

5. Ouellet-Hellstrom R, Stewart WF. Miscarriages among female physical therapists who report using radio- and microwave-frequency electromagnetic radiation. *Am J Epidemiol*. 1993;138(10):775–786.

6. Rosas DB, López H, Fernández N. Is magnetic resonance imaging teratogenic during pregnancy? Literature review. *Urología Colombiana*. 2017;26(3):219–228.

7. Kaplan G, Beler M, Unal I, et al. Diethylhexyl phthalate exposure amplifies oxidant and inflammatory response in fetal hy-

perglycemia model predisposing insulin resistance in zebrafish embryos. *Toxicol Ind Health.* 2024;40(5):232-243.

8. Zang L, Maddison LA, Chen W. Zebrafish as a model for obesity and diabetes. *Front Cell Dev Biol.* 2018;20(6):91. doi:10.3389/fcell.2018.00091

9. Rocha F, Dias J, Engrola S, et al. Glucose metabolism and gene expression in juvenile zebrafish (Danio rerio) challenged with a high carbohydrate diet: effects of an acute glucose stimulus during late embryonic life. *Br J Nutr.* 2015;113:403–413.

10. Gut P, Baeza-Raja B, Andersson O, et al. Whole-organism screening for gluconeogenesis identifies activators of fasting metabolism. *Nat Chem Biol.* 2013; 9:97–104.

11. Hansen NS, Strasko KS, Hjort L, et al. Fetal hyperglycemia changes human preadipocyte function in adult life. *J Clin Endocrinol Metab.* 2017;102(4):1141-1150.

12. Westerfield M.The zebrafish Book. Guide for the laboratory use of zebrafish (Danio rerio). *University of Oregon Press,* Eugene. 1995.

13. Cansız D, Unal I, Beler M, Alturfan AA, Emekli-Alturfan E. Assessment of developmental neurotoxicity using semi-automatic behavior analysis system for zebrafish. *Methods Mol Biol.* 2024;2753:409-419.

14. Lowry OH, Rosebrough NJ, Farr A., Randall RJ. Protein measurement with the Folin phenol reagent. *J Biol Chem.* 1951;193:265-275.

15. Yagi K. Simple assay for the level of total lipid peroxides in serum or plasma. *Methods Mol Biol* 1998;108:101-106.

16. Miranda KM, Espey MG, Wink DA. A rapid, simple spectrophotometric method for simultaneous detection of nitrate and nitrite. *Nitric Oxide.* 2001;5:62-71.

17. Habig WH, Jakoby WB. Assays for differentiation of glutathione S-transferases. *Methods Enzymol.* 1981;77:398-405.

18. Mylroie AA, Collins H, Umbles C, Kyle J. Erythrocyte superoxide dismutase activity and other parameters of copper status in rats ingesting lead acetate.*Toxicol Appl Pharmacol.* 1986;82:512-520.

19. Ellman GL, Courtney KD, Andres Jr V, Featherstone RM. A new and rapid colorimetric determination of acetylcholinesterase activity. *Biochem Pharmacol.* 1961;7:88-95.

20. Beutler E, Duron O, Kelly BM. Improved method for the determination of blood glutathione. *J Lab Clin Med.* 1963;61:882-888.

21. Livak KJ, Schmittgen TD. Analysis of relative gene expression data using real-time quantitative PCR and the 2(-Delta Delta C(T)) Method *Methods.* 2001;25:402-408.

22. Kim SH, Wu SY, Baek JI, Choi SY, Su Y, Flynn CR, et al. A post-developmental genetic screen for zebrafish models of inherited liver disease. *PLoS ONE.* 2015;10(5): e0125980. doi:10.1371/journal.pone.0125980

23. Mallozzi M, Bordi G, Garo C, Caserta D. The effect of maternal exposure to endocrine disrupting chemicals on fetal and neonatal development: A review on the major concerns. *Birth Defects Res C Embryo Today.* 2016;108(3);224-242.

24. Singh A, Castillo HA, Brown J, Kaslin J, Dwyer KM, Gibert Y. High glucose levels affect retinal patterning during zebrafish embryogenesis. *Sci Rep.* 2019;11(1):4121. doi:10.1038/s41598-019-41009-3

25. Li Y, Chen Q, Liu Y, et al. High glucose-induced ROS-accumulation in embryo-larval stages of zebrafish leads to mitochondria-mediated apoptosis. Apoptosis. 2022;27: 509–520.

26. Guru A and Arockiaraj J. Exposure to environmental pollutant bisphenol A causes oxidative damage and lipid accumulation in Zebrafish larvae: Protective role of WL15 peptide derived from cysteine and glycine-rich protein 2. *J Biochem Mol Toxicol.* 2023;37(1):e23223. doi:10.1002/jbt.23223

27. Erion DM, Park HJ, Lee HY. The role of lipids in the pathogenesis and treatment of type 2 diabetes and associated co-morbidities. *BMB Rep.* 2016;49(3):139-148.

28. Morris S, Cholan PM, Britton WJ et al. Glucose inhibits haemostasis and accelerates diet-induced hyperlipidaemia in zebrafish larvae. *Sci Rep.* 2021;11(1):19049. doi:10.1038/s41598-021-98566-9

29. Agha-Hosseini F, Mirzaii-Dizgah I, Farmanbar N, Abdollahi M. Oxidative stress status and DNA damage in saliva of human subjects with oral lichen planus and oral squamous cell carcinoma. *J Oral Pathol Med.* 2012; 41:736-740.

30. Torres-Ruiz M, Suárez Vi. López OJ, et al. Effects of 700 and 3500 MHz 5G radiofrequency exposure on developing zebrafish embryos. *Sci Total Environ.* 2024;915:169475. doi:10.1016/j.scitotenv.2023.169475

31. Briaud I, Rouault C, Bailbé D, Portha B, Reach G, Poitout V. Glucose-induced insulin mRNA accumulation is impaired in islets from neonatal streptozotocin-treated rats. *Horm Metab Res.* 2000;32(3):103-106.

32. Meo SA and Rubeaan KA. Effects of exposure to electromagnetic field radiation (EMFR) generated by activated mobile phones on fasting blood glucose. *IJOMEH.* 2013;26:235–241.

33. Al-Hussaniy HA, Alburghaif AH, Naji MA. Leptin hormone and its effectiveness in reproduction, metabolism, immunity, diabetes, hopes and ambitions. *J Med Life.* 2021;14:600-605.

34. Kelesidis T, Mantzoros CS. The emerging role of leptin in humans. *Pediatr Endocrinol Rev.* 2006;3(3):239-248.

How to cite this article

RESEARCH ARTICLE

Changes in Histological Features, Apoptosis and Necroptosis, and Inflammatory Status in the Livers and Kidneys of Young and Adult Rats

Emine Rumeysa Hekimoglu[1] ⓘ, Mukaddes Esrefoglu[1] ⓘ, Birsen Elibol[1] ⓘ, Seda Kirmizikan[1] ⓘ

[1]Bezmialem Vakıf University, Faculty of Medicine, Department of Histology and Embryology, Istanbul, Türkiye

ABSTRACT

Objective: Aging entails a gradual rise in low-grade inflammation affected by cellular degeneration and death. Inflammaging refers to the chronic, low-grade inflammation that occurs alongside the aging process. This study attempts to evaluate the hepatic and renal histological changes, apoptosis and necroptosis rates, and inflammaging status of 6-week-old and 10-month-old rats.

Materials and Methods: This study uses 12 male rats separated into two groups: Young Group (6-week-old rats; $n = 6$), and Adult Group (10-month-old rats; $n = 6$). Animals were sacrificed under anesthesia. The rats' livers and kidneys were removed, and each organ tissue was divided into two parts: one for the microscopic examination (H&E and TUNEL immunohistochemistry) and the other for biochemical determination (tumor necrosis factor-alpha [TNF-α], nuclear factor-kappa beta [NF-κB], interleukin1-Beta [IL-1β], IL6, receptor-interacting serine/threonine protein kinase [RIP], and RIP3).

Results: The histological features of the livers and kidneys of the 6-week-old rats were consistent with healthy mammalian organ features, while some histological changes were detected in sections of the 10-month-old rats. The apoptosis rate indicated by TUNEL immunohistochemistry was seen to have increased in the 10-month-old rats, while the necroptosis rate indicated by RIP3 Western-blotting analysis was conversely determined to have decreased. Significant increases in TNF-α and NF-κB levels were consistent with the increased apoptosis rate in the 10-month-old rats compared to the 6-week-old rats.

Conclusion: One of the striking results of this study is that the degenerative changes related to aging began to be seen even in 10-month-old rats. The researchers used healthy rats of this age as control subjects as well as to create experimental models.

Keywords: Apoptosis, Necroptosis, Young rats, Adult rats, Liver, Kidney

INTRODUCTION

The senescence of cells is an event where cells lose their dividing ability, often triggered by factors such as DNA damage or stress. Over time, senescent cells may proliferate in tissues and contribute to aging-related illnesses and aging itself. One hallmark of cellular senescence is the development of the senescence-associated secretory phenotype (SASP), wherein senescent cells secrete a variety of inflammatory cytokines, growth factors, and proteases.[1-3] Apoptosis and necroptosis are both programmed cell death routes that are mediated by specific molecular regulators.[4] Necroptosis represents a programmed cell death pathway that exhibits features overlapping with both apoptosis and necrosis. Unlike apoptosis, necroptosis is triggered by external factors such as inflammation, infection, or cellular stress when apoptosis is inhibited.[5] Different programmed cell death pathways are interconnected on multiple levels and include shared triggers, final execution events, and cell defense mechanisms. These pathways also include the potential for one type of cell death to trigger another type of cell death in the same or different cells.[6]

Aging entails a gradual rise in low-grade inflammation affected by cellular degeneration and death. Chronic, mild-grade inflammation involving inflammaging occurs alongside the aging process. This chronic inflammation is associated with an elevated risk of several age-related diseases, including adult-type diabetes, cardiac and vascular diseases, cancer, and neurodegenerative diseases. Inflammaging can exacerbate the progression of these conditions and contribute to their development by promoting tissue damage, impairing cellular function, and disrupting normal physiological processes. This inflammation is thought to be a result of various factors, such as the accumulation of cellular damage over time, dysregulation of the immune system, and the presence of aging cells.[7-9] In humans, inflammaging is marked by the elevation of circulating pro-inflammatory cytokines, notably interleukin-6 (IL-6), IL-1β, and tumor necrosis factor-alpha (TNF-α). These cytokines play

crucial roles in regulating the inflammatory response and are associated with various age-related diseases.[7,9,10]

This study attempts to evaluate the hepatic and renal histological changes, apoptosis and necroptosis rates, and inflammaging status of 6-week-old and 10-month-old rats. It also aims to discover the beginning of aging-related changes in rats to make suggestions about which age periods of animals should be preferred for yielding more realistic results. The experimental studies carried out so far have investigated age-related histological changes in much older rats than this study has used.

MATERIALS AND METHODS

Animals and Experimental Groups

This study includes 12 male Sprague-Dawley rats that were formed into two groups: Group 1 (Young Group), and Group 2 (Adult Group), each consisting of 6 rats. The rats in the Young Group are six weeks old, and the rats in the Adult Group were 10 months old. The animals were sacrificed under anesthesia. The abdominal cavities of the rats were opened, and the livers and kidneys were rapidly removed. Each liver and kidney tissue were divided into two parts, one for the microscopic examination and the other for the biochemical identification. The Animal Care and Experiment Committee of Bezmialem Vakif University School of Medicine approved the animal care and research procedure (Approval No. 2024/10).

Microscopic Evaluation

Light Microscopic Examination

The kidney and liver tissue samples were fixed in 10% buffered formalin. Following fixation, the tissue samples were dehydrated, cleared with xylol, and finally embedded in paraffin. For microscopic evaluation, sections measuring 5 µm in thickness were stained using hematoxylin-eosin (H&E) and Masson's trichrome techniques. Subsequently, the samples were inspected under a light microscope (Nikon Eclipse 920248, USA).

Immunohistochemical Staining

Sections were stained to detect apoptotic cell death using a TUNEL-based apoptosis kit (ApopTag® Plus Peroxidase In Situ Apoptosis Kit, S7101, Millipore, Darmstadt, Germany). The TUNEL technique was applied in accordance with the manufacturer's instructions. Two blinded reviewers counted the number of TUNEL-positive cells from five randomly selected fields for each sample. This counting process was conducted using ImageJ software (National Institutes of Health, Bethesda, MD, USA) under a microscope at 20X magnification.

Western Blotting

Kidney and liver tissues were dissected, complemented with phosphate-buffered saline (PBS) that included a protease inhibitor cocktail, homogenized, and centrifuged at 9,000 x g for 15 min at 4°C. The western blot method was performed as in previous studies.[11] The study used RIP (receptor-interacting serine/threonine protein kinase) and RIP3 (receptor-interacting serine/threonine kinase 3) to indicate the presence or absence of necroptosis. IL-1β (Novus Biologicals, USA), RIP, and RIP3 (Abcam, Boston, MA, USA), TNF-α, IL-6, and nuclear factor kappa B (NF-κB; Cell Signaling, Danvers, MA, USA) were used as the primary antibodies. Signal detection was carried out utilizing a luminol substrate (Elabscience, Houston, TX, USA) and recorded using a CCD camera with the Fusion FX7 system (Vilber Lourmat, Collegien, France). Verification of protein loading was accomplished using a monoclonal mouse antibody specific to glyceraldehyde 3-phosphate dehydrogenase (GAPDH; Abbkine, Atlanta, Georgia, USA).

Statistical Analysis

Statistical analysis was performed using SPSS 22.0. All data were expressed as mean ± standard error of the mean (*SEM*), and the difference between groups was analyzed using Student's t-test, with $p < 0.05$ being considered statistically significant.

RESULTS

Histology of the Liver and Kidney in the Young and Adult Rats

Various changes were detected in terms of the histological features and protein expressions related to both liver and kidney tissues between the 6-week and 10-month groups.

The H&E-stained liver sections from the 6-week-old rats appeared healthy, consistent with expectations. Classical liver lobule organization was obvious (Figure 1A). Hepatocytes possessing euchromatic nuclei and acidophilic cytoplasm containing soma basophilic granules were arranged as anastomosing cellular rows separated by sinusoidal capillaries. Periportal Kupffer cells and even bile canaliculi were observed between the adjacent hepatocytes (Figure 1B). Masson's trichrome-stained liver sections revealed collagen fiber organization. A thin layer of collagen fibers surrounded the thin-walled central vein (Figure 1C) and also observed within the portal space (Figure 1D). The H&E-stained liver sections from the 10-month-old rats were generally healthy, as expected. However, their sinusoid capillaries looked narrower than those of the 6-week-old rats (Figure 2A). Some deeply acidophilic stained hepatocyte groups were also interspersed among the healthy hepatocytes (Figure 2A). The nuclei of some of these hepatocytes seemed normal, while others were darker or paler than those of the
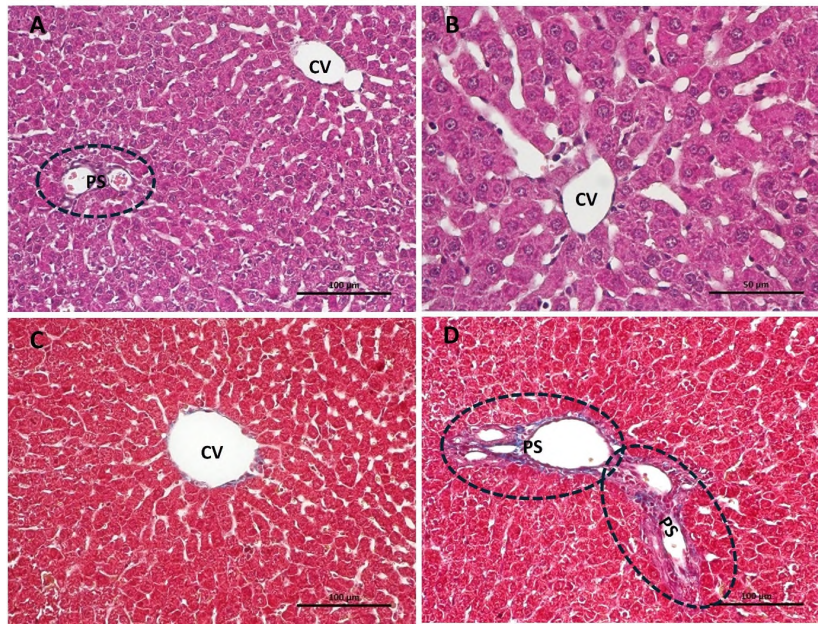
Figure 1. Histological features of the liver from 6-week-old rats. Central veins (CV) and portal spaces (PS) are regularly organized (A and B). A thin layer of collagen fibers surrounding central vein (C) and within the portal space (D) is observed A and B. Hematoxylin and Eosin; X20 (A) and X40 (B); Masson's trichrome; X20 (C) and X40 (D).
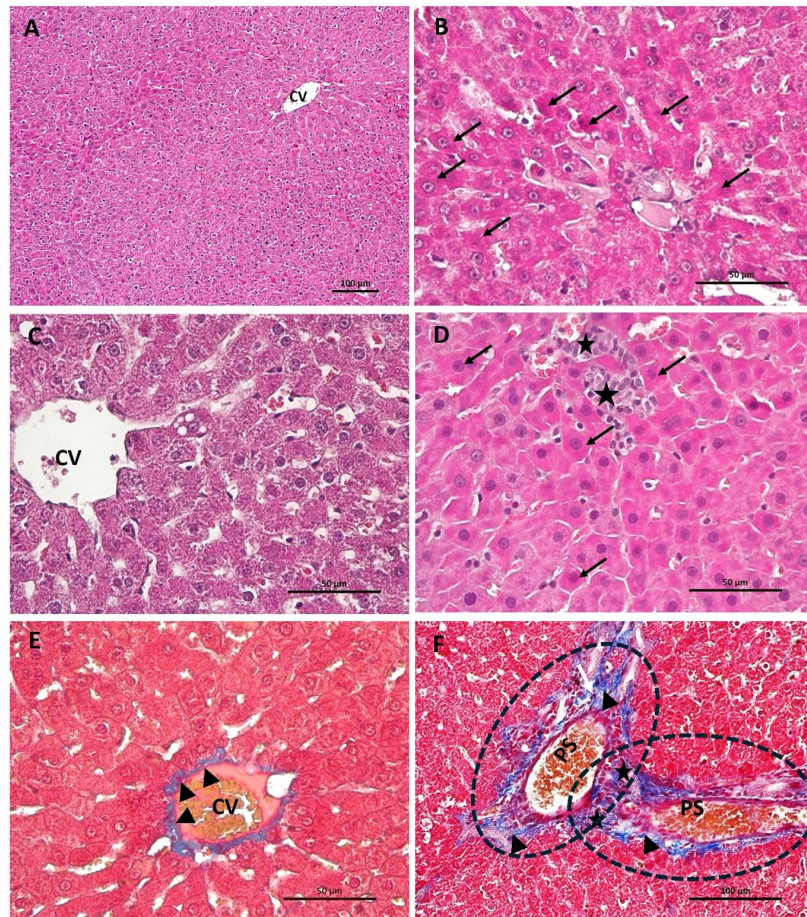
Figure 2. Histological features of the liver sections from 6-week-old rats. Deeply acidophilic stained hepatocyte groups are obvious among the regular hepatocytes (arrows) (A, B and D). Cytoplasmic vacuolization is evident both in deeply acidophilic stained hepatocytes (A, B and D) and healthy-appeared hepatocytes (C). Small inflammatory cell groups (black stars) are seen among deeply acidophilic cell groups (D) and within the portal spaces (PS) (F). The collagen fiber mass (marked by black arrowheads) encompassing the central vein (CV) (E) and within portal space (F) seems thicker than those of the previous group. Hematoxylin and Eosin, X20 (A), X40 (B) and X40 (C). Masson's trichrome, X40 (D) and X20 (E).

healthy hepatocytes. Additionally, cytoplasmic vacuolization was evident in both the apparently healthy hepatocytes (Figure 2B) and deeply acidophilic stained hepatocytes (Figure 2C). Occasionally, some small inflammatory cell groups were detected, especially among these cell groups (Figure 2D) as well as within the portal spaces. Masson's trichrome-stained liver sections revealed the collagen fiber mass around the central veins (Figure 2E) and within the portal spaces (Figure 2F) to be higher than those in the 6-week-old rats.

The H&E-stained kidney sections of the 6-week-old rats were healthy, as expected. Many glomeruli were detected surrounded by Bowman spaces in the cortex of the kidneys, as well as proximal and distal tubules, also as expected (Figure 3A). At higher magnifications, the macula densa, both layers of the Bowman capsule, striated border, and even basal striation of the proximal tubule cells became obvious (Figure 3B). Masson's trichrome-stained kidney sections revealed collagen fiber organization. A thin layer of collagen fibers was seen to surround the parietal layer of the Bowman capsule, but was only barely seen between the tubules (Figures 3C and 3D). The H&E-stained kidney sections of the 10-month-old rats were generally healthy, as expected. However, contraction of the Bowman space and tubule lumen was obvious in some places (Figure 4A). Under higher magnifications, the presence of some deeply acidophilic stained epithelial cells was detected in both the proximal (Figure 4B) and distal tubules. Regularly stained tubule epithelial cells also showed some abnormalities, including edema and heterochromatin condensation (Figure 4B). Interestingly, this group was detected to have some metaplastic changes related to the Bowman capsule. The simple squamous epithelium of the parietal layer of the Bowman capsule had transformed into a simple cuboidal epithelium, similar to that of the proximal tubule that included basal striation (Figure 4C). Some small inflammatory cell groups were detected in the interstitial area (Figure 4D). Masson's trichrome-stained kidney sections revealed the collagen fiber mass around the Bowman capsule and among the tubules (Figures 4E and 4F) to be higher than those in the 6-week-old rats.

IL-6, IL-1β, RIP3, RIP, NF-κB, and TNF-α Levels in the Young and Adult Rats' Liver and Kidney

RIP3 expression in the liver tissue was higher in the young rats compared to the adult rats ($p < 0.005$; Figure 5A). RIP expression was also higher in the young rats, though it did not reach the accepted level of significance (Figure 5B). The expressions of NF-κB and TNF-α were significantly higher in the adult animals compared to the young animals ($p < 0.05$ and $p < 0.005$, respectively; Figures 5C and 5D). In addition, no difference was found between the young and adult rats regarding IL-6 expression (Figure 5E).

IL-1β levels in the kidney tissue were notably higher in the young rats compared to the adult rats ($p < 0.05$; Figure 6A). In addition, RIP3 protein expression was slightly higher in the young rats compared to the adult rats ($p < 0.05$), whereas RIP protein expression was similar in both age groups (Figures 6B and 6C). Unfortunately, the Western-blotting protocol for NF-κB, TNF-α, and IL-6 failed despite repeated efforts.

Expression Patterns and Levels of TUNEL Positivity in the Young and Adult Rats' Liver and Kidney

The results of the mean % area measurement, which enables quantifying the percentage of tissue area that is positively stained for TUNEL, revealed the apoptosis levels to be slightly higher in the adult livers and kidneys compared to those of the younger rats (Figures 7A and 7B), though not statistically significant.

DISCUSSION

One of the fundamental mechanisms in the aging process is cellular senescence.[12] Senescent cells have a complex SASP, which includes an extension of pro-inflammatory variables with vital paracrine and autocrine impacts on cell and tissue biology. Both clinical evidence and experimental research have established connections for cellular senescence with the buildup of senescent cells and the generation and dissemination of SASP components, which contribute to age-related health issues.[13] Factors that initiate the formation of senescent cells encompass DNA damage, shortened telomeres, activated oncogenes, metabolic cues such as reactive oxygen species (ROS), physical strain, and impaired mitochondrial function.[14-17] A significant portion of senescent cells generates an SASP that is both pro-inflammatory and pro-apoptotic. The inducers, the length of time from induction, and microenvironmental factors of senescence vary according to cell type. SASP might be comprised of cytokines (e.g., IL-1a, IL-6, IL-8, TNF-α, interferon-γ) and chemokines, as well as growth factors, microRNAs, ROS, and exosomes.[18,19] Aging is characterized by an increase in mild chronic inflammation known as inflammaging, which is acknowledged as a crucial factor in the initiation of aging-related diseases.[20] In humans, inflammaging is defined by elevated levels of circulating pro-inflammatory cytokines, including IL-6, TNF-α, and IL-1β.[8] Although the current study detected no excessive pathological inflammation, hepatic expressions of NF-κB and TNF-α were significantly higher in the adult rats compared to the young ones.

In laboratory settings, Sprague-Dawley rats typically reach sexual maturity and adulthood at around 6-8 weeks of age. Adult life can be considered to begin around this age, as this is when they reach physical and sexual maturity. As for the onset of old age in Sprague Dawley rats, it generally starts around 18-24 months of age, at which point these rats may start exhibiting
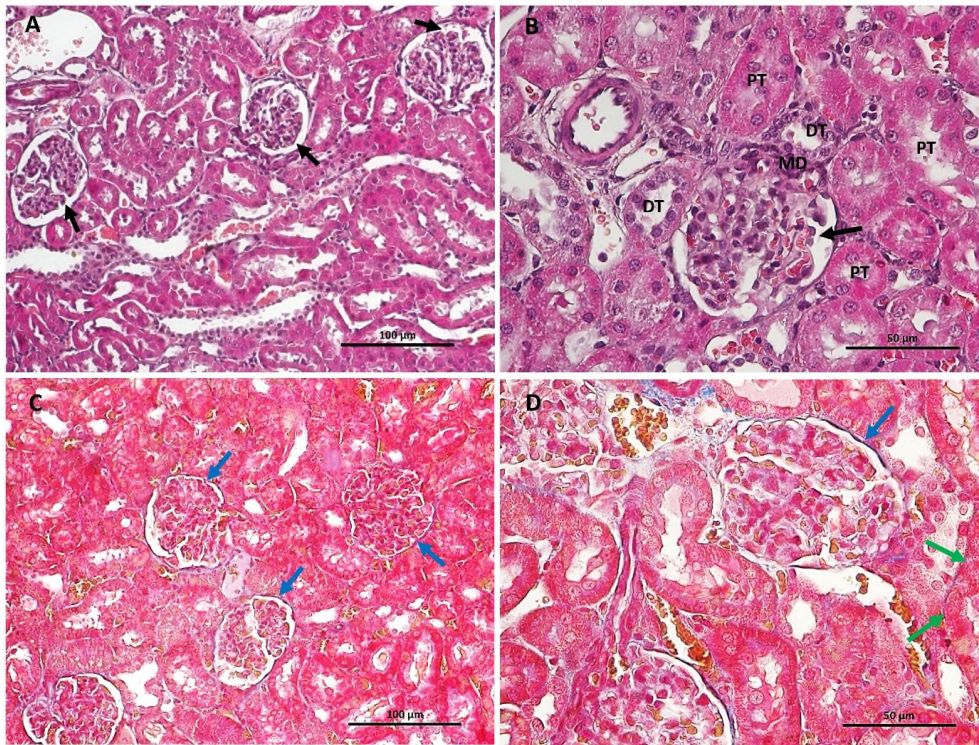
Figure 3. Histological features of the kidney sections from 6-week-old rats. Many glomeruli surrounded by Bowman spaces (black arrow), and proximal (PT) and distal tubules (DT) are detected in the cortex (A-D). Macula densa (MD), both layers of the Bowman capsule, striated border, and basal striation of the proximal tubule cells are seen (B). A thin layer of collagen fibers surrounding the parietal layer of the Bowman capsule (blue arrow) is seen (C and D). Note that collagen fibrils are barely seen between the tubules (green arrow) (D). Hematoxylin and Eosin, X20 (A) and X40 (B). Masson's trichrome, X20 (C) and X40 (D).

signs of aging. Due to both 8-month-old and 10-month-old rats typically being considered adults in the context of rat development, researchers generally use 8- or 10-week-old rats as subjects without hesitation, regardless of the age of the animals held by the animal research center. However, even the category of so-called adult rats can still have differences in cellular features, proliferation, and apoptotic, necrotic, or necroptotic cell death inflammation, organ morphology and physiology, and susceptibility to certain conditions. Consistent with this observation, while the histological features of the livers and kidneys of this study's 6-week-old rats are considered consistent with healthy mammalian organ features, some histological changes were detected in the sections of the 10-month-old rats. For instance, the presence of deeply acidophilic stained hepatocyte groups, vacuolization, and small inflammatory cell groups was evident in the liver sections. The presence of some deeply acidophilic stained epithelial cells was also detected in the kidney sections of this group in both the proximal and distal tubules, as well as cellular edema, nuclear heterochromatin condensation, and metaplastic changes related to the Bowman capsule. Also, some small inflammatory cell groups were observed in the kidney sections. In addition to the histological changes, the study also detected some differences in terms of the rates of apoptotic and necroptotic cell death and inflammatory mediators. The TUNEL immunohistochemistry indicated the apoptosis rate to have increased conversely, the RIP3 Western-blotting analysis indicated the necroptosis rate to have decreased in the

liver and kidneys of the 10-month-old rats. The levels of NF-κB and TNF-α expressions in the liver samples were notably elevated in the 10-month-old rats compared to the 6-week-old rats. As age advanced, the inflammatory cytokine levels in the liver were found to increase.[21] Inflammation and cell death are interrelated processes with significant overlap. Inflammatory signals can induce various forms of cell death, and cell death, particularly necrosis and necroptosis, can trigger and sustain inflammatory responses. Additionally, inflammation often results in the production of reactive oxygen species (ROS), which can cause cellular damage and death through oxidative stress mechanisms. Cytokines such as TNF-α, IL-1, and IL-6, produced during inflammation, can directly induce cell death. TNF-α, for instance, can trigger apoptotic pathways in certain contexts, leading to cell death. NF-κB, a key transcription factor activated by inflammatory signals, can regulate the expression of both pro-apoptotic and anti-apoptotic genes.

Regulated cell death modalities include apoptosis and necroptosis, which are mediated by dedicated molecular machines, and play a significant role in health and disease.[4] Numerous levels of connections exist among various forms of regulated cell death. These encompass shared molecular pathways such as common triggers, final execution steps, and cellular defense mechanisms. Moreover, the potential exists for one type of cell demise to induce a different type of cell death in the same or other cells.[4] Necroptosis could be considered the best-characterized form of regulated apoptosis.[22] Apopto-
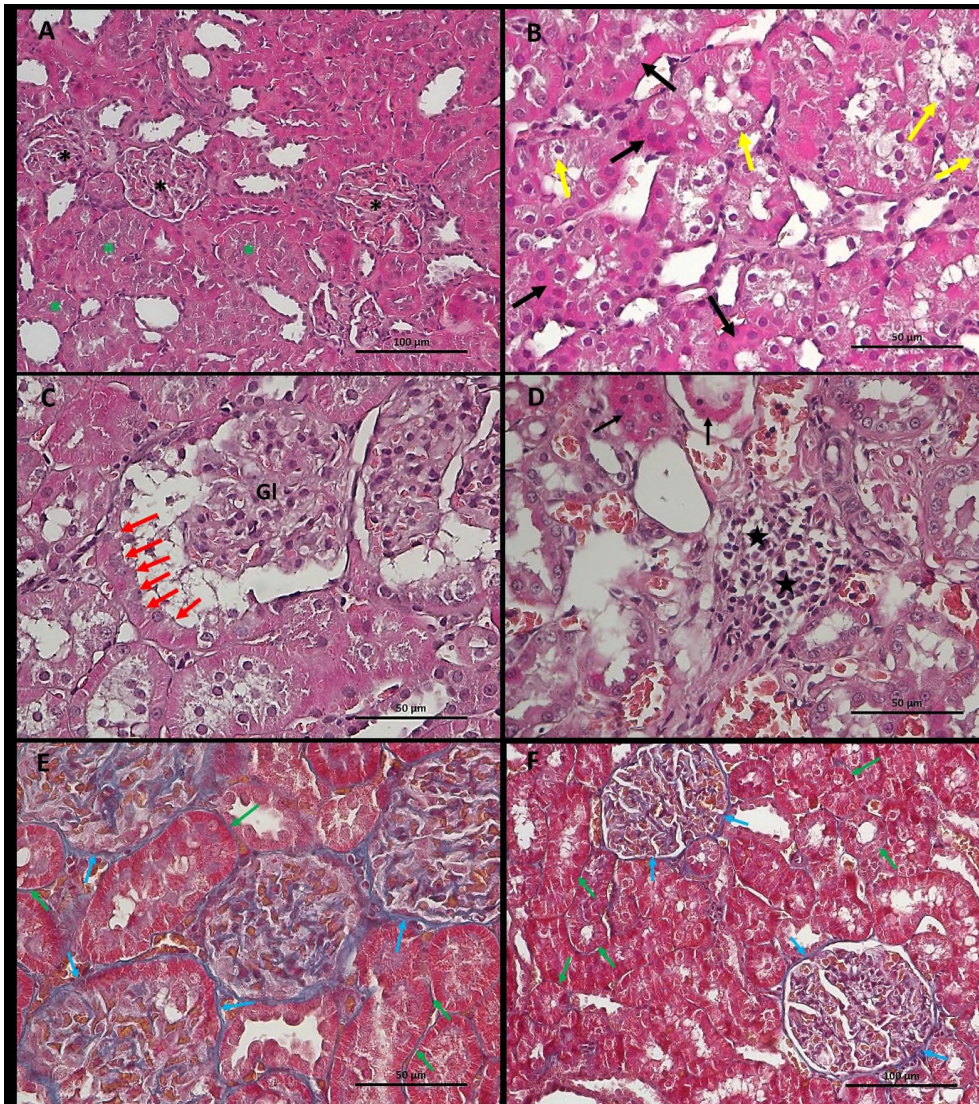
Figure 4. Histological features of the kidney sections from 10-month-old rats. Bowman spaces (marked by black asterisks), and the lumen of tubules seem contracted (marked by green asterisks). Some deeply acidophilic stained epithelial cells (black arrow) are detected within the tubular epithelium (A-D). Edema, and heterochromatin condensation (yellow arrow) are obvious within the tubular epithelial cells (B). Simple cuboidal epithelium similar to that of the proximal tubule (marked by red arrows) instead of simple squamous epithelium is detected in the parietal layer of Bowman capsule (C). Some small inflammatory cell groups (black star) are observed in the interstitial area (D). Collagen fiber mass around the Bowman capsule (blue arrow) and among tubules (green arrow) seems higher than those of the 8-month-old rats (E, F). A-D: Hematoxylin and Eosin, X20, X40, X40 and X40, respectively. E and F: Masson's trichrome, X20 and X40, respectively.

sis is triggered by signals of death, which can originate from either within the cell (intrinsic) or from external sources (extrinsic). Cellular stresses such as DNA damage, low oxygen levels, and oxidative stress stimulate the intrinsic pathway of apoptosis. These stimuli alter the cytoplasmic dynamics to promote pro-apoptotic factors, leading to the release of mitochondrial pro-apoptotic factors such as cytochrome c into the cytoplasm. Following this, the release of endonuclease G operates within the nucleus to facilitate DNA fragmentation and nuclear condensation. The initiation of apoptosis through the extrinsic pathway entails signaling via transmembrane receptors belonging to the TNF receptor family. Signaling through TNF receptor 1 leads to the activation of initiator caspase-8, ultimately re-

sulting in apoptosis.[23] Being a pleiotropic cytokine, TNF-α induces a diverse array of cellular reactions, spanning from inflammation and proliferation to programmed cell death.[24] TNF-α has been identified as capable of directly instigating two forms of cell death: apoptosis, which is dependent on caspase activity, and necroptosis, which occurs independently of caspase involvement.[25] In various cell types, the inhibition of caspases fails to prevent cell death following TNF-α stimulation but instead triggers an alternative form of cell demise known as necroptosis, characterized by cell lysis.[24,26] Necroptosis is triggered when receptor-interacting protein kinase-1 (RIPK1) binds to RIPK3, prompting its oligomerization and autophosphorylation. Subsequently, the active RIPK1/RIPK3
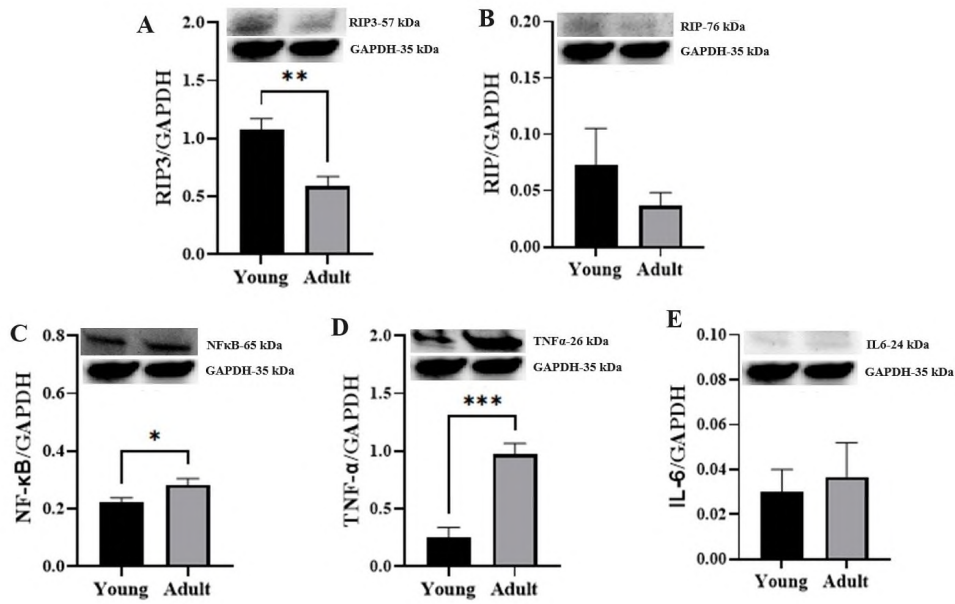
Figure 5. Semiquantitative analysis of (A) RIP3 to GAPDH, (B) RIP to GAPDH,(C) NF-κB to GAPDH, (D) TNF-α to GAPDH, and (E) IL-6 to GAPDH in the liver tissue by Western blotting for the young (n=6) and adult (n=6) animals. Representative photos belong to the samples pooled for each group. Data are presented as mean ± SEM, and * indicates for p<0.05, ** indicates for p<0.01, *** indicates for p<0.001.
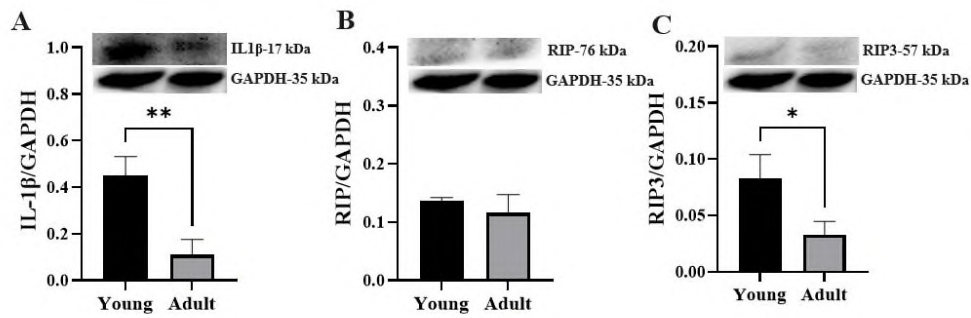
Figure 6. Semiquantitative analysis of **(A)** IL-1β to GAPDH, **(B)** RIP to GAPDH, and **(C)** RIP3 to GAPDH in the kidney tissue by Western blotting for the young (n=6) and adult (n=6) animals. Representative photos belong to the samples pooled for each group. Data are presented as mean ± SEM, and * indicates for p<0.05, ** indicates for p<0.01.
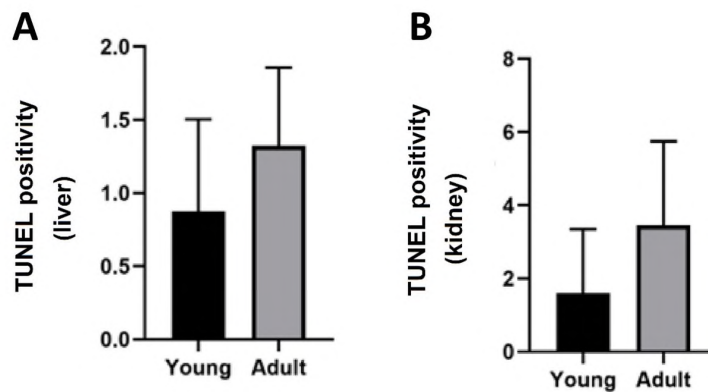
Figure 7. Expression patterns and levels of TUNEL positivity of the groups.

complex, known as the necrosome, activates the mixed lineage kinase domain-like (MLKL) pseudo-kinase protein. This activated MLKL relocates to the plasma membrane, resulting in permeabilization, rupture, and eventual death of the cell.[27-29] The binding of TNF-α to TNF receptor-1 instigates the formation of complex I, comprised of RIP1, cellular inhibitor of apoptosis proteins 1/2 [cIAP1/2], linear ubiquitin chain assembly complex [LUBAC], and inhibitor of nuclear factor-κB (IκB) kinases [IKKs]. This complex then stimulates the activation of NF-κB, leading to the induction of prosurvival genes.[30,31] Significant increases in TNF-α and NF-κB levels are consistent with the increased apoptosis rate the in liver 10-month-old rats compared to the 6-week-old rats in the current study. On the other hand, the study accumulated no signs of an aging-induced increased necroptosis rate. On the contrary, RIP3 levels in both the kidney and liver samples were significantly lower in the 10-month-old rats than in the 6-week-old rats, signifying decreased necroptosis rates. Mohammed et al. observed substantial elevations in the percentage of liver cells undergoing apoptosis and late apoptosis/necroptosis among rats over the age of 12 months.[32] Stahl et al. noted a close age-related correlation between necroptosis and liver inflammation, with both escalating notably in the latter stage of life at approximately 18 months of age, coinciding with the onset of certain age-associated pathologies in mice.[21] Marquez-Exposito et al. found no differences in gene and protein levels in the kidneys of healthy C57BL/6 mice compared to younger ones. Under the current study's experimental conditions, no age-related activation of necroptosis was observed.[22]

Apoptosis, or programmed cell death, can be both a natural and pathological process in aging rats, depending on the context and extent of the process. Apoptosis is a natural process that helps maintain tissue homeostasis by eliminating old, damaged, or unneeded cells. As rats age, there is a natural increase in the rate of apoptosis in some tissues as part of the aging process. This helps remove cells that have accumulated damage over time, which can prevent the onset of certain age-related diseases. When apoptosis occurs excessively, it can lead to the degeneration of tissues. In aging rats, this can contribute to the deterioration of vital organs and systems. In the current study slightly increased TUNEL positivity indicates aging-induced physiological apoptosis.

CONCLUSION

In conclusion, one notable finding from this study is that degenerative changes related to aging began to be seen even in 10-month-old rats. Healthy rats of this age were used as control subjects and to create experimental models. Both situations may have had the effect of unknowingly changing the results of the study. In most cases, even if researchers identify some slight histopathological or biochemical changes in the samples of control groups, these go ignored because they are considered unnatural. Because aging-related changes begin around 10 months, this study recommends researchers to use much younger rats in their studies to avoid unsubstantial results.

ORCID IDs of the author

Emine Rumeysa Hekimoglu   0000-0003-4300-7213
Mukaddes Esrefoglu   0000-0003-3380-1480
Birsen Elibol   0000-0002-9462-0862
Seda Kirmizikan   0000-0002-5652-778X

REFERENCES

1. Acosta JC, Gil J. Senescence: A new weapon for cancer therapy. *Trends Cell Biol.* 2012;22(4):211-219.

2. Coppe JP, Desprez PY, Krtolica A, Campisi J. The senescence-associated secretory phenotype: The dark side of tumor suppression. *Annu Rev Pathol.* 2010;5:99-118.

3. Childs BG, Durik M, Baker DJ, van Deursen JM. Cellular senescence in aging and age-related disease: from mechanisms to therapy. *Nat Med.* 2015;21(12):1424-1435.

4. Yuan J, Ofengeim D. A guide to cell death pathways. *Nat Rev Mol Cell Biol.* 2024;25(5):379-395.

5. Han J, Zhong CQ, Zhang DW. Programmed necrosis: Backup to and competitor with apoptosis in the immune system. *Nat Immunol.* 2011;12(12):1143-1149.

6. Sanz AB, Sanchez-Nino MD, Ramos AM, Ortiz A. Regulated cell death pathways in kidney disease. *Nat Rev Nephrol.* 2023;19(5):281-299.

7. Franceschi C, Garagnani P, Parini P, Giuliani C, Santoro A. Inflammaging: A new immune-metabolic viewpoint for age-related diseases. *Nat Rev Endocrinol.* 2018;14(10):576-590.

8. Ferrucci L, Fabbri E. Inflammageing: Chronic inflammation in ageing, cardiovascular disease, and frailty. *Nat Rev Cardiol.* 2018;15(9):505-522.

9. Hotamisligil GS. Inflammation and metabolic disorders. *Nature.* 2006;444(7121):860-867.

10. Salminen A, Kaarniranta K, Kauppinen A. Inflammaging: Disturbed interplay between autophagy and inflammasomes. *Aging-Us.* 2012;4(3):166-175.

11. Esrefoglu M, Kalkan TK, Karatas E, et al. Hepatoprotective actions of melatonin by mainly modulating oxidative status and apoptosis rate in lipopolysaccharide-induced liver damage.

Immunopharm Immunot. 2024;46(2):161-171.

12. López-Otín C, Blasco MA, Partridge L, Serrano M, Kroemer G. The hallmarks of aging. *Cell*. 2013;153(6):1194-1217.

13. Mehdizadeh M, Aguilar M, Thorin E, Ferbeyre G, Nattel S. The role of cellular senescence in cardiac disease: basic biology and clinical relevance. *Nat Rev Cardiol*. 2022;19(4):250-264.

14. Ishaq A, Tchkonia T, Kirkland JL, Siervo M, Saretzki G. Palmitate induces DNA damage and senescence in human adipocytes in vitro that can be alleviated by oleic acid but not inorganic nitrate. *Exp Gerontol*. 2022;163:111798. doi:10.1016/j.exger.2022.111798

15. Lagnado A, Leslie J, Ruchaud-Sparagano MH, et al. Neutrophils induce paracrine telomere dysfunction and senescence in ROS-dependent manner. *Embo J*. 2021;40(9):e106048. doi:10.15252/embj.2020106048

16. Palmer AK, Gustafson B, Kirkland JL, Smith U. Cellular senescence: At the nexus between ageing and diabetes. *Diabetologia*. 2019;62(10):1835-1841.

17. Miwa S, Kashyap S, Chini E, von Zglinicki T. Mitochondrial dysfunction in cell senescence and aging. *J Clin Invest*. 2022;132(13):e158447. doi:10.1172/JCI158447

18. Xu M, Pirtskhalava T, Farr JN, et al. Senolytics improve physical function and increase lifespan in old age. *Nat Med*. 2018;24(8):1246-1256.

19. Acosta JC, Banito A, Wuestefeld T, et al. A complex secretory program orchestrated by the inflammasome controls paracrine senescence. *Nat Cell Biol*. 2013;15(8):978-990.

20. Franceschi C, Campisi J. Chronic inflammation (inflammaging) and its potential contribution to age-associated diseases. *J Gerontol A Biol Sci Med Sci*. 2014;69 Suppl 1:S4-S9. doi:10.1093/gerona/glu057

21. Stahl EC, Delgado ER, Alencastro F, et al. Inflammation and ectopic fat deposition in the aging murine liver is influenced by CCR2. *Am J Pathol*. 2020;190(2):372-387.

22. Marquez-Exposito L, Tejedor-Santamaria L, Santos-Sanchez L, et al. Acute kidney injury is aggravated in aged mice by the exacerbation of proinflammatory processes. *Front Pharmacol*. 2021;12:662020. doi:10.3389/fphar.2021.662020

23. Tower J. Programmed cell death in aging. *Ageing Res Rev*. 2015;23(Pt A):90-100.

24. Walczak H. TNF and ubiquitin at the crossroads of gene activation, cell death, inflammation, and cancer. *Immunol Rev*. 2011;244:9-28.

25. Bertheloot D, Latz E, Franklin BS. Necroptosis, pyroptosis and apoptosis:An intricate game of cell death. *Cell Mol Immunol*. 2021;18(5):1106-1121.

26. Vandenabeele P, Galluzzi L, Vanden Berghe T, Kroemer G. Molecular mechanisms of necroptosis: an ordered cellular explosion. *Nat Rev Mol Cell Biol*. 2010;11(10):700-714.

27. Newton K, Manning G. Necroptosis and inflammation. *Annu Rev Biochem*. 2016;85:743-763.

28. Murphy JM, Czabotar PE, Hildebrand JM, et al. The pseudokinase MLKL mediates necroptosis via a molecular switch mechanism. *Immunity*. 2013;39(3):443-453.

29. Sun L, Wang H, Wang Z, et al. Mixed lineage kinase domain-like protein mediates necrosis signaling downstream of RIP3 kinase. *Cell*. 2012;148(1-2):213-227.

30. Silke J. The regulation of TNF signalling: What a tangled web we weave. *Curr Opin Immunol*. 2011;23(5):620-626.

31. Kanayama A, Seth RB, Sun LJ, et al. TAB2 and TAB3 activate the NF-κB pathway through binding to polyubiquitin chains. *Mol Cell*. 2004;15(4):535-548.

32. Mohammed S, Thadathil N, Selvarani R, et al. Necroptosis contributes to chronic inflammation and fibrosis in aging liver. *Aging Cell*. 2021;20(12):e13512. doi:10.1111/acel.13512

How to cite this article

REVIEW ARTICLE

From Pond Scum to Miracle Molecules: Cyanobacterial Compounds New Frontiers

Arbab Husain[1] ⓘ, Md Nematullah[2] ⓘ, Hamda Khan[3] ⓘ, Ravi Shekher[1] ⓘ, Alvina Farooqui[4] ⓘ, Archana Sahu[5] ⓘ, Afreen Khanam[1] ⓘ

[1]Mangalayatan University, Institute of Biomedical Education and Research, Department of Biotechnology and Life Sciences, Aligarh, India
[2]Integral University, Faculty of Pharmacy, Department of Pharmacy Practice, Lucknow, India
[3]Aligarh Muslim University Jawahar Lal Nehru Medical College, Department of Biochemistry, Aligarh, Uttar Pradesh, India
[4]Integral University, Faculty of Engineering, Department of Bioengineering, Lucknow, India
[5]Usha Martin University, Faculty of Health Sciences, Department of Pharmacy, Ranchi, India

ABSTRACT

Cyanobacteria are a diverse group of photosynthetic microorganisms known for their production of bioactive compounds with various biological activities. This review explores cyanobacterial bioactive compounds' current and future prospects and their roles in different fields. These compounds have great potential for pharmaceuticals, agriculture, and environmental remediation applications. Cyanobacterial bioactive compounds, such as cyanotoxins, peptides, polyketides, alkaloids, and terpenoids, exhibit remarkable properties, including antimicrobial, antifungal, antiviral, antioxidant, anti-inflammatory, and anticancer activities. Advances in genomics, metabolomics, synthetic biology, screening techniques, and bioinformatics have facilitated the identification, characterization, and manipulation of cyanobacterial compounds. The future prospects involve exploring untapped cyanobacterial diversity, integrating advanced technologies like machine learning and high-throughput screening, and sustainable production through biotechnological approaches. These efforts hold promise for discovering new bioactive compounds with unique properties and applications, contributing to the development of innovative pharmaceuticals, agricultural solutions, and environmental remedies.

Keywords: Cyanobacteria, Bioactive compounds, Pharmaceutical applications, Environmental remediation, Cyanobacterial diversity, Biotechnological approaches

INTRODUCTION

Cyanobacteria, also known as blue-green algae, are a diverse group of photosynthetic microorganisms that have gained significant attention for their ability to produce bioactive compounds with a wide range of biological activities.[1,2] These compounds hold great potential for various applications, including pharmaceuticals, agriculture, and environmental remediation. This review explores the current and future prospects of bioactive compounds derived from cyanobacteria, highlighting their promising roles in different fields. Cyanobacterial bioactive compounds exhibit remarkable properties, making them attractive candidates for drug discovery and development. They have demonstrated activities such as antimicrobial, antifungal, antiviral, antioxidant, anti-inflammatory, and anticancer properties.[3] These activities arise from cyanobacterial compounds' diverse chemical structures and functions. For example, cyanotoxins, a group of cyanobacterial bioactive compounds, have shown potential therapeutic applications in cancer treatment. Microcystins, a common cyanotoxin, have exhibited promising anticancer activity and are being investigated as potential leads for novel therapies.[4−6]

Furthermore, cyanobacteria produce a wide array of secondary metabolites, including peptides, polyketides, alkaloids, and terpenoids, which possess diverse bioactivities.[7] Cyanobacterial peptides have shown antimicrobial and anticancer activities, while cyanobacterial polyketides have demonstrated antifungal and antiviral properties. Cyanobacterial alkaloids and terpenoids have also shown potential as pharmaceutical leads and have garnered attention in drug discovery efforts.[8−10]

The current prospects of cyanobacterial bioactive compounds are promising due to advancements in various scientific disciplines. Genomics and metabolomics have facilitated the identification and characterizing of novel cyanobacterial compounds, providing valuable insights into their biosynthetic pathways and

regulatory mechanisms.[11] Synthetic biology approaches enable the manipulation of biosynthetic pathways, producing bioactive compounds with improved properties and yields. Additionally, innovative screening techniques and bioinformatics tools have enabled the efficient identification and isolation of novel compounds from cyanobacteria.[12,13]

Looking ahead, the future prospects of cyanobacterial bioactive compounds are exciting. Continued exploration of untapped cyanobacterial diversity holds promise for discovering new bioactive compounds with unique properties and applications.[14] Moreover, the sustainable production and scaling-up of cyanobacterial bioactive compounds through the integration of advanced technologies, such as machine learning and high-throughput screening, can accelerate the discovery and characterization of cyanobacterial compounds. Biotechnological approaches offer tremendous potential for meeting the increasing demand for natural products.[15]

In conclusion, cyanobacteria are valuable sources of bioactive compounds with diverse properties and applications.[16] The current advancements in genomics, metabolomics, synthetic biology, and screening techniques have paved the way for discovering and developing novel bioactive compounds from cyanobacteria.[17] The prospects involve the continued exploration of cyanobacterial diversity, the application of advanced technologies, and the sustainable production of bioactive compounds. These efforts will undoubtedly contribute to developing innovative pharmaceuticals, agricultural solutions, and environmental remedies.

CYANOBACTERIA

Cyanobacteria, a group of prokaryotic microorganisms also known as blue-green algae, are characterized by their ability to carry out oxygenic photosynthesis.[18] They play crucial ecological roles in various environments, including freshwater, marine ecosystems, and terrestrial habitats. Cyanobacteria have distinctive cellular structures, such as thylakoids, where photosynthetic pigments like chlorophyll-a, phycocyanin, and phycoerythrin are localized.[19]

The morphological diversity of cyanobacteria encompasses unicellular, filamentous, and colonial forms, which exhibit a range of adaptations to different ecological niches.[20] Some cyanobacteria can fix atmospheric nitrogen through specialized structures called heterocysts, allowing them to contribute to nitrogen availability in ecosystems.[21]

Cyanobacteria have gained significant attention for their production of bioactive compounds, which have diverse chemical structures and biological activities. These compounds exhibit antimicrobial, antiviral, antitumor, and antioxidant properties. For instance, cyanopeptides derived from cyanobacteria have shown promising antimicrobial and cytotoxic activities.[22−25]

Ongoing research on cyanobacteria focuses on understanding the genetic and metabolic mechanisms underlying their unique characteristics and bioactive compound production.[26] This knowledge holds potential for various applications in biotechnology, environmental remediation, and pharmaceutical development.[27] Cyanobacteria are photosynthetic prokaryotes that occupy diverse ecological niches and contribute significantly to global primary production. Their intricate cellular structures and metabolic capabilities enable them to thrive in various environments. Furthermore, their ability to produce bioactive compounds with valuable biological activities makes them a subject of interest for both ecological and biotechnological research (Figure 1).[28]

Secondary Metabolites of Cyanobacteria

Secondary metabolites produced by cyanobacteria are a diverse group of compounds that possess a wide range of properties and biological activities. These metabolites include peptides, polyketides, alkaloids, terpenoids, and other specialized molecules.[28]

Cyanobacterial Peptides

Cyanobacterial peptides are a diverse group of secondary metabolites produced by cyanobacteria. They exhibit various properties and activities, including antimicrobial, antiviral, and anticancer effects.[8,29] For example, microcystins, a class of cyanobacterial peptides, have been found to possess potent hepatotoxic and anticancer properties.[30,31]

Another example is cyanopeptolin, a peptide isolated from cyanobacteria, which has shown significant antimicrobial activity against various pathogens.[30]

Cyanobacterial Polyketides

Cyanobacterial polyketides are complex organic compounds produced through polyketide synthase pathways in cyanobacteria.[8] These metabolites exhibit diverse biological activities, including antimicrobial, antiviral, and cytotoxic effects. An example is jamaicamide, a polyketide produced by *Lyngbya majuscula*, which has displayed potent cytotoxicity against cancer cells.[32] Another noteworthy cyanobacterial polyketide is cryptophycin, which exhibits full antiproliferative activity against various cancer cell lines.[33]

Cyanobacterial Alkaloids

Cyanobacterial alkaloids are nitrogen-containing secondary metabolites produced by cyanobacteria.[34] They possess diverse biological properties, including cytotoxic, neurotoxic, and antifungal activities. Anatoxin-a, an alkaloid produced by several cyanobacterial species, is a potent neurotoxin.[35,36] Another well-known cyanobacterial alkaloid is saxitoxin, which exhibits full neurotoxic and paralytic effects.[37]
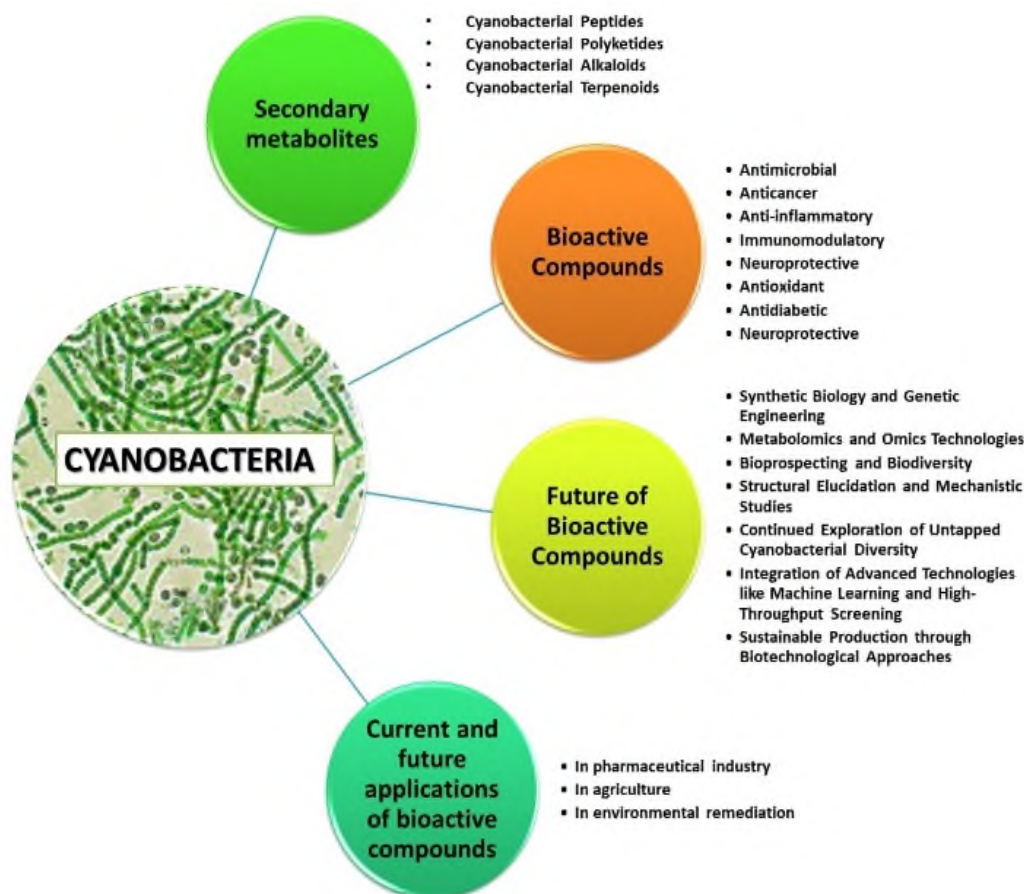
Figure 1. Bioactive compounds, future potential and diverse applications of Cyanobacteria.

Cyanobacterial Terpenoids

Cyanobacterial terpenoids are a diverse group of secondary metabolites with a terpenoid backbone produced by cyanobacteria. These compounds exhibit various biological activities, including antimicrobial, antiviral, and antifungal effects. For instance, nostocyclin, a terpenoid produced by *Nostoc* species, has demonstrated potent antimicrobial activity against various pathogens.[38] Another example is cryptosporioptide, a terpenoid derived from the cyanobacterium *Cryptosporiopsis* sp., which exhibits antifungal activity.[39]

Cyanobacteria and Its Bioactive Compounds

Microcystins

Microcystins are cyclic heptapeptides produced by various cyanobacteria, including species from the genera *Microcystis, Anabaena*, and *Planktothrix*. They are well-known for their hepatotoxicity and tumor-promoting properties. Microcystins inhibit protein phosphatases, disrupting cellular signaling pathways and causing liver damage.[40]

Cyanopeptides

Cyanopeptides are a diverse group of peptides produced by cyanobacteria, exhibiting a wide range of biological activities. These compounds possess antimicrobial, antiviral, cytotoxic, and immunosuppressive properties. They are of interest for their potential therapeutic applications.[31]

Anabaenopeptins

Anabaenopeptins are cyclic peptides predominantly produced by species of the cyanobacterial genus *Anabaena*. These compounds display a broad spectrum of bioactivities, including antimicrobial, antifungal, antiviral, and antitumor properties. They are considered promising candidates for drug development.[41]

Aeruginosins

Aeruginosins are a class of bioactive peptides produced by certain cyanobacteria, such as *Microcystis aeruginosa* and *Planktothrix spp*. These compounds exhibit diverse activities, including neurotoxicity, antiproliferative effects, and antibacterial properties.[31]

Lyngbyatoxins

Lyngbyatoxins are complex secondary metabolites produced by cyanobacteria, particularly from the genus *Lyngbya*. These compounds possess cytotoxic, neurotoxic, antifungal, and antimicrobial activities. They are of interest for their potential biomedical applications.[42]

Nodularins

Nodularins are cyclic peptides produced by certain cyanobacteria, including *Nodularia spumigena*. These compounds are known for their hepatotoxicity and tumor-promoting effects. Nodularins inhibit protein phosphatases, disrupting cellular signaling and leading to liver damage.[43]

Phycocyanin

Phycocyanin is a blue pigment and a significant component of the light-harvesting phycobiliprotein complex in cyanobacteria and algae. It is an accessory pigment for photosynthesis and exhibits antioxidant, anti-inflammatory, and immunomodulatory properties. Phycocyanin is of interest for various biotechnological and medicinal applications.[2,44]

Scytonemin

Scytonemin is a UV-absorbing pigment synthesized by certain cyanobacteria as a protective mechanism against high-intensity UV radiation. It exhibits strong photoprotective and antioxidant activities, making it of interest for applications in sunscreen formulations and photoprotection.[45]

Patellamides

Patellamides are cyclic peptides isolated from cyanobacteria, particularly from the genus *Prochloron*. These compounds exhibit potent cytotoxic and antimicrobial activities. They have attracted attention as potential drug candidates and are valuable tools for chemical biology studies.[46]

Geosmin

Geosmin is a volatile organic compound produced by various cyanobacteria and other microorganisms. It is responsible for the characteristic earthy odor associated with some bodies of water. Geosmin is also interested in biotechnology due to its potential use in the flavor and fragrance industries.[47]

Cylindrospermopsin

Cylindrospermopsin is a potent toxin produced by certain cyanobacteria, including species of the genus *Cylindrospermopsis*. It exhibits hepatotoxicity and has been implicated in animal and human poisonings. Cylindrospermopsin inhibits protein synthesis and affects cellular functions.[48,49]

General Properties of Bioactive Compounds in Cyanobacteria

Cyanobacteria, also known as blue-green algae, are photosynthetic microorganisms that produce a wide array of bioactive compounds with diverse properties and applications. These bioactive compounds have attracted significant attention due to their potential therapeutic, pharmaceutical, and industrial value. This article provides a comprehensive overview of the general properties of bioactive compounds found in cyanobacteria, supported by relevant citations.

Chemical Diversity

Bioactive compounds derived from cyanobacteria exhibit remarkable chemical diversity. They encompass a wide range of chemical classes, including peptides, alkaloids, polyketides, lipids, terpenoids, and pigments. This diverse array of chemical structures contributes to the broad spectrum of biological activities displayed by cyanobacterial bioactive compounds.[50–53]

Biological Activities

Cyanobacterial bioactive compounds possess various biological activities, making them valuable for numerous applications. They exhibit antimicrobial, antiviral, antifungal, anticancer, antiparasitic, anti-inflammatory, antioxidant, neuroprotective, and immunomodulatory properties.[54–57] These activities stem from the interaction of cyanobacterial compounds with specific targets, such as enzymes, receptors, and signaling pathways, in various biological systems.

Ecological Roles

Bioactive compounds in cyanobacteria play important ecological roles, contributing to their survival and competitive advantage in natural environments. Some compounds function as allelochemicals, enabling cyanobacteria to inhibit the growth of competing microorganisms and establish dominance.[58] Additionally, cyanobacterial compounds can act as signaling molecules, mediating cell-cell communication and physiological responses within cyanobacterial populations.[59]

Biosynthetic Pathways

The biosynthesis of cyanobacterial bioactive compounds involves complex enzymatic pathways. Biosynthetic gene clusters responsible for producing these compounds have been identified in cyanobacterial genomes through genomic analysis and comparative genomics. Understanding the biosynthetic pathways and regulatory mechanisms governing the production of bioactive compounds is crucial for their manipulation and optimization in biotechnological applications.[12]

Structural Elucidation

Structural elucidation of cyanobacterial bioactive compounds is critical in their characterization and understanding of their activity. Advanced analytical techniques such as mass spectrometry, nuclear magnetic resonance spectroscopy, and X-ray crystallography are employed to determine their chemical structures.[60] The elucidation of the structural features facilitates the development of structure-activity relationships and aids in designing analogs with improved properties.

Biotechnological Applications

Bioactive compounds from cyanobacteria have significant potential for various biotechnological applications. They can be explored for developing new drugs, pharmaceutical leads, nutraceuticals, cosmeceuticals, and agrochemicals.[61,62] Furthermore, cyanobacterial compounds have shown promise as sources of natural dyes, biofuels, and biosurfactants.[63,64] These applications highlight the importance of cyanobacterial bioactive compounds in various industries.

Bioactive compounds derived from cyanobacteria exhibit chemical diversity and possess a wide range of biological activities. Their ecological roles, biosynthetic pathways, structural elucidation, and potential biotechnological applications make them subjects of significant research interest. Further exploration of cyanobacterial bioactive compounds holds tremendous potential for the discovery of novel therapeutics, industrial applications, and sustainable solutions (Table 1).[29,31,41,42,65-71]

CURRENT RESEARCH ON BIOACTIVE COMPOUNDS OF CYANOBACTERIA

Cyanobacteria, commonly known as blue-green algae, are photosynthetic microorganisms that have gained significant attention for their production of bioactive compounds with diverse therapeutic properties. Current research in this field has focused on exploring these cyanobacterial compounds' bioactivity and potential applications. This article provides an overview of the recent research on bioactive compounds derived from cyanobacteria, highlighting their various biological activities, supported by relevant citations.

Antimicrobial Activity

Cyanobacterial bioactive compounds have shown significant antimicrobial activity against a range of pathogenic microorganisms.[72] For instance, it was demonstrated the antimicrobial potential of *Oscillatoria sancta* extracts against multidrug-resistant bacteria, including *Staphylococcus aureus* and *Escherichia coli*. Another study reported the antibacterial activity of a cyanobacterium, *Nostoc muscorum*, against clinically important human pathogens. These findings indicate the potential of cyanobacterial compounds as natural antimicrobial agents.[73,74]

Anticancer Effects

The bioactive compounds derived from cyanobacteria have exhibited promising anticancer effects. Research conducted by Jaki et al. demonstrated the cytotoxic activity of Nostoc commune extracts against human breast cancer cells.[75] Similarly, a study by Akbarizare et al. identified a cyanobacterial metabolite, largamides, which exhibited potent anticancer activity against colorectal cancer cells.[76] These studies highlight the potential of cyanobacterial compounds as a source of novel anticancer agents.

Anti-inflammatory and Immunomodulatory Properties

Cyanobacterial compounds have also shown significant anti-inflammatory and immunomodulatory properties. A study investigated the anti-inflammatory potential of *Phormidium persicinum* extracts and found them to inhibit the production of pro-inflammatory cytokines.[77] Furthermore, research demonstrated the immunomodulatory effects of a cyanobacterium, *Spirulina platensis*, which enhanced the activity of immune cells. These findings suggest the therapeutic potential of cyanobacterial compounds in inflammation-related disorders and immune modulation.[78]

Neuroprotective Effects

Current research has focused on exploring the neuroprotective effects of cyanobacterial bioactive compounds. A study investigated the neuroprotective activity of *Nostoc muscorum* extracts and demonstrated their ability to protect neuronal cells from oxidative stress-induced damage.[79] Similarly, cyanobacterial peptides, such as anabaenopeptins, have shown neuroprotective effects against amyloid-beta-induced neurotoxicity.[80] These studies suggest the potential of cyanobacterial compounds in developing neuroprotective therapies.

Antioxidant and Antidiabetic Properties

Cyanobacterial compounds have been investigated for their antioxidant and antidiabetic properties. Previous research by revealed the antioxidant activity of cyanobacterial extracts from *Microcystis aeruginosa*, which demonstrated free radical scavenging effects.[1,31] Additionally, a study by Kaushik et al. reported the antidiabetic potential of cyanobacterial bioactive compounds, as they showed inhibitory effects on critical enzymes involved in glucose metabolism.[81] These findings support the exploration of cyanobacterial compounds as potential antioxidants and antidiabetic agents.[81,82]

Current research on bioactive compounds derived from

Table 1. Bioactive compounds derived from cyanobacteria and their properties.

Bioactive Compound	Properties	References
Microcystins	Hepatotoxic, tumor-promoting, protein phosphatase inhibition	65
Cyanopeptides	Antimicrobial, antiviral, cytotoxic, immunosuppressive	31
Anabaenopeptins	Antimicrobial, antifungal, antiviral, antitumor	41
Aeruginosins	Neurotoxic, antiproliferative, antibacterial	29
Lyngbyatoxins	Cytotoxic, neurotoxic, antifungal, antimicrobial	42
Nodularins	Hepatotoxic, tumor-promoting, protein phosphatase inhibition	66
Phycocyanin	Antioxidant, anti-inflammatory, immunomodulatory	67
Scytonemin	UV-protective, antioxidant, antimicrobial	68
Patellamides	Antimicrobial, antifungal, cytotoxic, antiparasitic	69
Geosmin	Earthy odor, involved in cyanobacterial bloom formation	70
Cylindrospermopsin	Hepatotoxic, genotoxic, carcinogenic	71

cyanobacteria has highlighted their diverse therapeutic potential, including antimicrobial, anticancer, anti-inflammatory, neuroprotective, antioxidant, and antidiabetic activities. These findings underscore the importance of further exploration and investigation of cyanobacterial compounds for developing novel drugs and therapeutic interventions.

Neuroprotective Properties

Neurodegenerative diseases, such as Alzheimer's, Parkinson's, and Huntington's disease, present an increasing global health challenge due to the aging population. Despite intensive research, effective treatments for these devastating conditions remain elusive. In recent years, there has been growing interest in exploring natural compounds, and cyanobacteria have emerged as a promising source of bioactive molecules with potential neuroprotective properties.[83,84]

Several bioactive compounds derived from cyanobacteria have been investigated for their neuroprotective properties. For example, β-N-methylamino-l-alanine (BMAA), originally isolated from cyanobacteria, has been linked to neurotoxicity and implicated in neurodegenerative diseases such as amyotrophic lateral sclerosis and Alzheimer's disease.[85,86] However, research on BMAA's precise role in neurodegeneration is ongoing, and its potential therapeutic applications are yet to be fully elucidated. In addition to BMAA, other cyanobacterial compounds, such as anatoxin-a, have shown a potential to modulate neural pathways and reduce neuroinflammation, factors involved in the progression of neurodegenerative diseases.[87]

FUTURE OF BIOACTIVE COMPOUNDS OF CYANOBACTERIA

Bioactive compounds derived from cyanobacteria have shown immense potential in various therapeutic applications, ranging from antimicrobial and anticancer activities to neuroprotective and immunomodulatory effects. As research in this field continues to advance, the future of bioactive compounds of cyanobacteria holds great promise for drug discovery and development.

Synthetic Biology and Genetic Engineering

Advancements in synthetic biology and genetic engineering techniques offer exciting prospects for the future of cyanobacterial bioactive compounds. By manipulating the genetic makeup of cyanobacteria, researchers can enhance the production of specific bioactive compounds or engineer new compounds with improved properties. For example, genetic modifications in cyanobacteria have successfully increased the production of bioactive peptides and pigments.[88] Such approaches hold the potential for the sustainable and efficient production of bioactive compounds with enhanced therapeutic properties.

Metabolomics and Omics Technologies

Metabolomics and omics technologies enable comprehensive profiling and analysis of cyanobacterial metabolites, facilitating the discovery of novel bioactive compounds. Researchers

can identify and characterize previously unknown cyanobacterial metabolites by employing mass spectrometry, nuclear magnetic resonance, and other analytical techniques.[89] Additionally, omics approaches, such as genomics, transcriptomics, and proteomics, provide insights into cyanobacteria's biosynthetic pathways and regulatory mechanisms of bioactive compound production.[90] These technologies pave the way for discovering new bioactive compounds and optimizing production processes.[11]

Bioprospecting and Biodiversity

Cyanobacteria represent a vast and diverse group of organisms, offering untapped potential for discovering bioactive compounds. Exploring various cyanobacterial strains from different habitats can lead to identifying unique and potent bioactive compounds. Bioprospecting expeditions targeting unexplored environments, such as marine ecosystems and extreme environments, may yield valuable cyanobacterial species with novel bioactive compounds.[91,92] Furthermore, integrating culture-dependent and culture-independent approaches, along with high-throughput screening methods, can expedite the discovery of bioactive compounds from cyanobacteria.[93–95]

Structural Elucidation and Mechanistic Studies

To fully understand the potential of cyanobacterial bioactive compounds, extensive structural elucidation, and mechanistic studies are crucial. Advanced spectroscopic techniques, such as nuclear magnetic resonance spectroscopy and X-ray crystallography, enable the determination of the three-dimensional structures of bioactive compounds, providing insights into their interactions with targets and mechanisms of action. Elucidating the structure-activity relationships of cyanobacterial compounds will guide the design and optimization of novel therapeutic agents.[60,96]

Continued Exploration of Untapped Cyanobacterial Diversity

As a diverse group of microorganisms, cyanobacteria offer immense potential for discovering bioactive compounds. The future prospects of bioactive compounds derived from cyanobacteria rely on the continued exploration of untapped cyanobacterial diversity. By conducting extensive sampling and characterization efforts, researchers can uncover novel cyanobacterial species and strains that may harbor unique bioactive compounds.[97,98] These untapped resources hold the potential for discovering compounds with previously unknown biological activities and therapeutic applications.[99]

Integration of Advanced Technologies Like Machine Learning and High-Throughput Screening

The integration of advanced technologies such as machine learning, artificial intelligence, and high-throughput screening can revolutionize the discovery and development of cyanobacterial bioactive compounds. Machine learning algorithms can analyze vast datasets, identify patterns, and predict potential bioactivities.[100,101] This approach accelerates the screening process, enabling researchers to prioritize compounds with the highest likelihood of exhibiting desired biological properties. High-throughput screening allows for the rapid testing of large compound libraries, facilitating the identification of bioactive molecules efficiently.[91,102] By combining these advanced technologies, researchers can streamline the discovery and optimization of cyanobacterial bioactive compounds.

Sustainable Production through Biotechnological Approaches

Sustainable production methods are crucial for cyanobacterial bioactive compounds' future viability and scalability. Biotechnological approaches offer promising solutions in this regard. Techniques such as synthetic biology, metabolic engineering, and cultivation optimization can enhance the production of desired compounds.[103] By modifying cyanobacterial metabolic pathways, researchers can increase the yield and purity of target compounds. Cultivation optimization strategies, including nutrient optimization, light modulation, and bioreactor design, contribute to higher productivity and efficiency while minimizing environmental impacts.[104] These biotechnological approaches enable sustainable and cost-effective production of cyanobacterial bioactive compounds, facilitating their translation into practical applications.

CURRENT AND FUTURE APPLICATIONS OF BIOACTIVE COMPOUNDS OF CYANOBACTERIA IN PHARMACEUTICALS, AGRICULTURE, AND ENVIRONMENTAL REMEDIATION

Cyanobacterial bioactive compounds have diverse applications in pharmaceuticals, agriculture, and environmental remediation. These compounds exhibit a wide range of biological activities and have the potential to address various challenges in these fields.

A. In the pharmaceutical industry, bioactive compounds derived from cyanobacteria have shown significant potential for drug discovery and development. They have demonstrated activities such as antimicrobial, antifungal, antiviral, antioxidant, anti-inflammatory, and anticancer properties.[105] Cyanotoxins, a group of cyanobacterial bioactive compounds, have garnered attention for their potential therapeutic applications in cancer treatment.[106] For example, microcystins, a common cyanotoxin, have exhibited promising anticancer activity and are being investigated as potential leads for novel therapies.[107]

B. In agriculture, the bioactive compounds of cyanobacteria offer opportunities for sustainable crop protection and enhancement. They have demonstrated activity against plant

pathogens and pests, making them potential alternatives to synthetic pesticides.[108] Cyanobacterial compounds, including cyanotoxins, have also been explored for their allelopathic effects, which can contribute to weed control and crop protection. Furthermore, cyanobacterial biofertilizers show promise in improving nutrient availability and enhancing crop growth.[109]

C. Cyanobacterial bioactive compounds also play a role in environmental remediation. They have been studied for their potential in water and soil treatment. Cyanobacterial peptides, for instance, exhibit inhibitory effects on harmful bacteria in water sources, contributing to the control of waterborne diseases.[110] Moreover, the metal-binding and detoxification capabilities of cyanobacterial compounds have implications for the removal of heavy metals and pollutants from the environment.[111]

Looking ahead, the future applications of cyanobacterial bioactive compounds are promising. Continued exploration of cyanobacterial diversity and technological advancements will likely expand their range of applications. Integrating advanced techniques such as genomics, metabolomics, and synthetic biology can further enhance the discovery and development of novel compounds with improved properties.[112] Additionally, the sustainable production and scaling-up of cyanobacterial bioactive compounds through biotechnological approaches offer tremendous potential for meeting the increasing demand for natural products.[113]

CONCLUSION

In conclusion, cyanobacteria are valuable sources of bioactive compounds with diverse properties and applications. The current advancements in genomics, metabolomics, synthetic biology, and screening techniques have paved the way for discovering and developing novel bioactive compounds from cyanobacteria. The future prospects involve the continued exploration of cyanobacterial diversity, the application of advanced technologies, and the sustainable production of bioactive compounds. These efforts will undoubtedly contribute to developing innovative pharmaceuticals, agricultural solutions, and environmental remedies. Harnessing the potential of cyanobacteria and their bioactive compounds will offer new avenues for drug discovery and provide sustainable and eco-friendly solutions to various challenges in medicine, agriculture, and the environment. Therefore, further research and investment in this field are crucial to unlock the full potential of cyanobacterial bioactive compounds for the benefit of society.

ORCID IDs of the authors

Arbab Husain	0000-0002-9487-9284
Md Nematullah	0000-0002-5935-6699
Hamda Khan	0000-0003-2448-9878
Ravi Shekher	0000-0001-5984-0678
Alvina Farooqui	0000-0002-7260-0414
Archana Sahu	0000-0002-6526-2402
Afreen Khanam	0000-0002-5380-1667

REFERENCES

1. Husain A, Alouffi S, Khanam A, et al. Non-inhibitory effects of the potent antioxidant C-phycocyanin from Plectonema sp. on the *in vitro* glycation reaction. *Rev Rom Med Lab*. 2022;30(2):199-213.

2. Husain A, Alouffi S, Khanam A, Akasha R, Farooqui A, Ahmad S. Therapeutic efficacy of natural product 'c-phycocyanin' in alleviating streptozotocin-induced diabetes via the inhibition of glycation reaction in rats. *Int J Mol Sci*. 2022;23(22):14235. doi:10.3390/ijms232214235

3. Husain A, Farooqui A, Khanam A, et al. Physicochemical characterization of C-phycocyanin from *Plectonema* sp. and elucidation of its bioactive potential through in silico approach. *Cell Mol Biol*. 2022;67(4):68-82.

4. Rajneesh, Singh SP, Pathak J, Sinha RP. Cyanobacterial factories for the production of green energy and value-added products: An integrated approach for economic viability. *Renew Sustain Energy Rev*. 2017;69:578-595.

5. Khanam A, Ahmad S, Husain A. A Perspective on the impact of advanced glycation end products in the progression of diabetic nephropathy. *Curr Protein Pept Sci*. 2022;24(1):2-6.

6. Khanam A, Kavita K, Sharma RK, et al. *In-silico* exploration of cyanobacterial bioactive compounds for managing diabetes: Targeting alpha-amylase and beta-glucosidase. *Intell Pharm*. 2023;1(4):232-243.

7. Choudhary A, Naughton LM, Montánchez I, Dobson ADW, Rai DK. Current status and future prospects of marine natural products (MNPs) as antimicrobials. *Mar Drugs*. 2017;15(9):272. doi:10.3390/md15090272

8. Nandagopal P, Steven AN, Chan LW, Rahmat Z, Jamaluddin H, Mohd Noh NI. Bioactive metabolites produced by cyanobacteria for growth adaptation and their pharmacological properties. *Biology (Basel)*. 2021;10(10):1061. doi:10.3390/biology10101061

9. Alouffi S, Khanam A, Husain A, Akasha R, Rabbani G, Ahmad S. D-ribose-mediated glycation of fibrinogen: Role in the induction of adaptive immune response. *Chem Biol Interact*. 2022;367:110147. doi:10.1016/j.cbi.2022.110147

10. Khanam A, Alouffi S, Alyahyawi AR, et al. Generation of autoantibodies against glycated fibrinogen: Role in diabetic nephropathy and retinopathy. *Anal Biochem*. 2023;685:115393. doi:10.1016/j.ab.2023.115393

11. Lauritano C, Ferrante MI, Rogato A. Marine natural products from microalgae: An -omics overview. *Mar Drugs*. 2019;17(5):269. doi:10.3390/md17050269

12. Alam K, Hao J, Zhang Y, Li A. Synthetic biology-inspired strategies and tools for engineering of microbial natural product biosynthetic pathways. *Biotechnol Adv*. 2021;49:107759. doi:10.1016/J.BIOTECHADV.2021.107759

13. Khanam A, Alouffi S, Rehman S, Ansari IA, Shahab U, Ahmad S. An *in vitro* approach to unveil the structural alterations in d-ribose induced glycated fibrinogen. *J Biomol Struct Dyn*. 2021;39(14):5209-5223.

14. Majolo F, de Oliveira Becker Delwing LK, Marmitt DJ, Bustamante-Filho IC, Goettert MI. Medicinal plants and bioactive natural compounds for cancer treatment: Important advances for drug discovery. *Phytochem Lett*. 2019;31:196-207.

15. Li JWH, Vederas JC. Drug discovery and natural products: End of an era or an endless frontier? *Science*. 2009;325(5937):161-165.

16. Raja R, Hemaiswarya S, Ganesan V, Carvalho IS. Recent developments in therapeutic applications of Cyanobacteria. *Crit Rev Microbiol*. 2016;42(3):394-405.

17. Gulder TA, Moore BS. Chasing the treasures of the sea — bacterial marine natural products. *Curr Opin Microbiol*. 2009;12(3):252-260.

18. Saad A, Atia A. Review on freshwater blue-green algae (Cyanobacteria): Occurrence, classification and toxicology. *Biosci Biotechnol Res ASIA*. 2014;11(3):1319-1325.

19. Madhyastha HK, Vatsala TM. Pigment production in *Spirulina fussiformis* in different photophysical conditions. *Biomol Eng*. 2007;24(3):301-305.

20. Sánchez-Baracaldo P, Bianchini G, Di Cesare A, Callieri C, Chrismas NAM. Insights into the evolution of Picocyanobacteria and Phycoerythrin genes (mpeBA and cpeBA). *Front Microbiol*. 2019;10(JAN):45. doi:10.3389/fmicb.2019.00045

21. Di Rienzi SC, Sharon I, Wrighton KC, et al. The human gut and groundwater harbor non-photosynthetic bacteria belonging to a new candidate phylum sibling to Cyanobacteria. *Elife*. 2013;2:e01102. doi:10.7554/elife.01102

22. Altaf MM, Ahmad Khan MS, Ahmad I. Diversity of bioactive compounds and their therapeutic potential. *New Look to Phytomedicine Adv Herb Prod as Nov Drug Leads*. 2018:15-34.

23. Khalifa SAM, Elias N, Farag MA, et al. Marine natural products: A source of novel anticancer drugs. *Mar Drugs*. 2019;17(9):491. doi:10.3390/md17090491

24. Pandey VD. Cyanobacterial natural products as antimicrobial agents. *IntJ Curr Microbiol App Sci*. 2015;4(1):310-317.

25. Plaza M, Herrero M, Alejandro Cifuentes A, Ibáñez E. Innovative natural functional ingredients from microalgae. *J Agric Food Chem*. 2009;57(16):7159-7170.

26. Kleigrewe K, Gerwick L, Sherman DH, Gerwick WH. Unique marine derived cyanobacterial biosynthetic genes for chemical diversity. *Nat Prod Rep*. 2016;33(2):348-364.

27. Zahra Z, Choo DH, Lee H, Parveen A. Cyanobacteria: Review of current potentials and applications. *Environ*. 2020;7(2):13. doi:10.3390/ENVIRONMENTS7020013

28. Coates RC, Trentacoste E, Gerwick WH. Bioactive and novel chemicals from microalgae. *Handb Microalgal Cult Appl Phycol Biotechnol Second Ed*., 2013:504-531. doi:10.1002/9781118567166.CH26

29. Tikhonova I, Kuzmin A, Deeva D, et al. Cyanobacteria *Nostoc punctiforme* from abyssal benthos of Lake Baikal: Unique ecology and metabolic potential. *Indian J Microbiol*. 2017;57(4):422-426.

30. Fidor A, Konkel R, Mazur-Marzec H. Bioactive peptides produced by Cyanobacteria of the genus *Nostoc*: A Review. *Mar Drugs*. 2019;17(10):561. doi:10.3390/md17100561

31. Isaacs JD, Strangman WK, Barbera AE, Mallin MA, McIver MR, Wright JLC. Microcystins and two new micropeptin cyanopeptides produced by unprecedented *Microcystis aeruginosa* blooms in North Carolina's Cape Fear River. *Harmful Algae*. 2014;31:82-86.

32. Edwards DJ, Marquez BL, Nogle LM, et al. Structure and biosynthesis of the Jamaicamides, new mixed polyketide-peptide neurotoxins from the marine cyanobacterium *Lyngbya majuscula*. *Chem Biol*. 2004;11(6):817-833.

33. hih C, Teicher B. Cryptophycins: A Novel class of potent antimitotic antitumor depsipeptides. *Curr Pharm Des*. 2005;7(13):1259-1276.

34. Tan LT. Bioactive natural products from marine cyanobacteria for drug discovery. *Phytochemistry*. 2007;68(7):954-979.

35. Colas S, Marie B, Lance E, Quiblier C, Tricoire-Leignel H, Mattei C. Anatoxin-a: Overview on a harmful cyanobacterial neurotoxin from the environmental scale to the molecular target. *Environ Res*. 2021;193:110590. doi:10.1016/J.ENVRES.2020.110590

36. Osswald J, Rellán S, Gago A, Vasconcelos V. Toxicology and detection methods of the alkaloid neurotoxin produced by cyanobacteria, anatoxin-a. *Environ Int*. 2007;33(8):1070-1089.

37. Aráoz R, Vilariño N, Botana LM, Molgó J. Ligand-binding assays for cyanobacterial neurotoxins targeting cholinergic receptors. *Anal Bioanal Chem*. 2010;397(5):1695-1704.

38. Swain SS, Paidesetty SK, Padhy RN. Antibacterial, antifungal and antimycobacterial compounds from cyanobacteria. *Biomed Pharmacother*. 2017;90:760-776.

39. Abdel-Razek AS, El-Naggar ME, Allam A, Morsy OM, Othman SI. Microbial natural products in drug discovery. *Process*. 2020;8(4):470. doi:10.3390/PR8040470

40. Scoglio S. Microcystins in water and in microalgae: Do microcystins as microalgae contaminants warrant the current public alarm? *Toxicol Reports*. 2018;5:785-792.

41. Harms H, Kurita KL, Pan L, et al. Discovery of anabaenopeptin 679 from freshwater algal bloom material: Insights into the structure–activity relationship of anabaenopeptin protease inhibitors. *Bioorganic Med Chem Lett*. 2016;26(20):4960-4965.

42. Catherine Q, Susanna W, Isidora ES, Mark H, Aurélie V, Jean-François H. A review of current knowledge on toxic benthic freshwater cyanobacteria- Ecology, toxin production and risk management. *Water Res*. 2013;47(15):5464-5479.

43. Nowruzi B, Blanco S, Nejadsattari T. Chemical and molecular evidences for the poisoning of a duck by anatoxin-a, nodularin and cryptophycin at the coast of lake Shoormast (Mazandaran province, Iran). *Algologia*. 2018;28(4):409-427.

44. De Morais MG, Da Fontoura Prates D, Moreira JB, Duarte JH, Costa JAV. Phycocyanin from microalgae: Properties, extraction and purification, with some recent applications. *Ind Biotechnol*. 2018;14(1):30-37.

45. Stevenson CS, Capper EA, Roshak AK, et al. Scytonemin-A ma-

rine natural product inhibitor of kinases key in hyperproliferative inflammatory diseases. *Inflamm Res*. 2002;51(2):112-114.

46. Rumengan IFM, Modaso RH, Lintang R, Rumampuk ND, Posangi J. Cytotoxicity of methanol extracts of *Prochloron didemni* originated from ascidians *Lissoclinum patella* and *Didemnum molle* collected from Manado Bay, North Sulawesi. *IOP Conf Ser Earth Environ Sci*. 2020;517(1):012018. doi:10.1088/1755-1315/517/1/012018

47. Amaral SC do, Santos AV, Schneider MP da C, Silva JKR da, Xavier LP. Determination of volatile organic compounds and antibacterial activity of the amazonian cyanobacterium *Synechococcus* sp. strain GFB01. *Molecules*. 2020;25(20):4744. doi:10.3390/molecules25204744

48. Dinh QT, Munoz G, Simon DF, Vo Duy S, Husk B, Sauvé S. Stability issues of microcystins, anabaenopeptins, anatoxins, and cylindrospermopsin during short-term and long-term storage of surface water and drinking water samples. *Harmful Algae*. 2021;101:101955. doi:10.1016/j.hal.2020.101955

49. Mazmouz R, Chapuis-Hugon F, Mann S, Pichon V, Méjean A, Ploux O. Biosynthesis of cylindrospermopsin and 7-epicylindrospermopsin in *Oscillatoria* sp. strain PCC 6506: Identification of the cyr gene cluster and toxin analysis. *Appl Environ Microbiol*. 2010;76(15):4943-4949.

50. Ejike CECC, Collins SA, Balasuriya N, Swanson AK, Mason B, Udenigwe CC. Prospects of microalgae proteins in producing peptide-based functional foods for promoting cardiovascular health. *Trends Food Sci Technol*. 2017;59:30-36.

51. Hillwig ML, Liu X. A new family of iron-dependent halogenases acts on freestanding substrates. *Nat Chem Biol*. 2014;10(11):921-923.

52. Plech A, Salditt T, Münster C, Peisl J. Molecular biology of peptide and polyketide biosynthesis in cyanobacteria. *Appl Microbiol Biotechnol*. 2001;57(4):467-473.

53. Tillett D, Dittmann E, Erhard M, Von Döhren H, Börner T, Neilan BA. Structural organization of microcystin biosynthesis in *Microcystis aeruginosa* PCC7806: An integrated peptide-polyketide synthetase system. *Chem Biol*. 2000;7(10):753-764.

54. Dewi IC, Falaise C, Hellio C, Bourgougnon N, Mouget JL. Anticancer, antiviral, antibacterial, and antifungal properties in microalgae. *Microalgae Heal Dis Prev*. 2018:235-261.

55. Finamore A, Palmery M, Bensehaila S, Peluso I. Antioxidant, immunomodulating, and Microbial-modulating activities of the sustainable and ecofriendly *Spirulina*. *Oxid Med Cell Longev*. 2017;2017:1-14.

56. Ibrahim EA, Aly HF, Abou Baker DH, Mahmoud K, El-Baz FK. Marine algal sterol hydrocarbon with anti-inflammatory, anticancer and anti-oxidant properties. *Int J Pharma Bio Sci*. 2016;7(3):392-398.

57. Portmann C, Blom JF, Kaiser M, Brun R, Jüttner F, Gademann K. Isolation of aerucyclamides C and D and structure revision of microcyclamide 7806A: Heterocyclic ribosomal peptides from *Microcystis aeruginosa* PCC 7806 and their antiparasite evaluation. *J Nat Prod*. 2008;71(11):1891-1896.

58. Holland A, Kinnear S. Interpreting the possible ecological role(s) of cyanotoxins: Compounds for competitive advantage and/or physiological aide? *Mar Drugs*. 2013;11(7):2239-2258.

59. Kar J, Ramrao DP, Zomuansangi R, et al. Revisiting the role of cyanobacteria-derived metabolites as antimicrobial agent: A 21st century perspective. *Front Microbiol*. 2022;13:034471. doi:10.3389/fmicb.2022.1034471

60. Niveshika, Verma E, Mishra AK, Singh AK, Singh VK. Structural elucidation and molecular docking of a novel antibiotic compound from cyanobacterium *Nostoc* sp. MGL001. *Front Microbiol*. 2016;7(NOV):231637. doi:10.3389/FMICB.2016.01899/BIBTEX

61. Kumar J, Singh D, Tyagi MB, Kumar A. Cyanobacteria: Applications in biotechnology. *Cyanobacteria from Basic Sci to Appl*. 2018:327-346. doi:10.1016/B978-0-12-814667-5.00016-7

62. Vijayakumar S, Menakha M. Pharmaceutical applications of cyanobacteria-A review. *J Acute Med*. 2015;5(1):15-23.

63. Kumar L, Bharadvaja N. A review on microalgae biofuel and biorefinery: Challenges and way forward. *Energy Sources, Part A Recover Util Environ Eff*. 2020:1-24.

64. Singh NK, Dhar DW. Microalgae as second generation biofuel. A review. *Agron Sustain Dev*. 2011;31(4):605-629.

65. Ibelings BW, Chorus I. Accumulation of cyanobacterial toxins in freshwater "seafood" and its consequences for public health: A review. *Environ Pollut*. 2007;150(1):177-192.

66. Cerasino L, Salmaso N. Diversity and distribution of cyanobacterial toxins in the Italian subalpine lacustrine district. *Oceanol Hydrobiol Stud*. 2012;41(3):54-63.

67. Patel HM, Rastogi RP, Trivedi U, Madamwar D. Structural characterization and antioxidant potential of phycocyanin from the cyanobacterium *Geitlerinema* sp. H8DM. *Algal Res*. 2018;32:372-383.

68. Assunção J, Amaro HM, Malcata FX, Guedes AC. Cyanobacterial pigments: Photosynthetic function and biotechnological purposes. *Pharmacol Potential Cyanobacteria*. 2022:201-256. doi:10.1016/B978-0-12-821491-6.00008-9

69. Donia MS, Hathaway BJ, Sudek S, et al. Natural combinatorial peptide libraries in cyanobacterial symbionts of marine ascidians. *Nat Chem Biol*. 2006;2(12):729-735.

70. Wang Z, Shao J, Xu Y, Yan B, Li R. Genetic basis for geosmin production by the water bloom-forming cyanobacterium, *Anabaena ucrainica*. *Water*. 2014;7(1):175-187. doi:10.3390/W7010175

71. Wu Z, Yang S, Shi J. Overview of the distribution and adaptation of a bloom-forming cyanobacterium *Raphidiopsis raciborskii*: integrating genomics, toxicity, and ecophysiology. *J Oceanol Limnol*. 2022;40(5):1774-1791.

72. Singh T, Basu P, Singh TA, Boudh S, Shukla P. Cyanobacteria as source of novel antimicrobials: A boon to mankind. *Microorg Sustain Environ Heal*. 2020:219-230.

73. Shamim A, Mahfooz S, Hussain A, Farooqui A. Ability of Al-acclimatized Immobilized *Nostoc muscorum* to combat abiotic stress and its potential as a biofertilizer. *J Pure Appl Microbiol*. 2020;14(2):1377-1386.

74. Mahfooz S, Jahan S, Shamim A, Husain A, Farooqui A. Oxidative stress and response of antioxidant system in *Nostoc muscorum* exposed to different forms of zinc. *Turkish J Biochem*. 2018;43(4):352-361.

75. Jaki B, Orjala J, Heilmann J, Linden A, Vogler B, Sticher O. Novel extracellular diterpenoids with biological activity from the cyanobacterium *Nostoc commune*. *J Nat Prod*. 2000;63(3):339-343.

76. Akbarizare M, Ofoghi H, Hadizadeh M, Moazami N. *In vitro* assessment of the cytotoxic effects of secondary metabolites from *Spirulina platensis* on hepatocellular carcinoma. *Egypt Liver J*. 2020;10(1):11. doi:10.1186/s43066-020-0018-3

77. Blas-Valdivia V, Rojas-Franco P, Serrano-Contreras JI, et al. C-phycoerythrin from *Phormidium persicinum* prevents acute kidney injury by attenuating oxidative and endoplasmic reticulum stress. *Mar Drugs*. 2021;19(11):589. doi:10.3390/MD19110589

78. Pagarete A, Ramos AS, Puntervoll P, Allen MJ, Verdelho V. Antiviral potential of algal metabolites—A comprehensive review. *Mar Drugs*. 2021;19(2):94. doi:10.3390/md19020094

79. Pavón-Fuentes N, Marín-Prida J, Llópiz-Arzuaga A, et al. Phycocyanobilin reduces brain injury after endothelin-1- induced focal cerebral ischaemia. *Clin Exp Pharmacol Physiol*. 2020;47(3):383-392.

80. Romay C, Gonzalez R, Ledon N, Remirez D, Rimbau V. C-Phycocyanin: A biliprotein with antioxidant, anti-inflammatory and neuroprotective effects. *Curr Protein Pept Sci*. 2005;4(3):207-216.

81. Kaushik A, Sangtani R, Parmar HS, Bala K. Algal metabolites: Paving the way towards new generation antidiabetic therapeutics. *Algal Res*. 2023;69:102904. doi:10.1016/j.algal.2022.102904

82. Khanam A, Ahmad S, Husain A, Rehman S, Farooqui A, Yusuf MA. Glycation and antioxidants: Hand in the glove of antiglycation and natural antioxidants. *Curr Protein Pept Sci*. 2020;21(9):899-915.

83. Tabrizi S. Neurodegenerative diseases neurobiology pathogenesis and therapeutics. *J Neurol Neurosurg Psychiatry*. 2006;77(2):284. doi:10.1136/JNNP.2005.072710

84. Castaneda A, Ferraz R, Vieira M, Cardoso I, Vasconcelos V, Martins R. Bridging cyanobacteria to neurodegenerative diseases: A new potential source of bioactive compounds against alzheimer's disease. *Mar Drugs*. 2021;19(6):343. doi:10.3390/md19060343

85. Banack SA, Johnson HE, Cheng R, Cox PA. Production of the neurotoxin BMAA by a marine cyanobacterium. *Mar Drugs*. 2007;5(4):180-196.

86. Banack SA, Caller TA, Stommel EW. The Cyanobacteria derived toxin beta-n-methylamino-l-alanine and amyotrophic lateral sclerosis. *Toxins (Basel)*. 2010;2(12):2837. doi:10.3390/TOXINS2122837

87. Sini P, Dang TBC, Fais M, et al. Cyanobacteria, cyanotoxins, and neurodegenerative diseases: Dangerous liaisons. *Int J Mol Sci*. 2021;22(16):8726. doi:10.3390/ijms22168726

88. Spolaore P, Joannis-Cassan C, Duran E, Isambert A. Commercial applications of microalgae. *J Biosci Bioeng*. 2006;101(2):87-96.

89. Schwarz D, Orf I, Kopka J, Hagemann M. Recent applications of metabolomics toward cyanobacteria. *Metabolites*. 2013;3(1):72-100.

90. Pathania R, Srivastava A, Srivastava S, Shukla P. Metabolic systems biology and multi-omics of cyanobacteria: Perspectives and future directions. *Bioresour Technol*. 2022;343:126007. doi:10.1016/J.BIORTECH.2021.126007

91. Abida H, Ruchaud S, Rios L, et al. Bioprospecting marine plankton. *Mar Drugs*. 2013;11(11):4594. doi:10.3390/MD11114594

92. Paul SI, Majumdar BC, Ehsan R, Hasan M, Baidya A, Bakky MAH. Bioprospecting potential of marine microbial natural bioactive compounds. *J Appl Biotechnol Reports*. 2021;8(2):96-108.

93. Rotter A, Barbier M, Bertoni F, et al. The Essentials of marine biotechnology. *Front Mar Sci*. 2021;8:158. doi:10.3389/fmars.2021.629629

94. Zymański P, Markowicz M, Mikiciuk-Olasik E. Adaptation of high-throughput screening in drug discovery—Toxicological screening tests. *Int J Mol Sci*. 2012;13(1):427. doi:10.3390/IJMS13010427

95. Ferreira L, Morais J, Preto M, et al. Uncovering the bioactive potential of a cyanobacterial natural products library aided by untargeted metabolomics. *Mar Drugs*. 021;19(11):633.

96. Kim W, Chen TY, Cha L, et al. Elucidation of divergent desaturation pathways in the formation of vinyl isonitrile and isocyanoacrylate. *Nat Commun*. 2022;13(1):5343. doi:10.1038/s41467-022-32870-4

97. Van Wagoner RM, Drummond AK, Wright JLC. Biogenetic diversity of cyanobacterial metabolites. *Adv Appl Microbiol*. 2007;61:89-217.

98. Komárek J. A polyphasic approach for the taxonomy of Cyanobacteria: Principles and applications. *Eur J Phycol*. 2016;51(3):346-353.

99. Srinivasan R, Kannappan A, Shi C, Lin X. Marine bacterial secondary metabolites: A treasure house for structurally unique and effective antimicrobial compounds. *Mar Drugs* 2021;19(10):530. doi:10.3390/MD19100530

100. Hong K, Gao AH, Xie QY, et al. Actinomycetes for marine drug discovery isolated from mangrove soils and plants in China. *Mar Drugs*. 2009;7(1):24-44.

101. Wang K, Khoo KS, Leong HY, et al. How does the internet of things (IoT) help in microalgae biorefinery? *Biotechnol Adv*. 2022;54:107819. doi: 10.1016/j.biotechadv.2021.107819

102. Wase N V., Wright PC. Systems biology of cyanobacterial secondary metabolite production and its role in drug discovery. *Expert Opin Drug Discov*. 2008;3(8):903-929.

103. Sandybayeva SK, Kossalbayev BD, Zayadan BK, et al. Prospects of cyanobacterial pigment production: Biotechnological potential and optimization strategies. *Biochem Eng J*. 2022;187:108640. doi:10.1016/J.BEJ.2022.108640

104. Manirafasha E, Ndikubwimana T, Zeng X, Lu Y, Jing K. Phycobiliprotein: Potential microalgae derived pharmaceutical and biological reagent. *Biochem Eng J*. 2016;109:282-296.

105. Chu WL, Phang SM. Bioactive compounds from microalgae and their potential applications as pharmaceuticals and nutraceuticals. *Gd Challenges Biol Biotechnol*. 2019:429-469. doi:10.1007/978-3-030-25233-5_12

106. Pradhan B, Ki JS. Phytoplankton toxins and their potential therapeutic applications: A Journey toward the quest for potent pharmaceuticals. *Mar Drugs*. 2022;20(4):271. doi:10.3390/MD20040271/S1

107. Zanchett G, Oliveira-Filho EC. Cyanobacteria and Cyanotoxins: From impacts on aquatic ecosystems and human health to anticarcinogenic effects. *Toxins*. 2013;5(10):1896-1917. doi:10.3390/TOXINS5101896

108. Costa JAV, Freitas BCB, Cruz CG, Silveira J, Morais MG. Potential of microalgae as biopesticides to contribute to sustainable agriculture and environmental development. 2019;54(5):366-375.

109. Haque F, Banayan S, Yee J, Chiang YW. Extraction and applications of cyanotoxins and other cyanobacterial secondary metabolites. *Chemosphere*. 2017;183:164-175.

110. Levasseur W, Perré P, Pozzobon V. A review of high value-added molecules production by microalgae in light of the classification. *Biotechnol Adv*. 2020;41:107545. doi:10.1016/J.BIOTECHADV.2020.107545

111. Yaashikaa PR, Kumar PS, Jeevanantham S, Saravanan R. A review on bioremediation approach for heavy metal detoxification and accumulation in plants. *Environ Pollut*. 2022;301:119035. doi:10.1016/J.ENVPOL.2022.119035

112. Mishra A, Medhi K, Malaviya P, Thakur IS. Omics approaches for microalgal applications: Prospects and challenges. *Bioresour Technol*. 2019;291:121890.

doi:10.1016/J.BIORTECH.2019.121890

113. Olguín EJ, Sánchez-Galván G, Arias-Olguín II, et al. Microalgae-based biorefineries: challenges and future trends to produce carbohydrate enriched biomass, high-added value products and bioactive compounds. *Biol*. 2022;11(8):1146. doi:10.3390/BIOLOGY11081146

How to cite this article

Husain A, Nematullah MD, Khan H, Shekher R, Farooqui A, Sahu A, Khanam A. From Pond Scum to Miracle Molecules: Cyanobacterial Compounds New Frontiers. Eur J Biol 2024; 83(1): 94–105. DOI:10.26650/EurJBiol.2024.1357041

Bacterial Diversity of the Corpses

Ahmet Asan[1] iD

[1]Trakya University, Faculty of Science, Department of Biology, Balkan Campus, Edirne, Türkiye

ABSTRACT

The study presents the importance of forensic bacteriology, its use in forensic cases, the methods for bacteriological sampling from corpses, the types and species of bacteria isolated from human and pig corpses, which are most commonly used in forensic biology. The microbial changes that occur after death remain unclear. Postmortem microbiology is a relatively new field of research. After death, the failure of the immune system and other physical barriers leads to the proliferation and spread of microbes. In order for bacteriological information to be accepted within the scope of forensic bacteriology, the court must find suspicion to be present about whether the bacteria seen on the body will contribute to solving the case. Experts must be appointed to examine the issue in line with this suspicion, and these experts must prepare and submit their reports to the court at the requested time. When considering the literature studies, forensic bacteriology has been suggested to be a scientific discipline in the developmental stage and to only be able to provide circumstantial evidence in forensic cases as opposed to primary evidence. According to the literature review, most bacterial studies isolated from corpses were conducted in Romania. Although bacterial samples were isolated from various parts of the corpses, bacteria were mostly isolated from their blood samples. According to literature searches from various scientific journal databases, no study has occurred with a list of the bacteria isolated from corpses. This study is thought to be able to fill this important gap.

Keywords: Forensic bacteriology, Forensic microbiology, Bacteria, Forensic, Corpse

INTRODUCTION

Bacteria have prokaryotic cells, are usually thought of as undifferentiated single cells, and vary greatly in appearance, size, and function. For example, spherical bacteria such as *Staphylococcus and Streptococcus* have diameters between 0.75-1.25 µm and a density of 1.07 g/cm^3. Although most bacteria are unicellular, some bacteria are multicellular (e.g., Magnetoglobus). Among bacteria, 30 major phylogenetic lineages, called phyla, have at least one species that have been grown in a culture medium, but many phyla are found that have yet to be characterized. Some of these phyla contain thousands of described species, while others contain only a few species. More than 90% of cultured bacteria are grouped into four phyla: Actinobacteria, Bacillota (also known as Firmicutes[1-4]), Proteobacteria, and Bacteroidetes. Environmental deoxyribonucleic acid (DNA) sequence analysis provides evidence for the existence of at least 80 bacterial phyla.[5,6] However, according to the website www.bacterio.net[4], bacteria are only grouped under 43 phyla. Asan et al.'s[2,3,7] classification has been used for the Turkish scientific names of bacterial taxa.

According to Carter et al.[8], the bacteria most common in forensic bacteriology are found in three phyla: Actinobacteria, Firmicutes, and Proteobacteria. However, the prevalence of bacteria may vary depending on where the bacterial isolations are made. For example, Hyde et al.[9] reported Clostridia and Fusobacteria dominate the microbial communities on the faces and in the feces of vultures.

According to Garcia et al.[10], Actinomycetaceae, Bacteroidaceae, Alcaligenaceae and Bacilli play an important role in determining the postmortem interval (PMI). *Aeromonas* can be used to determine the cause of death, while *Corynebacterium* and *Helicobacter pylori* can be used to identify personal identity or geographical region. Although microbes dominate the living world, little is known about the vast majority of them. According to the American Academy of Microbiology, there are ten million times more bacteria and archaeal cells on our tiny planet than there are stars in the visible universe, and they may contain as much carbon as all plant and animal life combined.[11]

When checking the information in the literature, many publications are found to have information about bacterial checklists. The first publication on this subject was published in England

by Conlon and Paul[12] in 2020, which only has a list of bacterial pathogens that cause disease in humans. The most comprehensive bacterial checklist worldwide was published by Asan et al.[7] in 2021 as a 951-page book providing a list of the bacterial species, genera, families and phyla reported from Türkiye and isolated from all kinds of environments (e.g., humans, animals, plants, food, water, soil, air). In addition, the bacterial species, genera, families, and phyla included in this book are given Turkish scientific names for the first time. Later, lists of bacterial species that were not included in this book for various reasons or that were reported from Türkiye after the book's publication were published by Asan et al.[2,3] These two publications referred to as Asan et al.'s[7] books can be viewed as complementary. As seen, the world has few checklists regarding bacteria, and lists of bacterial species isolated from corpses are non-existent. This article has been prepared in order to fill this gap.

BACTERIA AND FORENSIC BACTERIOLOGY

One of the pioneering studies in forensic bacteriology was the work of Norris and Pappenheimer in 1905, which included bacteriological postmortem changes. After this study, bacteriological postmortem changes were investigated for many years, with Norris and Pappenheimer showing that bacteria could be found in corpses and later in lung tissue.[13]

Of the 96 causes of human illness and death around the globe, 29 are naturally occurring infectious diseases and cause the deaths of 14 million people a year globally, including 538 bacteria that are pathogenic to human. The abundance of bacteria also offers potential for forensic bacteriology.[14,15] Microorganisms can be used as evidence in many different forensic cases, but most studies are still in the experimental phase. Therefore, many opportunities exist for further research.[16]

The microbial changes that occur after death remain unclear, and postmortem microbiology is a relatively new field of research. After death, the failure of the immune system and other physical barriers leads to the proliferation and spread of microbes. To better understand the microbial changes that occur after death thanks to the emergence of new biomolecular approaches such as polymerase chain reaction (PCR) and sequencing, discussions can occur on the human postmortem microbiome, which encompasses the microbial populations colonizing internal organs and fluids and the microbes in decomposing remains. Postmortem microbiology covers PMI detection, the determination of mode and cause of death, and the isolation of microbes as markers of a particular type of death, biological crimes and their origins, trace evidence, healthcare-associated transmission diagnoses, evidence of sexual abuse, person identification, population studies, and the human microbiome's connection to personal effects and geolocation, as well as providing evidence for other crimes such as sexual assault and medical malpractice.[10,17-20] According to Narang et al.[15],

microbial forensics requires a multidisciplinary approach to biological crime detection, traces, and evidence. It also encompasses crime scene investigation, evidence collection, evidence processing, evidence preservation, evidence transportation, evidential analysis, interpretation of results, and presentation to the court and is also a requirement for civil security. Most forensic research that is used to better understand how to predict PMI requires the study of the physiochemical properties of decomposition and the effects of environmental factors.[21]

Forensic science deals with the identification and interpretation of critically important physical evidence (i.e., fingerprints, bloodstains, hairs, fibers, soil, and DNA). Eyewitness statements can be incomplete and inaccurate. To minimize these limitations, investigative statements can be compared with the interpretation of physical evidence. Detecting PMI is difficult, but if detected, PMI provides microbial evidence. Tozzo et al.[22] stated that the determination of PMI has always been an important issue and a challenge in the field of forensic science, with the methods for PMI estimation that have evolved over the last 20 years as advances in sequencing technologies having led to the availability of significant amounts of data and the ability to sequence all members of a bacterial community. Fatima et al.[23] also indicated similar opinions in their article and developed a scheme for sampling, sequencing, analysis, and forensic applications. Wang et al.[24] indicated artificial intelligence and next-generation sequencing (NGS) to have the potential to contribute to PMI estimation.

A variety of bacteria inhabit places such as the skin, oral cavity, and gastrointestinal tract of humans. The advent of advanced sequencing techniques has allowed for the study of the composition of this microbial community and track how it changes over time.[25] In general, decay is characterized by five stages: fresh decomposition, putrefaction, black putrefaction, butyric fermentation, and dry decomposition. During fresh decomposition, bacteria inside a corpse begin to digest the surrounding tissues. During decomposition, the bacteria inside the corpse perform anaerobic respiration, leading to the accumulation of gaseous by-products that swell the cadaver and eventually force fluids out of the body. The corpse is then exposed to the environment, facilitating wet tissue decomposition and leading to the dry stage of decomposition.[9]

Forensic science is concerned with the application of scientific knowledge to legal problems. To be called forensic, any scientific information must be prepared for presentation to a court of law.[26] In this sense, forensic microbiology data are not only available for review by scientists in the healthcare community but also by judges and juries.[17]

In order for bacteriological information to be accepted within the scope of forensic bacteriology, a suspicion about whether the bacteria seen on the body will contribute to solving the case must exist within the court. Experts must be appointed to examine the issue in line with this suspicion, and these experts

must prepare and submit their reports to the court at the requested time. However, having experts collect and evaluate the evidence in accordance with scientific methods is important. Forensic bacteriology being included in the scope of a standard procedure used for the investigation of certain crimes in all countries is a challenging claim. To be able to do this, the court personnel who appoint the expert witness are expected to be familiar with forensic bacteriology and to be convinced that forensic bacteriology can be useful in the investigation of certain crimes. This expectation is not equally present in all countries. Furthermore, because forensic bacteriology requires specialization and laboratory work, each country should have specialized bacteriologists and appropriate and adequate bacteriology laboratories. In addition, due to various types of bacteria being able grow on corpses, a bacteriologist is not expected to be an expert in all types of bacteria. In other words, bacteriologists who are experts on various groups of bacteria may be needed to diagnose and evaluate the bacteria growing on a corpse. Therefore, the lack and even inadequacy of bacteriologists in a country and the underdevelopment of bacteriology laboratories restrict the use of forensic bacteriology in criminal investigations.

When talking about forensic bacteriology, one thing should be clear. Bacteria that normally exist in the skin, oral cavity, urogenital system, and especially the intestines of a human being spread to the corpse after death because the immune system does not work and bacterial reproduction accelerates. However, the rate of reproduction of these bacteria in a corpse varies depending on the environment in which the corpse is found. For example, corpses in a cold environment exhibit slow bacterial growth. Other factors exist that affect the growth of bacteria in the body (e.g., oxygen levels in the tissues, pH). As a result, depending on the environment in which a corpse is found, bacteria begin to reproduce quickly or slowly in the body after death and contribute to decomposition. This is already a normal and expected process. According to Vass.[27] the decomposition of a corpse is a complex process that is based primarily on temperature and to a lesser extent on humidity. Vass also developed a formula for this purpose. For a person lying on the ground after death, Vass proposed the following formula to describe soft tissue decomposition[27]:

$$y = 1285 / x \qquad (1)$$

Where y is the number of days it takes for the body to become a skeleton and x is the average temperature in degrees Celsius during decomposition. For example, if the average temperature in the environment where a body is found is 7 ºC, then a person would become a skeleton in 183.57 days (1285/7), but this is a rough estimate because many factors are found to influence this. Or, if the average temperature of the environment is 22 ºC, then the period is 58.41 days (1285/22). As can be seen, the

rate of decomposition for a corpse increases as the average ambient temperature increases due to the intense activity of microorganisms. According to Vass[28], the following formula describes the decomposition of a human corpse above ground (aerobic; a different formula is used for underground-anaerobic decomposition [see Vass[28]]) and is used to estimate PMI in days:

$$PMI_{aerobic} = \frac{1285 \times (\text{decomposition}/100)}{0.0103 \times \text{temperature} \times \text{humidity}} \qquad (2)$$

Where 1285 is a constant representing the experimentally determined value for the accumulated degree days (ADD) when the release of volatile fatty acids (VFAs) from soft tissue stops. Once soft tissue decomposition ends or the remaining non-nutritive tissue hardens, dries, and mummifies, VFA production ceases. This occurs at approximately 1285 ADD. This ADD value marks the beginning of the post-skeletal stage of decomposition. ADD values less than 1285 indicate that VFAs are still being released and the corpse is in the pre-skeletal stage of decomposition. This formula should only be used when soft tissue remains on the body ($\leq$ 1285 ADD). Four variables have been identified with regard to weathering: temperature, humidity, pH, and partial pressure of oxygen. These variables have the greatest influence on weathering and are measured to create a formula for estimating the PMI for all objects located on or below the surface of the ground outside. The methodology is based on the premise that a standard amount of temperature or relative time is required for decomposition to complete. Vass[28] calculated this maximum temperature as 1285 ºC for ADD. According to Vass[28], when a decomposing body reaches an accumulated temperature of 1285 ºC, the soft tissue of the body has completely decomposed, leaving only the skeleton.[28,29] Decomposition is a single value or range between 1-100 and represents the best estimate of the extent of total body soft tissue decomposition. 0.0103 is a constant and represents an empirically determined measure of the effect of moisture on decomposition rates. Temperature is the average temperature in the area on the day the body was found, or the average temperature over a period of time, in degrees Celsius (e.g., 8 ºC). Humidity is a value between 1-100 and represents the average humidity in the area on the day the body was found or the average humidity over a period of time. Forensic bacteriology is concerned with the types of bacteria in a corpse based on the environment, bacterial reproduction, what this reproduction means, and its possible contribution to forensic investigations, especially for human deaths. Therefore, forensic bacteriology can be described as a relatively new discipline. Although forensic bacteriology is often argued as being a new discipline, previous assessments of the subject have occurred. For example, Donaldson wrote in 1928, "When we speak of the bacteriology of the dead body, we are actually referring to the decay of the dead body.[30] At death, the body may suddenly contain many

bacteria that have nothing to do with disease. In the example below, bacteriology was used to determine the cause of a person's death. In 1976, Takabe and Oya presented an autopsy case of food poisoning, probably caused by *Bacillus cereus*, and isolated and identified *Bacillus cereus* from the peritoneal exudate and intestinal contents of an 11-year-old boy who had died.[31] A similar case report can also be found in another study.[32]

Forensic bacteriology can also be used to seek answers to the following questions. In some cases, people who have been killed are buried in isolated places such as forests and covered with soil (according to Finley et al.[21], decomposition begins 4 min after death). Over time, biodegradation takes place due to organisms such as bacteria, fungi, insects, and nematodes. Nitrogen (N) and other elements pass into the soil. Microbial growth can increase with an increase in the substances needed by bacteria and fungi, as well as favorable environmental conditions such as temperature and pH. I wonder if bacteria exist that are more common where a body is buried than in other places. In other words, if certain bacteria and/or bacterial species are detected in a place that appear different externally in terms of bacterial growth and attract the attention of a bacteriologist, can a corpse also be said to be present there? Said yet another way, can some bacterial species be indicators in this regard? Isolating bacteria from a corpse or its environment is costly and time-consuming and requires dilution of the soil in a laboratory, the elimination of soil fungi and growth, and the identification of the bacteria in a medium. The answers to these questions are important, as can be seen in Haelewaters'[33] study, because knowing these answers can be useful for identifying places where people have been secretly buried after being killed. Tranchida et al.[34] stated the following on the subject: "Cadavers are an abundant source of organic matter. Various organisms (such as insects, bacteria, fungi, nematodes) can feed on them during decomposition." Lehman stated that the main purpose of forensic microbiology is to identify cause of death and the possible perpetrators of a crime.[35]

When forensic investigators need to solve a crime or find a body that has been secretly buried, they use different methods to study the changes that have occurred both in the body and in the soil where the body has decomposed. The aim of forensic taphonomy is to study the environmental conditions that influence the decomposition of a corpse in order to estimate PMI and determine the cause and manner of death.[36,37] The complex decomposition of human or other mammalian cadavers is closely influenced by biotic (e.g., bacteria, fungi, arthropods, nematodes) and abiotic (e.g., weather, climate, temperature, humidity) factors. Cadaver-associated microorganisms are part of the necrobiome, derived from the living host and the microbial communities living in the cadaver's environment. Previous studies have shown postmortem bacteria to be primarily of soil origin and to significantly influence the rate of cadaver decomposition. Although many studies have described the spatial and temporal changes in bacterial communities during decom-

position, current understanding of the succession pattern of post-decomposition mycoflora remains limited.[38]

Numerous living microorganisms exist that have the potential to assist postmortem medical investigations. Determining the exact cause of death and PMI are crucial data in forensic science for criminal deaths that have not been witnessed or when conflicting accounts are reported. For example, several studies have been conducted on identifying people using skin microbiota, estimating PMI, and identifying microorganisms.[39] Estimating PMI is important to an investigation, especially in cases where witnesses are unavailable.

A review study from Türkiye stated that microbiology can be used in forensic issues by taking into account the environmental conditions (humidity, temperature, oxygen) under which microorganisms can reproduce.[40] Another study by Efeoğlu et al.[41] took and analyzed soil samples for forensic microbiological analysis in 20 different regions within the provincial borders of Istanbul City and found concentrations of 83% bacteria and 17% fungi in the samples. The purpose of their study was to analyze microbiologically if physical evidence exists for soil contamination. Asan[42] also summarized forensic mycology in the world and in Türkiye as a review study from past to present.

THE USE OF FORENSIC BACTERIOLOGY

Microbiological analysis can be used to solve certain criminal cases; however, forensic microbiology is still under development. When making a legal assessment, evaluating not only the bacteriological evidence but also other biological evidence is useful. Microbial forensics is a multidisciplinary field that has recently been recognized as an effective method and a tool in forensic investigations. This growing field of forensic science encompasses a wide range of different disciplines such as biology, chemistry, physics, geology, mathematics, and computer science and can be applied in various fields regarding such things as bioterrorist acts, environmental protection, and environmental pollution, as it can provide reliable trace evidence at a crime scene.[43] Microorganisms can be used as biological weapons (i.e., biological crime), which involves the threat or use of microorganisms, toxins, pests, prions, or their associated by-products in criminal or terrorist acts and may result in outbreaks. Forensic microbiological issues may also be applicable to investigating the transmission of pathogenic microorganisms caused by sexual abuse and other physical crimes.[44]

For over a century, microbiology has played a relatively minor role in forensic science. In the early 1990s, the sequencing of amplified viral DNA was used to support a case that alleged several patients to have been infected with HIV from a dentist in Florida in the United States. The advent of PCR-mediated genotyping of bacteria has been seen as a valuable future tool in forensics. In the mid-1990s, fungal and pollen spore analyses were also developed, allowing researchers to differentiate

between soil types, which in turn allowed the association of substrate elements with specific sites.[19]

Studies of the thanatomicrobiome (biome of microorganisms found in the body, organs, and fluids postmortem) and the epinecrotic community (microorganisms found on decomposing corpses) can be used in forensic science. The change in species composition observed in each community is a valuable feature that provides much information. Some forensic investigations can use such visible changes in the microbiome and mycobiome to determine the cause of death or the actual place of death. Cause of death and microbial traces found at crime scenes can also provide evidence of criminality.[45] According to Kumari et al.[46], the microbiome can be used in forensic investigations. Furthermore, microbial forensics can be applied to issues for uses ranging from analyzing evidence, bioterrorism, and fraud to pathogen outbreaks and the spread of epidemics or unintentional release of biological agents or toxins. In such forensic investigations, both biological (e.g., bacteria, viruses, protists, fungi, and toxins) and non-biological (e.g., additives, growth media, delivery devices, intelligence) evidence are targeted for detection and characterization. Microbiomes are being used to clarify causes of death (e.g. drownings, toxicology, hospital-acquired infections, unpredictable infant mortality, and shaken baby syndrome) and to aid in identifying the deceased through skin, hair, and body fluid microbiomes. In addition, soil microbiomes help in geolocation, while postmortem time periods can be estimated using the thanato-microbiome and epinecrotic microbial community. The potential applications of microbiomes in various investigations make it a modern and reliable forensic investigation tool.[46] According to Fu et al.[38], the necrobiome is the postmortem community associated with cadavers and includes bacteria, fungi, arthropods, and other organisms and has been proposed as biological evidence for forensic investigation. Ogbanga et al.[47] studied the oral and skin microbiomes of people living in two different regions of Italy and found differences between the peoples of two regions regarding their microbiomes. They concluded the skin microbiome to be more discriminatory for human identification. This result may be useful for microbiome analysis immediately after death, but one must importantly take into consideration the fact that a microbiome will change after death when the temperature in the environment where a body is found is favorable for bacterial growth.

The ability to us bacteria in forensic bacteriology with regard to the decomposition of bodies is not clear in all cases and remains open to debate. Difficulty is had in claiming the field of forensic bacteriology to be able to provide primary evidence in identifying PMI and uncovering crime; however, it may also be useful in uncovering a variety of additional evidence. Metcalf et al.[25] conducted their research on a mouse model and stated determining PMI to be important in any death investigation but to also be prone to a number of errors and biases when using current techniques. Forensic entomology can be used for estimating PMI, but erroneous results can occur at the level of days or even months; therefore, microbes may provide a new method for estimating PMI.

Three stages occur after the death of a human being: bloating, decomposition, and skeletonization.[48] The information obtained from Metcalf et al.'s[25] study provides important contributions in this regard. During the bloating stage of the corpse (approximately days 6-9), the Lactobacillaceae and Bacteroidaceae families, endogenous anaerobes and facultative anaerobes are known to be common members of the intestinal environment. After abdominal rupture occurs, these taxa are significantly reduced, and exposure of the abdominal cavity to oxygen is increased by the *Rhizobiales* members of the families Phyllobacteraceae and Brucellaceae (e.g., *Pseudochrobactrum* and *Ochrobactrum* [*Brucella* is the current name of *Ochrobactrum*]). Furthermore, facultative anaerobes such as *Serratia*, *Escherichia*, *Klebsiella*, and *Proteus*, known as opportunistic pathogens, are abundant after laceration.[25] According to this information, bacteria detected in the abdominal cavity of a corpse may contribute to obtaining the estimated time of rupture and thus indirectly to the estimation of PMI. Palmiere et al.[49] stated that molecular approaches in bacteriology and the use of alternative biological samples in postmortem biochemistry may be useful for obtaining relevant information, even in corpses with severe decomposition changes.

ISOLATING BACTERIA FROM THE CORPSE AND ENVIRONMENT WHERE A CORPSE IS FOUND

The techniques used for microorganism identification and the methods and technologies in forensic microbiology are similar to those used in research and diagnostic microbiology. Currently, molecular sequencing and genotyping techniques are used for identification.[50] Correctly identifying the bacteria isolated in relation to an incident is important in order to contribute to criminal investigations. Tomaso and Neubauer[44] also stated that microbial forensics is a young scientific discipline. Although classical microbiological techniques are indispensable for forensic microbiological studies, new techniques such as rapid genome sequencing can also be utilized. The most commonly used assays in postmortem microbiology are antigen detection techniques, bacteriological cultures, and molecular techniques, especially as applied to bacteriology and virology. In most postmortem studies, antigenic techniques are considered indicative of preliminary assays that need to be confirmed by culture and molecular techniques. Less frequently, other analyses such as epidemiological typing are also required.[51] Identification in a microbiology laboratory depends on the quality of the sample collected. Therefore, a poor collection process with deficiencies in collection or transportation can lead to errors in the detection of etiologic agents. To avoid this, specific protocols need to be established for the collection of autopsy specimens. The correct interpretation of postmortem microbi-

ological results should take into account: a) the isolation site, b) the pathogenic potential of the organism, c) the age of the individual, especially regarding children, d) the usual bacterial flora of the isolation site, and e) the use of infection criteria in living individuals. The possibility for false negatives and false positives should be recognized in postmortem microbiological testing.[51] Importance is had in having environmental sampling that is sensitive, reliable and timely, as delay can lead to the loss of some evidence. Microbiological evidence can include samples of live microbial agents, protein toxins, nucleic acids, clinical samples from victims, environmental samples, contaminated clothing, or traces of specialized evidence.[15] The procedure followed by Ventura Spagnolo et al.[18] involves: storing the corpse at 4°C, collecting samples within 24 h and 48 h after death prior to evisceration, using appropriate collection media, sterilizing the surfaces of selected body sites, using sterile instruments, and immediately transferring collected samples to a microbiology laboratory.

Postmortem microbiology has been used in various research studies not only to confirm the presence of an underlying infectious disease process but also to determine cause of death. Cardiac blood, cerebrospinal fluid, and splenic tissue are promising samples for postmortem microbiological cultures, while lung tissue culture often yields false positive results.[52] According to Tuomisto et al.[53], pericardial fluid and the liver are the most sterile up to five days postmortem and offer the best postmortem microbiological sampling sites during that time period.

Of course, when working with bacteria found on corpses, one must take into account the possibility that they be pathogenic and/or allergenic to humans, and investigators should take precautions accordingly. Using the appropriate masks and gloves, as well as such things as disposable headgear and aprons, is important, as well as and carrying out the procedure as quickly and accurately as possible to avoid contamination. After death, however, determining whether the microorganisms to be isolated from the body for various purposes are actually of corpse origin, namely whether contamination has occurred or not, is important. Ventura Spagnolo et al.[18] explained avoiding contamination to be impossible. Robinson et al.[19] illustrated using the literature for possible sources of contamination. However, great care must be taken to prevent or minimize contamination when taking microbiological samples from a crime scene. The sampling personnel should be well trained, and forensic microbiological samples should be delivered to the laboratory as soon as possible to avoid deterioration. For sampling protocols, see Burcham et al.[17] and Singh et al.[54].

NGS has opened up new opportunities for microbiological sampling, especially from the environment. In culture-based sampling, only the type and density of living microorganisms in a medium can be investigated, because neither a dead microorganism nor its structure can grow in a medium. However, the NGS method is not culture-based and allows the DNA

structures of not only living microorganisms but also non-living/dead microorganisms to be detected, resulting in more data. For example, Metcalf et al.[25] conducted a 48-day laboratory experiment to characterize temporal changes in microbial communities using the Illumina HiSeq platform to characterize bacteria, archaea, and microbial eukaryotes by benefitting from a culture-independent combination. In forensic science, the NGS approach has recently been proposed for genotyping protocols regarding personal identification, lineage inference, and phenotypic prediction. In the near future, new protocols may replace their predecessors due to their high throughput characteristics, the rapid reduction of costs, and the development of specialized applications. Microbiology has always played an important role in the analysis of environmental samples during forensic investigations. Recent technological advances have increased the sensitivity and specificity of investigations while also having raised old and new technical questions. The first is the need for easy, repeatable and standardizable workflows, and the second is the need for expert scientists with regard to bioinformatics analysis.[55] According to Maehly[56], forensic bacteriology will develop alongside various forensic techniques to oppose the increase in crimes in the future.

BACTERIA FOUND ON CORPSES

The role of bacteria in corpse decomposition and the full spectrum of species involved in the process are not yet well known. Therefore, increasing current knowledge of the mycobiota found in corpses and understanding the physical, chemical, and biological factors that determine which species can participate in succession are necessary. These factors include temperature and humidity (and their changes over time), soil type and pH, the presence of animals, especially insects and rodents, the characteristics of the surrounding vegetation, the type and amount of different chemical compounds (e.g. heavy metals) in and around the corpse, and the amount of different gases and volatile compounds in the atmosphere.[36] By taking into account the literature on the subject, Schneider[57] outlined the main issues related to bacteriological investigations in the context of forensic autopsies and mentioned estimating the age of a corpse on the basis of bacteria-caused decomposition as an example. The bacterial genera and species detected in corpses in various countries are given on Table 1.

CONCLUSION

When a person dies (PMI), how they died, and who is likely to be responsible for their death are very important with regard to forensic cases. The bacteria that are usually isolated from corpse and a corpse's stage of decomposition can help to identify PMI and the persons who might be responsible for their death. Forensic bacteriology is a developing scientific discipline and much progress is needed. According to the literature

Table 1. Bacterial species and genera found in corpses.[13,18,31,32,49,52-54,58-66]

Bacterial genus or species	The corpse from which the bacterial genus and/or species was isolated.	Country	The place where bacteria are isolated	References
Bacillus cereus	Human	Japan	Peritoneal exudate and intestinal contents	Takabe and Oya[31]
Streptococcus pneumoniae	Human	South African Republic	Leptomeningeal tissue	Moar and Miller[32]
Acinetobacter, Aeromonas sobria, Enterobacter cloacae, Enterococcus faecalis, Escherichia coli, Klebsiella spp., Micrococcus tetragenus, Morganella morganii, Pseudomonas aeruginosa, Raoultella, Staphylococcus aureus, S. epidermidis, S. simulans, Stenotrophomonas maltophilia, Streptococcus pneumoniae, Streptococcus spp.	Human	China	Blood	Tang et al.[52]
Acinetobacter, Bacillus, Bacteroides, Citrobacter, Corynebacterium, Clostridium, Enterococcus, Enterobacter, Escherichia, Klebsiella, Lactobacillus, Micrococcus, Neisseria, Proteus, Peptostreptococcus, Propionibacterium, Stomatococcus, Serratia, Staphylococcus, Streptococcus	Human	Finland	Blood	Tuomisto et al.[53]
Citrobacter freundii	Human	France	Blood	Maujean et al.[58]
Citrobacter koseri , E. coli, Neisseria meningitidis	Human	France	Cerebrospinal fluid	Maujean et al.[58]
Acinetobacter baumannii, Aeromonas hydrophila, E. coli, K. pneumoniae, Morganella morganii, Proteus mirabilis, P. penneri, Providencia stuartii, Pseudomonas aeruginosa, P. putida, Shewanella putrefaciens, S. aureus, S. epidermidis, Streptococcus pneumoniae, S. viridans	Human	Romania	Blood	Dermengiu et al.[59]
Actibacter sediminis, Aerococcus suis, Arsenophonus nasoniae, Cellvibrio japonicus, Clostridium estertheticum, C. histolyticum, C. putrefaciens, Halomonas salifodinae, Ignatzschineria larvae, Moraxella pluranimalium, Myroides odoratimimus, P. mirabilis, Providencia heimbachae, P. stuartii, Pseudomonas brassicacearum, P. corrugata, P. fragi, P. orientalis, P. otitidis, P. panacis, P. peli, P. poae, P. protegens, P. syringae, Psychrobacter adeliensis, P. arcticus, P. cibarius, P. cryohalolentis, P. lutiphocae, P. namhaensis, Ruminococcus gnavus, Sphingobacterium composti, Sporosarcina globispora, Thermosyntropha lipolytica,	Swine	Romania	Mouth	Iancu et al.[60]

Table 1. Continued

Vitreoscilla stercoraria, Wohlfahrtiimonas chitiniclastica				
Aquaspirillum putridiconchylium, Bacteroides propionicifaciens, Ignatzschineria larvae, Myroides odoratus, Psychrobacter arcticus, P. alimentarius, P. cibarius, P. cryohalolentis, P. frigidicola, P. glacincola, P. namhaensis, Pseudomonas chlororaphis, P. lutea, P. poae, Plesiomonas shigelloides, Vitreoscilla stercoraria, Wohlfahrtiimonas chitiniclastica	Swine	Romania	Rectum	Iancu et al.[60]
Haemophilus influenzae, Listeria monocytogenes, N. meningitidis, S. pneumoniae	Human	It's not exactly known (Belgium ?, Italy?, Switzerla nd?)	Cerebrospinal fluid	Palmiere et al.[49]
E. coli, K. pneumoniae, M. morganii, P. aeruginosa, S. aureus, S. capitis, S. cohnii, S. epidermidis, S. haemolyticus, S. hominis, S. pettenkoferi, S. saprophyticus, S. simulans, S. warneri, Streptococcus pneumoniae	Human	Switzerla nd	Blood	Palmiere et al.[61]
Bacteroides fragilis, B. thetaiotaomicron, Citrobacter diversus, Clostridium cadaveris, C. innocuum, C. ramosum, C. tertium, E. faecalis, E. faecium, E. raffinosus, E. coli, Eubacterium limosum, Haemophilus influenzae, Klebsiella oxytoca, K. pneumoniae, M. morganii, P. aeruginosa, S. aureus, S. epidermidis, Streptococcus constellatus, S. parasanguinis	Human	Japan	Blood	Sunagawa and Sugitani[62]
E. coli, K. pneumoniae, S. pneumoniae	Human	Switzerla nd (Italy?, Switzerla nd?)	Blood	Palmiere and Tettamanti[63]
A. baumannii, E. coli, P. mirabilis, P. aeruginosa, Salmonella enteritidis, S. aureus, Streptococcus pyogenes	Human	Italy	Blood and pericardial and pleural fluids	Ventura Spagnolo et al.[18]
A. baumannii, Pseudomonas	Human	Romania	Blood, skin/wound, lung, pleural fluid, peritoneal fluid, abscess	Diac et al.[64]
Staphylococcus	Human	Romania	Blood	Diac et al.[64]
A. baumannii, A. lwoffii, Aeromonas sobria, Burkholderia cepacia, Citrobacter freundii, Clostridium difficile, C. sordellii, Comamonas acidovorans, E. cloacae, E. faecium, E. gallinarum, E. coli, Granulicatella adiacens, Klebsiella oxytoca, K. pneumoniae, Leuconostoc mesenteroides, P. vulgaris, P. aeruginosa, S. aureus,	Human	China	Blood	Zheng et al.[65]

Table 1. Continued

S. cohnii, S. epidermidis, S. saprophyticus, S. sciuri, Stenotrophomonas maltophilia, Streptococcus alactolyticus, S. hemolyticus				
Bacillus altitudinis, B. aryabhattai, B. badius, B. cereus, B. kochii, B. megaterium, B. methylotrophicus, B. muralis, B. simplex, B. subtilis, B. thuringiensis, Enterococcus durans, E. faecalis, Fictibacillus arsenicus, Lysinibacillus boronitolerans, L. fusiformis, Pediococcus acidilactici, Rummeliibacillus stabekisii, Staphylococcus cohnii, S. nepalensis, S. sciuri, S. xylosus, Vagococcus lutrae	Swine	USA	Skin	Singh et al.[54] (isolated by E. Junkins, unpublished data)
Bacteroides fragilis, B. ovatus, B, thetaiotaomicron, B. vulgatus, Bifidobacterium longum, Clostridium perfringens, C. sordellii, Enterobacter agglomerans, E. faecium, E. coli, K. pneumoniae, Lactobacillus curvatus, Staphylococcus sp., Streptococcus anginosus, S. oralis, Veillonella dispar	Human	France?	Blood	Mesli et al.[66]
Citrobacter, Clostridium, Dechloromonas, Desulfosporomusa, Enterococcus, Ewingella, Klebsiella, Lactobacillus, Lactococcus, Proteocatella, Pseudomonas, Psychrobacter, Zoogloea	Swine (In water)	USA	Epinecrotic biofilm	Benbow et al.[65]
A. baumannii, A. Iwoffii, Bacillus sp., Bacteroides fragilis, Moraxella catarrhalis, Citrobacter sp., Clostridium butyricum, C. septicum, Corynebacterium sp., E. cloacae, E. faecalis, E. faecium, E. coli, Hafnia alvei, Haemophilus influenzae, Klebsiella oxytoca, K. pneumoniae, Lactobacillus sp., Lactococcus sp., Neisseria sp., Pediococcus sp., Proteus vulgaris, P. aeruginosa, P. fluorescens, P. putida, Serratia liquefaciens, S. marcescens, Sphingomonas paucimobilis, S. aureus, S. intermedius, Stenotrophomonas maltophilia, Streptococcus mitis, S. parasanguinis, S. pneumoniae, S. salivarius	Human	Denmark	Various parts of the corpse	Christoffersen[13]

review, although some studies have included bacteria isolated from corpses, no checklist is yet to be found regarding the bacteria that have bene isolated from corpses. As far as is known, this study is the first one to collectively present the bacteria that have been isolated from corpses at the genus and species levels using information from the literature information (see Table 1). Table 1 also includes information about the countries and organisms from which the bacteria were reported to have been found. Thus, being able to access this list in future sci-

entific studies related to forensic bacteriology is considered to facilitate researchers.

ORCID IDs of the author

Ahmet Asan   0000-0002-4132-3848

REFERENCES

1. Oren A, Garrity GM. Valid publication of the names of forty-two phyla of prokaryotes. *Int J Syst Evol Microbiol.* 2021;71:005056. doi:10.1099/ijsem.0.005056

2. Asan A, Giray G, Aydoğdu H. Türkiye arke ve bakterileri listesine ilaveler-1 (New additions to the list of Archaea and Bacteria of Turkiye-1). *Bağbahçe Bil Derg.* 2022;9:91-99.

3. Asan A, Giray G, Aydoğdu H. Türkiye arke ve bakterileri listesine ilaveler: İkinci güncelleme. *Bağbahçe Bil Derg.* 2023;10:380-388.

4. Euzéby JP. LPSN-List of prokaryotic names with standing in nomenclature. 1997. Avaliable from: www.bacterio.net (Access: May 08, 2024).

5. Atlas RM. Microbiology fundamentals and applications. Sec. Ed. 984 pp. Macmillan Publishing Comp. New York, 1984.

6. Madigan MT, Aiyer J, Buckley DH, Sattley WM, Stahl DA. Brock biology of microorganisms. 16. Ed. Global Ed. 1129 pp. USA. Pearson Education Limited, 2022.

7. Altıntaş Kazar G, Asan H, Aygül A, et al. Türkiye Arke ve Bakterileri Listesi (Checklist of the Archaea and Bacteria of Turkey). Asan A, Aydoğdu H, Karaltı I, Kocagöz ZT. (eds), First Ed. İstanbul. 951 pp. Ali Nihat Gökyiğit Vakfı Yayını, 2021.

8. Carter DO, Junkins EN, Kodama WA. A primer on microbiology. pp 1-24. In: Carter DO, Tomberlin JK, Benbow ME, Metcalf, JL. (Eds). Forensic Microbiology. XXVI + 391 pp. By John Wiley & Sons Ltd, 2017.

9. Hyde ER, Metcalf JL, Bucheli SR, Lynne AM, Knight R. Microbial communities associated with decomposing corpses. pp 245-273. In: Carter DO, Tomberlin JK, Benbow ME, Metcalf JL. (Eds). Forensic Microbiology. XXVI + 391 pp. By John Wiley & Sons Ltd, 2017.

10. Garcia MG, Pérez-Cárceles MD, Osuna E, Legaz I. Impact of the human microbiome in forensic sciences: A systematic review. *Appl Environ Microbiol.* 2020;86):e01451-20. doi: 10.1128/AEM.01451-20

11. Clements JD. (Chair). Science needs for microbial forensics: Developing ınitial ınternational research priorities. XXIV + 228 pp. Washington D.C. The National Academies Press, 2014. www.nap.edu

12. Conlon CP, Paul J. A checklist of bacteria associated with infection in humans. In John Firth, Christopher Conlon, and Timothy Cox (eds), Oxford Textbook of Medicine, 6 edn (Oxford, 2020; online edn, Oxford Academic, 1 Jan. 2020), doi:10.1093/med/9780198746690.003.0151 (accessed 31 Jan. 2024). https://academic.oup.com/book/41095/chapter-abstract/351074866?redirectedFrom=fulltext

13. Christoffersen, S. The importance of microbiological testing for establishing cause of death in 42 forensic autopsies. *Forensic Sci Int.* 2015;250:27-32.

14. Taylor LH, Latham SM, Woolhouse ME. Risk factors for human disease emergence. *Philos Trans R Soc Lond Biol Soc.* 2001;356:983-989.

15. Narang D, Kulshreshtra R, Khan F, et al. Microbes in forensic medicine: A microbiologist perspective. *Int J Bioassays.* 2016;5.10:4913-4919.

16. Gunn A, Pitt SJ. Microbes as forensic indicators. *Trop Biomed.* 2012;29:311-330.

17. Burcham ZM, Jordan HR. History, current, and future use of microorganisms as physical evidence. pp 25-55. In: Carter DO, Tomberlin JK, Benbow ME, Metcalf JL. (Eds). Forensic Microbiology. XXVI + 391 pp. By John Wiley & Sons Ltd, 2017.

18. Ventura Spagnolo E, Mondello C, Stassi C, et al. Forensic microbiology: A case series analysis. *Euromediterranean Biomed J (Formerly: Capsula Eburnea).* 2019;14:117-121.

19. Robinson JM, Pasternak Z, Mason CE, Elhaik E. Forensic applications of microbiomics: A review. *Front Microbiol.* 2021;11:608101. doi:10.3389/fmicb.2020.608101

20. Moitas B, Caldas IM, Sampaio-Maia B. Forensic microbiology and geographical location: A systematic review. *Aust J Forensic Sci.* 2023; (In Press). doi:10.1080/00450618.2023.2191993

21. Finley SJ, Benbow ME, Javan GT. Microbial communities associated with human decomposition and their potential use as postmortem clocks. *Int J Legal Med.* 2015;129:623-632.

22. Tozzo P, Amico I, Delicati A, Toselli F, Caenazzo L. Postmortem interval and microbiome analysis through 16S rRNA analysis: A systematic review. *Diagnostics (Basel).* 2022;12:2641. doi:10.3390/diagnostics12112641

23. Fatima M, Hussain S, Babar M, Aftab U, Mushtaq N, Rehman HM. Microbiome and metagenome signatures: The potential toolkit for futuristic forensic investigations. *Int J Forensic Sci.* 2022;7:1-13.

24. Wang Z, Zhang F, Wang L, Yuan H, Guan D, Zhao R. Advances in artificial intelligence-based microbiome for PMI estimation. *Front Microbiol.* 2022;13:1034051. doi:10.3389/fmicb.2022.1034051

25. Metcalf JL, Wegener Parfrey L, Gonzalez A, et al. A microbial clock provides an accurate estimate of the postmortem interval in a mouse model system. *Elife.* 2013;15:e01104. doi:10.7554/eLife.01104

26. Wiltshire PEJ. Mycology in palaeoecology and forensic science. *Fungal Biol.* 2016;120:1272-1290.

27. Vass AA. Beyond the grave-understanding human decomposition. *Microbiol Today.* 2011;28:190-192.

28. Vass AA. The elusive universal post-mortem interval formula. *Forensic Sci Int.* 2011;204:34-40.

29. Cockle DL. Human decomposition and the factors that affect it: A retrospective study of death scenes in Canada. PhD Thesis. XXXIV + 413 pp. Simon Fraser University (Canada). 2013.

30. Donaldson R. Bacteriology in connection with forensic medicine. *J State Med.* (1912-1937). 1928;36:497-509.

31. Takabe F, Oya M. An autopsy case of food poisoning associated with *Bacillus cereus. Forensic Sci.* 1976;7:97-101.

32. Moar JJ, Miller SD. The value of autopsy bacteriology: A case report and review of techniques. *SA Med J.* 1984;66:192-193.

33. Haelewaters D. Hebeloma, pioneer genus in forensic mycology. *Fungi.* 2013;6:47-48.

34. Tranchida MC, Berruezo LEB, Stenglein SA, Cabello MN. Mycobiota associated with human cadavers: First record in Argentina. *Can Soc Forensic Sci J.* 2018;51:39-47.

35. Lehman DC. Forensic Microbiology. *Clin Lab Sci.* 2012;25:114-119.

36. Tranchida MC, Pelizza SA, Elíades LA. The use of fungi in forensic science, a brief overview. *Can Soc Forensic Sci J.* 2021;54: 35-48.

37. Yıldız SS. Ülkemizdeki adli vakalarda palinolojinin kullanımı

ve yararları (Usage and benefits of palynology in forensic cases in our country). PhD Thesis. Ankara. XVI + 128 pp. Hacettepe Üniversitesi Fen Bil Enst, 2021.

38. Fu X, Guo J, Finkelbergs D. Fungal succession during mammalian cadaver decomposition and potential forensic implications. *Scientific Rep.* 2019;9:12907. doi:10.1038/s41598-019-49361-0

39. Javan GT, Finley SJ. What is the "thanatomicrobiome" and what is its relevance to forensic investigations? (Chapter 6). In: Forensic Ecogenomics. The Application of Microbial Ecology Analyses in Forensic Contexts. pp. 133-143, 2018. doi:10.1016/B978-0-12-809360-3.00006-0

40. Berikten D. Adli Mikrobiyoloji. pp 322-325. In: Külekçi, Y. (Ed): Suç Araştırmalarında Kriminal Yaklaşımlar. Akademisyen Kitapevi. İstanbul, 2020. Link: https://books.akademisyen.net/index.php/akya/catalog/download/1807/1844/42346?inline=1 (Access: 22.1.2022).

41. Efeoğlu F, Çakan H, Kara U, Daş T. Forensic microbiological analysis of soil and the physical evidence buried in soil obtained from several towns in Istanbul. Cureus. 2022;14:e22329. doi:10.7759/cureus.22329

42. Asan A. Adli Mikoloji (Forensic mycology). Chapter 21. pp 584-618. In: Yamaç M, Asan A, Bıyık HH (Eds). Fungal Biyoteknoloji Uygulamaları. e-book. First Ed. Konya. Mikolojik Araştırmalar Derneği Yayınları No 1. 694 pp. Konya, 2023. https://fbuproje.org.tr/

43. Yousefsaber F, Naseri Z, Hasani AH. A short review of forensic microbiology. *Avicenna J Clin Microbiol Inf.* 2022;9:88-96.

44. Tomaso H, Neubauer H. Forensic Microbiology. Chapter 13. pp 293-306. 2011. www.intechopen.com

45. Speruda M, Piecuch A, Borzęcka J, Kadej M, Ogórek R. Microbial traces and their role in forensic science. *J Appl Microbiol.* 2022;132:2547-2557.

46. Kumari P, Prakash P, Yadav S, Saran V. Microbiome analysis: An emerging forensic investigative tool. *Forensic Sci Int.* 2022;340:111462. doi:10.1016/j.forsciint.2022.111462

47. Ogbanga N, Nelson A, Ghignone S, et al. The oral microbiome for geographic origin: An Italian study. *Forensic Sci Int Genetics.* 2023;64:102841. doi:10.1016/j.fsigen.2023.102841

48. Sidrim JJC, Moreira Filho RE, Cordeiro RA, et al. Fungal microbiota dynamics as a postmortem investigation tool: Focus on Aspergillus, Penicillium and Candida species. *J Appl Microbiol.* 2010;108:1751-1756.

49. Palmiere C, Vanhaebost J, Ventura F, Bonsignore A, Bonetti LR. Cerebrospinal fluid PCR analysis and biochemistry in bodies with severe decomposition. *J Forensic Leg Med.* 2015;30: 21-24.

50. Busic I. Forensic Microbiology. Zagreb. MSc Thesis. 47 pp. University of Zagreb, School of Medicine. Zagreb, 2022.

51. Fernandez-Rodriguez A, Alberola J, Cohen MC. Análisis microbiológico post mórtem [Post-mortem microbiology analysis]. *Enferm Infec Microbiol Clin.* 2013;31:685-691.

52. Tang RK, Liu Y, Liu YZ, et al. Evaluation of post-mortem heart blood culture in a Chinese population. *Forensic Sci Int.* 2013;231:229-233.

53. Tuomisto S, Karhunen PJ, Vuento R, Aittoniemi J, Pessi T. Evaluation of postmortem bacterial migration using culturing and real-time quantitative *PCR. J Forensic Sci.* 2013;58:910-916.

54. Singh B, Crippen TL, Tomberlin JK. An introduction to metagenomic data generation, analysis, visualization, and interpretation. pp 94-126. In: Carter DO, Tomberlin JK, Benbow ME, Metcalf JL. (Eds). Forensic Microbiology. XXVI + 391 pp. By John Wiley & Sons Ltd, 2017.

55. Giampaoli S, De Vittori E, Frajese GV, et al. A semi-automated protocol for NGS metabarcoding and fungal analysis in forensic. *Forensic Sci Int.* 2020;306:110052. doi:10.1016/j.forsciint.2019.110052

56. Maehly A. Die forensischen Wissenschaften gestern, heute und morgen. *Fresenius Z Anal Chem.* 1984;318:97-102.

57. Maujean G, Guinet T, Fanton L, Malicier D. The interest of postmortem bacteriology in putrefied bodies. *J Forensic Sci.* 2013;58:1069-1070.

58. Schneider V. Der wert bakteriologischer untersuchungen im rahmen gerichtlicher sektionen. *Z Rechtsmed.* 1985;94:81-92.

59. Dermengiu D, Curca GC, Ceausu M, Hostiuc S. Particularities regarding the etiology of sepsis in forensic services. *J Forensic Sci.* 2013;58:1183-1188.

60. Iancu L, Carter DO, Junkins EN, Purcarea C. Using bacterial and necrophagous insect dynamics for post-mortem interval estimation during cold season: Novel case study in Romania. *Forensic Sci Int.* 2015;254:106-117. (Erratum In: Forensic Sci Int 2016;258:80).

61. Palmiere C, Egger C, Prod'Hom G, Greub G. Bacterial translocation and sample contamination in postmortem microbiological analyses. *J Forensic Sci.* 2016;61:367-374.

62. Sunagawa K, Sugitani M. Post-mortem detection of bacteremia using pairs of blood culture samples. *Leg Med (Tokyo).* 2017;24:92-97.

63. Palmiere C, Tettamanti C. Positive bacteriological analyses in individuals with diabetes mellitus: Preliminary results from a forensic study. *Amer J Forensic Med Pathol.* 2018;39:126-129.

64. Diac I, Keresztesi AA, Cerghizan AM, Negrea M, Dogăroiu C. Postmortem bacteriology in forensic autopsies-A single center retrospective study in Romania. *Diagnostics (Basel).* 2022;12:2024. doi:10.3390/diagnostics12082024

65. Zheng Z, Zhang L, Zhao C, et al. A forensic study of cultivating postmortem heart blood in 131 autopsies suspected of infectious diseases. *Rom J Leg Med.* 2022;30:1-7.

66. Mesli V, Neut C, Hedouin V. Postmortem bacterial translocation. pp 192-211. In: Carter DO, Tomberlin JK, Benbow ME, Metcalf JL. (Eds). Forensic Microbiology. XXVI + 391 pp. By John Wiley & Sons Ltd, 2017.

How to cite this article

Induction of Apoptosis in BCR-ABL Fusion Associated Chronic Myeloid Leukemia Cells by *Camellia kissi* Wall. (Theaceae) Extract

Nguyen Anh Xuan[1] ⓘ, Nguyen Trung Quan[2] ⓘ, Bui Thi Kim Ly[3] ⓘ, Hoang Thanh Chi[3] ⓘ

[1]Hong Bang International University, Faculty Of Medical Laboratory, Ho Chi Minh City, Vietnam
[2]Vietnam National University Ho Chi Minh City, University of Science, Faculty of Biology and Biotechnology, Ho Chi Minh City, Vietnam
[3]Thu Dau Mot University, Department of Medicine and Pharmacy, Thu Dau Mot, Binh Duong, Vietnam

ABSTRACT

Objective: *Camellia kissi*, a prominent tea, lacks academic works. In a previous report, this plant substantially affected chronic myeloid leukemia cells. Understanding the mechanism of action of this tea species on leukemia cells will contribute to researching alternative treatment methods in the context of drug resistance in chronic myeloid leukemia, which is constantly increasing.
Materials and Methods: *C. kissi* comes from Lam Dong, Vietnam. The crude tea extract in methanol was obtained. The flow cytometry method with Annexin V and PI staining and the DNA fragmentation assays were used to indicate the apoptosis cells. The reversed transcription real-time PCR reactions were conducted to measure the mRNA level under the treatment.
Results: The results showed the apoptosis-inducing capacity of the *C. kissi* extract on K562 cells, and the impact was suggested to be through the induction of intracellular apoptosis and cell cycle arrest.
Conclusion: The apoptosis induction on K562 caused by *C. kissi* was reported for the first time. Initial recognition of the signaling pathway of inhibition is through the BCR-ABL/PTEN.

Keywords: *Camellia kissi*, Chronic myeloid leukemia, Leukemia, Gene expression.

INTRODUCTION

Leukemia is one of the most dangerous diseases, causing nearly 312,000 deaths in 2020 in the world; approximately 475,000 new cases of leukemia were recorded in the same year.[1] Asia accounts for about 50% of incidence and mortality cases.[2] Based on the cause and pathological condition, leukemia is divided into four standard types: Acute Myeloid Leukemia, Chronic Myeloid Leukemia, Acute Lymphoid Leukemia, and Chronic Lymphocytic Leukemia (CML).[3] The proportion of blood cancer groups varies depending on geographical area, in which CML accounts for about 20% of acute leukemia cases.[4] One of the essential signaling pathways in CML pathogenesis is through BCR-ABL protein fusion.[5] Continuous amplification of cell proliferation signals is the root cause of CML pathogenesis.[6] Besides the traditional treatments, targeting BCR-ABL drugs has been considered a promising treatment for CML in recent years. Drugs known as tyrosine kinase inhibitors (TKIs) that act on the protein fusion in use include Imatinib (Gleevec), Dasatinib (Sprycel), Nilotinib (Tasigna), Bosutinib (Bosulif), Ponatinib (Iclusig), and Asciminib (Scemblix).[7] However, reduced effectiveness due to drug resistance or side effects is a significant challenge in the treatment of CML.[8] For example, the accumulation of mutations in T315 causes multi-level drug resistance, so Ponatinib and Asciminib are preferred.[9] However, Asciminib causes thrombocytopenia, and Ponatinib has the risk of causing thrombosis.[10,11] Therefore, finding alternative treatment methods is necessary.

As mentioned, Asia faces a high incidence of leukemia, with rates constantly increasing. Thus, pathological studies need to be performed. Asian people have a unique living culture; they love using fresh, natural ingredients in their lives, including tea drinking culture.[12] Green tea plays a significant role in their lives and health, and it has been shown in studies to be effective on certain types of cancer, including leukemia.[13,14] *Camellia* is an outstanding tea genus with high biodiversity. Vietnam is one of the countries endowed with the most diverse of them.[15] High endemism in distribution makes some Vietnamese tea varieties be hidden from scientific research. *Camellia kissi* is one of the potential tea species, but academic information is lacking. Providing complete scientific information about bio-activity is vital in recognizing the prestige and significance of the conservation of this plant. Based on the previously published results of

potent proliferation inhibition on CML cells, this study aims to clarify the pathway in the mechanism of proliferation inhibition of *C. kissi* on K562 cells.

MATERIALS AND METHODS

Sample Preparation

C. kissi Wall. was harvested from Lam Dong province at the location coordinates of 11.481178.108.130521, Vietnam, with voucher No. PMT-C-01. The leaves were separated and cleaned with tap water. The leaves were left thoroughly dried in an oven with a steady temperature of 40°C. The dried sample was ground into a fine tea powder. Tea powder (200 g) was mixed into 600 mL of absolute methanol (Merck, Germany). After 24 h of shaking at 180 rounds per minute, the filtrate was collected; the filtrating process broadened three more times before filtrate pooling. By using a rotary evaporator, the crude methanol extract of *C. kissi* was obtained, and the extract (abbreviated as CKE) was prepared at a concentration of 300 µg/mL by weighting and dissolving with dimethyl sulfoxide (DMSO, Sigma-Aldrich, USA).

Cell Culture Conditions

Human Chronic Myeloid Leukemic cells, K562 (ATCC®CCL-243™) were cultured in RPMI 1640 (Roswell Park Memorial Institute Medium, Thermo Scientific, USA). The medium was added with 1% antibiotic and 10% fetal bovine serum (FBS, Thermo Scientific, USA). The trypan blue (Thermo Scientific, USA) exclusion method indicated cell density during the experiments. The initial cell concentration was set at 10^5 cells/mL Sub-culturing occurred every 72 h.

Cell Morphology Changes Screening

The tests took place in 6-well plates. The test volume was 3 mL for each well with 10^5 cells/mL, and the cells were treated with CKE in different concentrations. The cells were exposed to the extract for 72 h before collection. Next, 100 µL the treated cell biomass was smeared onto a slide, and then 90% ethanol covered the slide. The cells were stained with a 2.5 mg/mL solution of Wright's eosin methylene blue (Sigma-Aldrich, USA) dissolved in absolute methanol (Merck, Germany). After 2 min of incubation, the slide was washed with Wright's buffer (solution of 6.63 mg/mL of KH_2PO_4 and 2.56 mg/mL Na2HPO4, Sigma-Aldrich, USA). The cells' morphology was observed using a microscope (Olympus LS, Japan).

Apoptosis-Inducing Test

The solution of cell biomass at the density of 10^5 cells/mL was treated with CKE at 100 µg/mL. After 24 h of incubation, the cells were collected and dyed with the ANNEX100B kit (BioRad, USA).[16] The stained cells were analyzed on a flow cytometer (Accuri C6 Plus, BD Biosciences, USA).

DNA Fragmentation Assay

The cells at density 105 cells/mL were incubated with 100 µg/mL CKE for 24 h. The cells were collected and suspended in 100 µL of Dulbecco's phosphate buffer saline (Stemcell, Singapore). And then, 300 µL of trizol (Thermo Scientific, USA) was added to the mixture. The mix was incubated at 65°C for 15 min. 400 µL of Prec Buffer was added into the mix. Centrifugation at 10,000 g was conducted for 5 min. The precipitant was collected after removing the solution. The precipitant was washed twice with the wash solution. Total DNA was dissolved in 50 µL elution buffer (Favorgen Biotech, Taiwan). 10 µL of total DNA was analyzed using 2%-agarose-gel-electrophoresis supplemented with Redsafe dye (iNtRON Biotechnology, Korea).

mRNA Level Measurement

The cells at density 10^5 cells/mL were treated with 100 µg/mL CKE for 24 h. The cells were collected and the total mRNA was extracted using the trizol reagent (Thermo Scientific, USA). In detail, cells were harvested and, in 5 min, incubated with 750 µL trizol. The mixture was mixed with 150 µL chloroform (Merck, Germany). After 2 min of incubation, centrifugation at 10,000 g was conducted for 5 min to collect the supernatant. 300 µL of isopropanol was added to the supernatant collection. Centrifugation at 10,000 g was run for 5 min to remove the supernatant. The precipitant was washed with 750 µL ethanol 70%, and the centrifugation was repeated. Total RNA was stored in the elution buffer. The gene expression was detected by the RT-qPCR method with the combination of SensiFAST cDNA Synthesis and SensiFAST SYBR® No-ROX Kits (Meridian Bioscience, USA).[16] The used primers for analysis were named in Table 1.

Statistical Analysis

The results were collected in triplicate. The data was computed and analyzed using the GraphPad Prism software version 9.0.0. The image edition was performed by using ImageJ software.

RESULTS AND DISCUSSION

In many previous papers, apoptosis induction was observed as an impact of the extracts derived from tea.[17] *Camellia* is an outstanding member of Theaceae with the most species and diverse research activities. Thus far, the apoptosis-inducing effect has been recorded on many *Camellia* species, such as *Camellia sinensis* (L.) Kuntze[18], *Camellia ptilophylla* Hung T.Chang[19], *Camellia euphlebia* Merr. ex Sealy[20], and *Camellia oleifera* C. Abel[21]. However, the report on *C. kissi* has been ignored due to rarity and endemicity. The inhibitory effect of *C. kissi* extract

Table 1. The primers used for transcriptional-level evaluation.

Target	Forward primer	Reverse primer
GADPH	GAAGGTGAAGGTCGGAGTC	GAAGATGGTGATGGGATTTC
Fas	CACACTCACCAGCAACAC	TCCTTTCTCTTCACCCAAAC
Bcl-2	AAGATTGATGGGATCGTTGC	GCGGAACACTTGATTCTGGT
Bcl-XL	GTAGAGTGGATGGTCAGTG	TTGGACAATGGACTGGTTGA
Bax	TGGCAGCTGACATGTTTTCTGAC	TCACCCAACCACCCTGGTCTT
Caspase 3	GAACTGGACTGTGGCATTGA	CCTTTGAATTTCGCCAAGAA
Caspase 8	CTGCTGGGGATGGCCACTGTG	TCGCCTCGAGGACATCGCTCTC
Caspase 9	GGTGATGTCGGTGCTCTTGA	CGACTCACGGCAGAAGTTCA
Survivin	GTTGCGCTTTCCTTTCTGTC	TCTCCGCAGTTTCCTCAAAT
BCR-ABL	CGGGAGCAGCAGAAGAAGTTGTTC	CAGGCACGTCAGTGGTGTCTCTGTG
PIK3CA	GGTTGTCTGTCAATCGGTGACTGT	GAACTGCAGTGCACCTTTCAAGC
PIK3CB	TTGTCTGTCACACTTCTGTAGTT	AACAGTTCCCATTGGATTCAACA
mTor	GCTTGATTTGGTTCCCAGGACAGT	GTGCTGAGTTTGCTGTACCCATGT
PTEN	GGTTGCCACAAAGTGCCTCGTTTA	CAGGTAGAAGGCAACTCTGCCAAA
Erk	TCAAGCCTTCCAACCTC	GCAGCCCACAGACCAAA
p38a	TGAAATGACAGGCTACGTGG	GACTTCATCATAGGTCAGGC
CDK1	GGG TCA GCT CGC TAC TCA AC	AAG TTT TTG ACG TGG GAT GC
CDK2	TCATGGATGCCTCTGCTCTCAC	TGGAGGACCCGATGAGAATGGC
CDK4	CATTGGGGACTCTCACACTCTC	ATGGCTACCTCTCGATATGAG
TP53	TGTGGAGTATTTGGATGACA	GAACATGAGTTTTTTATGGC
pRB	ACTCCGTTTTCATGCAGAGACTAA	GAGGAATGTGAGGTATTGGTGACA

on K562 in a dose- and time-dependent manner was reported in a previous study with the half-maximal inhibitory concentration of 40.01± 3.12 µg/mL.[22] In the presence of SKE, the cell's morphology reflected many surface changes, indicating the apoptosis process (Figure 1). At 50 µg/mL CKE concentration, the K562's surface became smooth-surfaced protuberance, and the cell volume decreased. The fragmentation was observed during the treatment with 100 µg/mL CKE; the apoptotic bodies showed off. The simultaneous PI and Annexin V permeability confirmed the apoptosis induction. The results in Figure 2A indicated the increase of the co-positive stained cell population from 15% to 18% after a 24-hour treatment.

The integrity of the genome, which exhibited DNA decentralization, was evaluated after 24 h of treatment with CKE. As shown in Figure 3, the smears appeared in both treatments with CKE while absent in the control. The denaturation in the genome during apoptosis was demonstrated due to the cleaving of enzymes, especially caspase-3.[23] The programmatical cleavage created multiple fragmented products with around 180 bp difference in length.[24] The propodium iodide fluorescence analysis indicated the cell cycle arrestment at the G2 checkpoint (Figure 2B). The population of the cells harboring sister chromatins increased by almost ten percent after 24-hour CKE treatment, which indicated that cell division and cell proliferation decreased. Additionally, a slight development of the S phase was also recorded. The capacity of cell cycle arrest was

previously documented as the impact of *Camellia* plants, such as *C. sinensis* on human ovarian cancer cells and *C. oleifera* on human breast cancer cells.[25,26]

The mRNA levels showed the transcriptional regulation of the CKE on the K562. The 2-delta delta CT values expressed the target mRNA contents compared to the housekeeping gene *GAPDH*. The interaction of changing RNA expression of some genes in K562 caused by *C. kissi* was published for the first time. In the 24-hour experiment, the effect of the extract recorded an increase in mRNA levels of *Fas* and *Bax*, which represent a group of proteins upstream of the apoptosis signaling pathway. Besides, the decreased expression of *Bcl-2* family genes logically contributes to the perception of induction of apoptosis by CKE. Interestingly, the expression changes of *Caspase 9* and *Bcl-2* family mRNA suggest that the effector pathway may be closely linked to the mechanism of apoptosis induction by intracellular signals (Figure 4A). One of the prominent signaling pathways in CML is considered through the BCR-ABL fusion protein, which carries diverse downstream signals.[6] However, in this study, we found increased expression of *BCR-ABL* mRNA in cells but not of *Pi3K* or *MAPK* (Figure 4B). The *Pi3k* and *mTOR* were maintained during the tests but increased *PTEN* suggested an interaction pathway that requires further investigation.[27,28] Previously, the interaction between green tea and BCR-ABL was reported. The tea-derived catechins were expected to be a new inhibitor in CML treatment.[29-31]
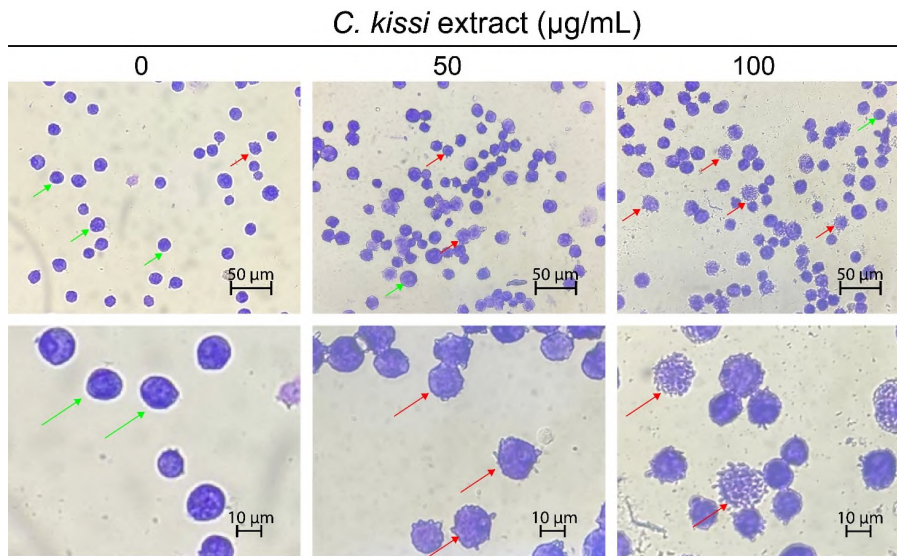
Figure 1. Cell morphology changes under the impact of *Camellia kissi* extract. The treatment at 100 µg/mL *C. kissi* extract was evaluated on K562, and the cell morphology was observed after 72 h of extract incubation. The cell morphology reflected several signs of apoptosis features, including shrinkage of the cell and smooth-surfaced protuberances (the red arrows) compared to the healthy cells (the green arrows).
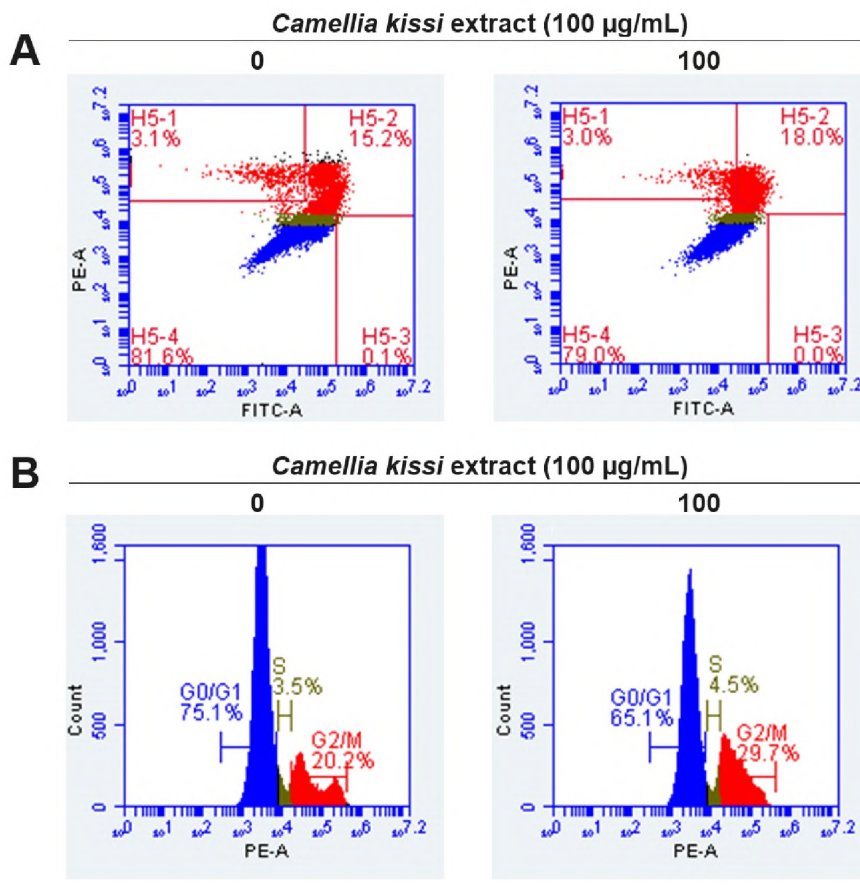

Figure 2. *Camellia kissi* extract induced apoptosis and cell cycle arrest on K562. Cells were exposed to 100 µg/mL *C. kissis* extract for 24 h before flow cytometry was performed. The results indicated the apoptosis-inducing effect of the extract, and the cell cycle was arrested at the M phase.
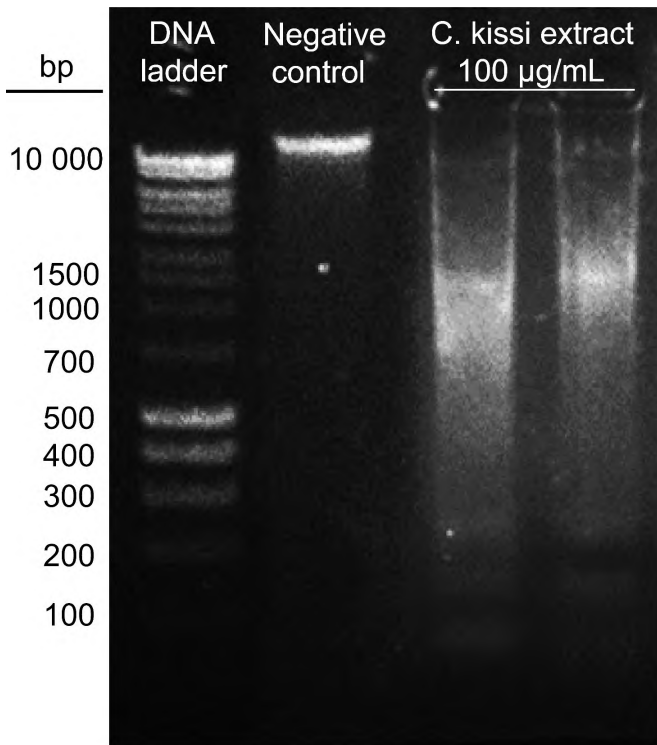
Figure 3. The DNA fragmentation under the influence of *Camellia kissi* extract. Cells were treated with *C. kissi* extract at 100 µg/mL for 24 h before DNA extraction. The 2%-agarose-gel-electrophoresis was conducted to analyze the DNA integrity. The results showed that the genome was cleaved into small polynucleotide fragments.
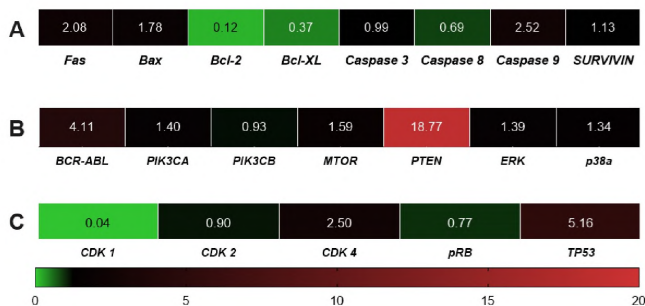

Figure 4. *Camellia kissi* extract regulated the mRNA level of several genes on K562. Cells were treated with *C. kissi* extract at 100 µg/mL for 24 h before total RNA extraction. The RT-qPCR was performed to analyze the mRNA level of several genes related to cell signaling, apoptosis, and cell cycle. The results showed that there were changes in mRNA levels in treated cells.

On the other hand, the number of cells at the G2 stage increased after 24 h of treatment, as mentioned above, for the collapse in the level of the *CDK1* described in Figure 4C, inferentially. CDK1 depletion was proposed to cause degradation of the CDK1/Cyclin A and CDK1/Cyclin B complexes, so the cells were trapped at the G2/M checkpoint.[32] Similarly, the increase in *CDK4* was also consistent with the decrease in cell number in the G1 phase under treatment. There was opposition in the expression of *TP53* and *pRB*; increased expression of *TP53* and decreased expression of pRP were observed. The increase in *TP53* was closely related to the decrease in CDK1/Cyclin B activity, leading to the cell's inability to pass the M checkpoint.[33] The results suggested the ability of *C. kissi* extract to induce K562 cell apoptosis via the intrinsic pathway through BCR-ABL/PTEN signaling. The cell arrest at G2/M was also observed as an effect of this extract. The research's development in the direction of protein analysis related to the discussed signaling pathways is necessary to have complete scientific information for this tea species.

CONCLUSION

This study documented the apoptosis-inducing ability of C. kissi leaf extract for the first time on K562 cells. The effect was considered to be mediated via the BCR-ABL pathways that led to apoptosis and G2 cell cycle arresting.

ORCID IDs of the authors

Nguyen Anh Xuan   0009-0001-7545-0888
Nguyen Trung Quan   0000-0002-6436-4693
Bui Thi Kim Ly   0000-0002-8433-7035
Hoang Thanh Chi   0000-0002-6638-1235

REFERENCES

1. Sung H, Ferlay J, Siegel RL, et al. Global cancer statistics 2020: GLOBOCAN estimates of incidence and mortality worldwide for 36 cancers in 185 countries. *CA Cancer J Clin*. 2021;71(3):209-249.

2. Dong Y, Shi O, Zeng Q, et al. Leukemia incidence trends at the global, regional, and national level between 1990 and 2017. *Exp Hematol Oncol*. 2020;9:14. doi: 10.1186/s40164-020-00170-6.

3. Levine R, Loriaux M, Huntly B, et al. The JAK2V617F activating mutation occurs in chronic myelomonocytic leukemia and acute myeloid leukemia, but not in acute lymphoblastic leukemia or chronic lymphocytic leukemia. *Blood*. 2005;106(10):3377-3379.

4. Lagunas-Rangel FA, Chávez-Valencia V, Gómez-Guijosa M, Cortes-Penagos C. Acute myeloid leukemia-genetic alterations and their clinical prognosis. *Int J Hematol Oncol Stem Cell Res*. 2017;11(4):328-339.

5. Sampaio MM, Santos MLC, Marques HS, et al. Chronic myeloid leukemia-from the Philadelphia chromosome to specific target drugs: A literature review. *World J Clin Oncol*. 2021;12(2):69-

94.

6. Mughal T, Goldman J. Chronic myeloid leukemia: Why does it evolve from chronic phase to blast transformation? *Front Biosci.* 2006;11(1):198-208.

7. Roskoski R, Jr. Targeting BCR-Abl in the treatment of Philadelphia-chromosome positive chronic myelogenous leukemia. *Pharmacol Res.* 2022;178:106156. doi: 10.1016/j.phrs.2022.106156.

8. Li Y, Zeng P, Xiao J, Huang P, Liu P. Modulation of energy metabolism to overcome drug resistance in chronic myeloid leukemia cells through induction of autophagy. *Cell Death Discov.* 2022;8(1):212. doi: 10.1038/s41420-022-00991-w.

9. Gleixner KV, Filik Y, Berger D, et al. Asciminib and ponatinib exert synergistic anti-neoplastic effects on CML cells expressing BCR-ABL1 (T315I)-compound mutations. *Am J Cancer Res.* 2021;11(9):4470-4784.

10. Pérez-Lamas L, Luna A, Boque C, et al. Toxicity of asciminib in real clinical practice: Analysis of side effects and cross-toxicity with tyrosine kinase inhibitors. *Cancers.* 2023;15(4):1045. doi:10.3390/cancers15041045

11. Merkulova A, Mitchell SC, Stavrou EX, Forbes GL, Schmaier AH. Ponatinib treatment promotes arterial thrombosis and hyperactive platelets. *Blood Adv.* 2019;3(15):2312-2316.

12. Pan SY, Nie Q, Tai HC, et al. Tea and tea drinking: China's outstanding contributions to the mankind. *Chin Med.* 2022;17(1):27. doi: 10.1186/s13020-022-00571-1.

13. Bange E, Timlin C, Kabel C, et al. Evidence for and against green tea and turmeric in the management of chronic lymphocytic leukemia. *Clin Lymphoma Myeloma Leuk.* 2018;18(10):e421-e6. doi: 10.1016/j.clml.2018.06.021.

14. Calgarotto A, Pericole FV, Favaro P, et al. Green tea in acute myeloid leukemia. *Blood.* 2013;122(21):5032. doi: 10.1182/blood.V122.21.5032.5032

15. Nguyet Hai Ninh L, Luong V, Nguyen Van C, et al. An updated checklist of *Theaceae* and a new species of *Polyspora* from Vietnam. *Taiwania.* 2020;65(2):216-227.

16. Quan N, Ly B, Chi H. The cytotoxic effect of *Vernonia amygdalina* Del. extract on myeloid leukemia cells. *Biomed Res Ther.* 2023;10(8):5855-5863.

17. Nakazato T, Ito K, Ikeda Y, Kizaki M. Green tea component, catechin, induces apoptosis of human malignant B cells via production of reactive oxygen species. *Clin Cancer Res.* 2005;11(16):6040-6049.

18. Er S, Dikmen M. *Camellia sinensis* increased apoptosis on U2OS osteosarcoma cells and wound healing potential on NIH3T3 fibroblast cells. *Cytotechnology.* 2017;69(6):901-914.

19. Gao X, Li X, Ho C-T, et al. Cocoa tea (*Camellia ptilophylla*) induces mitochondria-dependent apoptosis in HCT116 cells via ROS generation and PI3K/Akt signaling pathway. *Food Res Int.* 2020;129:108854. doi: 10.1016/j.foodres.2019.108854.

20. He D, Wang N, Sai X, Li X, Xu Y. *Camellia euphlebia* protects against corticosterone-induced apoptosis in differentiated PC12 cells by regulating the mitochondrial apoptotic pathway and PKA/CREB/BDNF signaling pathway. *Food Chem Toxicol.* 2019;126:211-222.

21. He X, Li H, Zhan M, et al. *Camellia nitidissima* chi extract potentiates the sensitivity of gastric cancer cells to paclitaxel via the induction of autophagy and apoptosis. *OncoTargets Ther.* 2019;12:10811-10825.

22. Xuan N, Tin S, Trung P, Chi H, Ly B. Investigate the anti-cancer effects of *Camellia kissi* methanol extract on K562 Leukemia cells. *JST-UD.* 2023;21(5):73-77.

23. Jänicke RU, Sprengart ML, Wati MR, Porter AG. Caspase-3 is required for DNA fragmentation and morphological changes associated with apoptosis. *J Biol Chem.* 1998;273(16):9357-9360.

24. Matassov D, Kagan T, Leblanc J, Sikorska M, Zakeri Z. Measurement of apoptosis by DNA fragmentation. *Methods Mol Biol* (Clifton, NJ). 2004;282:1-17.

25. Chen L, Chen J, Xu H. Sasanquasaponin from *Camellia oleifera* Abel. induces cell cycle arrest and apoptosis in human breast cancer MCF-7 cells. *Fitoterapia.* 2013;84:123-129.

26. Wang Y, Ren N, Rankin GO, et al. Anti-proliferative effect and cell cycle arrest induced by saponins extracted from tea (*Camellia sinensis*) flower in human ovarian cancer cells. *J Funct Foods.* 2017;37:310-321.

27. Steelman LS, Pohnert SC, Shelton JG, et al. JAK/STAT, Raf/MEK/ERK, PI3K/Akt and BCR-ABL in cell cycle progression and leukemogenesis. *Leukemia.* 2004;18(2):189-218.

28. Morotti A, Panuzzo C, Crivellaro S, et al. BCR-ABL inactivates cytosolic PTEN through Casein Kinase II mediated tail phosphorylation. *Cell cycle* (Georgetown, Tex). 2015;14(7):973-979.

29. Li XX, Liu C, Dong SL, et al. Anticarcinogenic potentials of tea catechins. *Front Nutr.* 2022;9:1060783. doi: 10.3389/fnut.2022.1060783.

30. Iwasaki R, Ito K, Ishida T, et al. Catechin, green tea component, causes caspase-independent necrosis-like cell death in chronic myelogenous leukemia. *Cancer Sci.* 2009;100(2):349-356.

31. Massimino M, Stella S, Tirrò E, et al. Non ABL-directed inhibitors as alternative treatment strategies for chronic myeloid leukemia. *Mol Cancer* 2018;17(1):56. doi: 10.1186/s12943-018-0805-1.

32. Fisher D, Krasinska L. Explaining redundancy in CDK-mediated control of the cell cycle: Unifying the continuum and quantitative models. *Cells.* 2022;11(13):2019. doi: 10.3390/cells11132019.

33. Rizzotto D, Englmaier L, Villunger A. At a crossroads to cancer: How p53-induced cell fate decisions secure genome integrity. *Int J Mol Sci.* 2021;22(19):10883. doi: 10.3390/ijms221910883.

How to cite this article